Functions of peroxisomal citrate synthase and peroxisomal malate dehydrogenase in lipid catabolism in Arabidopsis

Itsara Pracharoenwattana

A thesis submitted in partial fulfilment
of the requirements for the degree of

Doctor of Philosophy

The University of Edinburgh
2005

Declaration

I declare that this is my own work. Any contribution made by other parties is clearly acknowledged.

Contents

Acknowledgements

Firstly, I really would like to thanks my supervisor, Professor Steven Smith, for his patience, guidance, knowledge and support during the whole period of my PhD study. I also would like to thank Dr Johanna Cornah for her guidance, lab demonstration, help, conversation and ^{14}C-acetate feeding result. Thank you also to the past and present lab members, especially Sarah, Dave, Aileen, Susan, Dorthe, Hannah, Garry and Dan, for their enjoyable conversation and help. Thanks to John Finlay for TEM, Graham Wright for confocal microscopy and Robert Smith for GC-MS. I am also grateful to Dr Imogen Sparkes (Oxford) and Dr Alison Baker (Leeds) for their useful comments, clones and mutant seeds. Thanks also to lab members in the Garry Loake group for conversation and useful help. I would like to express my gratitude to the Royal Thai Government (The Development and Promotion of Science and Technology Talents Project) for giving me the opportunity to study in the United Kingdom.

Thanks to previous and current flatmates, Jane, Paula, Thierry and Steve, for enjoyable conversation, help, friendship and for coping with me. I would also like to thank Thai friends in Edinburgh and all over the place. Special thanks go to Pee Jay, Pee Toon and Neung who gave me lots of help and for being there when I needed someone to talk to. Thanks also to Pee Ob, Pee Lee, Pee Ake, Oa, Minn, Pee Jee, Pee Tik, Pee Bau, Pee Kay and Pee Jake for friendship and help. I would also like to thank Pee Jum, Pee Pom, Len, Pee Rut, Pee Kanit, Pee Wan, Pee Ben, Pee Noi and Pee Nai in Dusit Thai restaurant (Edinburgh) for their generosity, friendship and enjoyable conversation.

I would like to thank my family. Thanks to my father to let me do what I want to do. Thanks to my mother for her unconditional love, support, patience and encouragement. Thanks to my brother and sister for taking care of my parents through the period I stay abroad.

I am deeply grateful for all your support, without which, my PhD would not be possible.

Abbreviations

µM	micromolar
µmol	micromole
2,4-D	2,4-dichlorophenoxyacetic acid
2,4-DB	2,4-dichlorophenoxybutyric acid
ABA	abscisic acid
ABC	ATP binding cassette
ACO	aconitase
ACS	acyl-CoA synthetase
ACT	actin
ACX	acyl-CoA oxidase
AIM	abnormal inflorescent meristem
ALDP	adrenoleukodystrophy protein
BASTA	phosphinothricin
BOU	à bout de soufflé
bp	base pair
BSA	bovine serum albumin
CAC	carnitine acetylcarnitine carrier
CAT	catalase
CAT	carnitine acetyl-CoA transferase
CSY	citrate synthase
CTS	comatose
DEPC	diethyl pyrocarbonate
dH_2O	sterile distilled water
DMSO	dimethyl sulfoxide
dNTPs	2'-deoxynucleoside 5'-triphosphates
DTNB	5,5'-dithio-bis(2-nitrobenzoic acid)
DTT	dithiothreitol
EDTA	ethylene-diaminetetraacetic acid
ER	endoplasmic reticulum
GA	gibberellic acid
GC-MS	gas chromatography-mass spectrometry

GFP	green fluorescent protein
GGT	glutamate-glyoxylate aminotransferase
GOX	glycolate oxidase
GUS	glucuronidase
HPR	hydroxypyruvate reductase
ICL	isocitrate lyase
IPTG	isopropyl β–D-thiogalactoside
KAT	3-ketoacyl-CoA thiolase
LACS	long chain acyl-CoA synthetase
LB	lipid body
M	molar
Mb	megabase
MDH	malate dehydrogenase
MFP	multifunctional protein
MLS	malate synthase
mM	millimolar
mRFP	monomeric red fluorescent protein
mRNA	messenger RNA
nmol	nanomole
OD	optical density
PCR	polymerase chain reaction
PEPCK	phosphenolpyruvate carboxykinase
Pex	peroxin
PMDH	peroxisomal malate dehydrogenase
pmol	picomole
PMP	peroxisomal membrane protein
PTS	peroxisomal targeting signal
RNase	ribonuclease
rpm	revolutions per minute
RT-PCR	reverse transcription polymerase chain reaction
Rubisco	ribulose bisphosphate carboxylase/oxygenase
SDS	sodium dodecyl sulfate
SDS-PAGE	sodium dodecyl sulfate -poly acrylamide gel electrophoresis

SGT	serine-glyoxylate aminotransferase
TAG	triacylglycerol
TCA	tricarboxylic acid
TE	Tris-Cl, ethylenediaminetetraacetic acid
TEMED	N,N,N',N'-tetramethylethylenediamine
Tris	Tris(hydroxymethyl)aminomethane
Tween	polyethylenesorbitan monolaurate
UTR	untranslated region
XET	xyloglucan endotransglycosylase
X-Gal	4-bromo-4chloro-3-indoyl-β-D-galactopyranoside
X-Gluc	5-Bromo-4-chloro-3-indoyl-β-D-glucuronide

Abstract

In Arabidopsis, peroxisomal carbon metabolism to break down lipid reserves is known to be essential for germination and seedling growth. However, the metabolic pathways underlying this process remain to be elucidated. It is proposed that peroxisomal citrate synthase (CSY) is required for carbon transfer from peroxisomes to mitochondria during respiration of fatty acids in Arabidopsis seedlings. Two genes encoding peroxisomal CSY are expressed in Arabidopsis seedlings. Double mutant seeds in which both genes are knocked out are dormant, and unable to utilise their stored lipid. Germination can be achieved by removing the seed coat and supplying sucrose. The seedlings are resistant to 2,4-dichlorophenoxybutyric acid (2,4-DB), indicating a defect in peroxisomal β-oxidation. Beyond the seedling stage, double mutants also show an arrested growth phenotype, and crucially are unable to produce seeds. The double mutant phenotypes can be restored by complementation with a cDNA encoding CSY with either its native PTS2 targeting sequence or a heterologous PTS1 sequence. These results suggest that peroxisomal CSY is not just a glyoxylate cycle enzyme but is also required for fatty acid respiration and to break seed dormancy.

It is hypothesised that peroxisomal malate dehydrogenase (PMDH) serves to oxidise NADH produced by β-oxidation, and does not oxidise malate to provide oxaloacetate for the glyoxylate cycle. The Arabidopsis genome encodes eight putative NAD^+-dependent malate dehydrogenase enzymes, two of which are predicted to be PMDHs. Double mutant seeds in which these two *PMDH* genes are knocked out are unable to establish as seedlings unless exogenous sucrose is supplied. In this respect the double mutant is similar to a range of β-oxidation mutants. Seedlings are impaired in breakdown of stored lipid and insensitive to 2,4-DB, showing that β-oxidation is defective. The metabolism of [2-^{14}C]-acetate into sugars and organic acids is normal in double mutant seedlings, indicating that the glyoxylate cycle is still active. The phenotypes observed in the double mutant can be recovered by complementation with cDNAs encoding PMDHs with either authentic PTS2 or heterologous PTS1 sequences. In particular, PMDH is not required for the glyoxylate cycle, but appears to be required for fatty acid β-oxidation. Thus, critical roles in fatty acid β-oxidation are implied for peroxisomal CSY and MDH.

Chapter 1

Introduction

Chapter 1

Introduction

In nature, the seed represents the starting point of a new phase of plant growth and reproduction. Although common, the transition from seed to plant is a highly sophisticated process. Catabolism of storage reserves is one of the essential requirements at this stage, until the seedling becomes photoautotrophic. How this catabolism is achieved, has raised questions for the scientific community for more than a century. Recently, the breakthrough of genetic engineering technology together with the genome project of the model plant, *Arabidopsis thaliana*, have paved the way for a genetic approach to identify gene function and establish the role of specific genes in metabolism. This is achieved using molecular and biochemical analysis of Arabidopsis mutants. An abundance of research on the pathway of lipid catabolism has yielded some understanding, yet many aspects still remain undiscovered.

1.1 Germination and seedling establishment

The seed contains a new plant in miniature known as the embryo, and food reserves which provide carbon and energy for seedling growth before photosynthesis begins. Following the process of maturation and drying in the parent plant, the dried seed is

in a metabolically quiescent state. Matured seeds of most plant species exhibit primary dormancy (Debeaujon et al., 2000). Seed dormancy refers to the failure of a viable seed to germinate even when given favourable environmental conditions. This is a characteristic feature of seeds that are able to suspend developmental processes until the conditions necessary for germination are met (Bewley and Black, 1982). In nature, dormancy mechanisms ensure that seeds will germinate at the proper time. Abscisic acid (ABA) appears to be a dormancy inducing hormone which is indicated by the correlation between endogenous ABA and seed physiological stages. Dormant seeds contain a higher concentration of ABA than non-dormant seeds (Taiz and Zeiger, 2002). Moreover, the addition of ABA to mature non-dormant seeds inhibits their germination (Garciarrubio et al., 1997). The transition of dormancy to germination depends on the activation of developmental programmes and catabolism of metabolic reserves, which results in radicle emergence, seedling establishment and photoautotrophic growth (Bewley, 1997).

After hydration under suitable conditions, if it is not dormant, the seed reactivates its metabolism and commences germination. By definition, germination incorporates those events that start from the uptake of water (imbibition) by the quiescent dry seed and terminates with the elongation of the embryonic axis (Bewley, 1997). The visible consequence of germination is the protrusion of the radicle tip through the seed coat. The subsequent events are referred to as the seedling growth.

Water is needed to allow metabolism to begin. Uptake of water by the mature dry seed is triphasic, defined as: a rapid initial uptake of water or imbibition (phase I),

followed by a plateau phase (phase II) and ending up with an increase of water uptake (phase III) (Bewley, 1997; Figure 1.1).

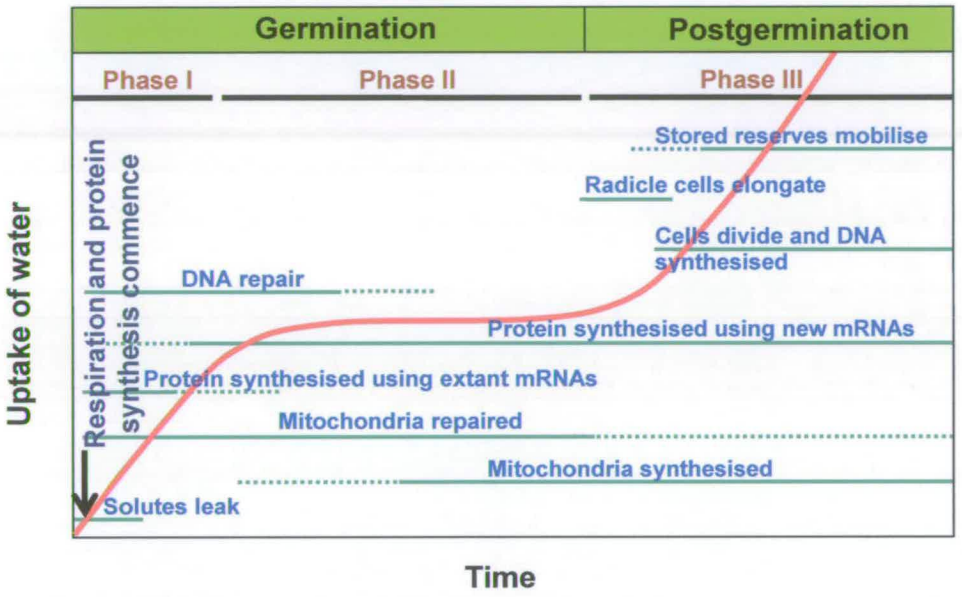

Figure 1.1 Time course of major events associated with germination and subsequent postgerminative growth (Bewley, 1997).

Uptake of water into the dry seed in phase I leads to a temporary structural perturbation to the membranes. Low molecular weight metabolites leak into the surrounding solution. This results in a transition of phospholipid membrane components from the gel phase which persists during maturation and drying, to the normal-hydrated liquid-crystalline state (Crowe and Crowe, 1992). Within a short time of hydration, membranes return to a stable configuration and leakage ceases. This event results in a resumption of the metabolic activity in cells (Bewley, 1997; Bewley et al., 2000). The metabolic activities now begin using the cellular structural and enzymatic components synthesised during maturation and conserved within dry seed. The metabolic activity commenced first is the resumption of respiratory

activity. Tissue of dry seed contains mitochondria. These mitochondria are poorly differentiated during the drying process; however, there are sufficient enzymes to drive respiratory metabolism. This is adequate to support the respiratory activity demand at the early stage of germination. Protein synthesis is another very early event. The machinery and components essential for protein synthesis are conserved within cells of matured dry embryo. As time continues, extant mRNAs are replaced by *de novo* transcription and turnover. New mRNAs are synthesised as germination proceeds. The majority of mRNAs initially accounts for the proteins essential to support basic cellular metabolism, but not restricted to germination (Bewley, 1997).

Once the radicle extends through the seed coat, the germination event is complete. The extension of the radicle is a turgor-driven process which may or may not be accompanied by cell division (Cosgrove, 1997). Bewley (1997) has claimed three possible explanations on how the radicle emerges. One possibility is that, as a result of the solute accumulation, the osmotic potential of the radicle cell is highly negative. This increases water uptake and results in a turgor pressure which is enough to force cell expansion. The second possibility is radicle elongation by the loosening of their cell walls. This can be achieved by the cleavage and rejoining of xyloglucan molecules, which allow expansion by microfibril separation. The reversible cleaving of xyloglucan is performed by xyloglucan endotransglycosylase (XET) (Wu et al., 1994). Expansins, which are proposed to be proteins responsible for disruption of hydrogen bonds between cell wall polymers, are also good candidates (McQueen-Mason and Cosgrove, 1995). The third possibility is that the seed tissues surrounding

the radicle tip weaken, allowing the radicle tip to elongate. All three mechanisms are expected to operate together to different extents to achieve radicle elongation.

After germination, the embryo of the germinated seed continues to grow and establishes a seedling. Seedling establishment is a crucial stage in the plant life cycle. To achieve this, seedlings must adapt both developmental and metabolic programs to the prevailing environmental conditions (Holdsworth et al., 1999). At this stage the germinated seed has a high energy demand to drive metabolic activities and cell division. As photosynthesis has not yet begun, the sole energy comes from storage reserves which are mainly macromolecules: proteins, lipids or carbohydrates. These have been accumulated during seed maturation and stored in cotyledons or endosperm. Besides the utilisation of endogenous storage reserves, resources from the environment such as mineral nutrients are also used. Additionally, regulation by environmental parameters is essential. For example, light through a complex system of photoreceptors and signal transduction pathways is known to affect seedling developmental programs (Chory, 1993). Following seedling establishment, the endogenous reserves are depleting, but photosynthesis has begun, so seedlings are now able to sustain their energy requirements.

1.2 Lipid mobilisation during seed germination and seedling growth

Lipids are highly concentrated metabolic energy stores containing more energy per given mass than either carbohydrates or proteins. Their hydrophobicity and insolubility in water allows lipids to segregate into droplets, which do not raise osmolarity of the cytosol. Moreover, lipids do not contain extra mass as solvation water, as do polysaccharides. Their inertness allows their intracellular storage in large quantity with little possibility of undesired chemical reaction with other constituents.

Lipids are major reserves especially in oil seed plants such as rapeseed, sunflower and castor bean. The carbon sources like the existing sucrose is available and enough to supply energy to a seed only at the early stage of germination. Once the seed is germinated, this carbon source is largely used up. To supplement this, lipid storage reserves are then broken down and converted into sucrose. Sucrose then can be utilised to support seedling growth. This mechanism allows germinating seed to grow and process from the heterotrophic stage into the phototrophic stage (Figure 1.2).

In plants, triacylgercerols (TAGs) are a group of lipids in which fatty acid molecules are linked by ester bonds to the three hydroxyl groups of glycerol, and are a common storage source of carbon and energy. However, TAG cannot be transported from cell to cell. Normally TAGs are stored in the cytosol in organelles called lipid bodies

(spherosomes or oleosomes). Once germination is achieved, TAGs are converted into a more mobile form of carbon, which is generally sucrose, for transport between cells. This conversion is achieved by several specialised metabolic pathways (Figure 1.3).

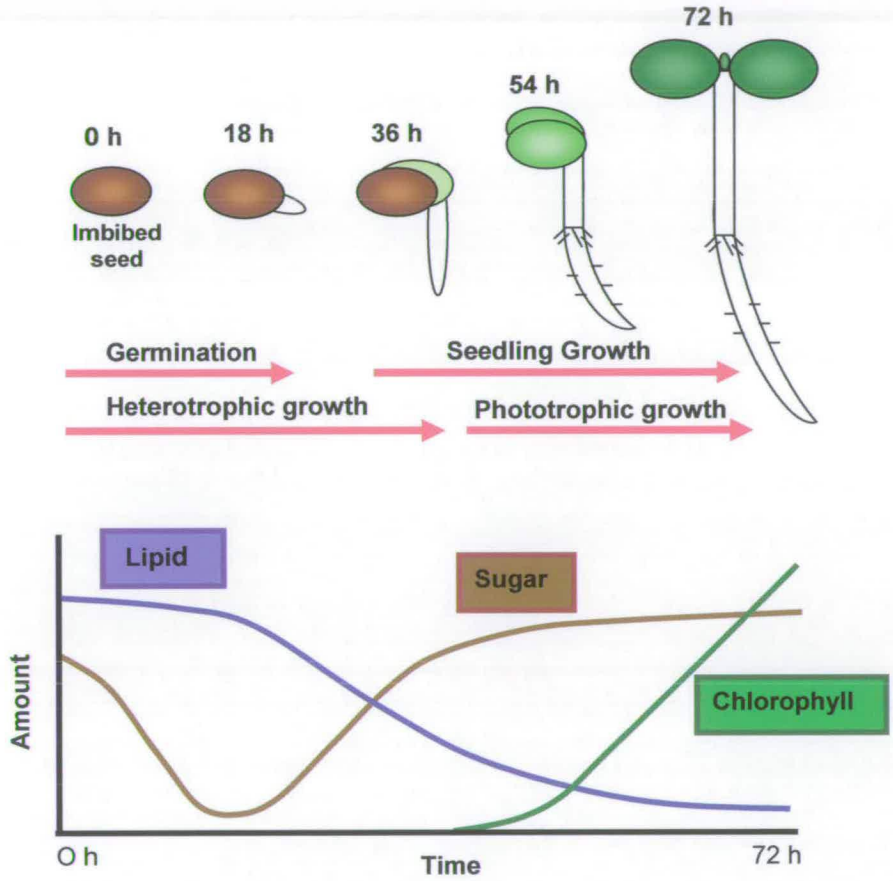

Figure 1.2 Schematic representation of time course of lipid breakdown in Arabidopsis, associated with germination and seedling growth.

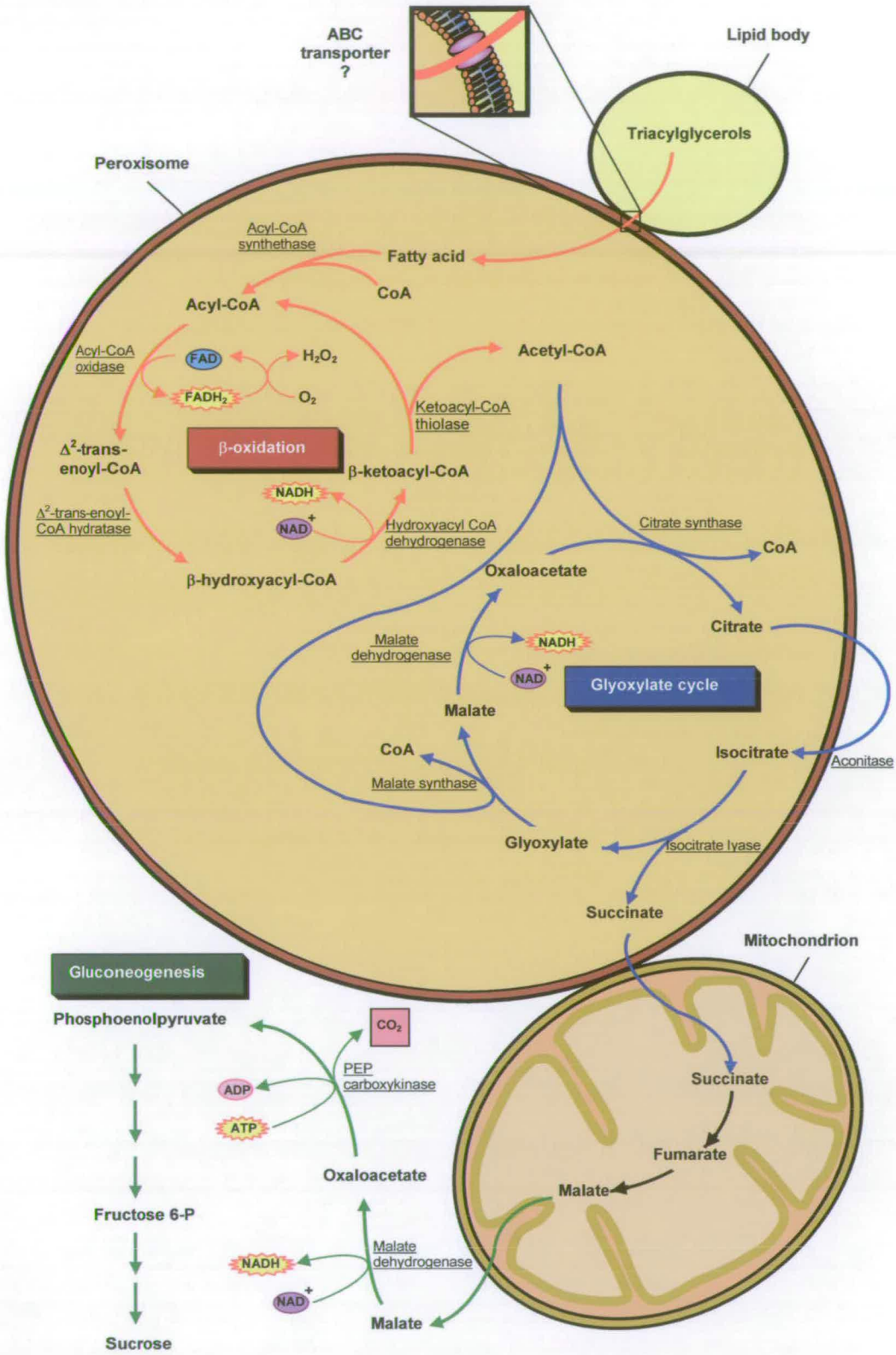

Figure 1.3 Representation of the metabolic pathways to breakdown triacylglycerols and convert them to sucrose.

1.3 Metabolic pathways to break down triacylglycerols

In animal cells, fatty acids released from TAGs are mobilised mainly in the mitochondrial matrix. By contrast, in plants this is carried out in the peroxisomes. TAG breakdown is not only used for metabolic energy production, but also provides metabolic precursors (Escher and Widmer, 1997). TAG mobilisation involves several consecutive pathways in various compartments (Figure 1.3). Firstly, TAGs stored in the lipid bodies are hydrolysed by lipase (Huang, 1992). Secondly, the fatty acids produced from lipase pass into the peroxisomes where β-oxidation occurs (Cooper and Beevers, 1969b). Thirdly, the acetyl-CoA produced from β-oxidation is condensed into succinate via the glyoxylate cycle (Breidenbach and Beevers, 1967). Fourthly, the succinate is exported from the peroxisomes into mitochondria and converted to malate through a partial citric acid cycle (Cooper and Beevers, 1969a). Finally, malate is transported back into the cytosol where the gluconeogenesis pathway converts it to sugar (Nishimura and Beevers, 1979). The metabolic conversion of TAGs into sugar is commonly represented as in Figure 1.3, but some details of this model, such as the role of peroxisomal malate dehydrogenase, may not be correct (see below).

1.3.1 Import of fatty acids into the peroxisome

The precise mechanism for fatty acid or acyl-CoA transport across the peroxisomal membrane in plants is still unknown. However, there is evidence that peroxisomal membrane transporters for such fatty acids do exist. ATP binding cassette (ABC) proteins are good candidates. ABC proteins function as ATP-binding dependent

pumps, ion channels and channel regulators (Theodoulou, 2000). In *Saccharomyces cerevisiae*, fatty acids appear to be activated externally and transported in the form of acyl-CoA by two ABC half proteins (Pat1p and Pat2p) (Hettema et al., 1996; Verleur et al., 1997). These contain an ATP binding cassette and are homologous to human ALDP (adrenoleukodystrophy protein; Mosser et al., 1993). ALDP is reported to be required for the import of very long chain fatty acid (VLCF) into peroxisome in human. Recently, the study of Arabidopsis mutants (*pxa1*, *cts* and *ped3)* in which this homologue is disrupted showed that fatty acid breakdown is blocked (Zolman et al., 2001; Footitt et al., 2002; Hayashi at al., 2002). This evidence indicates that an Arabidopsis ALDP homologue appears to be involved in fatty acid transport into peroxisomes. It remains to be determined whether fatty acids or fatty acyl-CoA is transported through the peroxisomal membrane. It was revealed that long-chain acyl-CoA is accumulated in *cts* seedlings (Footitt et al., 2002), indicating that fatty acids are initially activated into acyl-CoA by cytosolic long-chain acyl-CoA synthetase (cytosolic LACS) prior to transport into the peroxisomes. However, peroxisomal isoforms of LACS are still required subsequently (Fulda et al., 2004). This suggests that, during transport via the ABC transporter, acyl-CoA might be cleaved and the CoA returned to the cytosol, or more likely that unesterified fatty acid can be transported into peroxisomes.

1.3.2 β-oxidation

Fatty acids are activated into the fatty acyl-CoA by acyl-CoA synthetases (ACS; *EC 6.2.1.3*). This step requires ATP, Mg^{2+} and CoASH (Cooper, 1971). These enzymes have been observed in various organelles because these are also required for the

activation of fatty acid in lipid synthesis. It is suggested that ACSs are located on the peroxisomal membrane with the catalytic domains exposed to the matrix (Gerbling and Gerhardt, 1987). ACSs together with AMP binding proteins (AMPBP) belong to an AMPBP superfamily. This superfamily is classified by the existence of an AMP binding region and sequence analysis shows a high level of sequence similarity within the superfamily. It is suggested that the entire superfamily may have ACS activity (Graham and Eastmond, 2002; Hooks, 2002). In Arabidopsis there are 24 distinct members, of which at least 18 are expressed (Shockey et al., 2000). Some of these are putative peroxisomal ACS by their peroxisomal targeting sequences, but they remain to be characterised. Recently, Arabidopsis LACS6 and LACS7 have been characterised and demonstrated that their localisation is in peroxisomes (Fulda et al., 2002; 2004).

The activated acyl-CoA then enters the β-oxidation spiral which is catalysed by three proteins: (1) acyl-CoA oxidase, (2) the multifunctional protein and (3) L-3-ketoacyl-CoA thiolase. In each round of the β-oxidation spiral, acetyl-CoA (C_2) is cleaved from acyl-CoA (C_n). The remaining acyl-CoA (C_{n-2}) re-enters the β-oxidation spiral as many times as is necessary.

Acyl-CoA oxidase (ACX; *EC 1.3.3.6*) catalyses the reaction converting acyl-CoA into Δ^2-*trans*-enoyl-CoA. This reaction requires FAD as a co-factor, generating $FADH_2$. The reducing power ($FADH_2$) is then oxidised by flavoprotein dehydrogenase which directly transfers electrons to molecular oxygen and forms H_2O_2. Hydrogen peroxide is a damaging oxidant, so it is immediately converted to

H_2O and O_2 by catalase, which is abundant in peroxisomes. In animals, in which β-oxidation takes place in the mitochondria, this step is performed by acyl-CoA dehydrogenase (not by acyl-CoA oxidase). The reducing power resulting from this step can transfer through the respiratory chain to O_2, leaving H_2O as the product, together with ATP synthesis. Biochemical evidence suggested that plants contain multiple ACX isozymes with distinct but partially overlapping substrate chain-length specificities (Eastmond et al., 2000a). In Arabidopsis, four ACXs have been characterised (Eastmond, 2000a). ACX1 exhibited a preference for medium- to long-chain saturated acyl-CoAs whereas ACX2 showed a preference for long-chain unsaturated acyl-CoAs. ACX3 is a medium-chain and ACX4 is a short chain acyl-CoA oxidase.

The multifunctional protein (MFP) contains the domains for Δ^2-*trans*-enoyl-CoA hydratase (*EC 4.2.1.17*), L-3-hydroxyacyl-CoA dehydrogenase (*EC 1.1.1.35*), D-3-hydroxyacyl-CoA epimerase (*EC 5.1.2.3*) and Δ^3,Δ^2-enoyl-CoA isomerase (*EC 5.3.3.8*) activities. Fatty acids are catabolised toward L-isomers of 3-hydroxyacyl-CoA, hence for metabolism of saturated fatty acid and fatty acids containing a double bond at Δ^2 position with *trans* configuration, only the core activity of Δ^2-*trans*-enoyl-CoA hydratase and L-3-hydroxyacyl CoA dehydrogenase are required (Graham and Eastmond, 2002). With H_2O in the reaction, Δ^2-*trans*-enoyl-CoA hydratase converts Δ^2-*trans*-enoyl-CoA to L-3-hydroxyacyl-CoA. Next, L-3-hydroxyacyl-CoA dehydrogenase catalyses L-3-hydroxyacyl-CoA to 3-ketoacyl-CoA. This step requires NAD^+ as a co-factor and generates NADH as the reducing power. Since the majority of fatty acids found in plants are polyunsaturated, these (or their product

from β-oxidation core) sometimes contain a *cis* configuration double bond or double bond at odd numbered carbons. To continue the reaction in β-oxidation core, these are required to be converted into double bond at Δ^2 position with *trans* configuration. In this case, D-3-hydroxyacyl-CoA epimerase and Δ^3,Δ^2-enoyl-CoA isomerase activities are involved (Graham and Eastmond, 2002). Previous studies suggested that plants contain MFP isozymes, which exhibit broad specificity to chain-length of the substrates (Guhnemann-Schafer and Kindl, 1995). In Arabidopsis, two MFPs have been characterised (Richmond and Bleecker, 1999; Eastmond and Graham, 2000). Based on the homology to domains within MFPs, it is suggested that there might be various genes in Arabidopsis encoding mono-functional Δ^2-*trans*-enoyl-CoA hydratase and L-3-hydroxyacyl CoA dehydrogenase (Graham and Eastmond, 2002).

Thiolytic cleavage of 3-ketoacyl-CoA is performed by 3-ketoacyl-CoA thiolase (KAT; *EC 2.3.1.16*). This step generates acetyl-CoA (C_2) from acyl-CoA (C_n), therefore resulting in acyl-CoA (C_{n-2}) containing two carbon atoms shorter. The acyl-CoA then re-enters the β-oxidation pool again as many times as needed. Thiolases are probably the least characterised gene and protein family (Hooks, 2002). There are four putative thiolase genes in Arabidopsis which contain peroxisomal targeting signal sequences (Hooks, 2002). A previous study in the *kat2* (*ped1*) mutant suggested that KAT2 exhibits a broad chain-length specificity (Germain et al., 2001). However, further analysis may reveal differences in the substrate specificity of Arabidopsis thiolases.

1.3.3 Glyoxylate cycle and Gluconeogenesis

Acetyl-CoA, the two-carbon product from β-oxidation, is subsequently metabolised in the glyoxylate cycle. The glyoxylate cycle plays an important role allowing acetyl-CoA to be converted to carbohydrate. The glyoxylate cycle is a modified form of the tricarboxylic acid (TCA) cycle that bypasses the decarboxylative steps. This cycle condenses two molecules of acetyl-CoA (C_2) into succinate (C_4). This pathway possesses two key enzymes which are isocitrate lyase (ICL; *EC 4.1.3.1*) and malate synthase (MLS; *EC 4.1.3.2*). Another three enzymes which also appear in the TCA cycle are apparently required; these are citrate synthase (CSY; *EC 4.1.3.7*), aconitase (ACO; *EC 4.2.1.3*) and malate dehydrogenase (MDH; *EC 1.1.1.37*). CSY, ICL, MLS and MDH are localised in the peroxisome (Huang et al., 1983). By contrast, ACO is reported as a cytosolic enzyme in castor bean, potato (Courtois-Verniquet and Douce, 1993) and pumpkin (De Bellis et al., 1994; Hayashi et al., 1995).

The glyoxylate cycle initially synthesises citrate (C_6) from acetyl-CoA (C_2) and oxaloacetate (C_4) by CSY. Citrate is transported into the cytosol where ACO is localised. Isocitrate is then formed and transported back into the peroxisome. Isocitrate (C_6) is then cleaved by ICL to give glyoxylate (C_2) and succinate (C_4). Next MLS combines glyoxylate (C_2) with another acetyl-CoA (C_2) to produce malate (C_4), which is then oxidised into oxaloacetate by MDH. This oxaloacetate can join another acetyl-CoA to continue the cycle. The subcellular location of the steps of malate oxidation are not necessarily as shown in Figure 1.3 (see below).

Succinate from the glyoxylate cycle is transported into the mitochondria and metabolised by TCA cycle enzymes, and converted to malate. The malate is converted into oxaloacetate, probably by cytosolic MDH. Next, using ATP, the irreversible reaction of phosphoenolpyruvate carboxykinase (PEPCK; *EC 4.1.1.49*) converts oxaloacetate (C_4) to give phosphoenolpyruvate (C_3) and CO_2. From phosphoenolpyruvate, gluconeogenesis can proceed to the production of sucrose.

1.4 Regulation of the pathways in lipid mobilisation

It is demonstrated that the gene expression pattern for β-oxidation, glyoxylate cycle and gluconeogenesis is reflected in the pattern of enzyme activity, indicating a regulation at the transcriptional level (Rylott et al., 2001). In most plants including Arabidopsis, the level of mRNA and enzyme activity appears to correlate with the period of lipid mobilisation during germination and seedling growth (Figure 1.4). For example, *ACX1*, *ACX2*, *ACX3* and *ACX4* genes encode the family of acyl-CoA oxidase enzymes (Eastmond et al., 2000a; Rylott et al., 2001), *MFP2* gene encoding multifunctional protein (Eastmond and Graham, 2000), *KAT2* (*PED1*) gene encoding thiolase (Germain et al., 2001; Rylott, 2001), *ICL* gene encoding isocitrate synthase (Eastmond et al., 2000b), *MLS* gene encoding malate synthase (Cornah et al., 2004) and *PEPCK* gene encoding phosphoenolpyruvate carboxykinase (Rylott et al., 2003a). During germination only some of the gene family members are markedly induced, for example, *MFP2* and *KAT2* which are the main expressed genes from the multifunctional protein and thiolase families respectively (Eastmond and Graham, 2000; Germain et al., 2001). Apparently for MFP2 and KAT2, which are believed to

have broad substrate specificity, a single gene product is adequate to perform catabolism for short, medium and long-chain fatty acyl-CoA. In contrast, ACX has narrow substrate specificity. Each ACX is responsible for catalysing oxidation of particular chain-length fatty acyl-CoA. In this case, four genes among the ACX family members are all significantly expressed (Eastmond et al., 2000a).

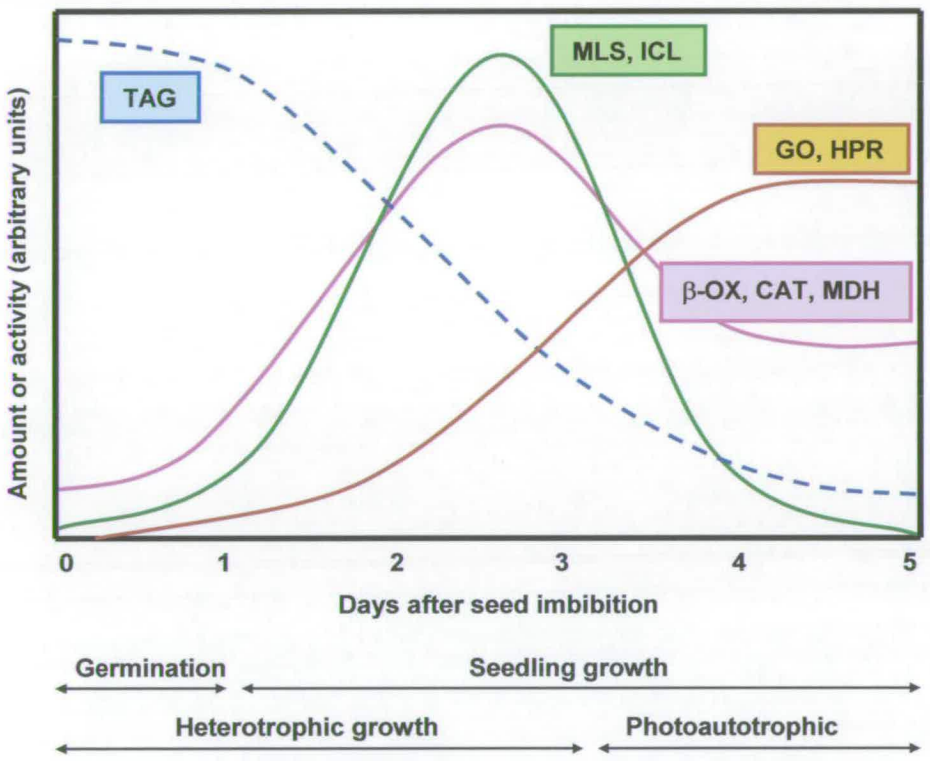

Figure 1.4 Schematic representation of developmental changes in TAG and peroxisomal enzymes in cucumber cotyledons during germination and seedling growth in the light. TAG, triacylglycerols; β-ox, enzymes of fatty acid β-oxidation; ICL, isocitrate lyase; MLS, malate synthase; GO, glycolate oxidase; HPR, hydroxyl pyruvate reductase; CAT, catalase; MDH, malate dehydrogenase (Cornah and Smith, 2002).

Rylott et al. (2001) demonstrated that in Arabidopsis, genes involved in β-oxidation, glyoxylate cycle and gluconeogenesis all display a similar pattern of expression which shows a greatly increased level up to a peak at day 2 followed by a decline, which suggests the possibility of common regulation mechanism. However, both mRNA and enzyme activity of the glyoxylate cycle enzymes, ICL and MS, are undetectable in Arabidopsis seedlings after day 3. By contrast, the β-oxidation and gluconeogenesis genes still remain active after this stage. Furthermore this characteristic is still found in a wide range of mature plant tissues including leaves, roots, bolts, inflorescence and siliques (Eastmond et al., 2000a; Eastmond and Graham, 2000; Froman et al., 2000), whereas expression of glyoxylate cycle genes is not detected. This indicates an additional role for β-oxidation and gluconeogenesis, in Arabidopsis at least, compared to the glyoxylate cycle, whose primary role is that of lipid mobilisation during germination and seedling growth.

The mechanism for co-ordinate transcriptional control of these genes during germination and seedling growth is unknown. In most plants, abscisic acid (ABA) has a role to inhibit, while gibberellic acid (GA) has a role to promote germination. In cereals ABA and GA play a direct role in the regulation of genes involved in mobilisation of carbohydrate and protein reserves (Ritchie and Gilroy, 1998; Lovegrove and Hooley, 2000). It is possible that lipid mobilisation in Arabidopsis is influenced by GA and ABA. As shown by a previous study, GA is required for an induction of *PEPCK1* and *ICL* in both embryo and endosperm, and ABA inhibits this induction in the embryo (Penfield et al., 2004).

When the leaf begins to senesce, β-oxidation genes show an increase of mRNA level (Eastmond et al., 2000a; Eastmond and Graham, 2000; Froman et al., 2000). In addition, glyoxylate cycle genes, *ICL* and *MLS* are also found to be induced in barley, cucumber, and tobacco during senescence (Gut and Matile, 1988; Graham et al., 1992; Mclaughlin and Smith, 1994). It is possible that senescence-induced lipase plays a central role in the control of senescence enhanced gene expression. Probably it is due to de-esterification of membrane lipids resulting in loss of membrane integrity that could generate the signals for the induction of genes involved in lipid metabolism (Hong et al., 2000; Graham and Eastmond, 2002).

Carbohydrate starvation in maize root tip results in an increase of overall β-oxidation activity (Dieuaide et al., 1992). Previous studies showed that MLS and ICL are induced during carbohydrate starvation and repressed by high sugars in a variety of tissues and cell types (Graham et al., 1994a; Graham et al., 1994b; Ismail et al., 1997). Seedlings grown on media supplemented with 29 mM sucrose have reduced cotyledonary lipid breakdown (Eastmond et al., 2000b) and it is completely blocked in seedlings grown on media in the presence of low (0.1 mM) nitrogen and 100 mM sucrose (Martin et al., 2002). It is possible that the feedback control of lipid mobilisation can be achieved at the post-transcriptional or post-translational level by inhibition of key enzyme or protein function.

1.5 Plant peroxisomes and their functions

Found in eukaryotes, peroxisomes are single membrane-bound organelles which, viewed best by transmission electron microscopy, are 0.5 to 1.5 μm in diameter. Unlike mitochondria and chloroplasts, peroxisomes are devoid of DNA. Peroxisomal proteins are therefore all nuclear encoded. An important function of the peroxisome is to detoxify the cell by degrading H_2O_2. This can be achieved by the enzyme, catalase, that coverts H_2O_2 into H_2O and O_2. Moreover these multipurpose organelles are responsible for a wide variety of essential metabolic pathways in eukaryotes including photorespiration, β-oxidation of fatty acid and synthesis of cholesterol or penicillin.

Plant peroxisomes have specific physiological functions depending on the type of tissue in which they are found, and on metabolic and developmental state of the organism (Johnson and Olsen, 2001). Peroxisomal membrane proteins known as porins provide permeability to small metabolites such as glycolate, glycerate and inorganic ions (Reumann, 2000). Plant peroxisomes can be classified into several classes, namely glyoxysomes, leaf peroxisomes and unspecialised peroxisomes (Beevers, 1979). Each is present at different stages in the life cycle and sequesters peroxisomal enzymes that are specific for the physiological roles of such organs. Leaves, roots, embryos and seedlings each possess different peroxisomes specialised to tissue specific functions. Leaf peroxisomes contain enzymes required for photorespiration. Young seedling peroxisomes possess the enzymes required for lipid conversion to succinate to supply energy to the seedlings until they become

photoautotrophic. Peroxisomes in a *Rhizobium*-infected cell in root nodules contain enzymes involved in nitrogen metabolism (Webb and Newcomb, 1987). During biotic and abiotic stress responses, the enzymes involved in jasmonic acid biosynthesis (Stintzi and Browse, 2000) and enzymes involved in the metabolism of reactive oxygen species (Corpas et al., 2001) are found in the peroxisomes.

In green leaves, peroxisomes are mainly involved in the metabolic recycling of 2-phosphoglycolate generated by the oxygenase activity of RubisCO during photorespiration. The pathway for metabolism of 2-phosphoglycolate involves the co-ordinated reactions of sixteen enzymes and at least six translocators distributed between chloroplasts, peroxisomes and mitochondria (Reumann, 2002; Figure 1.5). The peroxisomal enzymes that are involved in photorespiration include the glycolate oxidase (GOX), glutamate-glyoxylate aminotransferase (GGT), serine-glyoxylate aminotransferase (SGT), hydroxypyruvate reductase (HPR), malate dehydrogenase (MDH) and catalase (CAT). Catalase is involved in the detoxification of hydrogen peroxide formed as a result of glycolate oxidation. The membrane of plant peroxisomes contains porin-like channels that enable a broad range of small negatively charged metabolites to pass across the membrane by facilitated diffusion (Reumann, 2000). Photorespiration is inevitable due to the activity of RubisCO and is believed to prevent the plants from photooxidation and photoinhibition, especially under the high light intensity and low intracellular CO_2 concentration by dissipating excess ATP and NADPH generated from the light reaction (Kozaki and Takeba, 1996).

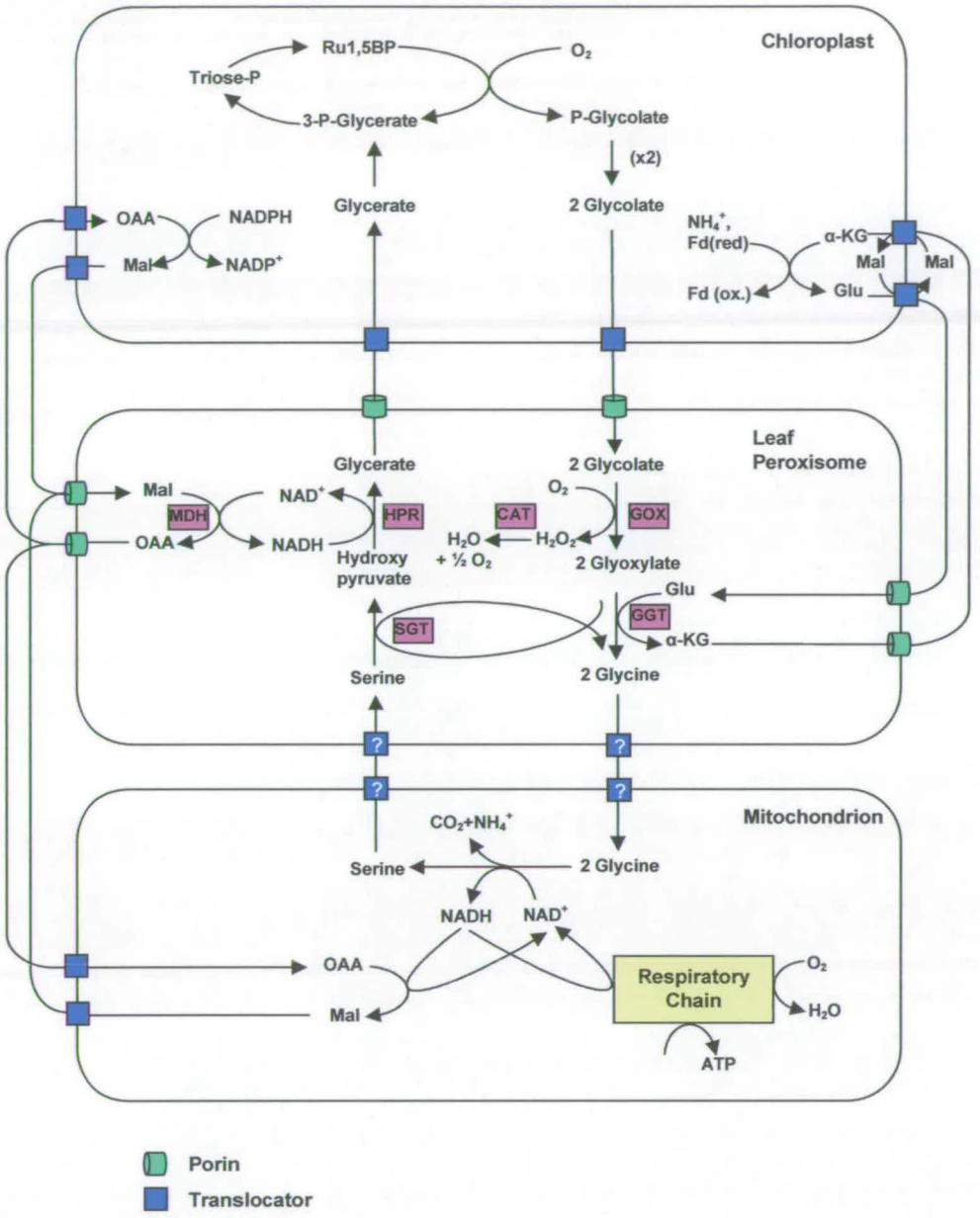

Figure 1.5 Reactions and transport of intermediates of the photorespiratory C2 cycle. GOX: glycolate oxidase, GGT: glutamate-glyoxylate aminotransferase, SGT: serine-glyoxylate aminotransferase, HPR: hydroxypyruvate reductase, MDH: malate dehydrogenase and CAT: catalase (Reumann, 2002).

The mechanism of peroxisome biogenesis in plants remains to be discovered. A model for peroxisome biogenesis has been proposed that the peroxisome is generated from a pre-peroxisomal vesicle which is derived from the endoplasmic reticulum (ER) (Johnson and Olsen, 2001; Mullen et al., 2001). However, there are several studies that are inconsistent with this hypothesis (Sacksteder and Gould, 2000). Another hypothesis proposes that peroxisomes are formed from a pre-peroxisomal vesicle called a 'protoperoxisome' (Purdue and Lazarow, 2001; Lazarow, 2003). The peroxisome formation process requires Pex3, Pex16 and Pex19. Pex19 is believed to facilitate insertion of Pex3, Pex16 and also other peroxisomal membrane proteins (PMPs) into the bilayer of the protoperoxisome (Lazarow, 2003). Next, this structure enables other matrix proteins to be imported and then the mature peroxisomes are developed. The peroxisomes are also able to multiply themselves by fission from the pre-existing peroxisomes (Mullen et al., 2001). There is a little known about how PMPs are assembled into the peroxisome membrane. It is proposed that some PMPs are inserted directly from the cytosol into the peroxisomal membrane (Johnson and Olsen, 2001). These PMPs are termed PMPs TypeII such as PMP22, PMP34, PMP47 and PMP70. Their functions are unknown and unlikely to be required for peroxisome biogenesis. Another group of PMPs which are referred to as Type I are believed to be targeted earlier to the ER or possibly a pre-peroxisomal vesicle before the peroxisome is formed. PMPs Type I are shown to be required for peroxisomal biogenesis, for instance, Pex2, Pex3, Pex15 and Pex16.

There is evidence for peroxisomes in dry seed but they increase in size during seedling development (Trelease, 1984). The question was raised how glyoxysomes

are replaced by leaf peroxisomes during plant growth. Previously, there were two hypotheses. In one the glyoxysomes are destroyed and replaced by new leaf peroxisomes (the two population hypothesis) (Kagawa and Beevers, 1975), while in the other glyoxysomes are re-pakaging and interconverted into leaf peroxisomes (the single population hypothesis) (Trelease et al., 1971). The latter hypothesis has been confirmed by the immunocytochemistry study of pumpkin peroxisomes (Nishimura et al., 1986). Hayashi et al. (2000b) further established that glyoxysomes are functionally transformed into leaf peroxisomes during greening and subsequently transformed back into glyoxysomes during senescence of the cotyledons. These transformations of structure and function depend upon nuclear genes, and transport of new proteins into the peroxisome.

1.6 Import of peroxisomal proteins

As mentioned previously, peroxisomes are devoid of DNA, thus peroxisomal proteins are nuclear encoded. As shown in table 1.1 the peroxisomal proteins contain one of the two peroxisome targeting signals (PTSs), each of which is necessary and sufficient to import protein from the cytosol into the peroxisomal matrix. PTS1 is the first identified PTS. This is a carboxyl terminal tripeptide which consists of prototype Ser-Lys-Leu (SKL) or related types of [C/A/S/P]-[K/R]-[I/L/M] (Hayashi et al., 1997), such as SRM, SRI, SKL and SKM. Even though such a short targeting motif, it is sufficient to import peroxisomal proteins and the majority of peroxisomal proteins carry a PTS1 signal.

The second type termed PTS2 is found within the first 30 amino acid at the amino terminus. The PTS2 is comprised of the nonapeptide motif which is R-$(X)_6$-H/Q-A/L/F (Kato et al., 1996, 1998; Mullen, 2002). The subtype R-$(X)_6$-HL is highly common among PTS2-containing proteins. Unlike PTS1, the PTS2 signal is cleaved after import into the peroxisomal matrix. Downstream of a PTS2 sequence is a conserved cysteine residue which is believed to be essential for proteolytic processing of PTS2-containing proteins in peroxisomes (Kato et al., 1998).

The mechanism for the import of proteins through the peroxisomal membrane remains to be established. Recently, peroxisomal protein import through the machinery (a docking complex) at the peroxisomal membrane was proposed (Figure 1.6). It is proposed that after translation, proteins containing PTS1 or PTS2 may form oligomeric structures (Kato et al., 1999) and then combine with their cytosolic receptors. Pex5p is a cytosolic receptor for PTS1 proteins (Brickner et al., 1998), and Pex7p for PTS2 proteins (Schumann et al., 1999). In yeast *Saccharomyces cerevisiae*, Pex18p and Pex21p are further required for import of PTS2 proteins (Purdue and Lazarow, 2001); on the other hand, in the yeast *Yarrowia lipolytica* Pex20p is required instead of Pex18p and Pex21p (Einwachter et al, 2001). In mammals, there are two forms of Pex5p, a short form (Pex5pS) and a long form (Pex5pL). Only Pex5pL can bind to Pex7p forming a Pex5pL-Pex7p complex, which is required for PTS2 protein import (Matsumura et al., 2000). It is believed that Pex18p/Pex21p, Pex20p and Pex5pL are responsible for similar functions required by the PTS2 pathway (Brown and Baker, 2003). Since Arabidopsis Pex5p is the homologue of

Table 1.1 Typical plant peroxisomal proteins with the indicated physiological functions and targeting signals

Protein	Function	Plant (Reference)	Sequence (Putative signal in Bold)
PTS1 proteins[a]			
Ala:glyoxylate aminotransferase1	Photorespiration	Arabidopsis (Liepman and Olsen, 2001)	HHIPLIP**SRI**
Catalase	Peroxide metabolism	Cottonseed (Mullen et al., 1997)	ASRLNVR**PSI**
Isocitrate lyase	Glyoxylate cycle	*Brassica napus* (Comai et al.,1989)	TSLVVAK**SRM**
Isocitrate lyase	Glyoxylate cycle	Castor bean (Beeching and Northcote, 1987)	GSEVVAK**ARM**
Glycolate oxidase	Photorespiration	Spinach (Volokita and Somerville, 1987)	GPSSRAV**ARL**
12-Oxophytodienoic acid reductase	Jasmonate biosynthesis	Arabidopsis (Stintzi and Browse, 2000)	YPFLAPS**SRL**
Uricase (nodulin-35)	Purine metabolism	Soybean (Suzuki and Verma, 1991)	ASLSRLW**SKL**
PTS2 proteins[b]			
Citrate synthase	Glyoxylate cycle	Pumpkin (Kato et al., 1995)	X15 - **RLAVLAAHL**SAASLE
Malate dehydrogenase	Glyoxylate cycle	Watermelon (Gietl, 1990)	X9 - **RIARISAHL**HPPKSQ
Thiolase	Fatty acid β-oxidation	Arabidopsis (Hayashi et al., 1998)	X6 - **RQRVLLEHL**RPSSSS

[a]PTS1 at extreme carboxyl terminus of protein

[b]PTS2 in amino terminal portion of protein

X_n indicates the number of residues between the amino terminus of the protein and the signal

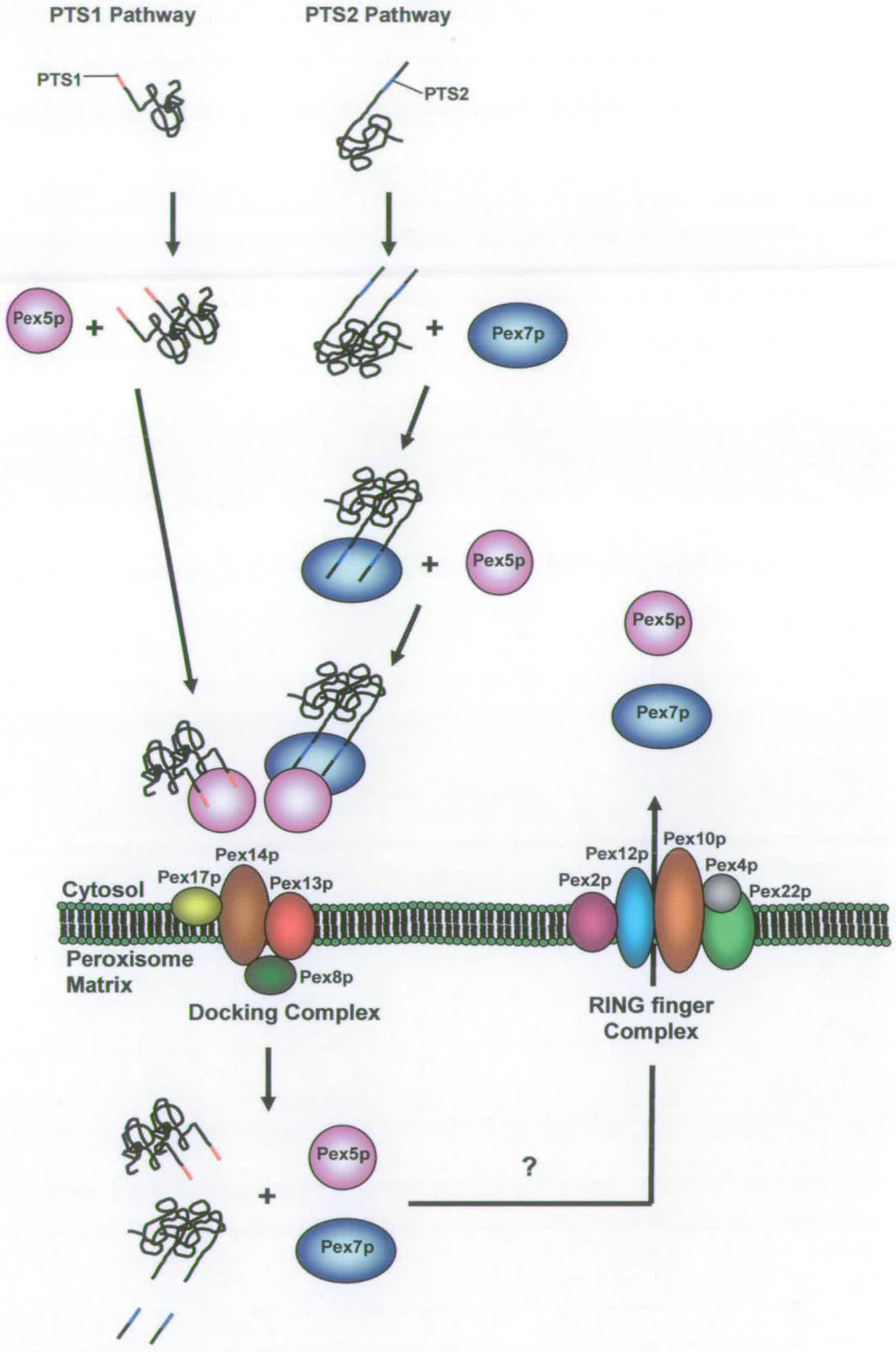

Figure 1.6 The mechanism for the import of PTS1- and PTS2- containing proteins through the peroxisomal membrane.

Pex5pL in mammals, PTS1 and PTS2 import pathways may be similar in plants and mammals.

The docking complex includes three peroxins, Pex13p, Pex14p and Pex17p (Brown and Baker, 2003). Pex17p is a peripheral peroxisomal membrane protein which is believed to form part of the complex by reacting with Pex14p to form a tight core complex. Pex13p is an integral peroxisomal membrane protein and a study in yeast proposed that Pex13p is able to bind with Pex7p with its amino-terminus and Pex5p with its carboxy-terminus (Pires et al., 2003). Pex14p is an intrinsic peroxisomal membrane protein involved in binding to Pex5p. In Arabidopsis PTS1 binds to the tetratricopeptide repeat (TPR) in Pex5p, whereas PTS2 first binds to the WD40 repeat in Pex7p which then bind to Pex5p (Hayashi and Nishimura, 2003). The two amino-terminal domains of Pex14p (i.e. ^{58}I- ^{65}L and ^{78}R-^{97}R) capture the receptor-cargo complexes by binding to WXXXF/Y repeats that exist in the middle of Pex5p (Nito et al., 2002). Pex5p and Pex14p mediate the import both PTS1- and PTS2-containing proteins through the docking complex. Pex8p is believed to be required for the matrix protein import machinery (Brown and Baker, 2003).

After docking, the cytosolic receptor might release its cargo into the peroxisomal matrix and may remain itself in the cytosol. However, cytosolic receptors are shown to be localised to the cytosol, peroxisomal membrane and peroxisomal matrix (Olsen, 1998). It is possible that the receptor binding with its cargo is able to pass through translocation machinery into peroxisomal matrix. The receptors might recycle back to the cytosol possibly via the RING finger complex, which consists of Pex2p,

Pex10p and Pex12p, with two of them (Pex10p and Pex12p) able to bind with Pex5p (Brown and Baker, 2003). It is also thought that Pex22p and Pex4p are involved in the recycling of Pex5p (Brown and Baker, 2003).

It is possible that there are other peroxins involved in the import of peroxisomal proteins that remain to be discovered. In plants there are numerous peroxins and peroxin homologues whose functions remain to be established.

1.7 Re-examination of lipid mobilisation in plants

1.7.1 Fate of acetyl-CoA derived from β-oxidation

As mentioned previously, acetyl-CoA derived from β-oxidation of triacylglycerols during germination is used to support growth during early seedling development. This process is achieved by the glyoxylate cycle which condenses two molecules of acetyl-CoA into one molecule of succinate. In castor bean, the lipid reserve is stored in endosperm which senesces after germination. Therefore substrate demand for respiration within this tissue is negligible. The majority of lipids are converted into sucrose and transported to the growing tissues of the seedling. In many oilseeds like Arabidopsis, sunflower and cucumber, the lipid reserve is stored in the cotyledons of the embryo. As these cotyledons subsequently differentiate from storage organs into photosynthetic tissue, a high substrate demand for respiration is required. Thus, in these oilseeds, much acetyl-CoA is likely to be respired using the TCA cycle within the cotyledon itself rather than being processed for intercellular transport via the glyoxylate cycle and gluconeogenesis.

There is evidence that lipids are respired in some plants. The respiration of TAGs in sunflower (*Helianthus annuus*) (Salon et al., 1988) and lettuce (*Lactuca sativa*) (Raymond et al., 1992) have been shown by feeding seedlings with [^{14}C]-fatty acids or [^{14}C]-fatty acyl-CoA. It is found that the radioactivity is incorporated into the intermediates of TCA cycle but not in glyoxylate. Furthermore at this stage (early germination), MS and ICL, the key enzymes in the glyoxylate cycle are not detected. These results establish that storage lipids can be respired in some plants. A recent study using an Arabidopsis *icl* mutant in which the glyoxylate cycle is disrupted showed that the glyoxylate cycle is not necessary for germination and seedling establishment (Eastmond et al., 2000b). In *icl* seedlings, sucrose, which is normally derived from glyoxylate cycle and then gluconeogenesis, is highly reduced. However the stored lipids disappear and most is metabolised to CO_2. This implies that in *icl* seedlings the lipids are still utilised by respiration.

The question raised is how, in the absence of the glyoxylate cycle, carbon produced from β-oxidation is exported from the peroxisome to the mitochondrion. Eastmond and Graham (2001) have proposed two possible ideas as outlined here.

One is based on data from *Saccharomyces cerevisiae* (van Roermund et al., 1995; 1999) which claimed that there is a pathway to transport acetyl units from the peroxisome to the mitochondrion (Figure 1.7A). In yeast mutants lacking the glyoxylate cycle, disruption of the peroxisomal citrate synthase gene, indicated the presence of an alternative pathway, the 'acetylcarnitine shuttle', for the transport of acetyl units from peroxisome to mitochondrion. In the peroxisome, this pathway

produces acetylcarnitine in which acetyl-CoA and carnitine are substrates for carnitine acetyl-CoA transferase (CAT). The product, acetylcarnitine, is then exported to the mitochondria, where acetyl-CoA is reformed and enters the TCA cycle and carnitine transports back to peroxisome. In yeast a single gene encodes both peroxisomal and mitochondrial CAT (Elgersma et al., 1995). A carnitine acetylcarnitine carier (CAC) located at the mitochondrial membrane is responsible for import of acetylcarnitine from the cytosol into mitochondria (van Roermund et al., 1999). However, the precise mechanism of the acetylcanitine pathway in yeast remains to be established. There is no evidence to suggest that this pathway exists in plants and there are no gene candidates revealed with similar identity to the sequence of yeast *CAT* gene.

Recently, Arabidopsis mutant seedlings, in which an acylcarnitine carrier homologue 'BOU' is disrupted, showed a slow rate of TAGs breakdown and a block in the transition from seed to seedling (Lawand et al., 2002). It was proposed that BOU plays a role in transferring carbon skeletons derived from β-oxidation from peroxisomes into mitochondria. However, BOU is required only in the light but not in the dark, so it not consistent with the role in TAGs breakdown during germination because β-oxidation and the glyoxylate cycle are working both in the light and the dark. The *bou* mutant is impaired in the synthesis of polar lipids, indicating a role in membrane biogenesis in the light.

The second proposal is based on data obtained from the sunflower (*Helianthus annuus*) (Salon et al., 1988) and lettuce (*Lactuca sativa*) (Raymond et al., 1992)

(Figure 1.7B). These studies used particulate fractions prepared from germinating seeds to investigate the incorporation of [^{14}C]-fatty acids or [^{14}C]-fatty acyl-CoA into other substrates. The radioactivity was recovered in citrate and intermediates in the TCA cycle. No radioactivity was found in glyoxylate. This indicates that acetyl-CoA is condensed into citrate by peroxisomal citrate synthase (peroxisomal CSY) even in the absence of the glyoxylate cycle. It was proposed that citrate formed from acetyl-CoA produced by β-oxidation of fatty acids is metabolised by the TCA cycle in mitochondria. On the other hand, inhibition of peroxisomal CSY by (5,5'-dithiobis)2-nitrobenzoic acid (DTNB), an inhibitor for peroxisomal CSY but not mitochondrial CSY, leads to a significant accumulation of acetyl-CoA. This suggests that peroxisomal CSY is involved in the metabolism of acetyl-CoA produced from β-oxidation. These studies concluded that citrate and oxaloacetate might shuttle between the peroxisomes and mitochondria so that the TCA cycle can operate between these two organelles. Consistent with this proposal is the recent observation that aconitase is not the peroxisomal enzyme (Courtois-Verniquet and Douce, 1993; De Bellis et al., 1994; Hayashi et al., 1995). Therefore citrate is usually exported from peroxisome to cytosol to operate the glyoxylate cycle.

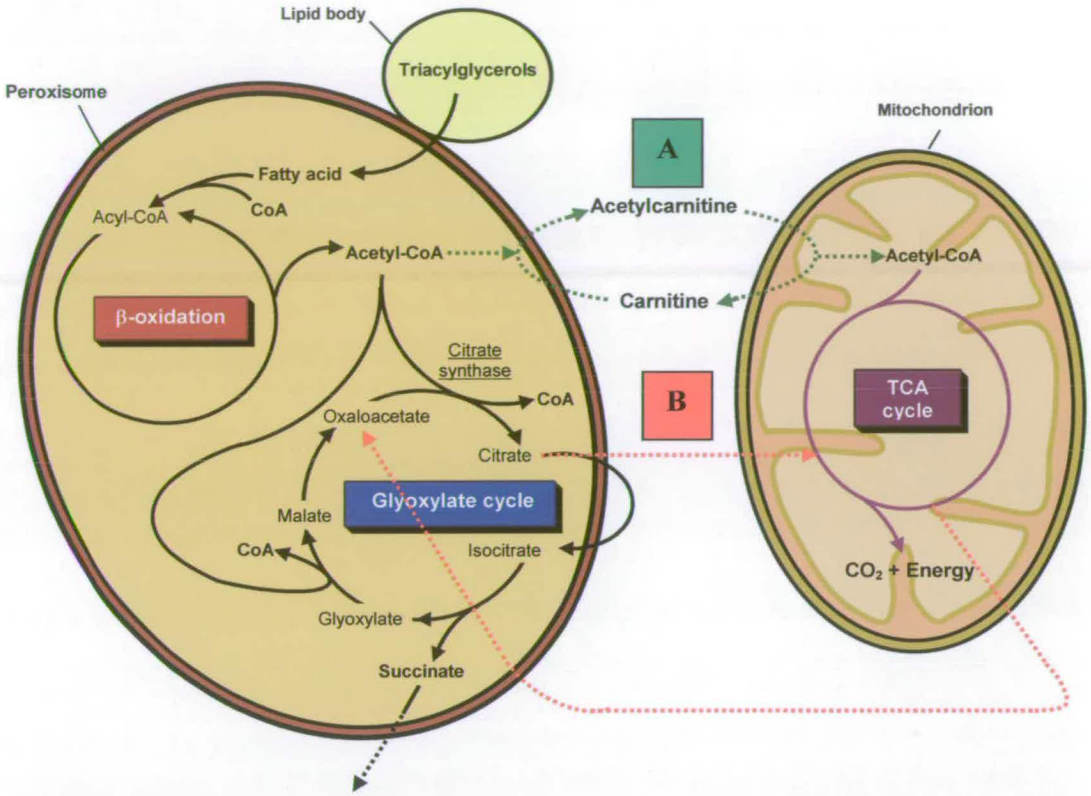

Figure 1.7 Two possible routes by with carbon from acetyl-CoA in peroxisomes might be made available for respiration; **(A)** is based on data from yeast, **(B)** is based on data from sun flower and lettuce.

1.7.2 Re-oxidation of reducing equivalents

In peroxisomal lipid catabolism through the β-oxidation spiral and glyoxylate cycle, reduced cofactors are produced (two $FADH_2$ and three NADH appear for each exported succinate). They must be reoxidised so that the pathway is able to continue to work. As mentioned previously, $FADH_2$ produced by acyl-CoA oxidase, is directly oxidised by transfer to molecular oxygen. However, it is still unclear how NADH (produced by hydroxyacyl-CoA dehydrogenase in β-oxidation and malate dehydrogenase in the glyoxylate cycle) becomes reoxidised. The peroxisomal

membrane appears to be impermeable to NAD^+ and NADH as shown in castor bean peroxisomes (Cooper and Beevers, 1969b; Donalson, 1982). In addition, a report showed that the yeast peroxisomal membrane is impermeable to NAD^+ and NADH *in vivo* (Van Roermund et al., 1995). Thus the NAD^+ and NADH are unlikely to be exported to another cellular compartment for reoxidation, for example the mitochondrial membrane where the electron transport chain system is located. Escher and Widmer (1997) have discussed two possible ideas for the reoxidation of NADH, which are as follows.

(i) NADH-driven electron transport

This idea was proposed after the discovery of an NADH dehydrogenase associated with the peroxisomal membrane. This is believed to be a flavoprotein that can transfer electrons from reducing equivalent to ferricyanide and cytochrome c *in vitro* (Hicks and Donaldson, 1982; Donaldson and Fang, 1987; Luster and Donaldson, 1987). These might be responsible for a short-chain electron transfer system which transports electrons from the peroxisomal matrix to the cytosol. The cytosolic electron acceptor is still unknown but dehydroascorbate has been proposed (Bowditch and Donaldson, 1990).

Recently, the peroxisomal membranes from pea leaves and potato tubers have been shown to transport electron *in vitro* using oxygen or oxidised ascorbate to accept electrons from the membrane dehydrogenases (Lopez-Huertas et al., 1999; Struglics et al., 1993). Furthermore integral membrane protein PMP18 (cyt b_5 homologue), PMP32 and PMP29 have been discovered in pea leaf peroxisomes and shown to

catalyse NADH-dependent production of superoxide ($O_2^{-\bullet}$) during electron transfer to O_2 *in vitro* (Lopez-Huertas et al., 1997; 1999). Besides evidence from such experiments *in vitro*, currently there is insufficient evidence to establish that this proposed mechanism is responsible for NADH reoxidation in plant peroxisomes.

(ii) Transferring redox equivalents to another cellular compartment via appropriate shuttle

This hypothesis was proposed by Mettler and Beevers (1980). It states that by using a malate-aspartate shuttle, reducing equivalents are exported as malate which is reoxidised into oxaloacetate in the cytosol or mitochondrial matrix (Figure 1.8). The oxaloacetate returns to the peroxisome after conversion to aspartate, which is reconverted subsequently into oxaloacetate. In order to balance carbon and nitrogen, an oxoglutarate-glutamate exchange also occurs. In this scheme, peroxisomal malate dehydrogenase (PMDH) performs oxaloacetate reduction in the β-oxidation step, which consumes NADH and generates malate (Figure 1.9B), rather than malate oxidation in the glyoxylate cycle as previously assumed (Figure 1.9A). The direction of the reaction catalysed by PMDH will depend on the balance of the reactants under physiological conditions. The oxidation of malate by PMDH in peroxisomes is unfavourable since a high ratio of NADH/NAD^+ is generated by peroxisomal β-oxidation (Esher and Widmer, 1997).

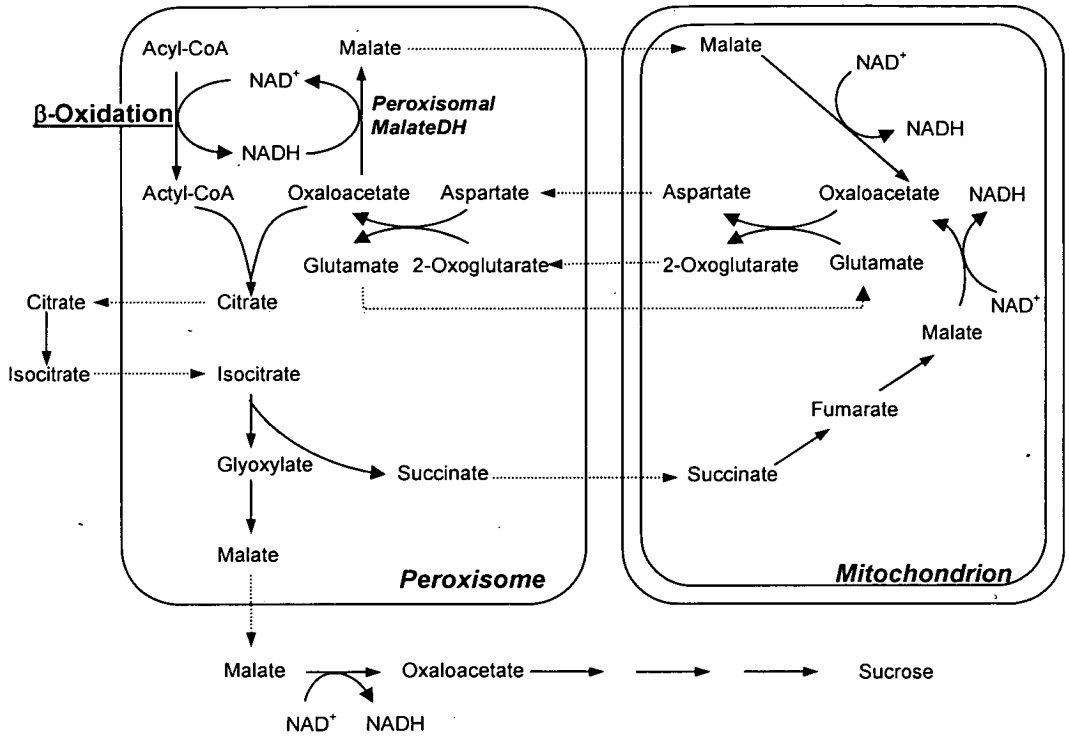

Figure 1.8 Reoxidation of NADH via a malate-aspartate shuttle, proposed by Mettler and Beevers, (1980)

Figure 1.9 (Next page) Hypothesis that peroxisomal malate dehydrogenase does not oxidise malate to provide oxaloacetate for the glyoxylate cycle **(A)**, but serves to oxidise NADH produced by β-oxidation **(B)**.

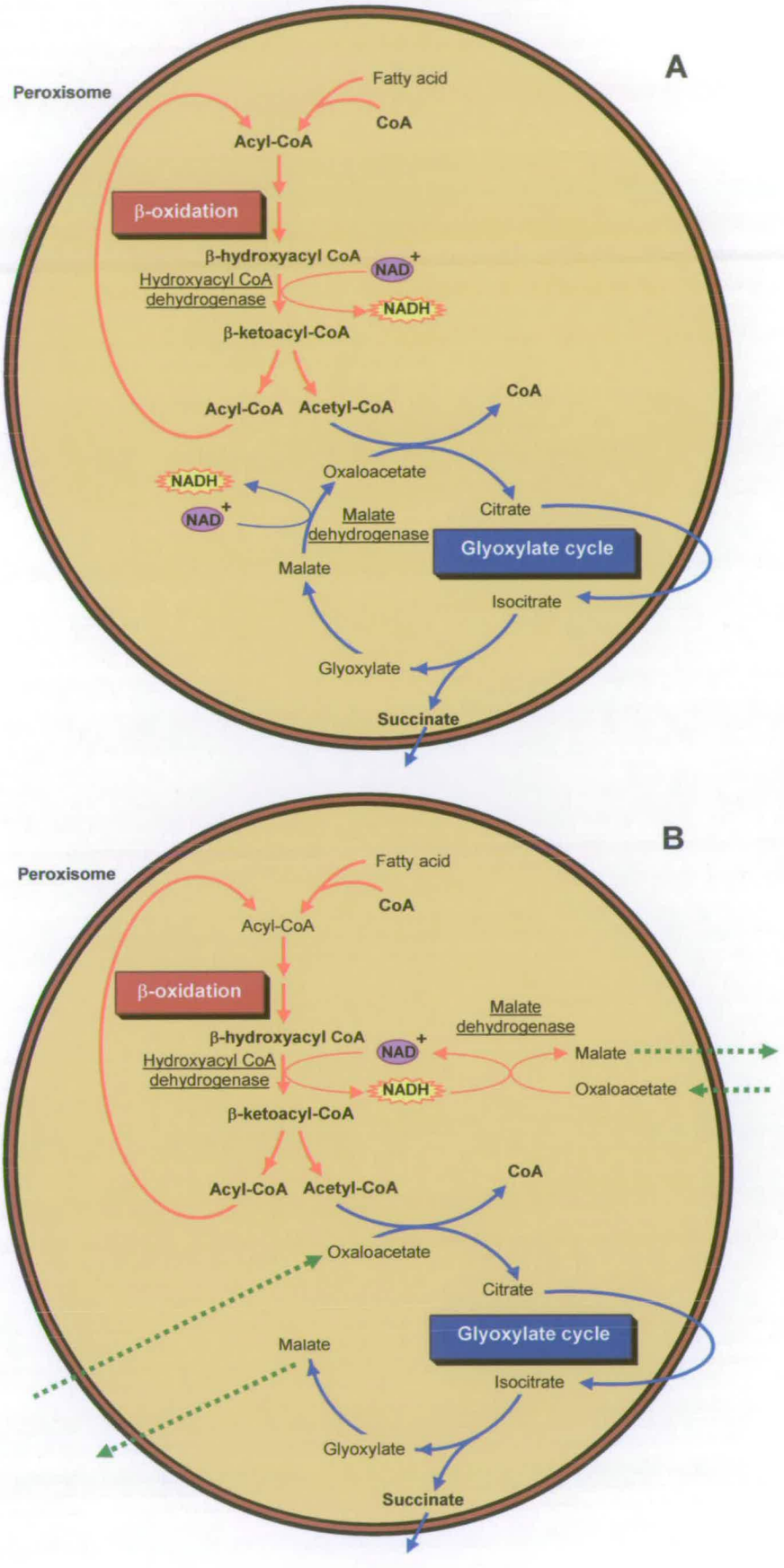
A
Peroxisome
Fatty acid
CoA
Acyl-CoA
β-oxidation
β-hydroxyacyl CoA
NAD+
Hydroxyacyl CoA dehydrogenase
NADH
β-ketoacyl-CoA
Acyl-CoA
Acetyl-CoA
CoA
Oxaloacetate
NADH
NAD+
Malate dehydrogenase
Citrate
Glyoxylate cycle
Malate
Isocitrate
Glyoxylate
Succinate
B
Peroxisome
Fatty acid
CoA
Acyl-CoA
β-oxidation
Malate dehydrogenase
β-hydroxyacyl CoA
NAD+
Malate
Hydroxyacyl CoA dehydrogenase
NADH
Oxaloacetate
β-ketoacyl-CoA
Acyl-CoA
Acetyl-CoA
CoA
Oxaloacetate
Citrate
Glyoxylate cycle
Malate
Isocitrate
Glyoxylate
Succinate

There is supporting evidence about the role of PMDH in *Saccharomyces cerevisiae* (van Roermund et al., 1995). It is suggested that PMDH is involved in the reoxidation of NADH generated during β-oxidation. Knockout mutants with disruption of the *PMDH* gene resulted in blocking β-oxidation *in vivo*. As a result of the failure to reoxidise NADH, hydroxyacyl-CoA, which is normally oxidised by hydroxyacyl-CoA dehydrogenase together with co-factor NAD^+, is accumulated. In these mutants, β-oxidation activity can be recovered in a cell lysate (*in vitro*), as NADH can be reoxidised when the peroxisomal membrane is disrupted.

1.8 Reverse genetic approach to investigate gene function

1.8.1 Reverse genetic approach

A forward genetic approach begins with a mutant phenotype followed by determining what gene is causing the altered phenotype. On the other hand, the reverse genetic approach begins with a mutated gene sequence and subsequently looks for the resulting phenotype. A mutation in a gene can be induced in several ways, but insertion mutagenesis is particularly powerful. The resulting gene knockouts or null mutants provide the possibility to establish gene function (Krysan et al., 1996; Krysan et al., 1999).

The principle of this reverse genetic technique is based on the assumption that insertion mutagenesis by T-DNA (by *Agrobacterium tumefaciens*) or transposons occurs at random sites within the plant genome. Among a sufficiently large population, it is assumed that at least one plant exists in which the gene of interest is

disrupted (Krysan et al., 1999; Thorneycroft et al., 2001). The foreign DNA is not only used to disrupt the expression of the gene into which it is inserted, but also used as the marker to identify gene mutation. The screening of the transgenic population to find the desired mutants is performed by PCR (Krysan et al., 1996), using combinations of gene-specific and T-DNA (or transposon) primers (Thorneycroft et al., 2001). The resulting PCR fragment known as a 'junction fragment' indicates a positive plant in which an insert has disrupted the target gene. To confirm that these plants are knockout mutants, southern blotting and gene sequencing are employed. Subsequently, northern blotting or RT-PCR is used to reveal the absence of transcripts. A more recent approach has been the systematic sequencing of junction fragments in individual plants from a large population. Such sequence information can then be screened for insertions in target genes. This approach has reached the point of a web-based publicly accessible resource (Sessions et al, 2003; Alonso et al., 2003; Rosso et al. 2003; Strizhov et al., 2003; Li et al., 2003)

1.8.2 Arabidopsis as an experimental system

Arabidopsis thaliana, a small flowering annual dicotyledonous plant, was discovered by Johannes Thal in the sixteenth century. It was first reported in 1943 by Freidrich Laibach that Arabidopsis is potentially a model organism for genetic studies (Laibach, 1943). The suitability of Arabidopsis as a model for genetic and developmental biological research has been summarised (Sommerville and Koornneef, 2002). For example, it produces a large number of progeny and develops rapidly. It is easy to grow in a limited space. It produces fertile hybrids and has a relatively low chromosome number and DNA content.

Arabidopsis is a member of Brassicaceae family, as well as rapeseed, lettuce and cabbage. Although a weed, Arabidopsis has no agronomic significance, but offers advantages in genetics and molecular biology research. It has a rapid life cycle (about 8 weeks from germination to mature seed) and one of the smallest genomes (5 chromosomes and 125 Mb DNA) among plant species. Recently the Arabidopsis genome project has determined the complete genome sequence, to be used as a reference database for plant genomics. Importantly, Arabidopsis is able to be efficiently transformed by *Agrobacterium tumefaciens* that contains a gene of interest in a Ti-plasmid (Bechtold et al., 1993). In this aspect, it has made it possible to create insertion mutants with random integration of T-DNA inserts into the plant genome. Recently, the availability and accessibility of Arabidopsis mutant database resources have provided a large collection of knockout mutants disrupted in the majority of genes (Sessions et al, 2003; Alonso et al., 2003, Rosso et al., 2003, Strizhov et al., 2003, Li et al., 2003). A lot of aspects on plant growth and development have been established by characterisation of mutants in which such genes are disrupted. These have led to more understanding of fundamental aspects of plant metabolism.

1.9 Arabidopsis mutants with defects in lipid metabolism

In the last few years, many mutants related to peroxisome function have been characterised. Mutations that cause defects in β-oxidation reveal a significant effect on Arabidopsis seed germination and seedling growth (Table 1.2). For example, Arabidopsis *cts*, *pxa1* and *ped3* in which an ATP-binding cassette (ABC) transporter is disrupted revealed a severe defect in β-oxidation (Russell et al., 2000; Zolman et

al., 2001; Footitt et al., 2002; Hayashi at al., 2002). This ABC transporter is proposed to be required for import of fatty acids into peroxisomes. The *cts* seeds are unable to germinate even when exogenous sucrose is supplied. Germination can be achieved by removing the seed coat and providing sucrose but the mutant seedlings are still unable to catabolise their TAGs. Propionic acid and butyric acid can rescue the germination phenotype as these short-chain fatty acids are believed not to require the ABC transporters for fatty acid transport through peroxisomal membrane (Footitt et al., 2002). A defect in β-oxidation activity in *cts* seedlings is apparently revealed by the insensitivity to pro-herbicide 2,4-dichlorophenoxybutyric acid (2,4-DB). In contrast, wild type seedlings showed a sensitive response to 2,4-DB as β-oxidation converts 2,4-DB into 2,4-dichlorophenoxyacetic acid (2,4-D), which results in inhibition of root growth (Wain and Wightman, 1954; Figure 1.10).

There are nine long-chain acyl-CoA synthetase (LACS) isozymes in Arabidopsis (Hooks et al., 1999; Shockey et al., 2002). Knocking out two genes which belong to the *LACS* gene family leads to abnormal seedling establishment in Arabidopsis. The *lacs6:lacs7* mutants are able to germinate but fail to establish as seedlings unless exogenous sucrose is supplied (Fulda et al., 2004). The mutants are unable to metabolise their TAGs. Since LACS is specific to long-chain fatty acids, *lacs6:lacs7* seedlings are still able to convert 2,4-DB to 2,4-D.

Table 1.2 Mutants with the disruption of genes involved in lipid catabolism.

Mutant	Defective protein	Phenotype	Evidence revealing defect in lipid catabolism in seedlings	Reference
cts	ABC transporter (Comatose)	Seed dormancy	1. Fail to breakdown TAGs 2. LB persist [d] 3. 2,4-DB insensitive	Russell et al., 2000; Zolman et al., 2001; Footitt et al., 2002; Hayashi at al., 2002
lacs6:lacs7	Long-chain acyl-CoA synthetase	Fail to establish seedling[a]	1. Fail to breakdown TAGs[b] 2. LB persist [bd]	Fulda et al., 2004
acx3:acx4	Acyl-CoA oxidase	Embryo lethal	1. Fail to breakdown TAGs[bc] 2. 2,4-DB insensitive[c]	Rylott et al., 2003b
aim1	Multifunctional protein	Abnormal inflorescence	1. 2,4-DB insensitive	Richmond and Bleecker, 1999
kat2	3-ketoacyl thiolase	Fail to establish seedling[a]	1. Fail to breakdown TAGs 2. LB persist[d] 3. 2,4-DB insensitive	Hayashi et al., 1998; Germain et al., 2001
icl	Isocitrate lyase	Impaired seedling growth[a]	None	Eastmond et al., 2000b
mls	Malate synthase	Impaired seedling growth[a]	None	Cornah et al., 2004

[a]In the absence of sucrose

[b]Partial effect

[c]Tested on *acx2* and *acx4* single mutant as the *acx3:acx4* is embryo lethal

[d]Observed in cotyledons from 5 day-old seedlings

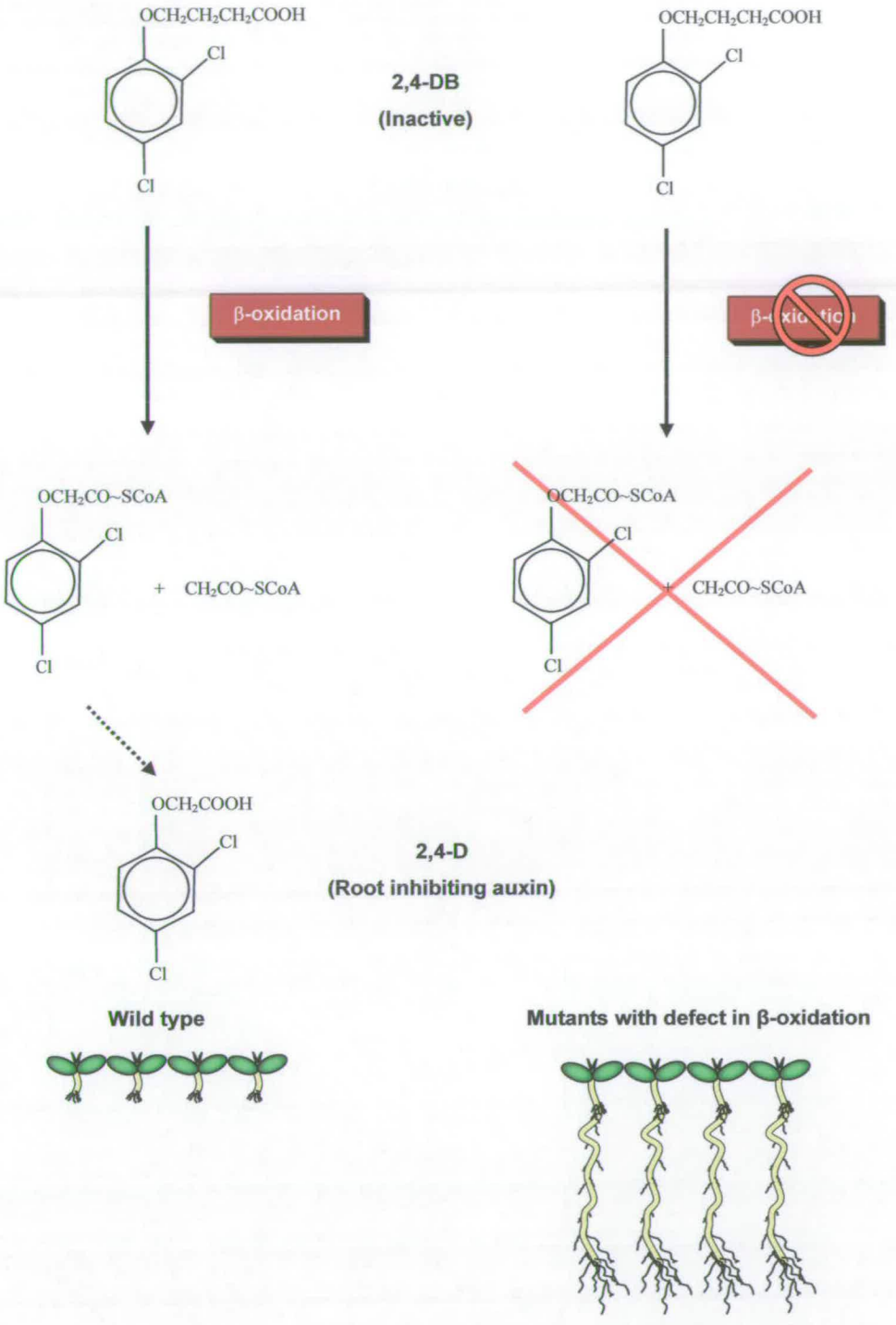

Figure 1.10 Conversion of 2,4-dichlorophenoxybutyric acid (2,4-DB) to 2,4-dichlorophenoxyacetic acid (2,4-D) via β-oxidation. Mutants with a defect in β-oxidation are insensitive to 2,4-DB.

There are at least four acyl-CoA oxidase (ACX) isozymes, two of which have been evaluated for their role in Arabidopsis seedlings (Eastmond, 2000a). The lipid utilisation, seedling growth and establishment are normal in single mutants *acx3* and *acx4*, in which one ACX gene is disrupted. However each single mutant is partially insensitive to 2,4-DB, suggesting that β-oxidation is deficient. Also, there is an accumulation of short-chain fatty acyl-CoA in *acx4* and an accumulation of medium chain fatty acyl-CoA in *acx3* (Rylott et al., 2003b). Crucially, the double mutant *acx3:acx4* is embryo lethal. This indicates that β-oxidation is essential for seed development.

The Arabidopsis mutant (*aim1*) in which one of the two multifunctional proteins (MFP) is mutated showed an abnormal inflorescence meristem (AIM) phenotype (Richmond and Bleecker, 1999). Mutant seedlings showed a sensitivity to 2,4-DB, indicating that β-oxidation is inefficient. This mutant established that β-oxidation is required for inflorescence and floral development.

The *KAT2* gene is the major expressed gene among the 3-ketoacyl-CoA thiolase (KAT) family. Seeds of Arabidopsis knockout mutant *kat2* or *ped1* are able to germinate but unable to establish as seedlings (Hayashi et al., 1998; Germain et al., 2001). Seedling establishment can be rescued by supplying exogenous sucrose. These mutants do not metabolise their TAGs and are insensitive to 2,4-DB, indicating that β-oxidation is defective.

Unlike those mutants previously mentioned, the Arabidopsis *icl* mutant seedlings in which the glyoxylate cycle is disrupted are able to catabolise their TAGs (Table 1.2). Without supplying exogenous sucrose, the germination and seedling growth can be achieved normally even if the growth phenotype is slightly impaired, compared to wild type (Eastmond et al., 2000b). It is concluded that the glyoxylate cycle is not essential for germination and, in *icl* mutants, isocitrate may be transported to be respired in the TCA cycle. Recently, another Arabidopsis glyoxylate cycle mutant, *mls*, has been characterised (Cornah et al., 2004). The results reveal that *msl* has a milder phenotype when compared to *icl*. It is suggested that in the *mls* mutant, the glyoxylate may be converted into sugar by using the photorespiratory pathway.

1.10 Aims of the project

What still remains to be investigated about peroxisome functions includes the following. The first is to establish how acetyl-CoA produced from β-oxidation is transferred to mitochondria during germination and seedling growth in Arabidopsis. The question is whether it is based on a mechanism similar to that found in yeast in which acetyl-CoA could be transferred using an acetyl-carnitine shuttle or is based on the proposed mechanism from studies in sunflower and lettuce. Importantly, Arabidopsis knockout mutants in which peroxisomal citrate synthase (peroxisomal CSY) genes are disrupted can test these hypothesises. If Arabidopsis obligately uses the latter mechanism, peroxisomal CSY will be critical. Mutants will therefore display a severe phenotype on germination and seedling growth. Furthermore, characterisation of this mutant will lead to an understanding of the roles and

physiological functions of peroxisomal CSY. Based on the observations that peroxisomal CSY is found in many plant tissues at different stages of development, it is likely that peroxisomal CSY is not just a glyoxylate cycle enzyme.

Another line of investigation is to test the hypothesis that peroxisomal malate dehydrogenase (PMDH) serves to oxidise NADH produced by β-oxidation, and does not oxidise malate to provide oxaloacetate for the glyoxylate cycle. Arabidopsis in which *PMDH* genes are knocked out will test this hypothesis. If PMDH performs a function in the glyoxylate cycle, mutants without PMDH are expected to reveal characteristics similar to glyoxylate cycle mutants. In contrast, if PMDH has a role in β-oxidation, mutants are expected to be unable to carry out β-oxidation. This will reveal a severe phenotype on germination and seedling growth, similar to phenotypes observed in those β-oxidation mutants.

Chapter 2

Materials and Methods

2.1 Chemicals
2.2 Bacterial strains and media
2.3 Plant materials
2.4 Plant growth conditions and pollination
2.5 DNA analysis
2.6 RNA analysis
2.7 DNA cloning
2.8 Gene transfer into Arabidopsis
2.9 Protein analysis
2.10 Biochemical analysis
2.11 Microscopy
2.12 Homology search and sequence analysis

Chapter 2

Materials and Methods

2.1 Chemicals

All chemicals were supplied by Sigma Chemical Co., Dorset, UK, unless otherwise stated.

2.2 Bacterial strains and media

2.2.1 Bacterial strains

Escherichia coli strain DH5α; *Sup*E44 Δ*lac* U169 (Φ80*lac*ZΔM15) *hsd*R17 *rec*A1 *end*A1 *gyr*A96 *thi*-1 *rel*A1

Escherichia coli strain BL21 (DE3) (Novagen, Nottingham, UK) carrying λDE3 gene and a chromosomal copy of the T7 RNA polymerase gene under control of the *lacUV5* promoter

Agrobacterium tumefaciens, strain GV 3101 C58 containing Ti pMP90RK (Koncz and Schell, 1986, Van Larabeke et al., 1974)

2.2.2 LB medium

LB broth was prepared containing 1% (w/v) tryptone (Difco, MD, USA), 0.5% (w/v) yeast extract (Difco, MD, USA), 1% (w/v) NaCl, pH 7.2 with NaOH. 1.5% (w/v) Bacto-agar (Difco, MD, USA) was supplemented for LB agar.

2.2.3 Plasmids

The plasmids used in this experiment were as follows.

Vector	Source and/or Reference	Use
pGEM-T easy	Promega, Southampton,UK	Cloning PCR product and sequencing
pGreen0179-hygro	Hellens et al., 2000	Ti Binary vector
pGreen0049-kan	Hellens et al., 2000	Ti Binary vector
pJitt166	Hellens et al., 2000	Cloning 35S cassette
pBluescript-CSY3 cDNA	Riken (pda02633); Seki et al., 2002	Amplifying CSY3 cDNA
pUNI 51-PMDH1 cDNA	ABRC (U14754); Yamada et al., 2003	Amplifying PMDH1 cDNA
pUNI 51- PMDH2 cDNA	ABRC (U12728); Yamada et al., 2003	Amplifying PMDH2 cDNA
pGreen-ICL::GFP4	Dr. Johanna Cornah, University of Edinburgh	Amplifying *GFP4*
pGEM-mRFP	Dr. Kumiko Samejima, University of Edinburgh	Amplifying *mRFP*
pCambia-CFP::SKL	Sparkes et al., 2003	Transformation of CFP-SKL
pCambia-PEX10::YFP	Sparkes et al., 2003	Transformation of PEX10-YFP
pET21a (+)	Novagen, Nottingham, UK	Bacterial expression vector

2.3 Plant materials

Wild-type Arabidopsis used was Columbia 0 (NASC accession N1092), unless otherwise stated. The mutant stock lines used in this project were as follows.

Line	Gene disruption	Source and/or Reference
csy1(Col)	Peroxisomal citrate synthase 1 (*CSY1*)	Insert Watch; Tissier et al., 1999 (SINS:03_23_03)
csy2-1 (Col)	Peroxisomal citrate synthase 2 (*CSY2*)	Syngenta; Sessions et al., 2000 (Garlic_367_E07.b.1a.Lb3Fa)
csy2-2 (Col)	Peroxisomal citrate synthase 2 (*CSY2*)	Syngenta; Sessions et al., 2000 (Garlic_1160_D05.b.1a.Lb3Fa)
csy3-1 (Col)	Peroxisomal citrate synthase 3 (*CSY3*)	Syngenta; Sessions et al., 2000 (Garlic_662_D07.b.1a.Lb3Fb)
csy3-2 (Col)	Peroxisomal citrate synthase 3 (*CSY3*)	SALK; Alonso et al., 2003 (N612543)
pmdh1 (Col)	Peroxisomal malate dehydrogenase (*PMDH1*)	Gabi-Kat; Rosso et al., 2003 (363B11)
pmdh2 (Col)	Peroxisomal malate dehydrogenase (*PMDH1*)	Gabi-Kat; Rosso et al., 2003 (326G02)
cts-1 (Col)	ABC transporter or Comatose (*CTS*)	Footitt et al., 2002
icl-1 (Col)	Isocitrate synthase (*ICL*)	Eastmond et al., 2000b
mls-1(Col)	Malate synthase (*MS*)	Cornah et al., 2004
kat2 (Col)	Thiolase 2 (*KAT2*)	Germain et al., 2001

2.4 Plant growth conditions and pollination

2.4.1 Seed sterilisation

Arabidopsis seeds were sterilised in microcentrifuge tubes by rinsing once with 70% (v/v) ethanol. The seeds were then treated with 10% (v/v) sodium hypochlorite solution (commercial bleach, Fisher Scientific, Loughborough, UK) supplemented with one drop of Triton-X for 10 min, followed by several rinses of sterile water. In some cases, chlorine vapour treatment was used to sterilise seeds by preparing 3 ml of concentrated hydrochloric acid in 100 ml of sodium hypochlorite to generate chlorine gas in a sealed desiccator. The microcentrifuge tubes containing the seeds were put into the sealed desiccator for 6-16 h.

2.4.2 Growing Arabidopsis on plates

Sterilised seeds were sown on petri dishes containing ½ MS agar (Murashige and Skoog, 1962) containing 0.22 % (w/v) MS salt and 0.8 % (w/v) Bactor-agar (Difco, MD, USA), pH 5.8 with KOH. In some cases, 1-3 % (w/v) sucrose was supplemented as indicated. For screening transgenic lines, the selection was made by adding appropriate antibiotics (50 μg/ml kanamycin or hygromycin) into the medium. Seeds were sown on appropriate medium and stratified at 4°C for 2 d to synchronise seed germination. The plates were then put in a growth cabinet at 22°C under constant light (100 μmol photons.m^{-2}.s^{-1}).

2.4.3 Growing Arabidopsis in soil

Plants were grown on a 3:1 mixture of Levingston's compost:grit in the growth room at 22°C, 60-80% humidity and 100 μmol photons.$m^{-2}.s^{-1}$ light intensity with either long day or short day conditions (16 h or 8 h photoperiod). Seeds were collected from mature dry siliques and allowed to dry further at room temperature for at least 2 weeks, before being stored up to 1 year at 4°C for subsequent use.

2.4.4 Cross-pollination

Female parents were emasculated by using the fine forceps to remove all the immature anthers from the floral buds. Pollination was performed by smearing the mature anthers of male parents onto the stigma of the emasculated female parents. The female cross pollinated flowers were covered with cling film for 3 d to protect cross pollination from other undesired anthers. After 2-3 weeks the seeds from mature siliques were collected and allowed to ripen at room temperature for at least 2 weeks before sowing.

2.5 DNA analysis

2.5.1 Arabidopsis DNA preparation for PCR

One small leaf or half a leaf was put in a microcentrifuge tube and 400 μl of Edwards buffer (200 mM Tris-Cl pH 7.5, 250 mM NaCl, 25 mM EDTA 0.5% (w/v) SDS; Edwards et al., 1991) was added. The leaf was mashed well with a plastic pestle. The sample was mixed by vortexing and centrifuged for 5 min at 18,000g. Then 300 μl of supernatant was transferred into a new tube and 300 μl isopropanol was added and

mixed. The samples were left for 2 min and centrifuged again for 5 min at 18,000g. The supernatant was decanted away and the DNA pellet was left exposed to the air for 15-20 min before being resuspended in 20 µl of TE buffer (10 mM Tris-Cl, pH 8.0, 1 mM EDTA). One µl of DNA solution was used as the template for a 20 µl PCR reaction.

2.5.2 Quantitative analysis of DNA

To quantify concentration of DNA, the sample was diluted with dH_2O and measured in a spectrophotometer at 260 nm. The concentration was given by the formula:

$$\text{DNA concentration } (\mu g/ml) = 50 \times A_{260} \times \text{Dilution factor}$$

2.5.3 Polymerase chain reaction (PCR)

a) Oligonucleotide preparation

Oligonucleotides were supplied by MWG Biotech Co., Ebersberg, Germany for using in PCR and sequencing experiments. All oligonucleotides are listed as shown in table 2.1.

Table 2.1 Oligonucleotide sequences

Name	Sequence (5' to 3')	Gene
SC_Com_For	CAC GGC TCC GGT TCG ATC TTC G	*CSY1, CSY2, CSY3*
SC_Com_Rev	CCA GTG TGA CAA GTA TCC AGC	*CSY1, CSY2, CSY3*
740_For	CTG AGC CGA ATC AGG TGT TGC	*CSY1*
750_For	GTC TGA TAC CGT CGG ATT GG	*CSY2*
790_For	CGG AAG GAA AAC AGG ATT CTC C	*CSY3*
410_For	GCG ATA ATC TCC GAT CTA GAT CCG	*CMDH1*

410_Rev	CGG ACA AAG CCC TGA AAG GC	*CMDH1*
330_For	CGG CGA TAA TTT TCC GAT CTC G	*CMDH2*
330_Rev	CAG CTG AGA AAA GAC CGG	*CMDH2*
720_For	GCC AGC TTC AAG TTC ACT AGA AGC	*CMDH3*
720_Rev	GCT AGC TCT CGT GCA GAG TC	*CMDH3*
780_For	CAG ATT GCT GAC GGG TCA GG	*PMDH1*
780_Rev	GCC GTA CAC TTC ATC GAT CC	*PMDH1*
660_For	CTC AGA TGG AGG CCA AGA AC	*PMDH2*
660_Rev	GCT GAT ACA CTT CCT CTG C	*PMDH2*
720_For (2)	CGT GAT AAT GAT CGG C	*CMDH3*
720_Rev (2)	ACC GAA AAC GAG TAA ACC	*CMDH3*
750intron_For	GTA TCC TGT GTT ACA GAC ACG	*CSY2*
790intron_Rev	CTG ATA CTC TAT TGG GTG CAG	*CSY3*
ACT2_21F	CAA CCA ATC GTG TGT GA	*ACTIN2*
ACT2_1267R	CTG TGA ACG ATT CCT GGA	*ACTIN2*
ICL5'	GCA GAG GGA GGC AAG AAT GAG CAT G	*ICL*
ICL3'	TAA CAC TCG GCC TTG CTC ATT TGA C	*ICL*
MS5'	ATG GAG CTC GAG ACC TCA GTT TAT C	*MS*
MS3'	GAG CCT TGA GAC ATT GAT AGG GTA G	*MS*
LACS7_For	GTA TGG TGG TGT TGC TGT CG	*LACS7*
LACS7_Rev	ATG GTT CTG GCA CCA AAG TC	*LACS7*
ACOX1_For	GCG AAG CTT AGA AGA TCA TTC TCC TC	*ACX1*
ACOX1_Rev	GCG AAG CTT AGA AGA TCA TTC TCC TC	*ACX1*
ACOX2_For	CTT CCA ACT CAT GAT TCC AAA GGA GTC	*ACX2*
ACOX2_Rev	CAG CAG CCA CCT GTT GCA GAA GTA CAG	*ACX2*
MFP2_For	CCT TGA CAT AGT CGG GAG GA	*MFP2*
MFP2_Rev	GGC ATT CCA AAC TTG CTG AT	*MFP2*
Kat2_For	GAG TCC ATG ACT ACC AAT CCA ATG CC	*KAT2*
Kat2_Rev	CCC AAG AGA AGC AAG AGT TGT GGT TG	*KAT2*
MCS1_For	AGC AGG ACC GTC TGA AGA AA	*CSY4*
MCS1_Rev	CGG AAT AAC CTT GCC ACT GT	*CSY4*

MCS2_For	TCA ACA GAG TTG GCT CAT CG	*CSY5*
MCS2_Rev	AGT GCC CTG TCC CAT ATC AG	*CSY5*
LB3	TAG CAT CTG AAT TTC ATA ACC AAT CTC GAT ACA C	Syngenta KO GENES
dspm1	CTT ATT TCA GTA AGA GTG TGG GGT TTT GG	Insert Watch KO GENES
DS5	ACG GTC GGG AAA CTA GCT CTA C	GeneTrap KO GENES
GabiKat	ATA TTG ACC ATC ATA CTC ATT GC	Gabi-Kat KO GENES
LBa1	TGG TTC ACG TAG TGG GCC ATC G	SALK KO GENES
35S-731For	CAT TTG GAG AGG ACA GCC C	35S Promoter
SacII_CaMV_For	GCA TCC CGC GGC GCT GAA ATC ACC AGT CTC T	CaMV Terminator
SacI_CaMV_Rev	GCA TCG AGC TCC GAG GAT ATC GCA TGC TCC G	CaMV Terminator
HindIII_790_For	GCA TCA AGC TTT TTC TTC GCT CCC TTT CTT C	*CSY3*
EcoRI_CaMV_Rev	GCA TCG AAT TCC GAG GAT ATC GCA TGC TCC G	CaMV Terminator
790_CaMV_For	AGG GTG TTT GTC CGC CTT GTC GCT GAA ATC ACC AGT CTC T	*CSY3::CaMV*
790_CaMV_Rev	AGA GAC TGG TGA TTT CAG CGA CAA GGC GGA CAA ACA CCC T	*CSY3::CaMV*
35S-790_For	CAT GGC GTG CAG GTC GAC GGT TTC TTC GCT CCC TTT CTT C	*35S::CSY3*
35S-790_Rev	GAA GAA AGG GAG CGA AGA AAC CGT CGA CCT GCA CGC CAT G	*35S::CSY3*
XbaI-35S_For	GCA TCT CTA GAG AGC TCG GTA CCC CTA CTC C	35S Promoter
SmaI-790_Rev	GCA TCC CCG GGA CAA GGC GGA CAA ACA CCC T	*CSY3*
790upst-1_For	CGA TGG TAA AGC GAG CCG	*CSY3*
790dwst-1_Rev	GGT GCG TTC GTC GAC GAT CG	*CSY3*
HindIII_790	GCA TCA AGC TTG TTC AAT ACT CCT GAC CGC AG	*CSY3*
750upst-1_For	GTC TTC ACT GCC CTT GCC C	*CSY2*
750dwst-1_Rev	GAT ATT TCT TCC CCG TAC GC	*CSY2*
HindIII_750	GCA TCA AGC TTT CAA TAC ACT TAC CCG CAG	*CSY2*
790_GFP_For	GCG GAT ACG AGT GTC GCA ATG AGT AAA GGA GAA GAA C	*CSY3::GFP*
790_GFP_Rev	GTT CTT CTC CTT TAC TCA TTG CGA CAC TCG TAT CCG C	*CSY3::GFP*
750_GFP_For	CAT CGG CTC ACA TTA CCG CTA TGA GTA AAG GAG AAG AAC	*CSY2::GFP*
750_GFP_Rev	GTT CTT CTC CTT TAC TCA TAG CGG TAA TGT GAG CCG ATG	*CSY2::GFP*
GFP_XbaI_Rev	GCA TCA GAT CTT TAT TTG TAT AGT TCA TCC ATG CC	*GFP*
780HindIII_For	GCA TCA AGC TTC CAG AAG GAG ATA TAA CCA TGG ATC CAA ACC AAC GTA TC	*PMDH1*
780XbaI_Rev	GCA TCT CTA GAT TAT TTC TTC GCA AAG GTA ACA CC	*PMDH1*

780_GFP_For	GGC GAT ACT TGG AGC AGC TGG TAT GAG TAA AGG AGA AGA AC	*PMDH1::GFP*
780_GFP_Rev	GTT CTT CTC CTT TAC TCA TAC CAG CTG CTC CAA GTA TCG CC	*PMDH1::GFP*
660HindIII_For	GCA TCA AGC TTC CAG AAG GAG ATA TAA CCA TGG AGT TTC GTG G	*PMDH2*
660XbaI_Rev	GCA TCT CTA GAT CAT TTT CTG ATG AAT TCA ACA CC	*PMDH2*
660_GFP_For	ATT CTT GGA GCT GCA GGT GGA ATG AGT AAA GGA GAA GAA C	*PMDH2::GFP*
660_GFP_Rev	GTT CTT CTC CTT TAC TCA TTC CAC CTG CAG CTC CAA GAA T	*PMDH2::GFP*
GFP_EcoRI_Rev	GCA TCG AAT TCT TAT TTG TAT AGT TCA TCC ATG CC	*GFP*
HindIII_RFP_F	GCA TCA AGC TTA TGG CCT CCT CCG AGG ACG TCA TC	*RFP*
HindIII_RFP_F2	GCA TCA AGC TTC GCC ACC ATG GCC TCC TCC GAG GAC GTC ATC	*RFP*
RFPSRL_F600_Rev	GCT CCC TGG GAT GAT GGA TGG CGC CGG TGG AGT GGC GGC	*RFP::SRL*
EcoRI_RFPSRL_R	GCA TCG AAT TCT CAC AGC CTG GAC AGC TCC CTG GGA TGA TGG ATG GCG CC	*RFP::SRL*
RFP399_For	CCC CGT AAT GCA GAA GAA GA	*RFP*
HindIII_780_62	GCA TCA AGC TTC GCC ACC ATG GAT CAG ATT GCT GAC GGG TCA GGT TTG	*PMDH1*
HindIII_660_64	GCA TCA AGC TTC GCC ACC ATG GAG GCC AAG AAC TCT GTA ATC G	*PMDH2*
HindIII_790_61	GCA TCA AGC TTC GCC ACC ATG GGA AAA CAG GAT TCT CCA GCG ATC G	*CSY3*
EcoRI_SRL_Rev	GCA TCG AAT TCT CAC AGC CTG GAC AGC TCC CTG GGA TGA TGG AT	SRL Sequence
XbaI_SRL_Rev	GCA TCT CTA GAT CAC AGC CTG GAC AGC TCC CTG GG	SRL Sequence
780SRL_Rev	ACA GCT CCC TGG GAT GAT GGA TTT TCT TCG CAA AGG TAA CAC CTT TAT G	*PMDH1::SRL*
660SRL_Rev	ACA GCT CCC TGG GAT GAT GGA TTT TCT GAT GAA TTC AAC ACC TTT C	*PMDH2::SRL*
790SRL_Rev	ACA GCT CCC TGG GAT GAT GGA TAA CTG AAG ATC CAG CCA AAC GTC	*CSY3::SRL*
780_F824	AGT TTG CAG ATG CTT GCC T	*PMDH1/2*
780NheI_For	GCA TCG CTA GCA TGG ATC CAA ACC AAC GTA TCG CG	*PMDH1*
780XhoI_Rev2	GCA TCC TCG AGT TTC TTC GCA AAG GTA ACA CCT TTA	*PMDH1*
660NheI_For	GCA TCG CTA GCA TGG AGT TTC GTG GAG ATG CCA ACC	*PMDH2*
660XhoI_Rev2	GCA TCC TCG AGT TTT CTG ATG AAT TCA ACA CCT TTC	*PMDH2*
pET_Pro_Primer	AAT ACG ACT CAC TAT AGG GG	pET Promoter
pET_Ter_Primer	GCT AGT TAT TGC TCA GCG G	pET Terminator
T3 Promoter Primer	ATT AAC CCT CAC TAA AGG GA	T3 Promoter
T7 Promoter Primer	TAA TAC GAC TCA CTA TAG GGA GA	T7 promoter
SP6 Promoter Primer	GAT TTA GGT GAC ACT ATA G	SP6 Promoter
MMDH1_For	CCC TAG ACA TCT CAT CGC C	*Mitochondrial MDH1*

MMDH1_Rev	TTG GGT ACG CTT AGT AAG GG	*Mitochondrial MDH1*
MMDH2_For	GTC GAT CAC ATC AAC ACC CG	*Mitochondrial MDH2*
MMDH2_Rev	GAA GAA GAC AAC TCT ACC GG	*Mitochondrial MDH2*

b) PCR reaction

The PTC-200 DNA engine (MJ Research, MA, USA) was used to carry out PCR reactions. Typically, a 20 µl reaction mixture was set up containing 12 µl of sterile dH_2O, 2 µl of 10 x PCR buffer (500 mM Tris-Cl, pH 8.3, 0.5 % (w/v) BSA, 5 % (w/v) Ficoll, 10 % (w/v) sucrose 300 mM KCl, 30 mM $MgCl_2$, 10 mM Tetrazine), 2 µl of mixed dNTP (2 mM of each deoxynucleoside 5' triphosphate, Promega, Southampton, UK), 1 µl of 2.5 µM forward primer, 1 µl of 2.5 µM reverse primer and 1 µl of 0.1 Unit/µl Taq DNA polymerase. The PCR was performed using the following cycle.

94°C for 30 s

94°C for 30 s
57°C for 30 s
72°C for 2 min
} 25-35 cycles

72°C for 2 min

The PCR products were subsequently analysed by agarose gel electrophoresis or stored at 4°C until required.

c) Purification of PCR products

If the PCR products were required for further PCR, cloning or sequencing experiments, the samples were purified a using QIAGEN PCR Purification Kit. (QIAGEN, Sussex, UK). In the final step, the DNA samples were eluted with 40 µl either dH_2O or 10 mM Tris-Cl, pH 8.5.

2.5.4 Restriction analysis of DNA

200-300 ng of plasmid DNA, or unspecified amount of PCR product, was digested in a 10 µl reaction mixture containing appropriate digestion buffer and 1 Unit of restriction enzyme. The samples were incubated at the appropriate temperature for 1-3 h. If a large amount of digested products were required, the reactions described were scaled up.

2.5.5 DNA gel electrophoresis

Horizontal agarose gel electrophoresis was used to separate the resulting DNA fragment products. The appropriate mass of agarose (0.75-1.5% (w/v)) was weighed and added into the volume of 0.5 X TBE buffer (45 mM Tris-base, 45 mM boric acid, 1 mM EDTA, pH 8.0 (adjust with HCl)) in an Erlenmeyer flask. The agarose was swirled and microwaved until it was melted. The agarose was allowed to cool to around 55°C and 10 µg/ml of ethidium bromide was supplemented. The melted agarose was poured onto a gel electrophoresis tray and the comb was inserted. When the gel was set, the comb was removed and the gel was transferred into the electrophoresis chamber and filled with 0.5 X TBE buffer until it covered the gel. In some cases, the appropriate volume of sample was mixed with 3 X gel loading dye

(0.25 % (w/v) bromophenol blue, 0.25% (w/v) xylene cyanol FF, 15% (w/v) Ficoll (Type 400)) equivalent to 1/3 of the final volume. Samples were loaded into the wells alongside a ladder DNA marker and then run using 100 V (constant) for approximately 1 h. The agarose gel was then removed and was examined on the UV transilluminator.

2.5.6 Purification of DNA from agarose gel

Ethidium bromide stained DNA fragments were visualised under the low-energy UV transilluminator. The desired DNA fragments were excised from the gel and purified by following the gel extraction protocol of "OIAGEN's QIAquick Gel Extraction Kit" (QIAGEN, Sussex, UK). In the final step, the DNA sample was eluted with 40 µl either dH_2O or 10 mM Tris-Cl, pH 8.5.

2.5.7 DNA sequencing

Plasmid DNA and PCR products were sequenced by PCR reactions, using DYEnamic ET Terminator Cycle Sequencing Kit. A 10 µl PCR reaction mixture was set up containing 4 µl of DNA template (200-500 ng plasmid or 50-90 ng PCR product), 3 µl of 1 X sequencing buffer, 1 µl of 5 µM primer, 2 µl of DYEnamic. The PCR reactions were carried out by the DNA sequencing facility in the ICAPB, The University of Edinburgh.

2.6 RNA analysis

2.6.1 Isolation of plant RNA

a) Large scale RNA extraction

1 g of plant tissue was ground into a fine powder with a pre-cooled pestle and mortar in liquid nitrogen. The tissue was then transferred into a pre-cooled 15 ml plastic centrifuge tube (Falcon) and to this was added 5 ml of extraction buffer (100 mM Tris-Cl pH 8.5, 6% (w/v) para-aminosalicylic acid sodium salt, 1% (w/v) tri-isopropylnaphthalene sulfonic acid sodium salt) and 5 ml of 1:1 phenol/chloroform. The mixture was mixed well by vortex and centrifuged at 2,500g at 4°C for 10 min. The aqueous phase was transferred into a baked glass centrifuge tube (Corex) and 500 µl of 3 M sodium acetate, pH 5.5 (adjust with glacial acetic acid) and 12.5 ml of ethanol was added and vortexed before being covered with parafilm and left at -20°C for 2 h. The sample was centrifuged at 10,000g at 4°C for 10 min and the pellet was resuspended with 2 ml of DEPC-H_2O. 2 ml of 5 M LiCl was further added and mixed before the sample was incubated at 4°C for 1 h. Then the centrifugation was repeated and pellet was resuspended in 300 µl of DEPC-H_2O and transferred into a microcentrifuge tube. Then 30 µl of 3 M sodium acetate, pH 5.5 and 750 µl of ethanol were added and the sample was incubated at -20°C for 2 h. Finally the pellet was recovered by centrifugation at 18,000g at 4°C for 10 min and resuspended in 100 µl DEPC-H_2O. The RNA samples were stored at -70°C for subsequent analysis.

b) Small scale RNA extraction using RNeasy Plant Mini Kit (QIAGEN, Sussex, UK).

Up to 100 mg of plant tissue was ground to a fine powder with a pre-cooled pestle and mortar in liquid nitrogen. The tissue was transferred into a microcentrifuge tube and 450 µl of RLT buffer (composition not disclosed by manufacture) was added into the sample. The sample was mixed well before being transferred into a QIAshredder spin column and centrifuged for 2 min at 18,000g. The flow-through fraction was then transferred into a new microcentrifuge tube and a half volume of 96-100% ethanol was added and mixed well. The sample was then applied onto an RNeasy mini column and centrifuged for 1 min at 18,000g. The flow-through was decanted away and 700 µl RW1 buffer (composition not disclosed by manufacture) was added and the centrifugation was repeated. The column was transferred into a new collection tube and was washed twice by adding 500 µl RPE buffer (composition not disclosed by manufacture) followed by centrifugation. To elute, the RNeasy mini column was put into new microcentrifuge tube and 30-50 µl RNase-free water was added and centrifuged for 1 min. The RNA samples were kept at -70°C until subsequent analysis.

2.6.2 Quantitative analysis of RNA

To quantify concentration of RNA, the sample was diluted with DEPC-H_2O and measured in a spectrophotometer at 260 nm. The concentration was given by the formula:

$$\text{RNA concentration } (\mu g/ml) = 40 \times A_{260} \times \text{Dilution factor}$$

2.6.3 Reverse transcriptase cDNA synthesis

A 20 µl cDNA synthesis was set up containing 1 X RT Buffer, 0.5 mM each dNTP (Promega, Southampton, UK), 1 µM Oligo-dT Primer (Promega, Southampton, UK), 10 units RNase inhibitor (Promega, Southampton, UK), 50 ng - 2 µg RNA template and 4 units Omniscript Reverse Transcriptase (QIAGEN, Sussex, UK) (in the case of RNA template of less than 50 ng, Sensiscript Reverse Transcriptase (QIAGEN, Sussex, UK) was used instead). The samples were incubated at 37°C for 1 h and kept at -20°C until subsequent analysis.

2.6.4 cDNA amplification

An RT-PCR reaction was set up in a 20 µl PCR reaction using an appropriate primer pair. Typically 1 µl of cDNA was used as the template. In some case cDNA was diluted (1/10 or 1/100) as appropriate for qualitative PCR.

2.7. DNA cloning

2.7.1 Plasmid DNA Preparation and Purification

Transformed single colonies were transferred independently into 5 ml of LB medium supplemented with appropriate antibiotic (50 µg/ml ampicillin or kanamycin). Cultures were incubated overnight at 37°C and shaken at 250 rpm. Each suspension culture was transferred into a 15 ml plastic centrifuge tube (Falcon) and centrifuged at 2,500g for 10 min with a Sorvall RC5B centrifuge (Dupont, New Jersey, USA). The supernatant was decanted and the subsequent steps followed the plasmid

preparation protocol of "QIAprep Spin Miniprep Kit" (QIAGEN, Sussex, UK). In the final step plasmid was eluted with 40 µl either dH_2O or 10 mM Tris-Cl, pH 8.5.

2.7.2 Transformation of competent cells

a) Preparation of competent cells

A 5 ml overnight pre-culture of *E. coli* DH5α strain was transferred into 500 ml LB medium supplemented with 5 ml of 1 M $MgCl_2$. The culture was incubated at 18°C for about 2-3 d until the A_{600} of 0.5-0.7 was reached. The culture was placed on ice for 10 min. The cell pellet was then harvested by centrifuge at 2,500g at 4°C for 10 min and resuspended in 80 ml of ice cold TB buffer (10 mM Pipes, 55 mM $MnCl_2$, 15 mM $CaCl_2$, 250 mM KCl, pH 6.7 (adjust with KOH prior to adding $MnCl_2$)). The centrifugation step was repeated to harvest the pellet. Cells were resuspended by gently swirling in 20 ml TB buffer supplemented with DMSO (to a final concentration of 7% (v/v)) and incubated on ice for 10 min. The 300 µl of competent cell aliquots were prepared, chilled in liquid nitrogen and stored at -70°C.

b) Heat-shock transformation

Approximately 50 ng of plasmid DNA or 2 µl of ligation reaction was added into 50 µl of competent *E. coli* cells in a microcentrifuge tube. The sample was gently mixed well and stored on ice for 30 min. Cells were then transferred into a preheated 42°C water bath and left for 90 s before being rapidly transferred back onto ice for 1-2 min. LB (200 µl) was added to the cells and incubated at 37°C in a water bath for 45 min before using a glass rod to aseptically spread cells on LB agar plates containing the

appropriate antibiotic (50 μg/ml ampicillin or kanamycin). The culture plates were incubated at 37°C overnight.

2.7.3 Cloning of RT-PCR product into pGEM-T easy vector (Promega, Southampton, UK)

The RT-PCR product amplified by Taq DNA polymerase was directly used to ligate with pGEM-T easy vector (Promega, Southampton, UK). A 10 μl ligation reaction was set up containing 1-3 μl of RT-PCR product, 1 X ligation buffer, 50 ng of pGEM-T easy vector and 3 Units of T4 DNA ligase (Promega, Southampton, UK). Ligation reactions were incubated at 4°C overnight. Next day 2 μl of each reaction was used for transformation into competent *E. coli* DH5α and then cells were spread onto ampicillin (50 μg/ml) LB plates containing X-Gal (40 μg/ml) and IPTG (200 μg/ml). Plates were incubated at 37°C overnight and the white colonies were selected.

2.7.4 Cloning of DNA fragments into plasmid vectors

a) Amplification of target DNA fragment

The correct frame of the target DNA fragment was amplified using PCR. In some cases, PCR primers were designed to include an extra sequence (end protection and restriction site sequences) at the 5' end followed by 20-25 bases at the 3' portion that was used to hybridise with the target region (Old and Primose, 1994). The amplified DNA fragment was then produced with the extra sequence which coded for restriction sites at the end of the amplified products. Instead of using Taq DNA

polymerase, the Pfu DNA polymerase was used to obtain better results with proof reading activity. A 50 µl PCR reaction mixture was set up containing 1 X Pfu DNA polymerase buffer (Promega, Southampton, UK), 200 µM each dNTP (Promega, Southampton, UK), 1 µM forward primer, 1 µM reverse primer, 0.5 µg DNA template, 2 Units of Pfu DNA polymerase (Promega, Southampton, UK). The Pfu mediated-PCR was performed using the following cycle.

94°C for 30 s

94°C for 30 s
52°C for 30 s
72°C for 2-5 min* } 25-35 cycles

72°C for 2 min

*The extension time was 2 min for every 1 kb to be amplified.

b) Creating sticky ends on vector and amplified product

Vector (20 µl) was digested in a 50 µl reaction mixture containing 1 X digestion buffer and 5 Units of restriction enzymes. The reaction mixture was incubated at 37°C for 1-2 h followed by heating at 65°C for 15 min to inactivate the enzymes. Then 10 µl of shrimp alkaline phosphatase (SAP) and 6.6 µl of 10 X SAP buffer (Rhoche Scientific, Heidelberg, Germany) were added. Following the incubation at 37°C for 10-20 min the enzyme was subsequently inactivated by heating at 65°C for 15 min. The digested vectors were separated by gel electrophoresis and purified using a gel extraction Kit (QIAGEN, Sussex, UK). In some cases, amplified PCR products were used. The restriction reaction was also set up in 50 µl and incubated at

37°C for 1-2 h. After denaturing restriction enzymes at 65°C for 15 min, the digested PCR products were directly purified using a PCR purification Kit (QIAGEN, Sussex, UK).

c) Ligation of DNA fragments into plasmid vector

Each 10 µl ligation reaction was set up with 1 X ligation buffer, 1 Unit of T4 DNA ligase (Rhoche Scientific, Heidelberg, Germany) and a vector to DNA fragment molar ratio 1:1. The samples were incubated at 4°C overnight. 2 µl from each reaction were used for transformation into competent *E. coli* DH5α.

2.8. Gene transfer into *Arabidopsis*

2.8.1 Agrobacterium transformation

a) Competent cell preparation

Overnight culture (5 ml) of *Agrobacterium tumefaciens* strain GV1301 C58 was inoculated into 500 ml LB medium supplemented with 100 µg/ml rifampicin and 10 µg/ml gentamycin. When an A_{680} of 0.5-1.0 was reached, the culture was chilled on ice for 10 min and centrifuged for 3 min at 500g to remove cell clumps. The supernatant was poured into new a new Universal bottle and centrifuged at 2,500g for 10 min at 4°C. The cell pellet was resuspended in ice-cold 20 mM $CaCl_2$ (1ml per 50 ml original culture). Competent cells (200 µl) were transferred into 1.5 ml aliquots, rapid-frozen with liquid nitrogen and stored at -70°C.

b) Heat-shock Transformation

A thawed aliquot of competent *Agrobacterium* was added 5-10 μl of plasmid DNA. The cells were then rapid-frozen in liquid nitrogen and thawed in a 37°C water bath for 5 min. LB medium (1 ml) was added, and mixed by gentle pipetting and inversion. Following the incubation at 30°C with gentle shaking for 2-4 h, cells were centrifuged at 2,500g for 10 min and resuspended in 100 μl LB. Finally, cells were spread onto LB agar supplemented with 100 μg/ml rifampicin, 10 μg/ml gentamycin and 50 μg/ml kanamycin. The transformed colonies appeared after the plates were incubated for 2-3 d at 30°C.

2.8.2 *Arabidopsis* transformation

a) Plant growth

Arabidopsis plants were grown in soil in the growth room under long day condition. After the flowers were produced, the primary bolts of each plant were clipped to encourage the growth of secondary bolts. A week later, the green siliques were removed and the plants were ready for transformation.

b) Floral dipping transformation

A single colony of *Agrobacterium* containing plasmid for transformation was inoculated into 5 ml LB with antibiotic (100 μg/ml rifampicin, 2.5 μg/ml gentamycin and 50 μg/ml kanamycin) and grown overnight with shaking at 30°C. The overnight culture was transferred into 500 ml LB with antibiotics and grown again until A_{680} about 0.8 was reached. The cell pellet was then recovered by centrifuging at 2,500g

for 10 min and then resuspended in 500 ml of 5% (w/v) sucrose containing 0.01% (v/v) silwet L-77. Flowers of each plant were dipped into Agrobacterium solution for 10-20 s with gentle swirling. Plants were covered with a plastic bag for 24 h and watered well. Plants were re-dipped again 5-7 d later. Seeds were harvested 3-4 weeks after the transformation and the transformed plants were selected by sowing the seeds on ½ MS medium containing either 50 μg/ml hygromycin or 50 μg/ml kanamycin (appropriate antibiotic was based on plant selectable makers of plasmid constructs).

2.9 Protein analysis

2.9.1 Quantification of protein content

The protein content of samples was determined as described by Bradford (1976) using the Bio-Rad Protein assay reagent (Bio-Rad, Hamburg, Germany). Each 1 ml assay cuvette was set up containing 1-10 μl of protein sample, 200 μl protein assay solution and dH_2O to 1 ml. Following incubation for 5 min, the absorbance at 595 nm of samples was measured. Bovine serum albumin was used as the standard marker.

2.9.2 *In vitro* protein expression

The expression vector pET 21a (+) (Novagen, Nottingham, UK) was engineered to express histidine tagged-recombinant proteins. These were made up to encode 6 histidine residues attached at the carboxy terminus of the target proteins. The vectors were then transformed into *E. coli* protein expression strain BL21 (DE3) (Novagen,

Nottingham, UK). A transformed single colony was selected from LB agar supplemented with 50 μg/ml ampicillin and transferred into 5 ml of LB medium supplemented with 100 μg/ml ampicillin. Next day the overnight suspension culture was transferred into 500 ml of LB medium supplemented with 100 μg/ml ampicillin and incubated at 37°C and 250 rpm. When an A_{600} of 0.6 was reached, the protein expression was induced by adding 500 μl of 1 M IPTG. During the period of time, 1 ml of suspension culture was collected for measurement of A_{600} and the appropriate volume of suspension culture was removed (1 ml per A_{600} unit) to prepare protein samples for monitoring protein expression.

2.9.3 Protein purification

a) Cell extract preparation

After 3 h induction with IPTG, 250 ml of suspension culture was harvested by centrifugation at 10,000g for 10 min using pre-weighed centrifuge tubes. The supernatant was decanted and the pellet was allowed to drain. About one gram of wet cell paste was resuspended with 5 ml of BugBuster reagent (Novagen, Nottingham, UK) by pipetting. Then 125 Units Benzoase Nuclease (Novagen, Nottingham, UK) and 5,000 Units rLysozyme solution (Novagen, Nottingham, UK) were added. The cell suspension was incubated on a shaking platform at a slow setting for 15-20 min at room temperature. The cell debris was removed by centrifugation at 16,000g for 20 min at 4°C and the supernatant was used in the next step.

b) Column Chromatography (Novagen, Nottingham, UK)

Target protein purification was performed using a pre-charged His-Bind Column (Novagen, Nottingham, UK). After the column cap was removed, the storage buffer in the upper chamber was poured off and the lower Luer plug was opened. The column was equilibrated by allowing 10 ml of 1 X binding buffer to flow through the column. Then 5 ml of cell extract was loaded. After the cell extract had drained, to the column was added 10 ml of 1 X binding buffer then 10 ml of 1 X wash buffer. Finally the target protein was eluted with 5 ml 1 X elute buffer. Fractions (1 ml) of protein sample were captured and the protein content measured. In some cases an Amicon protein concentrator (Millipore, MA, USA) was used to concentrate protein as necessary.

2.9.4 Production of antisera

One ml of each purified recombinant protein at a concentration of 1mg/ml was sent to the Scottish National Blood Transfusion Service for rabbit antisera generation.

2.9.5 Sodium dodecyl sulfate-polyacrylamide gel electrophoresis (SDS-PAGE)

a) Preparation of bacterial protein samples

An appropriate volume of suspension culture was transferred into a microcentrifuge tube and spun at 12,000g for 1 minute. The supernatant was removed and the pellet was resuspended in 1 ml of ice cold 0.5 mM Tris-Cl pH 7.5 before centrifugation was repeated. The supernatant was removed and the pellet was resuspended with 100 µl of dH_2O. Then 100 µl of 2 X gel loading buffer (100 mM Tris-Cl pH 6.8, 200 mM

dithiothreitol, 20 % (v/v) glycerol, 4 % (w/v) SDS, and 0.2 % (w/v) bromophenol blue) was added and mixed. The sample was boiled for 5 min and centrifuged at 12,000g for 10 min. The supernatant was transferred to a new microcentrifuge tube and used for SDS-PAGE.

b) Preparation of plant protein samples

100 mg of plant tissue was ground in a mortar with 1 ml extraction buffer (50 mM Tris-Cl pH 6.8, 2% (v/v) β-mercaptoethanol, 10 % (v/v) glycerol). Each homogenised sample was spun at 12,000g for 10 min and then 150 µl of supernatant was transferred into another tube and mixed with 50 µl of sample loading buffer (50 mM Tris-Cl pH 6.8, 2% (v/v) β-mercaptoethanol, 10 % (v/v) glycerol, 8 % (w/v) SDS and 0.1 % (w/v) bromophenol blue). The samples were boiled for 5 min and used for SDS-PAGE.

c) Gel electrophoresis

Two glass plates were cleaned using lint free tissue and water, followed by ethanol. The plates and spacers were assembled, forming a "sandwich". The sandwich was positioned on the pouring stand. Then 10 ml of 12% separating gel (3.3 ml H_2O, 4 ml 30% (w/v) acrylamide mix (acrylamide/bis-acrylamide = 29:1), 2.5 ml 1.5 M Tris-Cl pH 8.8, 100 µl 10% (w/v) SDS, 100 µl 10 % (w/v) ammonium persulphate and 4 µl TEMED) was prepared. The mixture was mixed briefly and poured into the sandwich. Water saturated butanol was carefully overlayed onto the gel surface to a depth of 2-3 mm. The gel was allowed to set for 30 min. The butanol was then poured off and the top of the gel was washed with dH_2O and dried with filter paper.

Next 5 ml of 5 % stacking gel (3.4 ml H_2O, 0.83 ml 30% (w/v) acrylamide mix (acrylamide/bis-acrylamide = 29:1), 0.63 ml 1 M Tris-Cl pH 6.8, 50 µl 10% (w/v) SDS, 50 µl 10 % (w/v) ammonium persulphate and 5 µl TEMED) was prepared. The mixture was poured into the sandwich until the level reached the top of the lower plate. The comb was inserted, avoiding air bubbles. The gel was allowed to set for 20 min. The comb was then carefully pulled out and the gel assembly was placed in the electrophoresis tank. Outer buffer reservoir and inner buffer reservoir were filled with Tris-glycine electrophoresis running buffer (25 mM Tris-base, 250 mM glycine, 0.1% (w/v) SDS, pH 8.3 (adjust with HCl)). The samples were then loaded into wells alongside a standard molecular weight marker (BioRad, Hemel Hempstead, UK) using a long tip micropipette (avoid spilling samples into adjacent wells). The power supply was connected and run at 25 mA (per gel) for 50 min.

d) Staining gel

Once the electrophoretic front had reached the bottom shown by the movement of dye, the power pack was switched off. The gel was carefully removed from the sandwich and placed in clean staining box. By gentle orbital shaking, staining with 100-200 ml of staining solution (0.25% (w/v) Coomassie Brilliant Blue R250, 45% (v/v) methanol, 10% (v/v) glacial acetic acid) followed. After 30 min the staining solution was removed and then 300 ml of destaining solution (45% (v/v) methanol, 10% (v/v) glacial acetic acid) was subsequently added and shaken gently overnight. Next day, the gel was viewed on a light box and photographed.

2.9.6 Western blot analysis

a) SDS protein transfer

The SDS gel and the membrane Hybond^{TM}-C super (Amersham, Chalfont, UK) were equilibrated for 15 min in the Bjerrum and Schafer-Nielsen transfer buffer (48 mM Tris-base, 39 mM glycine, 20% (v/v) methanol, non adjusted pH 9.2). A Bio-Rad protein transfer apparatus (Bio-Rad, Hamburg, Germany) was used to transfer SDS protein onto the membrane. The stack was set up by putting a pre-soaked (with transfer buffer) filter paper onto the anode excluding any air bubbles, and the pre-wet membrane was put on the top. The equilibrated gel was then carefully put on the membrane, followed by another pre-soaked filter paper. The cathode and safety cover were placed onto the stack. The power supply was set for 12 V and switched on for 45 min.

b) Detection with antibody

The non specific-binding sites of the membrane were blocked by immersing the membrane in 5% (w/v) non-fat dried milk in TBS-T buffer (20 mM Tris-Cl pH 7.6, 8% (w/v) NaCl, 0.1% (v/v) Tween 20) on an orbital shaker at room temperature for 1 hour or at 2-8°C overnight. The membrane was rinsed twice in TBS-T buffer (>4ml/cm^2 membrane) for 2 min each time. The appropriate amount of rabbit primary antibody was diluted in TBS-T buffer and the membrane was immersed in the diluted antibody solution on the orbital shaker at room temperature for 1 hour. Then the membrane was washed by briefly rinsing twice with two change of TBS-T buffer, immersing in TBS-T buffer (>4ml/cm^2 membrane) on the orbital shaker for 15 min, then 3 x 5 min rinses with fresh TBS-T buffer. Then the membrane was

transferred into 1/5,000 diluted secondary antibody (HRP-labelled anti rabbit-goat antibody, Amersham, Chalfont, UK) in TBS-T buffer and incubated at room temperature on the orbital shaker for 1 hour. The washing procedure was repeated and excess wash buffer was drained. The membrane (protein side up) was put onto a sheet of saran wrap and ECL detection reagent (2 ml of solution A and 50 µl of solution B, Amersham, Chalfont, UK) was applied onto the membrane. The membrane was incubated at room temperature for 3-5 min and then the detection reagent was drained off. Finally the membrane was wrapped with saran wrap before being put into an X-ray cassette and exposed with film for 5-10 s.

2.10 Biochemical analysis

2.10.1 Enzyme assay

a) Citrate synthase enzyme assay

The crude enzyme was extracted by grinding 100 mg plant tissue with 1 ml extraction buffer (150 mM Tris-Cl pH 8.0, 10 mM KCl, 1 mM EDTA, 10% (v/v) glycerol, 0.1 mM PMSF). The homogenised sample was centrifuged at 18,000g for 10 min at 4°C. The supernatant was transferred into a new microcentrifuge tube and used for enzyme assay. Citrate synthase activity was assayed with 5,5'-dithio-bis(2-nitrobenzoic acid) (DTNB) as described by Srere (1969). A 1 ml reaction was set up containing 100 mM Tris-Cl pH 8.0, 100 µM DTNB, 1 mM $MgCl_2$, 1 mM Oxaloacetate and 200 µM acetyl CoA. The reaction was started by adding enzyme solution to avoid inhibition of the enzyme by DTNB (Schnarrenberger et al., 1980;

Kato et al., 1995) The reaction product was measured at 412 nm using an extinction coefficient of $\varepsilon = 1.36 \times 10^6$ $M^{-1}.cm^{-1}$.

b) Malate dehydrogenase enzyme assay

The crude enzyme extract was prepared by grinding 100 mg plant tissue with 1 ml PBS buffer (137 mM NaCl, 2.7 mM KCl, 4.3 mM Na_2HPO_4, 1.4 mM KH_2PO_4, pH 7.4 (adjust with HCl)). The homogenised sample was centrifuged at 18,000g for 10 min at 4°C. The supernatant was transferred into a new microcentrifuge and used for enzyme assay. Malate dehydrogenase activity was assayed by measuring the decrease in absorbance at 340 nm resulting from oxidation of NADH ($\varepsilon = 6.2 \times 10^3$ $M^{-1}.cm^{-1}$). A 1 ml reaction mixture was set up containing 200 µM oxaloacetate, 200 µM NADH and enzyme in PBS buffer.

2.10.2 Fatty acid analysis

Fatty acids were analysed using the fatty acid methyl esters (FAMEs) method according to Browse et al. (1986). Heptadecanoic acid (C17:0) was prepared as an internal standard (ISTD) by applying 10 µl of 1 mg/ml heptadecanoic acid in chloroform into each 2 ml screw-top glass vial. The ISTD vials were dried using a SpeedVac. Each batch of 20 seedlings was boiled in 200 µl dH_2O for 5 min and seedlings were transferred into the ISTD vial. To each vial was then added 200 µl of hexane and 0.5 ml of 1 N HCl (in methanol). The vials were tightly sealed with teflon-lined screw-caps, votexed and placed in a rack in an 85°C oven for 2 h. The samples were then removed and transferred into a pre-cooled rack in a -20°C freezer for 10 min. The caps were removed and 0.25 ml 0.9% (v/v) KCl in water was added.

The samples were re-capped and vortexed. The top (hexane) layer containing FAME derivatives was carefully transferred into new vials and dried in the SpeedVac with low heat. The samples were kept at -20°C for subsequent GC-MS analysis. The GC-MS analysis was carried out by the Department of Chemistry, University of Edinburgh.

2.10.3 Sodium [2-^{14}C] acetate feeding experiment

The metabolism of sodium [2-^{14}C] acetate was performed by Dr Johanna Cornah according to Eastmond et al. (2000) with modifications according to Cornah et al. (2004). Triplicate batches of 100, 2-day old Arabidopsis seedlings, grown on 1% (w/v) sucrose in continuous light were prepared. The seedlings were incubated in the dark (to prevent re-fixation of $^{14}CO_2$) at 20°C in 200 µl of medium containing 1 mM sodium [2-^{14}C] acetate (20 MBq.mmol^{-1}) and 50 mM Mes-KOH (pH 5.2) for 4 h. During the incubation evolved $^{14}CO_2$ was trapped in a well containing 200 µl 5 N KOH. The KOH solution with incorporated ^{14}C was kept for subsequent quantification. The soluble components of the seedlings were then extracted in three 1 ml aliquots of 80% (v/v) ethanol at 80 °C followed by 1 ml water at 40 °C. The total soluble extracts were combined and the hydrophobic components were extracted with 1.5 ml chloroform. The ethanol-soluble components were dried, resuspended in water and then further separated into neutral, basic and acidic fractions by ion exchange chromatography. The soluble components were passed sequentially over Dowex anion and cation-exchange resins (500 µl bed volumes) (Supelco, PA, USA), and the neutral components eluted with 2 x 0.6 ml aliquots dH_2O. The basic and acidic components were eluted with 2 x 0.75 ml aliquots 2 N

NH_4OH and 2 N formic acid, respectively. The amount of ^{14}C present in each fraction quantified by scintillation counting.

2.11 Microscopy

2.11.1 Fluorescence and confocal microscopy

A Nikon TE200 flourescence microscope (Tokyo, Japan) or a confocal laser scanning microcope (CLSM) (BioRad Radiance 2100 Rainbow, Deisenhofen, Germany) was used to analyse the expression of green fluorescence protein (GFP) and red fluorescence protein (RFP). To perform the analysis, plant materials such as seedlings and leaves were transferred onto slides, submerged in water and covered with cover slips. For fluorescence microscopy, the fluorescein isothiocyanate filter sets (excitation/emission) for GFP (460-500 nm/510-560 nm), or RFP (528-533 nm/600-660 nm) were used. For confocal microscopy, a 480-500 nm wavelength of excitation, and emission of 510 to 550 nm (GFP), or 580 to 620 nm (RFP), or 605-685 nm (chloroplast) were used.

2.11.2 Transmission electron microscopy

Transmission electron microscopy (TEM) was carried out as in the method described by Carde (1987). Plant tissue was prepared by being fixed primarily in modified Karnovsky fixative (Karnovsky, 1965) containing 2% (v/v) formaldehyde (from paraformaldehyde) and 2.5% (v/v) glutaraldehyde in 0.1 M sodium cacodylate buffer, pH 7.2 (adjust with HCl) for 1 hour. Specimens were then washed three times with 0.1 M sodium cacodylate buffer (pH 7.2) for 20 min each time and post fixed for 1 hour in 1% (w/v) osmium tetroxide in 0.1 M sodium cacodylate buffer (pH 7.2). The

specimens were again washed three times in 0.1 M sodium cacodylate buffer (pH 7.2) and then 1% (w/v) tannic acid in 0.1 M sodium cacodylate buffer (pH 7.2) was subsequently added for 1 hour. Washing in dH_2O and dehydration through gradually increasing alcohol series followed (10%, 20%, 50%, 70%, 80%, 90%, and 100% respectively for 10 min each time and two changes of dry absolute alcohol for at least 1 h). Spurr's resin was infiltrated into the tissue by using propylene oxide as an intermediate step after dehydration. The blocks were subsequently sectioned on a Leica UCT ultramicrotome using a diamond knife to produce 90nm (gold) sections. These were collected and stained using a double staining technique as described by Daddow (1983). Sections were then viewed on a transmission electron microscope FEI CM120 Biotwin and pictures were made using Kodak SO163 film for plates.

2.12 Homology search and sequence analysis

Several bioinformatic tools were used for sequence search and analysis. The sequence searches in Arabidopsis were performed using TAIR (Huala et al., 2001; http://www.arabidopsis.org) and TIGR (Bevan et al., 2001; http://www.tigr.org/tdb/e2k1/ath1/) databases. BLAST at the NCBI (Wheeler et al., 2000; Altschul et al., 1990; Gish et al., 1993; Madden et al., 1996; Zhang et al., 1997; Zhang et al., 1997 2000; http://www.ncbi.nlm.nih.gov/ BLAST/) was used for general homology search whereas, TAIR (Huala et al., 2001; http://www.arabidopsis.org/wublast/index2.jsp) was used for Arabidopsis homology search. Multiple alignments of nucleotide and protein sequences were carried out using ClustalX and GeneDoc programmes (Thompson et al., 1997; Nicholas et al.,

1997). Phylogenetic trees were performed using ClustalW at EMBL-EBI (Kersey et al., 2004; http://www.ebi.ac.uk/clustalw/). The trees were constructed using Phylodendron (version 0.8d, by D.G. Gilbert, http://iubio.bio.indiana.edu/treeapp/). The translation tool of a nucleotide to a protein sequence was performed using translate tool at ExPASy (Gasteiger et al., 2003; http://us.expasy.org/tools/ dna.html).

Chapter 3

The Function of Peroxisomal Citrate Synthase

3.1 Identification of peroxisomal citrate synthase genes in Arabidopsis

3.2 Analysis of peroxisomal citrate synthase gene expression

3.3 Analysis of peroxisomal citrate synthase subcellular localisation

3.4 Isolation and characterisation of citrate synthase knock-out mutants

3.5 Citrate synthase double mutants

3.6 Complementation of the double mutant with *CSY* genes

3.7 Defect in fatty acid β-oxidation in the double mutant

Chapter 3

The Function of Peroxisomal Citrate Synthase

3.1 Identification of peroxisomal citrate synthase genes in Arabidopsis

To identify the potential peroxisomal citrate synthase genes, firstly a databank sequence search was carried out to identify all citrate synthase genes in Arabidopsis. The genome project of Arabidopsis has revealed that there are five genes predicted to encode citrate synthases (CSY) in the Arabidopsis genome. In this project these genes are named as *CSY1* (At3g58740), *CSY2* (At3g58750) *CSY3* (At2g42790) *CSY4* (At2g44350) and *CSY5* (At3g60100). Based on their encoded protein annotation and subsequent phylogenetic tree analysis (Figure 3.1), these CSYs are divided into two major groups. The first group is comprised of CSY4 and CSY5, which are predicted to be mitochondrial with mitochondrial targeting sequences at their N-termini. CSY4 has been identified as a mitochondrial CSY (Millar et al., 2001; Hazlewood et al., 2004). The second major group of CSYs consists of CSY1, CSY2 and CSY3. Each of these is predicted to be peroxisomal with an obvious type 2 peroxisomal targeting sequence (R-X_6-HL) at the N-terminus (Table 3.1). Members of group two are more similar in sequence to pumpkin peroxisomal citrate synthase (Kato et al., 1996) than are members of group one. In addition, there are characteristic differences between CSYs in group one and group two. For example, the CSYs in group one contain 17

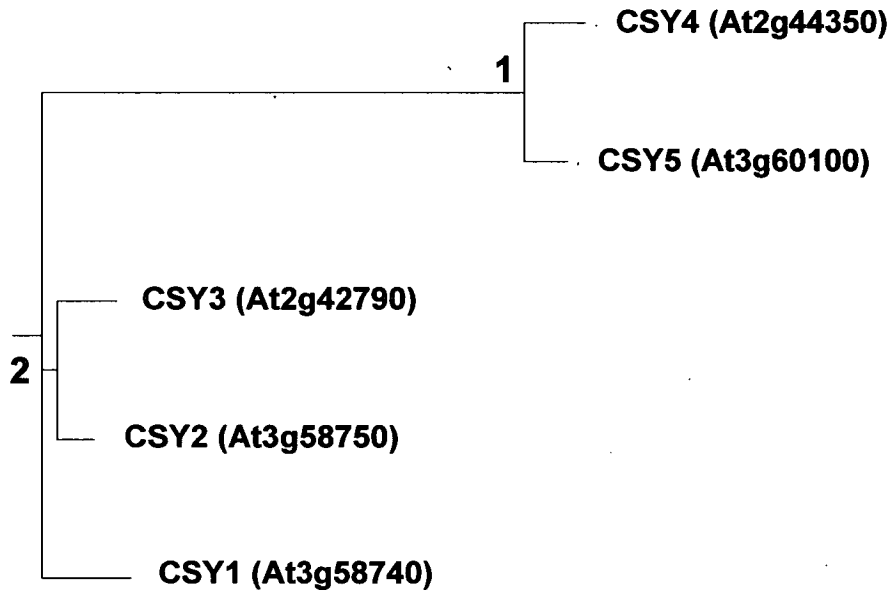

Figure 3.1 Phylogenetic tree of five CSY proteins from Arabidopsis. Sequences were aligned with the ClustalX programme (Thompson et al., 1997) and the tree was constructed by Phylodendron (version 0.8d, by D.G. Gilbert, http://iubio.bio.indiana.edu/treeapp/).

or 19 exons whereas there are only 12 or13 exons for CSYs in group two (Table 3.1). The isoelectric point (PI) is less than 7 in group one and over 7 in group two (Table 3.1). CSY1, CSY2 and CSY3 which belong to group two are unique from CSY4 and CSY5 in group one and so are the good candidates for peroxisomal CSYs.

Table 3.1 Genes predicted to encode citrate synthase in Arabidopsis genome[a]

Gene	Number of exon	Prediction of subcellular localisation	Encoded protein		Protein property		
			N-terminus (first 20 aa)	C-Terminus (last 3 aa)	PI	Length (aa)	MW (kDa)
CSY1 (At3g58740)	12	Peroxisomes	MEISERARARLAVLNAHLTV[b]	TKL	8.16	480	52.88
CSY2 (At3g58750)	12	Peroxisomes	MEISQRVKARLAVLTAHLAV[b]	SAL	8.86	514	56.56
CSY3 (At2g42790)	13	Peroxisomes	MEISERVRARLAVLSGHLSE[b]	SSV	7.79	509	56.16
CSY4[c] (At2g44350)	19	Mitochondria	MVFFRSVSAFTRLRSRVGQQ	SSA	6.88	473	52.63
CSY5 (At3g60100)	17	Mitochondria	MVMQDLKSQMQEIIPEQQDR	LNR	5.98	433	48.21

[a]Information for gene/protein annotations were obtained from The Arabidopsis Information Resource (Huala et al., 2001; www.arabidopsis.org)

[b]Highlighted are peroxisome targeting sequence type 2 (PTS2) : R-X_6-HL

[c]Mitochondrial citrate synthase (Millar et al., 2001; Hazelwood et al., 2004)

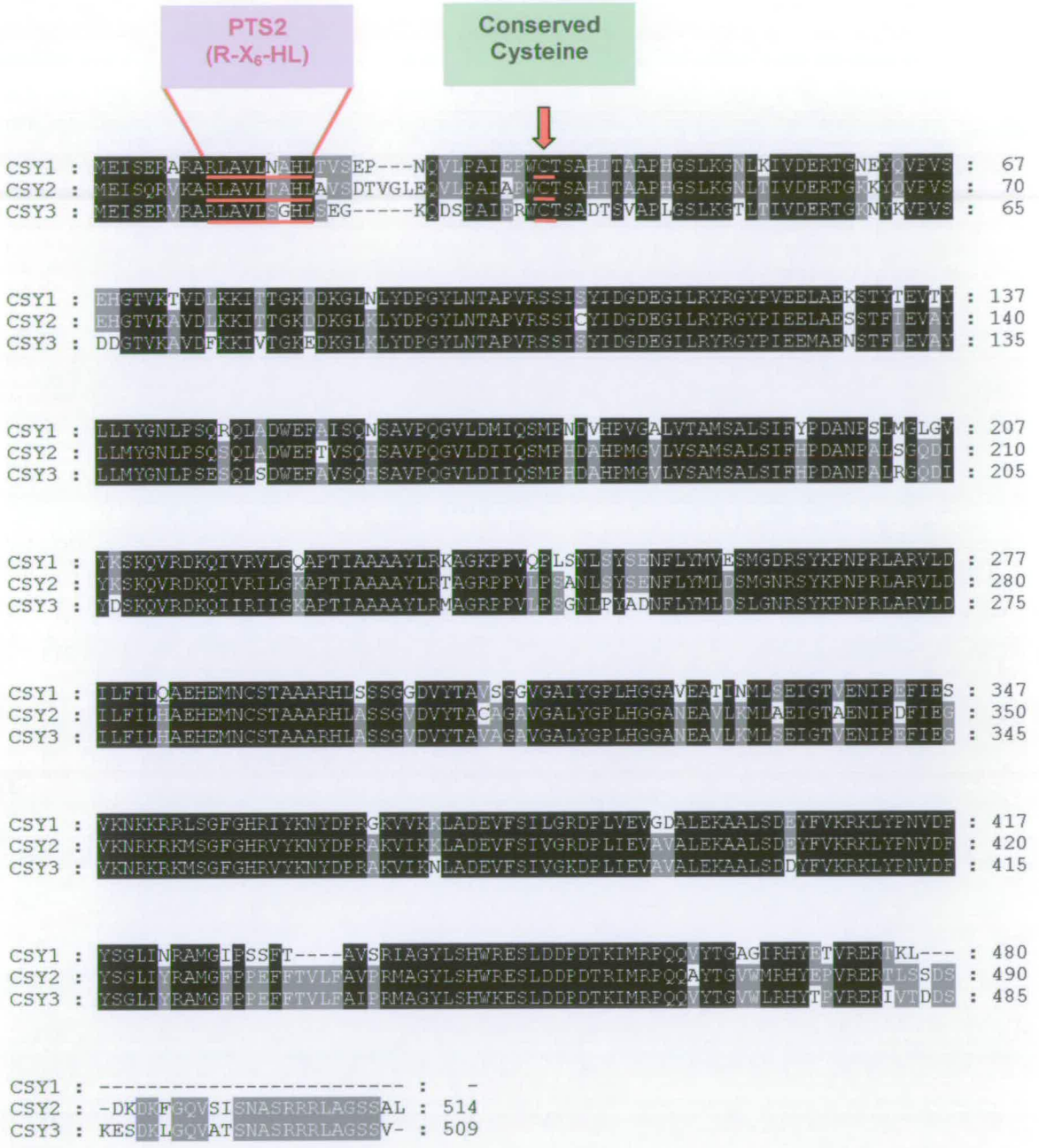

Figure 3.2 Multiple alignments of putative peroxisomal citrate cynthase proteins (CSY) were carried out using ClustalX and GeneDoc programmes (Thompson et al., 1997; Nicholas et al., 1997). The peroxisomal targeting signal type 2 sequences (PTS2) and conserved cysteine residues are highlighted.

Protein identity analysis showed that at least 77% identity scores were found among members in CSY group two. By contrast the identity of CSY group one against group two are less than 30%. Protein multiple alignments of CSY1, CSY2 and CSY3 showed a high similarity within the group (Figure 3.2). In addition, CSY2 and CSY3 showed even greater similarity. Their C-terminal peptide sequences are longer than CSY1 and the homology was greater in CSY2 and CSY3 along the whole peptide sequence. CSY1 and CSY2 are neighbouring genes on chromosome 3 and have probably arisen by gene duplication. CSY3 may have arisen more recently by duplication of CSY2 and insertion into chromosome 2. For CSY1, CSY2 and CSY3, each contains a predicted type 2 peroxisomal targeting sequence (PTS2) at the N-terminus. This comprises the nonapeptide motif R-$(X)_6$-H/Q-A/L/F (Kato et al., 1996, 1998; Mullen, 2002), downstream of which is a conserved cysteine residue. This conserved cysteine is essential for proteolytic processing of PTS2-containing proteins following import into peroxisomes at least in plants and mammals (Kato et al., 1998, Kato et al., 2000). Therefore CSY1, CSY2 and CSY3 are proposed to be peroxisomal and chosen for this study of peroxisomal citrate synthase.

3.2 Analysis of peroxisomal citrate synthase gene expression

3.2.1 Verifying the RT- PCR products

To determine which of the putative *CSY* genes are expressed in germinating seeds and developing seedlings, gene-specific oligonucleotide primers were designed so that transcripts of each gene could be detected by RT-PCR. Because the nucleotide sequences of *CSY1*, *CSY2* and *CSY3* showed strong similarity to each other, the

specificity of particular primer pairs to such desired template to be amplified was monitored. To test the RT-PCR products obtained with each primer combination they were digested with restriction endonucleases which could distinguish different gene products. In this case *Eco*RI and *Hin*dIII were employed to generate the resulting fragments (Figure 3.3). The results showed that RT-PCR products obtained with each primer pair were of the predicted sizes and were digested with specific endonucleases to products of the expected sizes. Additionally the RT-PCR products were subsequently identified by nucleotide sequencing to confirm that RT-PCR products corresponded to the predicted gene in each case.

3.2.2 RT-PCR analysis

The expression profiles of the predicted peroxisomal CSY genes were then examined. RT-PCR analysis using RNA template isolated from various tissues of mature Arabidopsis showed that *CSY2* and *CSY3* genes are expressed throughout the shoot, but *CSY1* expression is detected only in siliques (Figure 3.4A). The expression of *CSY1* was subsequently detected in developing seeds during the period when TAG accumulates in the embryo (Figure 3.4B). To examine expression of *CSY* genes in seedlings, RNA was isolated at daily intervals from day 1 to day 8. RT-PCR analysis showed that *CSY2* and *CSY3* are both expressed strongly during germination and seedling development stages, while *CSY1* RNA was not detected. Expression of *CSY2* and *CSY3* could also be detected in imbibed seeds (day 0) but the RNA template from such seeds was less reliable for RT-PCR (results not shown).

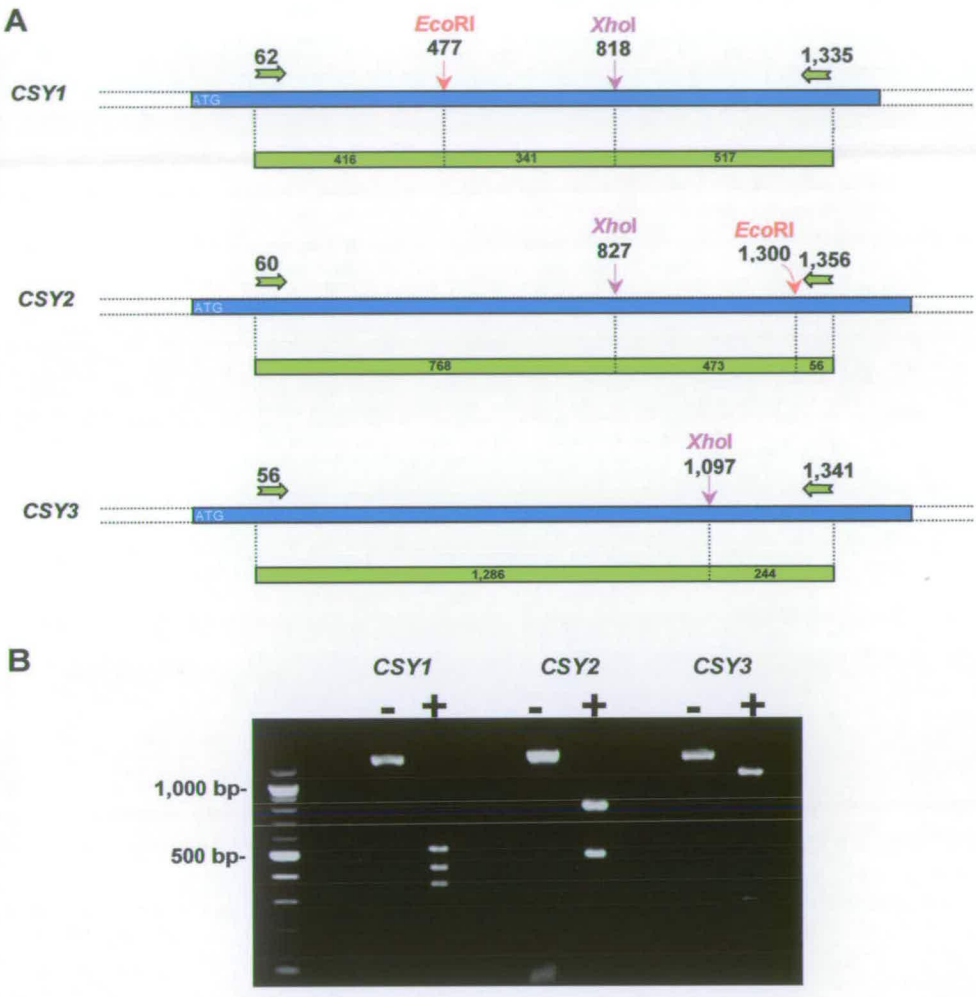

Figure 3.3 Characterisation of three Arabidopsis peroxisomal citrate synthase (*CSY*) cDNAs. **(A)**, Schematics of the primer locations (green arrows) and unique *Eco*RI and *Xho*I restriction endonuclease sites (red and pink arrows respectively) in the *CSY1*, *CSY2* and *CSY3* cDNAs. **(B)**, RT-PCR products produced from each *CSY* cDNA using primers illustrated, without (-) and with (+) subsequent digestion with restriction endonucleases.

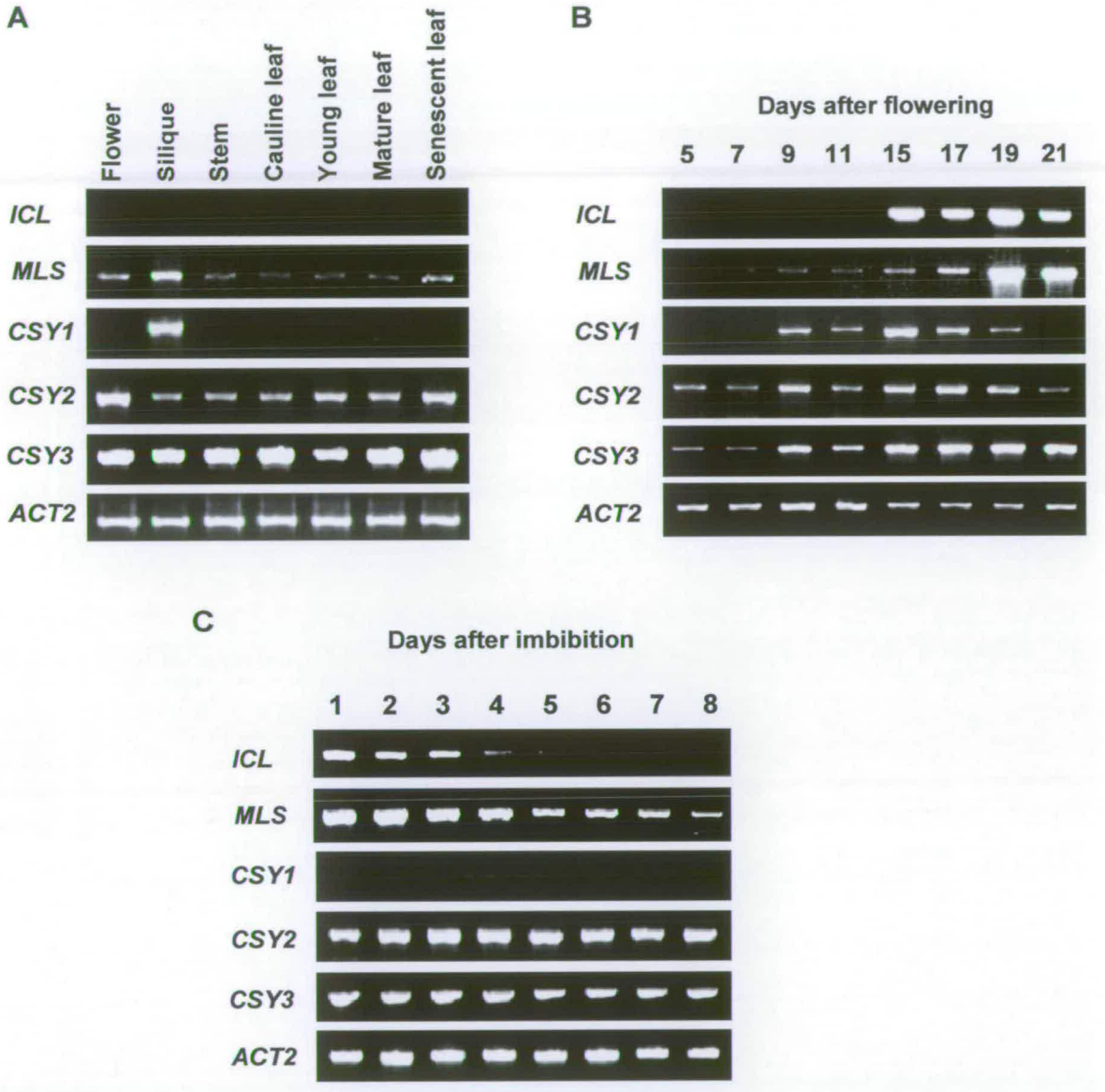

Figure 3.4 Gene expression pattern of peroxisomal *CSY* genes detected by RT-PCR; **(A),** in different organs of 6 week old Arabidopsis plants; **(B)**, in maturing Arabidopsis seeds; **(C)**, in developing seedlings.

Transcripts for isocitrate lyase (*ICL*) and malate synthase (*MLS*), the unique enzymes for the glyoxylate cycle are abundant after the onset of seed germination and decline thereafter to a very low or undetectable level. In contrast, *CSY2* and *CSY3* genes are expressed strongly during germination, seedling development and at mature plant stages. This indicates a potential role for peroxisomal CSYs in addition to that of a glyoxylate cycle enzyme.

3.3 Analysis of peroxisomal citrate synthase subcellular localisation

A number of publications have demonstrated that PTS2, including the nonapeptide motif R-$(X)_6$-HL, at the N-termini enables peroxisomal proteins to be localised in the peroxisome (Kato et al., 1995; Johnson and Olsen, 2003; Fulda et al., 2002; Hayashi et al., 2002; Mano et al., 2002). This includes a previous study in pumpkin, in which CSY localisation was proved to be peroxisomal and was targeted by PTS2 (Kato et al., 1996). To confirm that Arabidopsis CSY2 and CSY3 are also localised in the peroxisome and are targeted by PTS2 leader sequences, several constructs were generated, encoding the putative PTS2 sequences of CSY2 and CSY3 fused to green fluorescent protein (GFP).

3.3.1 Construction of p35S::CSY2-GFP and p35S::CSY3-GFP

The construct p35S::CSY2-GFP was constructed by PCR using Pfu polymerase. The CSY2 leader sequence template was prepared by PCR amplification from genomic DNA between position -349 and +196 (where A of start codon = 1) using 750upst-

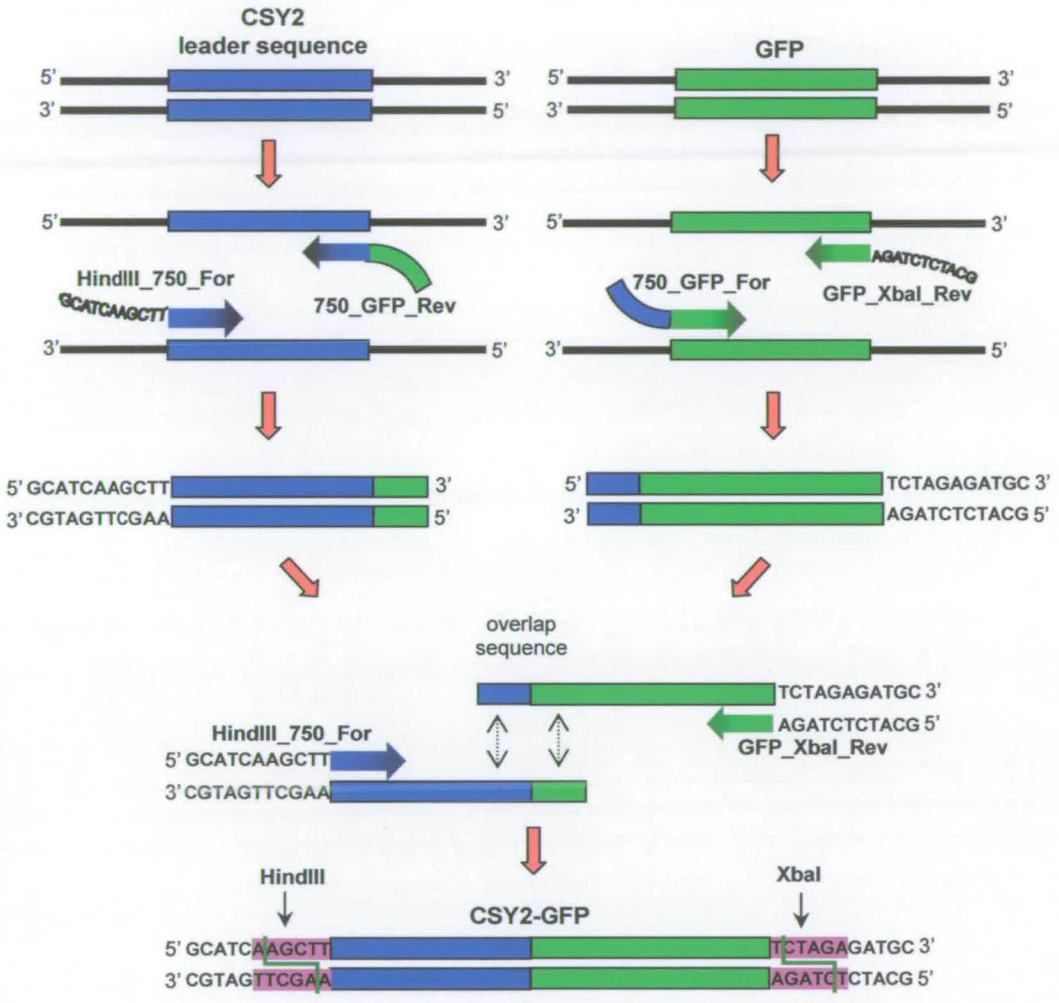

Figure 3.5 Cloning schematic diagram of CSY2 leader sequence fused with GFP by PCR. The restriction sites *Hind*III and *Xba*I were introduced at the 5' and 3' end respectively.

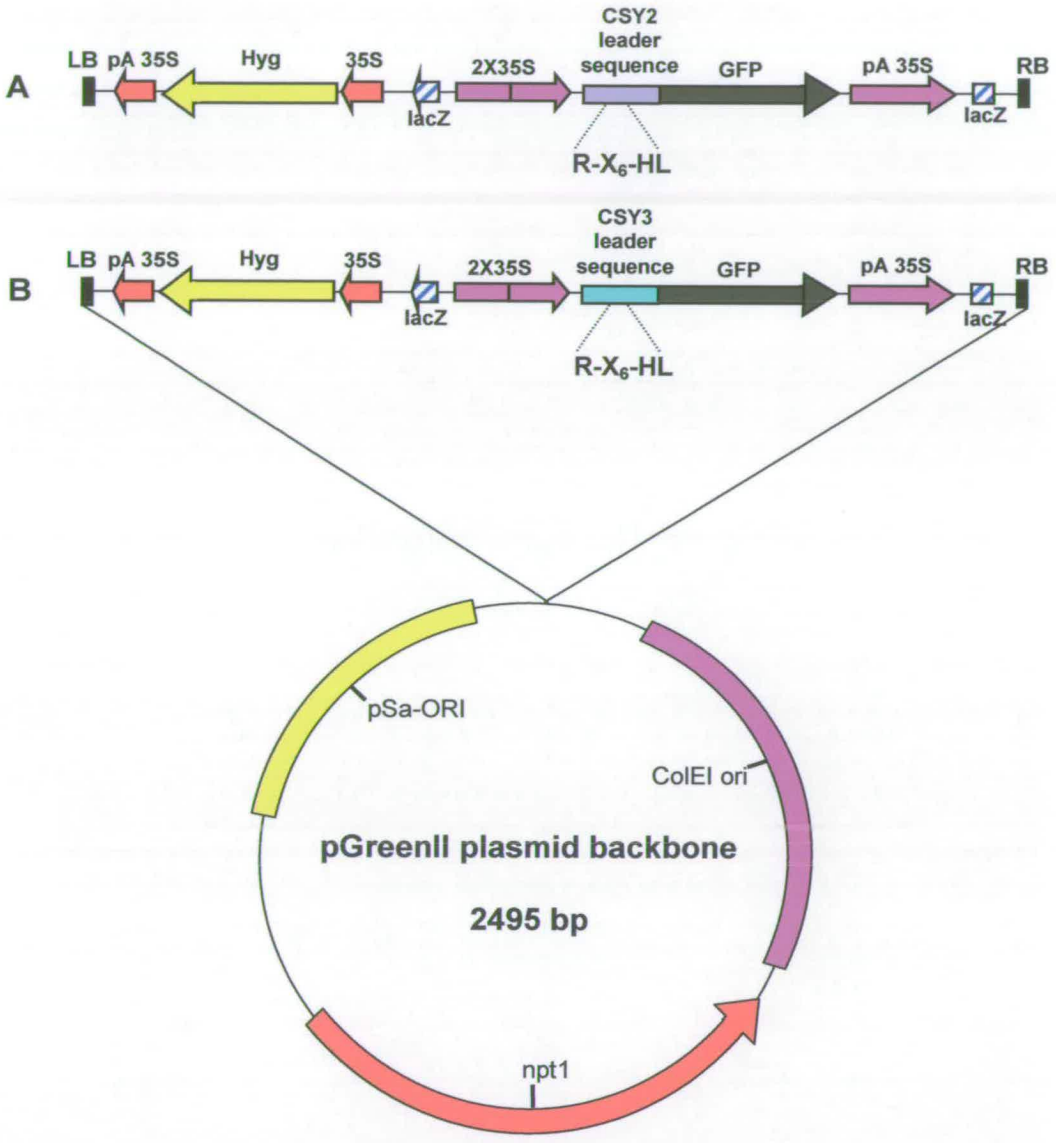

Figure 3.6 Schematic diagram of binary vector p35S::CSY2-GFP **(A)** and p35S::CSY3-GFP **(B)**

1_For and 750dwst-1_Rev primers. The overlapping PCR fusion was then used to construct a CSY2-GFP fragment (Figure 3.5). Firstly *Hin*dIII_750 and 750_GFP_Rev primers were used to amplify the CSY2 leader fragment with the introduction of a *Hin*dIII site at the 5' end and the first 20 bp of GFP fragment at the 3' end. In another PCR Reaction, 750_GFP_For and GFP_XbaI_Rev primers were use to amplify the GFP fragment with the introduction of an *Xba*I site at the 3' end and the last 20 bp of CSY2 leader sequence at the 5' end. The complementary overlapping sequence 20-25 bp of 3' end in the CSY2 fragment and the 5' end in the GFP fragment enabled the CSY2-GFP fusion fragment to be amplified by Hindlll_750 and GFP_XbaI_Rev primers. This PCR fragment was then cut by restriction enzymes and subcloned into pJitt166 between the double 35S promoter and CaMV terminator at *Hin*dIII and *Xba*I sites (Hellens et al., 2000). The complete cassette of CSY2-GFP with CaMV promoter and terminator was then restriction digested by *Kpn*I and *Xho*I and inserted into pGreen0179 at *Kpn*I and *Xho*I sites (Hellens et al., 2000). This plasmid is called p35S::CSY2-GFP (Figure 3.6A).

The p35S::CSY3-GFP construct (Figure 3.6B) was made by the same procedures described for making the construct p35S::CSY2-GFP, using 790upst-1_For, 790dwst-1_Rev, HindIII_790, 790_GFP_For and 790_GFP_Rev primers instead of 750upst-1_For, 750dwst-1_Rev, HindIII_750, 750_GFP_For and 750_GFP_Rev primers respectively.

3.3.2 Construction of the peroxisomal marker p35S::mRFP-SRL

A peroxisomal marker was created using a p35S::mRFP-SRL construct. This was made encoding monomeric red fluorescent protein (mRFP) (Campbell et al., 2002) fused to the C-terminal 10 amino acids of pumpkin (Cucurbita cv Kurokawa Amakuri) malate synthase which contain the PTS1 signal sequence Ser-Arg-Leu (SRL). This PTS1 had been used to target β-glucuronidase into peroxisomes in Arabidopsis (Hayashi et al., 1996) and had recently been verified to transport RFP (DsRed) to peroxisomes in Arabidopsis (Lin et al, 2004). Due to the p35S::CSY2-GFP and p35S::CSY3-GFP constructs containing the 35S-hygro cassette as a plant selectable marker, pGreen0049 (Hellens et al., 2000) encoding the kanamycin plant selectable marker cassette was used to construct p35S::mRFP-SRL.

The mRFP-SRL fragment was generated by PCR using Pfu polymerase (Figure 3.7). First the mRFP gene was amplified with the HindIII_RFP_For primer to introduce a *Hin*dIII site at the 5' end, and the RFP_600_Rev primer to avoid the stop codon and introduce a partial PTS1 sequence at the 3' end. The second amplification using HindIII_RFP_For and RFP_SRL_EcoRI_Rev primers was carried out to introduce the complete PTS1 sequence and restriction site *Eco*RI.

The mRFP-SRL fragment was subcloned into pJitt166 between the double 35S promoter and CaMV terminator at the *Hin*dIII and *Eco*RI sites (Hellens et al., 2000). The complete mRFP-SRL cassette controlled by the 35S promoter and terminator was then cloned into *Kpn*I and *Sac*I sites of the T-DNA region in pGreen0049 binary

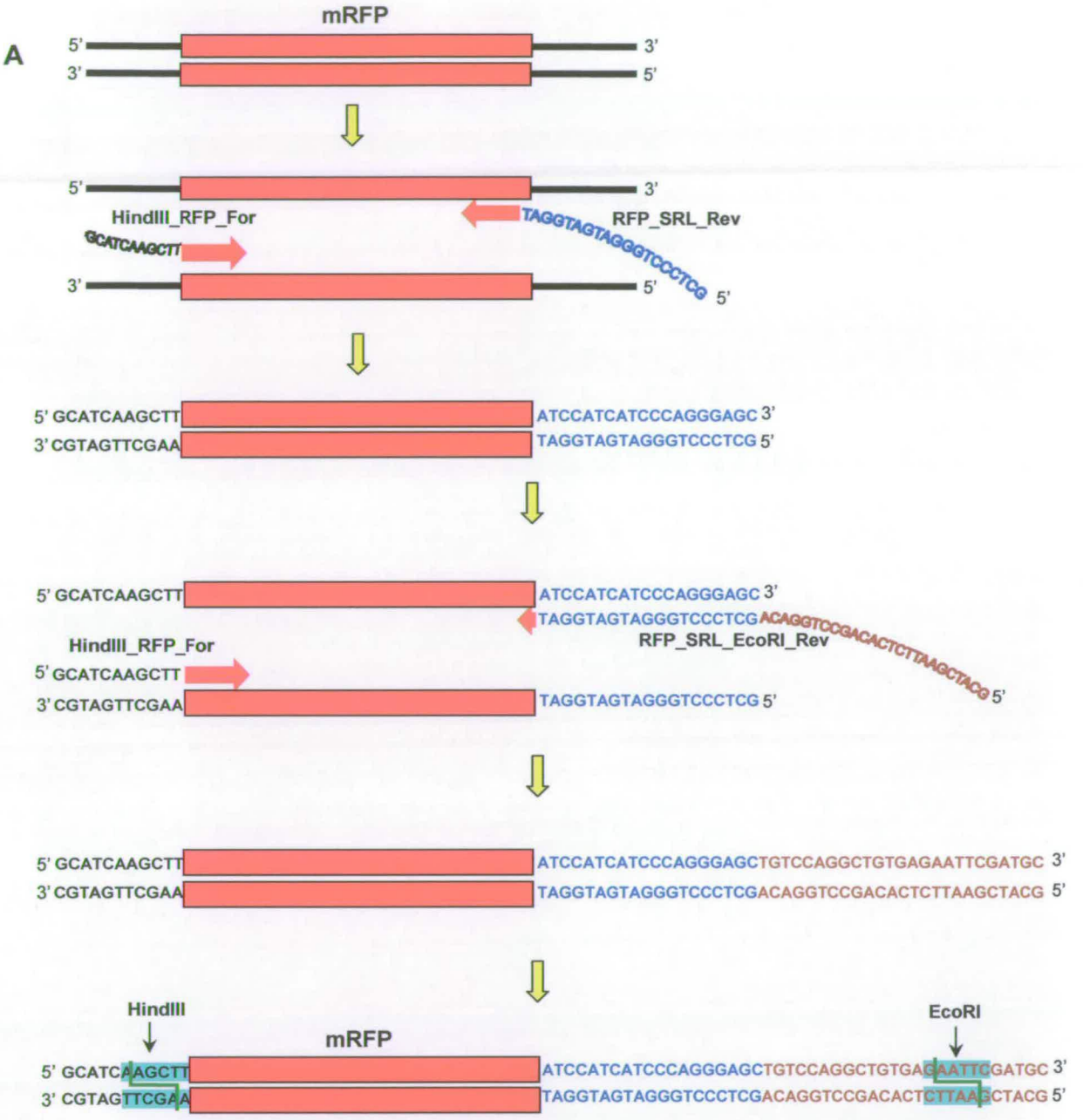
A
mRFP
5'
3'
3'
5'
5'
3'
HindIII_RFP_For
GCATCAAGCTT
TAGGTAGTAGGGTCCCTCG
RFP_SRL_Rev
3'
5'
5'
5' GCATCAAGCTT
ATCCATCATCCCAGGGAGC 3'
3' CGTAGTTCGAA
TAGGTAGTAGGGTCCCTCG 5'
5' GCATCAAGCTT
ATCCATCATCCCAGGGAGC 3'
TAGGTAGTAGGGTCCCTCG
ACAGGTCCGACACTCTTAAGCTACG 5'
RFP_SRL_EcoRI_Rev
HindIII_RFP_For
5' GCATCAAGCTT
3' CGTAGTTCGAA
TAGGTAGTAGGGTCCCTCG 5'
5' GCATCAAGCTT
ATCCATCATCCCAGGGAGCTGTCCAGGCTGTGAGAATTCGATGC 3'
3' CGTAGTTCGAA
TAGGTAGTAGGGTCCCTCGACAGGTCCGACACTCTTAAGCTACG 5'
HindIII
mRFP
EcoRI
5' GCATCAAGCTT
ATCCATCATCCCAGGGAGCTGTCCAGGCTGTGAGAATTCGATGC 3'
3' CGTAGTTCGAA
TAGGTAGTAGGGTCCCTCGACAGGTCCGACACTCTTAAGCTACG 5'
B
mRFP
ATCCATCATCCCAGGGAGCTGTCCAGGCTGTGA
I H H P R E L S R L -

Figure 3.7 (Previous Page) (A), Cloning schematic diagram of mRFP fused to the C-terminal 10 amino acids of pumpkin malate synthase which contains the PTS1 signal sequence Ser-Arg-Leu (SRL). **(B),** The peroxisomal marker mRFP-SRL protein.

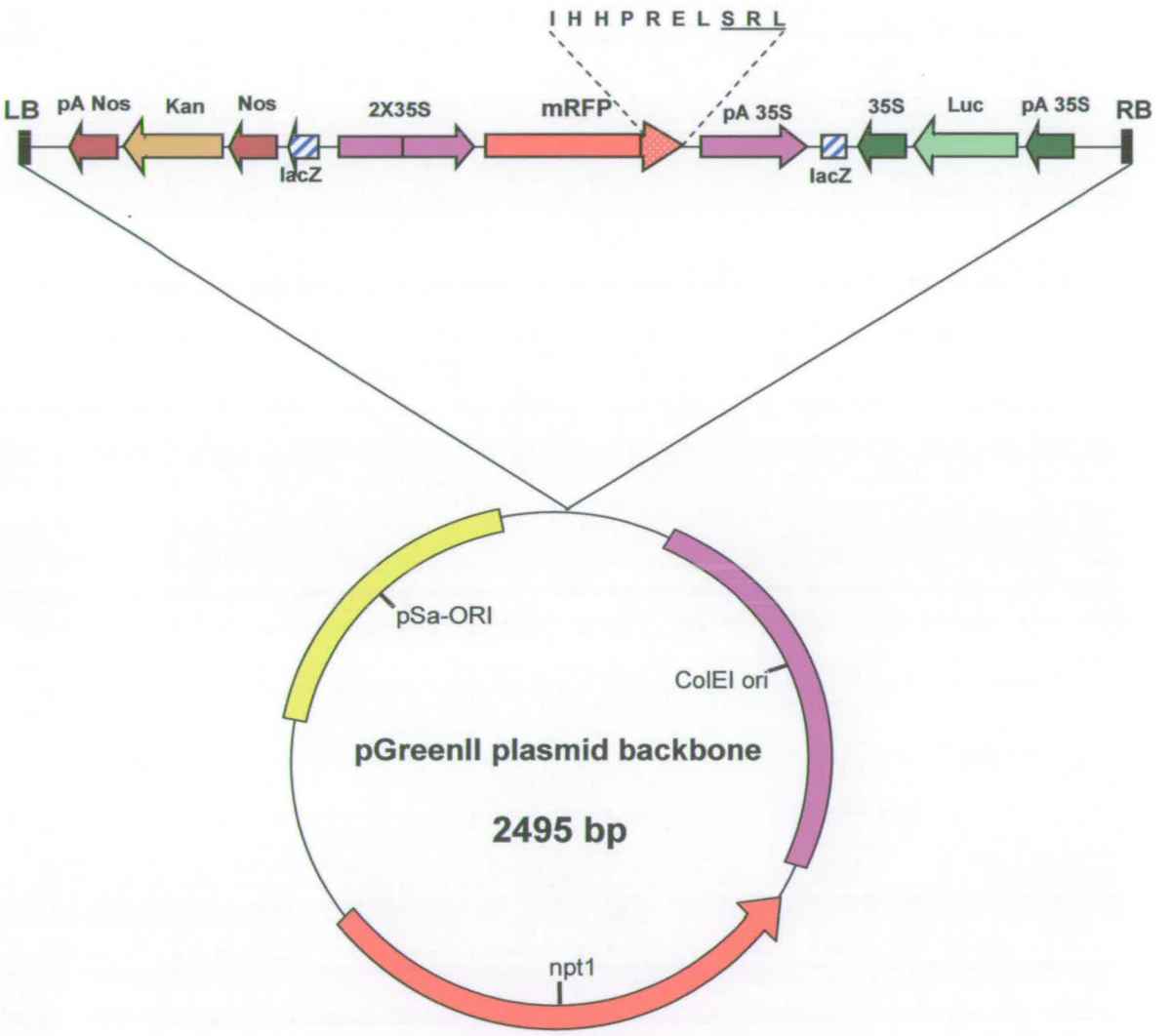

Figure 3.8 Schematic diagram of binary vector p35S::mRFP-SRL.

vector (Hellens et al., 2000). This engineered pGreen is called p35S::mRFP-SRL (Figure 3.8).

3.3.3 Localisation of CSY2-GFP and CSY3-GFP

Arabidopsis were subjected to Agrobacterium floral dipping transformation (Clough, and Bent, 1998) using the p35S::CSY2-GFP and p35S::CSY3-GFP binary vectors. The T_0 transgenic plants, CSY2-GFP and CSY3-GFP, were obtained through hygromycin selection and subsequently the presence of the transgenes was confirmed by PCR analysis (results not shown). In each transgenic line, GFP expression in leaf epidermal cells was visualised using fluorescence microscopy. CSY2-GFP and CSY3-GFP located to punctuate spherical structures similar in size to plant peroxisomes (0.5-1.5 μm) (Figure 3.9A and 3.9B). In order to confirm that these microbodies with GFP expression are peroxisomes, another round of Agrobacterium floral dipping transformation with a peroxisomal marker construct was carried out. The T_2 plants expressing CSY2-GFP and CSY3-GFP were transformed with the p35S::mRFP-SRL binary vector. The transgenic plants with GFP/mRFP co-expression (CSY2-GFP/mRFP-SRL and CSY3-GFP/mRFP-SRL) were obtained through selection with hygromycin and kanamycin.

To demonstrate co-localisation of GFP and mRFP, confocal observation of root hair cells from 7 day old seedlings co-expressing of both constructs was performed (Figure 3.9C and 3.9G). The images revealed that the distribution of CSY2-GFP and CSY3-GFP occurred in punctuate spherical structures (Figure 3.9D and 3.9H) and resembled the distribution of the peroxisomal marker mRFP-SRL (Figure 3.9E and

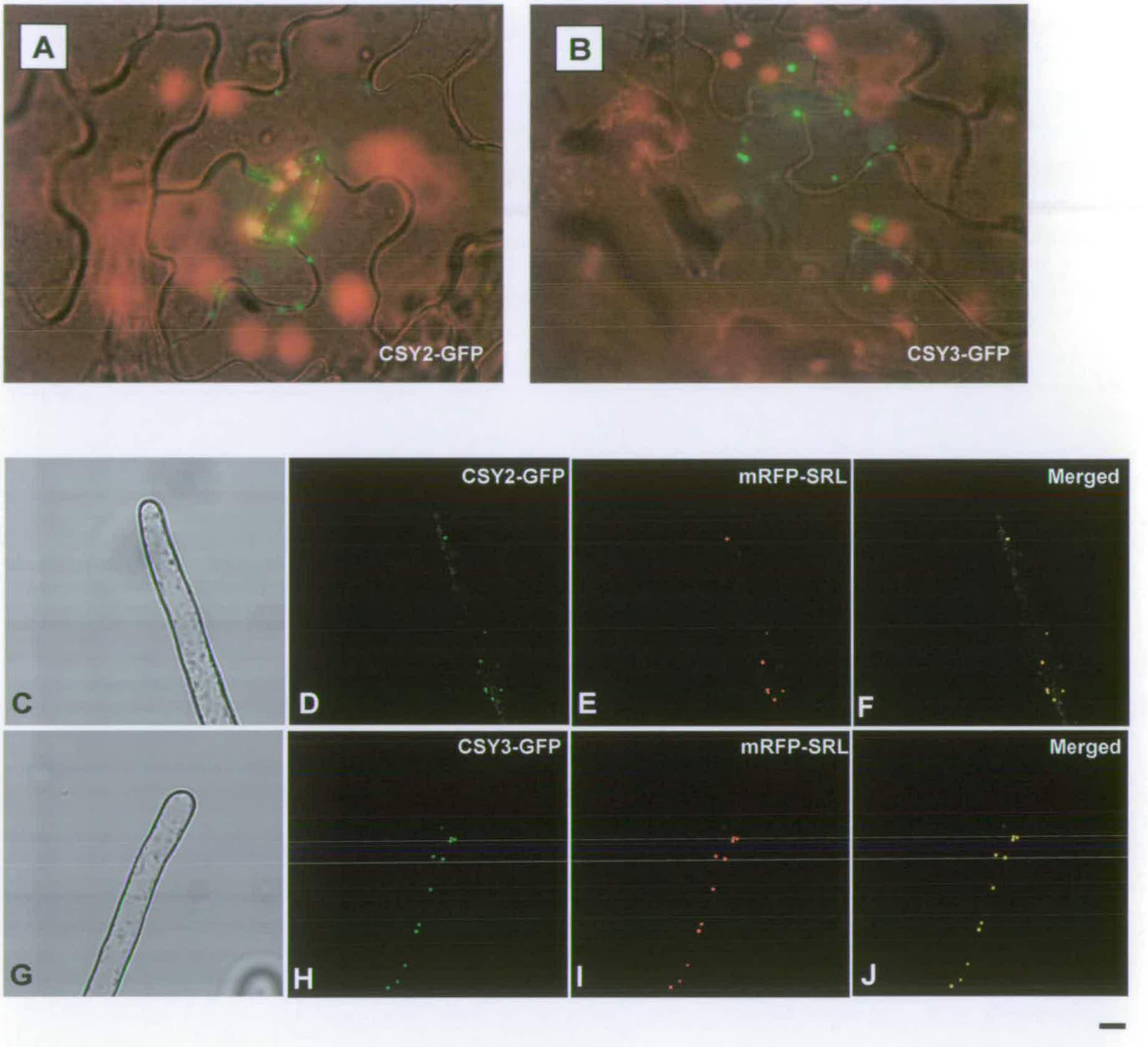

Figure 3.9 Localisation of CSY2-GFP and CSY3-GFP in peroxisomes of leaf epidermal cells **(A and B)**. Confocal images of root hair cells of transgenic Arabidopsis plants expressing CSY2- or CSY3-GFP and mRFP-SRL. Images are bright-field **(C and G)**, GFP signal **(D and H)**, mRFP signal **(E and I)** and merged GFP and mRFP **(F and J)** images. Scale bar = 10 µm.

3.9I). The merged images of GFP and mRFP (Figure 3.9F and 3.9J) confirmed that CSY2-GFP and CSY3-GFP co-localised with mRFP. The peroxisomal localisation of the mRFP-SRL protein was independently confirmed by Dr Imogen Sparkes (Oxford Brookes University). No evidence was found for targeting of GFP or mRFP to organelles other than peroxisomes. Therefore, CSY2 and CSY3 are peroxisomal proteins which are targeted by the PTS2 signal.

3.4 Isolation and characterisation of citrate synthase knock-out mutants

Potential knock-out (KO) mutants with T-DNA insertions in the structural genes *CSY2* and *CSY3* were found in databases of Arabidopsis KO centres. Seeds from these lines were ordered and each homozygous KO mutant was isolated through PCR screening. To screen, two PCR reactions were performed in each plant with the following primer combinations; (i) T-DNA LB primer and one gene-specific primer (to amplify the junction fragment) and (ii) two gene-specific primers (to amplify the genomic fragment). Figure 3.10 demonstrates the principle of PCR based screening. In this case screening for *csy2-1* is illustrated. Wild type plants allowed only genomic fragments to be amplified. On the other hand, homozygous plants, with T-DNA insertions in both alleles of the structural genes, allowed only junction fragments to be amplified. The heterozygous plants with one allele disrupted allowed both genomic fragments and junction fragments to be amplified.

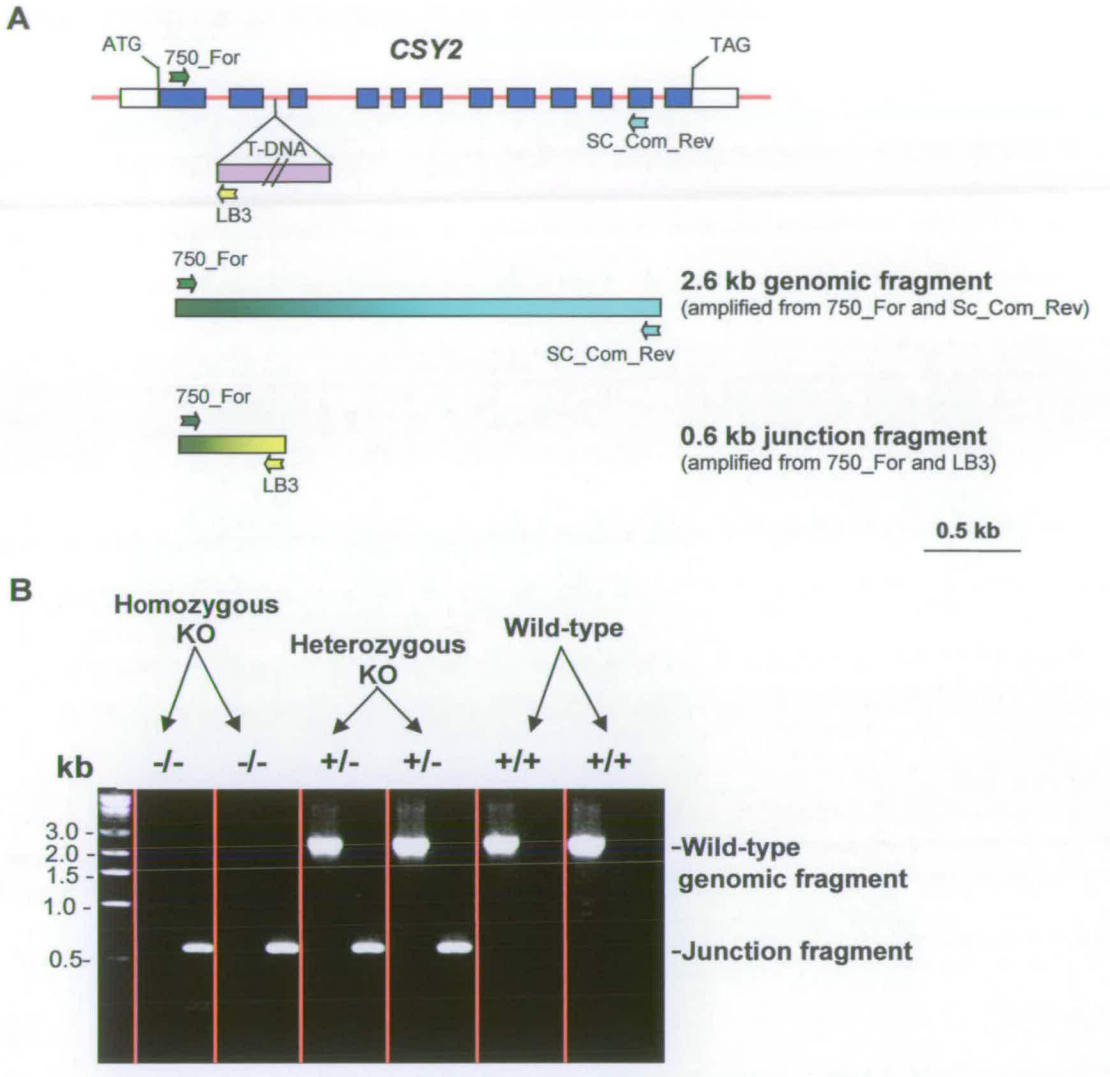

Figure 3.10 PCR-based screening for *csy2-1* mutant. **(A)**, Gene structure of *CSY2* showing position of the T-DNA. Exons are blue boxes, introns red lines and untranslated regions white boxes. **(B)**, PCR-based screening to distinguish homozygous knockout mutants, heterozygous plants and wild type plants.

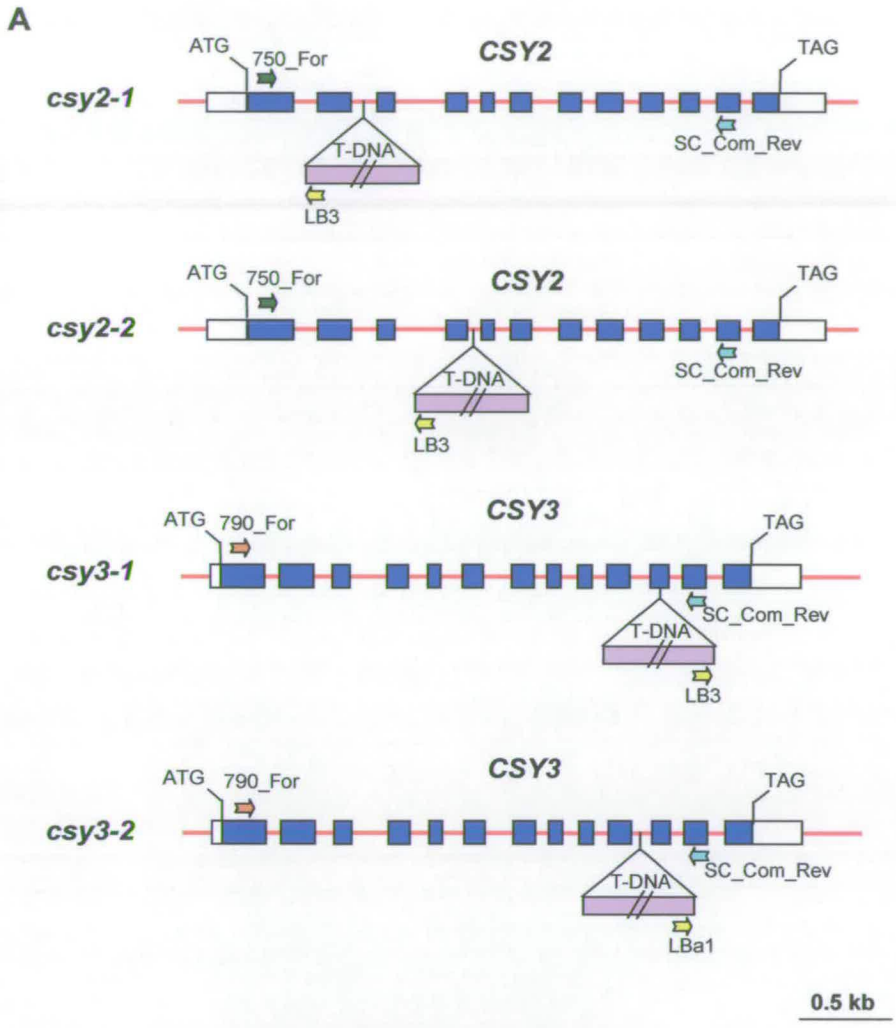

Figure 3.11 (A), Diagram showing gene structure of *CSY2* and *CSY3* with positions of the T-DNAs in individual mutants. Exons are blue boxes, introns red lines and untranslated regions white boxes. **(B),** RT-PCR with RNA isolated from 2-day old seedlings.

Table 3.2 Null mutants of *CSY* genes

Mutant	Source	Plant Selectable Maker	Gene disruption	Position of T-DNA insertion (A of start codon = 1)	Direction of left border
csy2-1	Syngenta	Basta	*CSY2*	853	Toward 5' end
csy2-2	Syngenta	Basta	*CSY2*	1475	Toward 5' end
csy3-1	Syngenta	Basta	*CSY3*	2410	Toward 3' end
csy3-2	Salk	Kanamycin	*CSY3*	2312	Toward 3' end

The homozygous KO plants that gave the resulting PCR junction fragment without a gene-specific genomic fragment were collected. Two independent mutants for each of *CSY2* and *CSY3* were isolated and named *csy2-1*, *csy2-2*, *csy3-1* (Syngenta; Sessions et al., 2002) and *csy3-2* (Salk; Alonso et al., 2003) (Table 3.2). The junction fragments from each line were then subjected to nucleotide sequencing using the T-DNA LB primer and one gene-specific primer. The results showed that the nucleotide sequence from each junction fragment corresponded to the genomic sequence of the gene which was expected to contain the T-DNA insertion. The position of the T-DNA insertion in the structural gene in each mutant was determined as shown in Table 3.2 and Figure 3.11A. To confirm the absence of RNA in these mutants, RT-PCR analysis was performed using RNA template from day 2 seedlings. Results reveal that *csy2-1* and *csy2-2* have no detectable CSY2 RNA and *csy3-1* and *csy3-2* have no detectable CSY3 RNA (Figure 3.11B).

CSY is believed to be involved in fatty acid breakdown to supply seedlings with energy and carbon skeletons. Knocking out *CSY* may therefore reveal phenotypes in germination and seedling growth. To determine whether *csy2* and *csy3* reveal any

obvious phenotype, the germination and seedling growth in *csy2* and *csy3* were compared to wild type in various conditions. In the absence of sucrose, *csy2* and *csy3* seeds are able to germinate normally but seedling growth was slightly impaired compared to that of wild type in both light and dark conditions (Figure 3.12A; Table 3.3, 3.4). When grown in the presence of 1% (w/v) sucrose, mutant and wild type seedling growth is indistinguishable. Furthermore, growth and development of *csy2* and *csy3* mutants in soil beyond the seedling stage is indistinguishable from wild type (results not shown).

Previous studies have shown that mutants defective in β-oxidation are not sensitive to the pro-herbicide 2,4-dichlorophenoxybutyric acid (2,4-DB) (Hayashi et al., 1998; Richmond and Bleecker, 1999; Zolman et al., 2001; Footitt et al., 2002). On the other hand, the mutants defective in glyoxylate cycle, *mls* and *icl*, have phenotypes like wild type plants which show sensitivity to 2,4-DB as β-oxidation is still sufficient to convert 2,4-DB into the root inhibiting auxin, 2,4-dichlorophenoxyacetic acid (2,4-D) (Pracharoenwattana, unpublished result). An experiment was carried out to determine the reponse of *csy2* and *csy3* to 2,4-DB. The results showed that *csy2, csy3* and wild type show similar sensitivity to 2,4-DB, suggesting that defects in peroxisomal β-oxidation in *csy2* and *csy3* mutants are not detectable (results not shown). However, it might be that knocking out only one CSY gene in *csy2* and *csy3* is not sufficient to reveal β-oxidation deficiency.

Total citrate synthase (CSY) activity was measured in wild type, *csy2-1*, and *csy3-1* seedlings at daily intervals (Figure 3.12B). Total CSY activity is highest at days 0 to

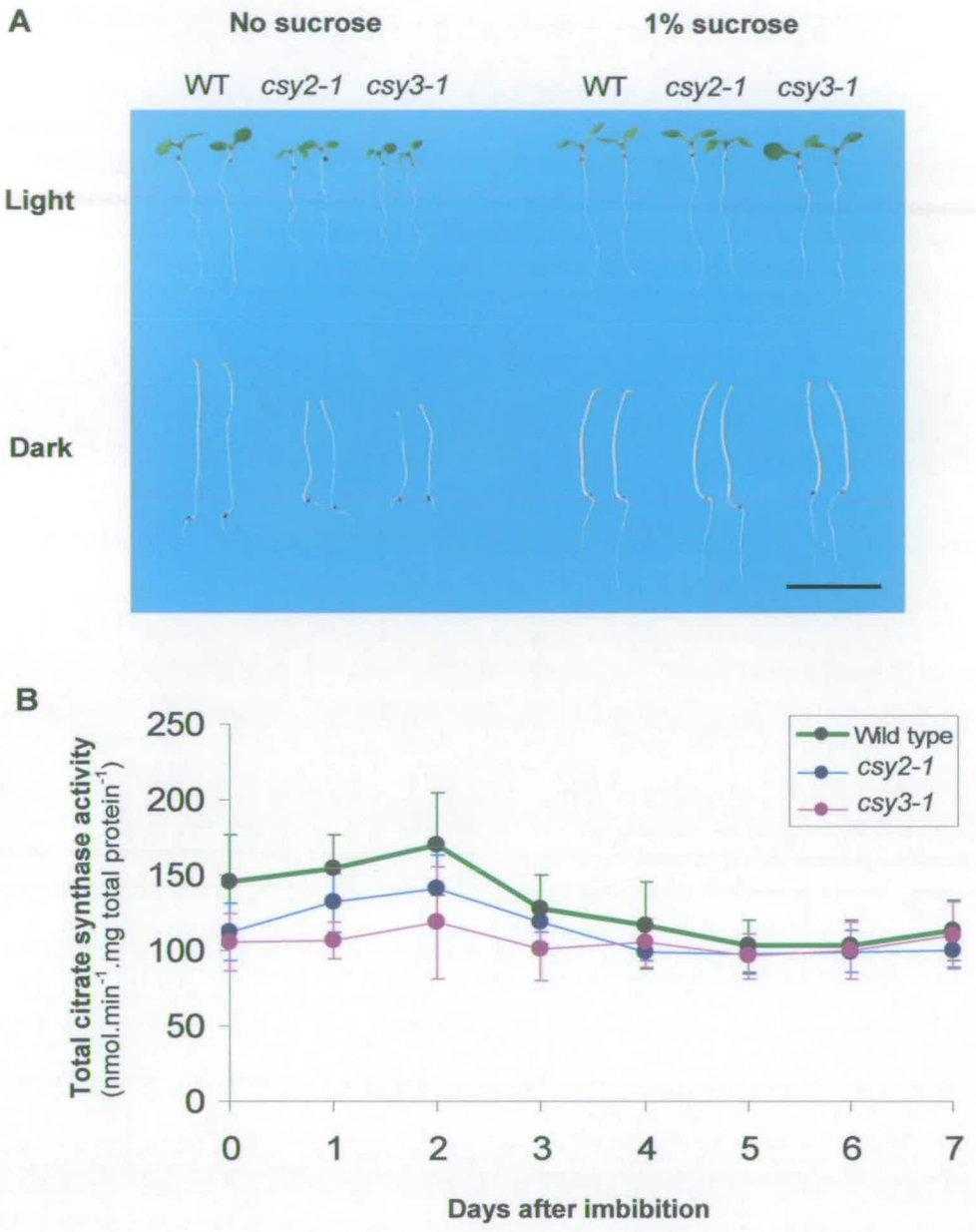

Figure 3.12 (A), Phenotypes of *csy* mutants. Seedlings were grown vertically on plates for 5 days in continuous light or dark in the presence or absence of 1% (w/v) sucrose. Scale bar = 1 cm. **(B),** Citrate synthase enzyme activity in total cell extracts of wild type and *csy* mutant seedlings from 0 to 7 days after imbibition. Data plotted are the mean ± SD, where green symbols are wild type, blue symbols are *csy2* and pink symbols are *csy3*. Three experiments each with three replicates were performed.

2 when TAG mobilisation begins, and is thereafter lower. This indicates a role for CSY in germination and seedling development. Both mutants have a small, but consistent, reduction in CSY activity at days 0 to 2 relative to wild type. The reduction of CSY activity in *csy2* is less than that of *csy3*, corresponding to the milder phenotype observed in *csy2*. The small reduction in total CSY activity in mutants is presumably due to the redundancy of *CSY* genes in Arabidopsis.

Table 3.3 Shoot length of wild type, *csy2* and *csy3* seedlings that were grown on plates in continuous light or dark in the presence or absence of 1% (w/v) sucrose for 5 days.

Condition	No sucrose			1% sucrose		
	WT	*csy2-1*	*csy3-1*	Wt	*csy2-1*	*csy3-1*
Light	0.12 ± 0.01	0.10 ± 0.01	0.01 ± 0.00	0.13 ± 0.01	0.13 ± 0.03	0.12 ± 0.02
Dark	1.32 ± 0.23	1.14 ± 0.14	0.93 ± 0.06	1.51 ± 0.27	1.22 ± 0.12	1.19 ± 0.16

Table 3.4 Root length of wild type, *csy2* and *csy3* seedlings that were grown on plates in continuous light or dark in the presence or absence of 1% (w/v) sucrose for 5 days.

Condition	No sucrose			1% sucrose		
	WT	*csy2-1*	*csy3-1*	Wt	*csy2-1*	*csy3-1*
Light	1.37 ± 0.21	1.24 ± 0.18	1.01 ± 0.13	1.60 ± 0.13	1.62 ± 0.19	1.51 ± 0.13
Dark	0.33 ± 0.07	0.25 ± 0.06	0.18 ± 0.02	0.95 ± 0.11	0.69 ± 0.11	0.55 ± 0.10

3.5 The citrate synthase double mutants

Mutants of *csy2* and *csy3* were crossed to make double mutants. The F1 double heterozygotes were allowed to self to generate F2. The F2 seeds were plated on medium containing 1% (w/v) sucrose which has been shown to be necessary and sufficient for seedling establishment in several β-oxidation mutants (Hayashi et al., 1998; Richmond and Bleecker, 1999; Germain et al., 2001; Zolman et al., 2001; Fulda et al., 2004). The F2 plants were subsequently grown in soil and genotype screening was carried out by PCR. The expected frequency of homozygous double mutants in F2 generation is 1 in 16. 400 plants were screened but surprisingly no such double mutant was detected. All the F2 plants which could grow and become mature plants were found to carry at least one *CSY* gene. However, it was observed that an appreciable proportion of F2 seeds were unable to germinate even though exogenous sucrose was provided. As shown in table 3.5 the progeny with the dormant seed phenotype fit the ratio of expected *csy2:csy3* double mutants in all cases of self-fertilised parents.

Table 3.5 Segregation of *csy2* and *csy3* alleles confers the double mutant ratio for the non-germinated seeds.

Parent (to be self-crossed)	Batch	Progeny (%)		χ^2 value (*P*)
		Germinated seed	Non-germinated seed	
CSY2/csy2-1, CSY3/csy3-1[a]	1	96	4	0.86 (>0.1)
	2	97	3	1.80 (>0.1)
	3	96	4	0.86 (>0.1)
CSY2/csy2-2, CSY3/csy3-1[a]	1	98	2	3.08 (>0.05)
	2	96	4	0.86 (>0.1)
	3	96	4	0.86 (>0.1)
CSY2/csy2-1, CSY3/csy3-2[a]	1	95	5	0.27 (>0.5)
	2	98	2	3.08 (>0.05)
	3	97	3	1.80 (>0.1)
CSY2/csy2-2, CSY3/csy3-2[a]	1	96	4	0.86 (>0.1)
	2	97	3	1.80 (>0.1)
	3	95	5	0.27 (>0.5)
CSY2/csy2-1, csy3-1/csy3-1[b]	1	80	20	1.33 (>0.1)
	2	82	18	2.61 (>0.1)
	3	72	28	0.48 (>0.1)
csy2-1/csy2-1, CSY3/csy3-1[b]	1	71	29	0.85 (>0.1)
	2	84	16	4.32 (>0.01)
	3	73	27	0.21 (>0.5)
CSY2/csy2-2, csy3-1/csy3-1[b]	1	79	21	0.85 (>0.1)
	2	78	22	0.48 (>0.1)
	3	80	20	1.33 (>0.1)
csy2-2/csy2-2, CSY3/csy3-1[b]	1	78	22	0.48 (>0.1)
	2	73	27	0.21 (>0.5)
	3	77	23	0.21 (>0.5)

[a]Double heterozygous mutant; expected 6.25% double homozygous mutant in progeny generation.

[b]Homozygous for one gene and heterozygous for another; expected 25% double homozygous mutant in progeny generation.

A previous study showed that the *cts* (comatose) mutants fail to germinate even when provided with sucrose, but can be induced to germinate by removal of the seed coat (Foottit et al., 2002). To determine if *csy2:csy3* mutants have a similar dormant phenotype, seeds from the F1 heterozygotes which failed to germinate after 5 days, incubation in the presence of 1% (w/v) sucrose, were surgically disrupted to remove the embryo, and incubated further in the presence of 3% (w/v) sucrose. Such embryos grew and developed into seedlings although they grew more slowly than wild type (Figure 3.13A). Genomic DNA and total RNA were isolated from those seedlings and were subjected to PCR and RT-PCR analysis (Figure 3.13B). The results showed that they were homozygous *csy2:csy3* double mutants. However, unlike seeds of the *cts* mutant, which can be induced to germinate by incubation with propionic or butyric acids, in *csy2:csy3* double mutants these organic acids did not apparently increase the frequency of germination (results not shown).

The *csy2:csy3* double mutants fail to establish mature plants when transferred to soil (Figure 3.13C and 3.13D) and crucially are unable to produce flowers and seeds (Figure 3.13D and 3.13E). Thus the best strategy to obtain homozygous *csy2:csy3* seeds as plant material for experimentation were from plants homozygous for either *csy2* or *csy3* and heterozygous for the other. For instance, double-mutant seeds were obtained from plants heterozygous for *csy2* and for homozygous *csy3* (Figure 3.14). It is expected that in the progeny generation, 25% will be homozygous *csy2:csy3* and hence dormant seeds. Another 75%, which can grow and develop normally are expected to contain as least one functional *CSY* gene as it is sufficient for plant growth and development. After several days incubation at 20°C, homozygous

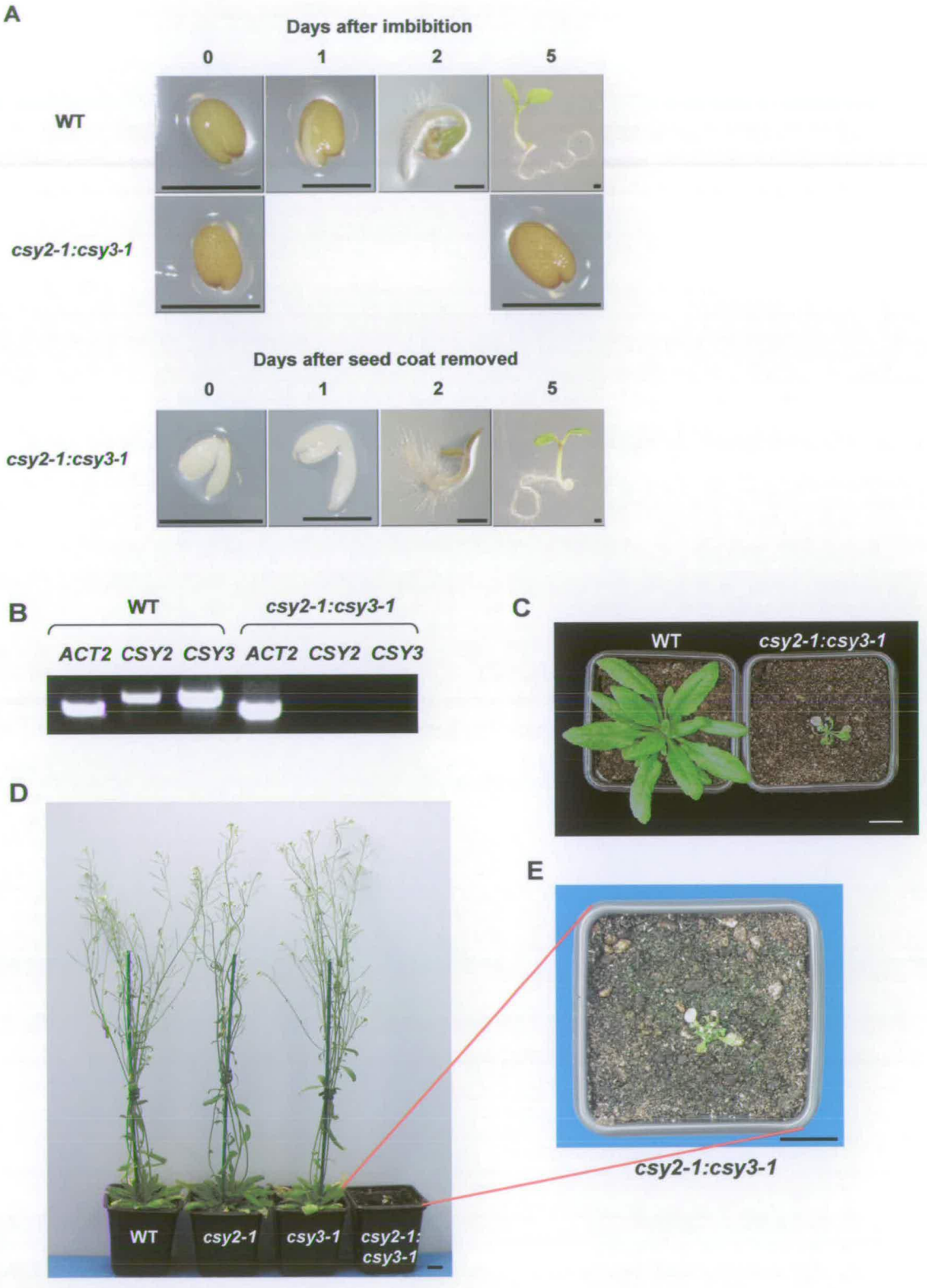
A
Days after imbibition
0
1
2
5
WT
csy2-1:csy3-1
Days after seed coat removed
0
1
2
5
csy2-1:csy3-1
B
WT
csy2-1:csy3-1
ACT2 CSY2 CSY3 ACT2 CSY2 CSY3
C
WT
csy2-1:csy3-1
D
WT
csy2-1
csy3-1
csy2-1:
csy3-1
E
csy2-1:csy3-1

Figure 3.13 (Previous Page) Characterisation of *csy2:csy3* double mutants. **(A),** Wild type seedling during first 5 days after imbibition compared to *csy2-1:csy3-1* double mutant at days 0 and 5 in the light on ½ MS medium plus 1% (w/v) sucrose. Bottom, *csy2-1:csy3-1* after seed coat removal and plated on ½ MS Medium plus 3% (w/v) sucrose. Scale bars = 1 mm. **(B),** RT-PCR of ACT2 (actin), *CSY2* and *CSY3* RNAs from 2-day old wild type and *csy2-1:csy3-1* seedlings. **(C),** Phenotypes of 4 week-old wild type and *csy2-1:csy3-1*. Scale bars = 1 cm. **(D),** Phenotypes of 7 week-old wild type, *csy2-1*, *csy3-1* and *csy2-1:csy3-1*. Scale bars = 1 cm. **(E),** *csy2-1:csy3-1* phenotype same as **(D)** from top view. Scale bars = 1 cm.

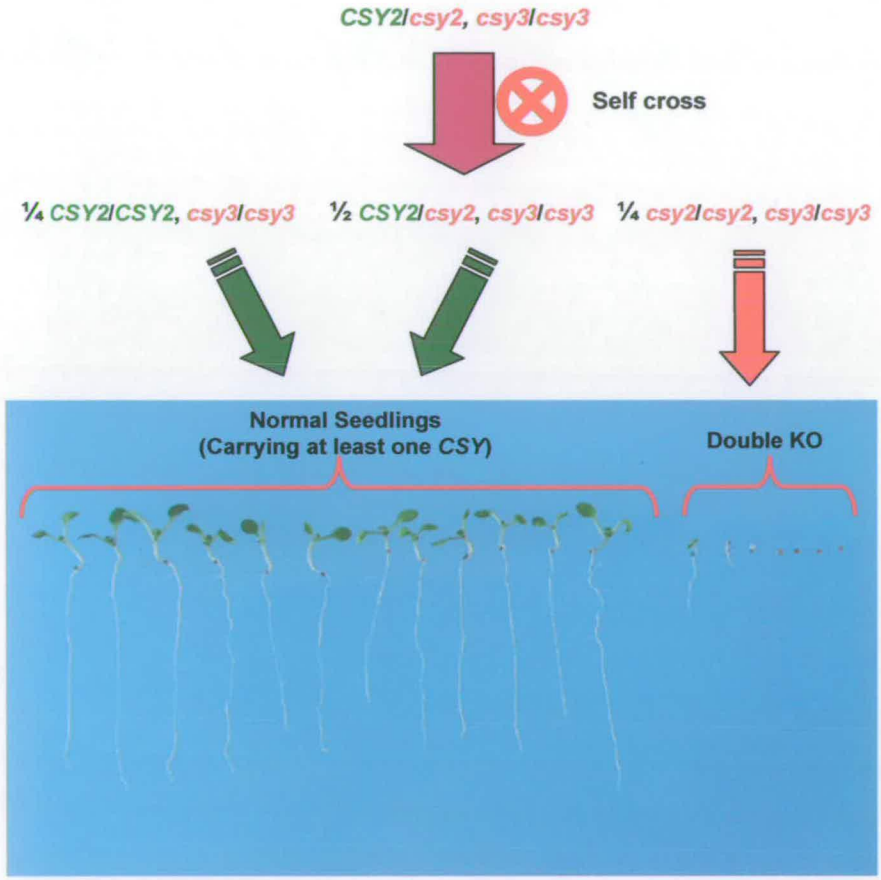

Figure 3.14 Illustration of strategy to supply homozygous *csy2:csy3* seeds from parent plants which are heterozygous for *csy2* and homozygous for *csy3*.

csy2:csy3 seeds were identified by means of their failure to germinate. Such non-germinated seeds were surgically treated to disrupt the seed coat and plated on medium containing 3% (w/v) sucrose. Such seeds and seedling could be used for analysis of the double mutant phenotype. However some homozygous *csy2:csy3* are able to germinate spontaneously without any surgical treatment (Figure 3.14) but such *csy2:csy3* seedlings are very small and stressed compared to wild type.

To determine the reduction of CSY activity in *csy2:csy3* seedlings, *csy2:csy3* seeds which had not germinated after 2 days, incubation on medium in the presence of 1% (w/v) sucrose, were isolated and forced to germinate by seed coat removal. The *csy2:csy3* seeds were allowed to grow for 2 days. These seedlings were assayed for CSY activity, together with 2-day-old wild type, *csy2* and *csy3* seedlings which had germinated normally. The results show that the *csy2:csy3* seedlings contain only about 25% of CSY activity compared to wild type (Figure 3.15). The remaining CSY is presumably mitochondrial.

To demonstrate that the *csy2:csy3* phenotype is due to the disruption of *CSY* genes and not due to secondary mutations which could have occurred during transformation by T-DNA, four independent double knockouts were generated from all possible combinations of the two single knockout *csy2* and two single knockout *csy3* mutants. In all cases the homozygous *csy2:csy3* mutants were isolated and subsequently confirmed to be missing *CSY2* and *CSY3* mRNA by RT-PCR. The dormant seed phenotype was observed in all homozygous *csy2:csy3* mutants and the mature plants showed the arrested phenotype when compared to wild type (results not shown).

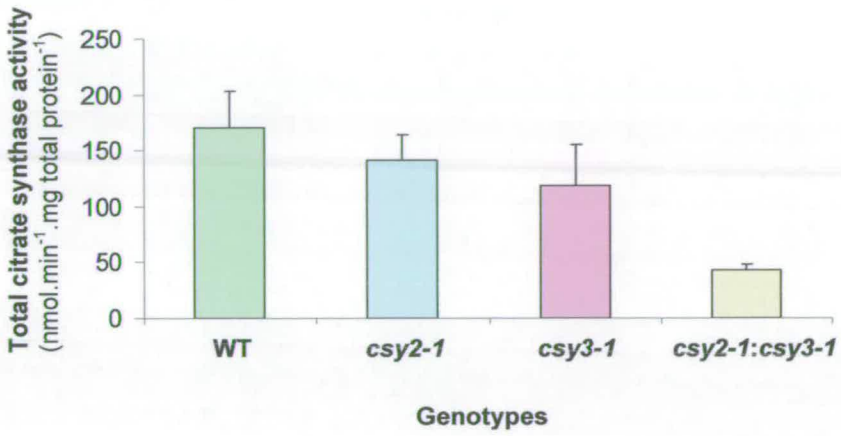

Figure 3.15 Total citrate synthase enzyme activity in 2-day old seedlings grown in continuous light in the presence of 1% sucrose. Data are the mean ± SD where green box is wild type, blue box is *csy2-1*, pink box is *csy3-1* and yellow is *csy2-1:csy3-1*. Three experiments each with three replicates were performed.

3.6 Complementation of the double mutant with *CSY* genes

To confirm that the phenotype in *csy2:csy3* is caused specifically by the lack of a functional *CSY* gene and not due to inherent disruption of expression of other specific genes caused as a consequence of T-DNA insertion in a *CSY* gene, transgenic complementation was employed.

The first construct was generated from full-length *CSY3* cDNA containing the native PTS2 targeting sequence at the N-terminus. Pfu polymerase was used to amplify the cDNA coding sequence with HindIII_790_For and EcoRI_790_Rev primers. During the amplification, the restriction sites *Hin*dIII and *Eco*RI were introduced into the 5' end and the 3' end of the fragment respectively. The PCR product was then digested with *Hin*dIII and *Eco*RI and inserted in between the double 35S promoter and CaMV terminator of pGreen0179-2x35S::Ter (Pracharoenwattana, unpublished result) to generate p35S::CSY3 (Figure 3.16A). Plants which were heterozygous *CSY2/csy2* and homozygous *csy3/csy3* were subjected to Agrobacterium floral dipping transformation. Fourteen T_0 plants carrying the transgene were obtained through hygromycin selection (in the presence of sucrose). The PCR was subsequently carried out to identify and isolate only the plants that displayed the homozygous *csy2:csy3* genotype among T_0 plants. This PCR detection was on the basis that in the homozygous *csy2:csy3* mutant containing *CSY3* cDNA transgene, *CSY2* and *CSY3* genomic fragments would fail to amplify but the *CSY3* cDNA transgene would amplify. Several homozygous *csy2:csy3* mutants containing the transgene were obtained.

A previous study showed that a PTS2 sequence can be responsible for dual targeting of citrate synthase to both peroxisome and mitochondria in yeast (Lee et al., 2000). To demonstrate that the homozygous *csy2:csy3* mutant phenotype is due to the disruption of CSY in the peroxisome but not mitochondria, another complementation was been carried out. The second construct with a modified *CSY3* cDNA was generated in which the first 60 bases, corresponding to the PTS2 signal sequence were deleted. The cDNA was then provided with a PTS1 sequence, corresponding to last 10 amino acids of the pumpkin *MLS* gene (as in section 3.3.2). This PTS1 sequence has been confirmed to be a peroxisomal targeting sequence (Hayashi et al., 1996). The construct was made by PCR using Pfu polymerase. The fragment was amplified with the introduction of a *Hin*dIII site at the 5'end using HindIII_790_61 primer and introduction of the PTS1 signal sequence and *Eco*RI site at the 3' end using 790_SRL_Rev primer and EcoRI_SRL_Rev primers. The ΔCSY3-SRL PCR fragment was then digested with *Hin*dIII and *Eco*RI and inserted between the double 35S promoter and CaMV terminator of pGreen0179-2x35S::Ter (Pracharoenwattana, unpublished result) to generate p35S::ΔCSY3-SRL (Figure 3.16B). Plants which were heterozygous *CSY2/csy2* and homozygous *csy3/csy3* were subjected to Agrobacterium floral dipping transformation. The T_0 transformants were obtained through hygromycin selection. PCR was subsequently used to verify *csy2:csy3* mutants containing the transgene from those T_0 plants.

The homozygous *csy2:csy3* plants containing either 35S::CSY3 cDNA or 35S::ΔCSY3-SRL transgenes are able to germinate and grow normally (Figure 3.17).

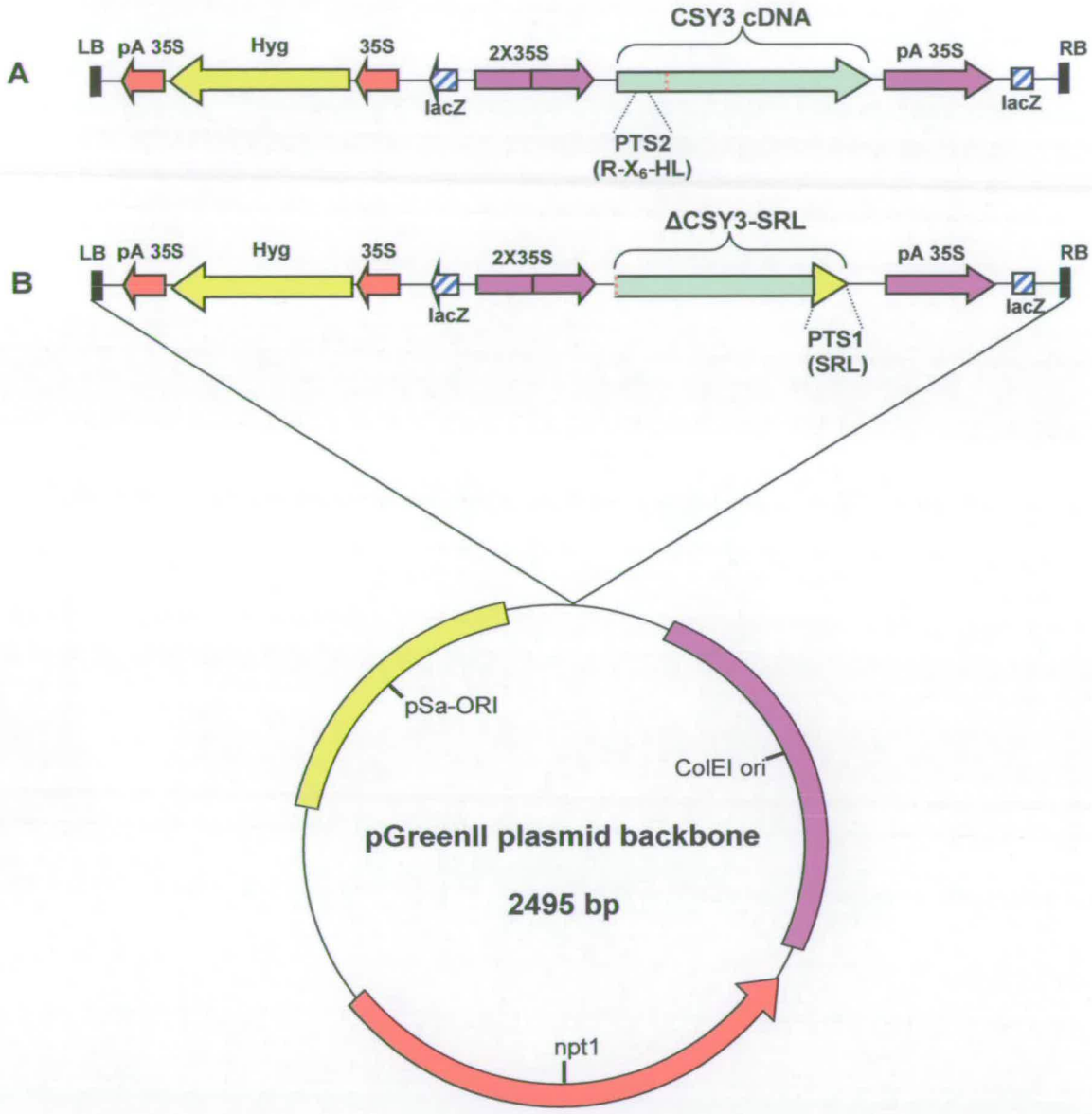

Figure 3.16 Schematic diagram of binary vector p35S::CSY3 **(A)** and p35S::ΔCSY3-SRL **(B)**

Figure 3.17 (Next Page) (A), Diagram showing CSY3 containing the native PTS2 (R-X_6-HL) at the N-terminus (i) and ΔCSY3-SRL which is truncated CSY3 in which PTS2 is replaced with PTS1 (SRL) (ii). **(B)**, 4-week-old phenotypes of (i) wild type, (ii) *csy2-1:csy3-1, (iii) csy2:csy3* complemented with *CSY3* cDNA with authentic PTS2 sequence, (iv) *csy2:csy3* complemented with *CSY3* cDNA with PTS2 sequence replaced by PTS1. **(C)**, the same as **(B)** but allowed to grow further for 7 weeks.

A

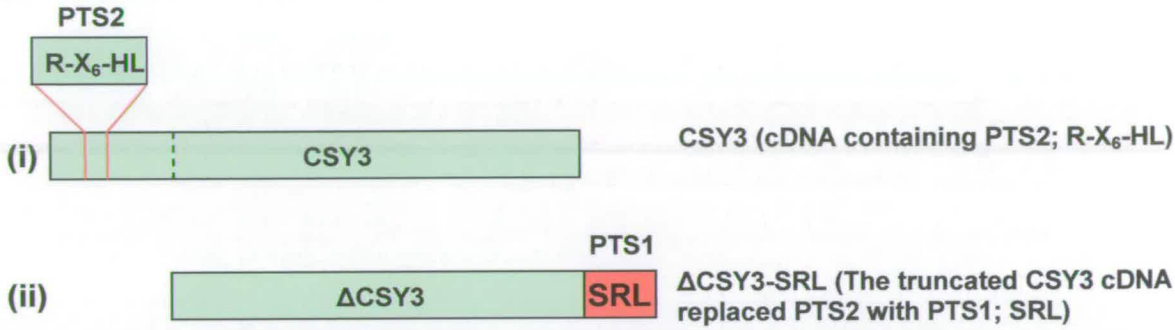

B

(i) WT (ii) *csy2:csy3* (iii) PTS2 (iv) PTS1

C

(i) WT (ii) *csy2:csy3* (iii) PTS2 (iv) PTS1

This result shows that the dormant seed and impaired plant growth phenotype is caused by the absence of peroxisomal CSY.

3.7 Defect in fatty acid β-oxidation in the double mutant

To examine lipid reserve mobilisation in the *csy2:csy3* double mutant, transmission electron microscopic examination of cotyledons was carried out. The sections were prepared from rare *csy2:csy3* double mutant seedlings which germinated spontaneously and grew for 5 days. The genotype of such seedlings was confirmed by RT-PCR analysis of one cotyledon while the other was used for electron microscopy. The results showed a striking inability to break down lipid bodies in *csy2:csy3* double mutant (Figure 3.18C and 3.18D). In comparison lipid bodies are not present in wild type seedlings at day 5 (Figure 3.18A and 3.18B). These results are consistent with those observed with *kat2/ped1* (Hayashi et al., 1998; Germain et al., 2001) and *cts1* (Footitt et al., 2002) seedlings (see section 1.9). Cells from wild type cotyledons were highly vacuolated with plenty of well-developed chloroplasts containing abundant starch granules. In contrast, cells from *csy2:csy3* double mutant cotyledons revealed small vacuoles and unusual chloroplasts. Like peroxisomes observed in the *kat2* mutant (Germain et al., 2001), peroxisomes containing unusual structures are found (Figure 3.18D). However the peroxisomes in *csy2:csy3* double mutant seedlings at day 5 were not obviously very large as compared to wild type, and are therefore similar to those observed in *cts* mutants (Footitt et al., 2002).

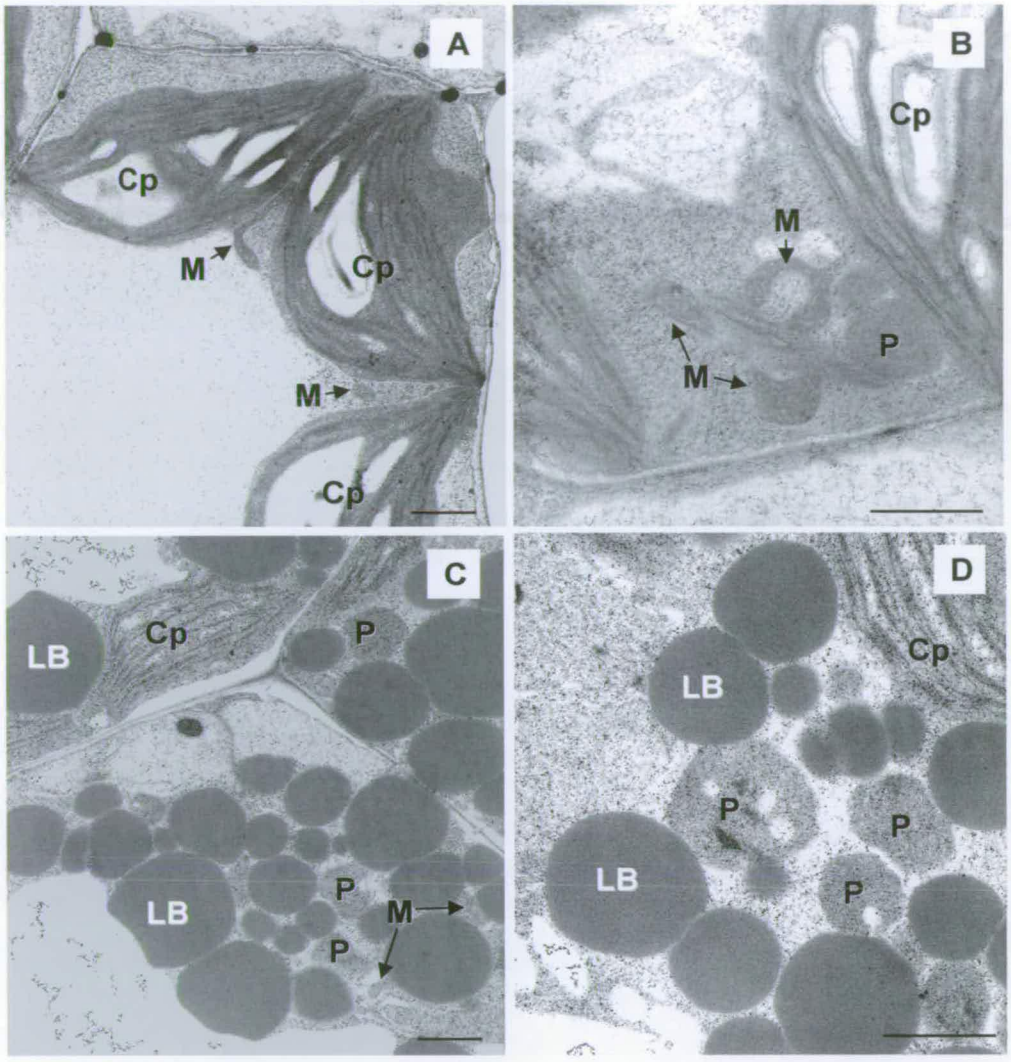

Figure 3.18 Transmission electron micrograph from cotyledon of 5-day old wild type **(A)** and **(B)** and *csy2-1:csy3-1* which germinated spontaneously **(C)** and **(D)**. Scale bars are 1 µm. P, peroxisomes; M, mitochondria; Cp, chloroplasts; LB, lipid bodies.

To provide further information that lipid mobilisation is blocked, triacylglycerol (TAG) content was measured in *csy2:csy3* double mutants compared to wild type. TAG was determined by the quantitation of eicosenoic acid (20:1) using gas chromatography and mass spectrometry (Browse et al., 1986). Embryos were removed from dormant seeds at day 1.5 and grown for 2, 3, 4 and 5 days and TAG quantification carried out. During the period of time the TAG content in *csy2:csy3* double mutants does not change while the TAG content in wild type decreases rapidly and is almost absent at day 5 (Figure 3.19). It is not possible to identify homozygous mutant seed before 1.5 days. Nevertheless, since TAG does not decline after day 1.5, and is similar in amount to that of wild type seedlings at day 0, TAG content in the double mutant presumably not decline between day 0 and day 1.5.

To establish that the block of TAG mobilisation in *csy2:csy3* double mutants is due to a defect in β-oxidation, the resistance to pro-herbicide 2,4-dichlorophenoxybutyric acid (2,4-DB) was tested. This compound can be converted by peroxisomal β-oxidation to the herbicide 2,4-dichlorophenoxyacetic acid (2,4-D) resulting in an inhibition of root growth (Wain and Wightman, 1954). Previous experiments showed that mutants defective in β-oxidation are unable to metabolise 2,4-DB and seedlings were then found to be resistant to 2,4-DB (Hayashi et al., 1998; Richmond and Bleecker, 1999; Zolman et al., 2001; Footitt et al., 2002). The *csy2:csy3* double mutant embryos obtained by surgical removal from dormant seeds were grown on medium containing 2,4-DB and 3% (w/v) sucrose. The results showed that the *csy2:csy3* double mutant seedlings are resistant to 2,4-DB while wild type, *csy2,* and

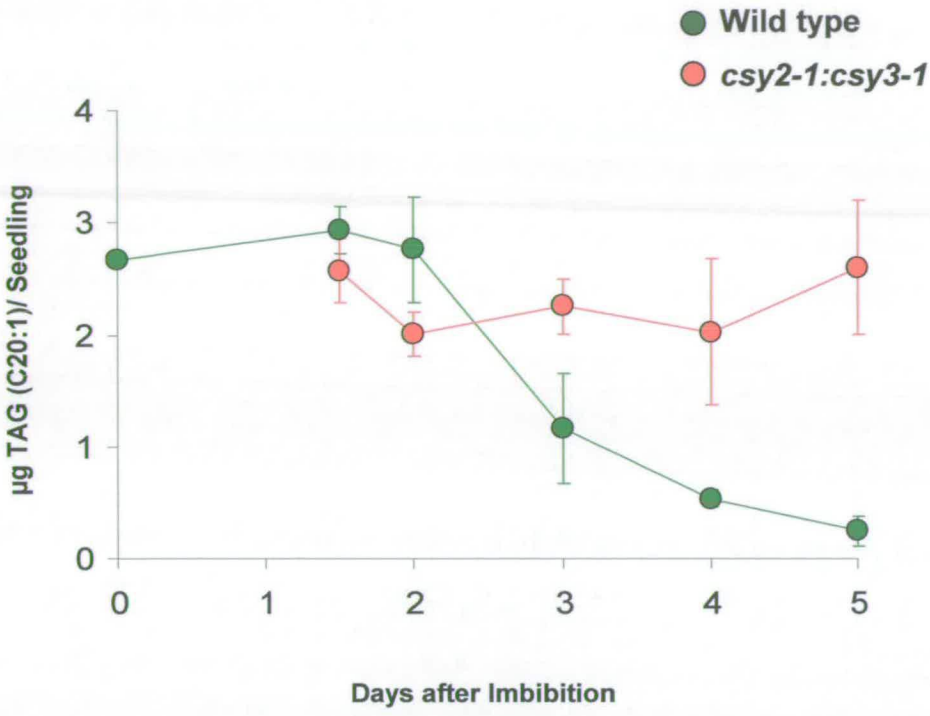

Figure 3.19 TAG content of wild type (green symbols) and *csy2:csy3* (red symbols) seedlings. C20:1, used as a marker for TAG, was detected by GC-MS in triplicate batches of 20 seedlings grown in continuous light on ½ MS medium plus 3% (w/v) sucrose. Data are the mean ± SD.

csy3 are sensitive (Figure 3.20A). This result indicates that peroxisomal β-oxidation is defective in the *csy2:csy3* double mutant.

RT-PCR analysis on 2-day-old seedlings revealed that the gene encoding the major mitochondrial CSY (*CSY4*) is expressed normally, confirming that the *csy2:csy3* double mutant phenotype is not due to the disruption of mitochondrial CSY (Figure 3.20B). Furthermore genes encoding key β-oxidation enzymes including *LACS7*, *ACX2*, *MFP2*, *KAT2* are expressed normally in *csy2:csy3* double mutant compared to wild type (Figure 3.20B). This indicates that there is not a generalised depression of expression of such β-oxidation relevant genes, but rather a specific block in peroxisomal CSY which leads to the block in β-oxidation.

During starvation and senescence structural molecules including lipids are degraded and the resulting nutrients transported to younger actively growing tissue or storage (Hooks, 2002). β-oxidation genes are induced to increase the activity of lipid mobilisation. Previous reports demonstrated that genes involved in β-oxidation are induced during tissue starvation including *ACX3* and *ACX4* (Froman et al., 2000, Eastmond et al., 2000a), *MFP2* (Eastmond and Graham, 2000), and *KAT2* (Froman et al., 2000). To determine whether peroxisomal *CSY* genes are expressed in a similar way to the β-oxidation genes, RT-PCR analysis on starved tissue was carried out. The starved tissue was prepared from detached leaves which were incubated in the dark for 0, 2 and 4 days. The RT-PCR results showed that expression of *CSY2* and *CSY3* genes is increased together with those of β-oxidation (*LACS7*, *ACX2*, *MFP2*, *KAT2*) (Figure 3.21). The major mitochondrial CSY4 is not increased as this does not

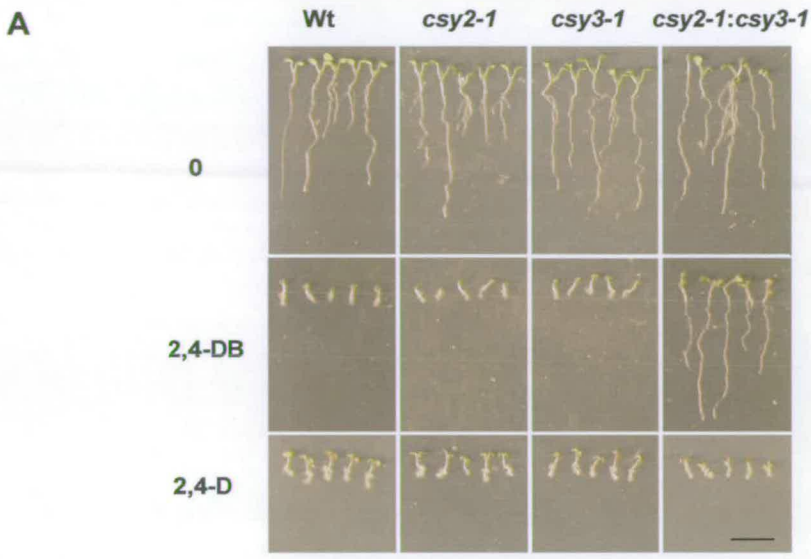
A
Wt
csy2-1
csy3-1
csy2-1:csy3-1
0
2,4-DB
2,4-D

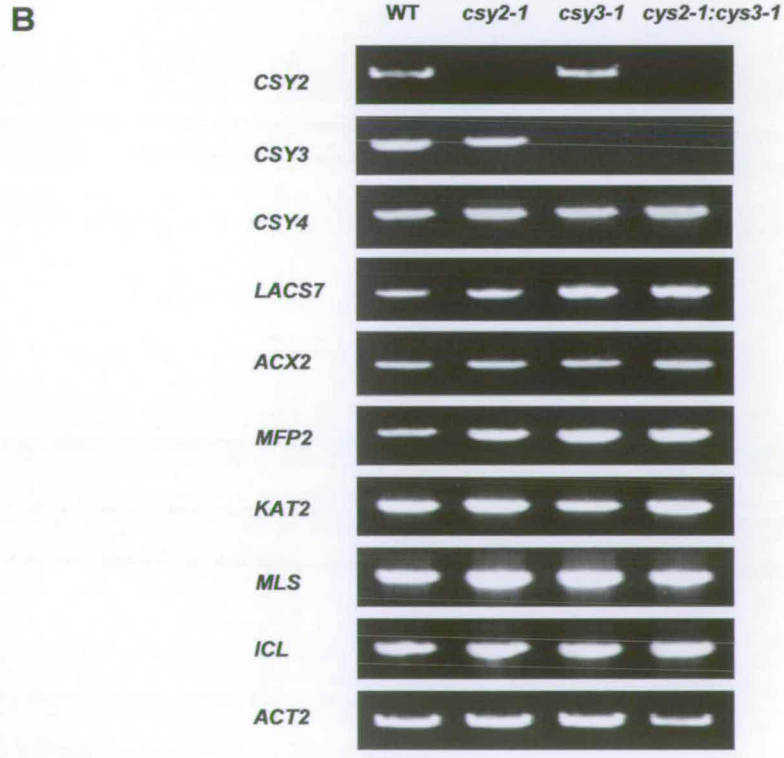
B
WT
csy2-1
csy3-1
cys2-1:cys3-1
CSY2
CSY3
CSY4
LACS7
ACX2
MFP2
KAT2
MLS
ICL
ACT2

Figure 3.20 (Previous Page) (A), Seedlings on ½ MS plus 3% (w/v) sucrose (control) and plus 200 ng/ml 2,4-DB or 50 ng/ml 2,4-D. Scale bar =1 cm. **(B),** Expression of citrate synthase (CSY), β-oxidation and glyoxylate cycle genes detected by RT-PCR using RNA isolated from 2-day old light-grown seedlings. The amount of cDNA template in each RT-PCR reaction was normalised to the signal from the *ACT2* gene. *CSY4*, mitochondrial citrate synthase; *LACS7*, peroxisomal long chain acyl-CoA synthetase; *ACX2*, acyl-CoA oxidase 2; *MFP2*, multifunctional protein 2; *KAT2*, 3-ketoacyl-CoA thiolase; *MLS*, malate synthase; *ICL*, isocitrate lyase.

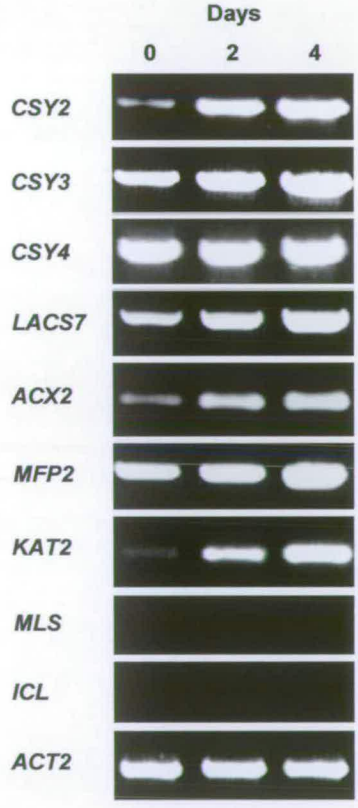

Figure 3.21 Expression of β-oxidation genes in starved leaves detected by RT-PCR using RNA isolated from detached leaves after 0, 2 and 4 days incubation in the dark. *CSY*, citrate synthase *CSY4*, mitochondrial citrate synthase; *LACS7*, peroxisomal long chain acyl-CoA synthetase; *ACX2*, acyl-CoA oxidase 2; *MFP2*, multifunctional protein 2; *KAT2*, 3-ketoacyl-CoA thiolase; *MLS*, malate synthase; *ICL*, isocitrate lyase.

play a role in β-oxidation. Expression of genes encoding unique enzymes for the glyoxylate cycle (*ICL* and *MLS*) is not detected in this case, indicating that the glyoxylate cycle is not active. These results suggest that peroxisomal CSY is more than just a glyoxylate cycle enzyme, but is also required for β-oxidation and fatty acid respiration.

Chapter 4

The Function of Peroxisomal Malate Dehydrogenase (PMDH)

4.1 Identification of *PMDH* genes in Arabidopsis

4.2 Expression analysis of *PMDH* genes

4.3 Analysis of PMDH subcellular localisation

4.4 Isolation of *pmdh1* and *pmdh2* knockout mutants

4.5 Analysis of the double mutant

4.6 In vitro expression of PMDH proteins and western blot analysis

4.7 Complementation of the double mutant with *PMDH* genes

Chapter 4

The Function of Peroxisomal Malate Dehydrogenase (PMDH)

4.1 Identification of *PMDH* genes in Arabidopsis

The genome project of Arabidopsis has revealed that there are eight genes predicted to encode NAD^+-dependent malate dehydrogenase (MDH) in the Arabidopsis genome (there is one $NADP^+$-dependent malate dehydrogenase, which localized in chloroplasts). These MDHs are known to be compartmentalised in several organelles: peroxisomes, mitochondria and chloroplasts, as well as in the cytosol. Based on gene annotations and subsequent phylogenetic tree analysis (Figure 4.1), these MDHs are divided into 4 major groups. One group which is believed to be peroxisomal is comprised of At2g22780 and At5g09660, and here named PMDH1 and PMDH2 respectively. Both reveal a similar sequence to watermelon PMDH (Gietl 1990; Gietl et al., 1994). PMDH1 and PMDH2 are predicted to be peroxisomal because of an obvious type 2 peroxisomal targeting sequence (PTS2) at the N-terminus (Figure 4.2). This PTS2 is a nonapeptide motif R-$(X)_6$-H/Q-A/L/F (Kato et al., 1996; 1998; Mullen, 2002), downstream of which is a conserved cysteine residue. This conserved cysteine is essential for proteolytic processing of PTS2-containing

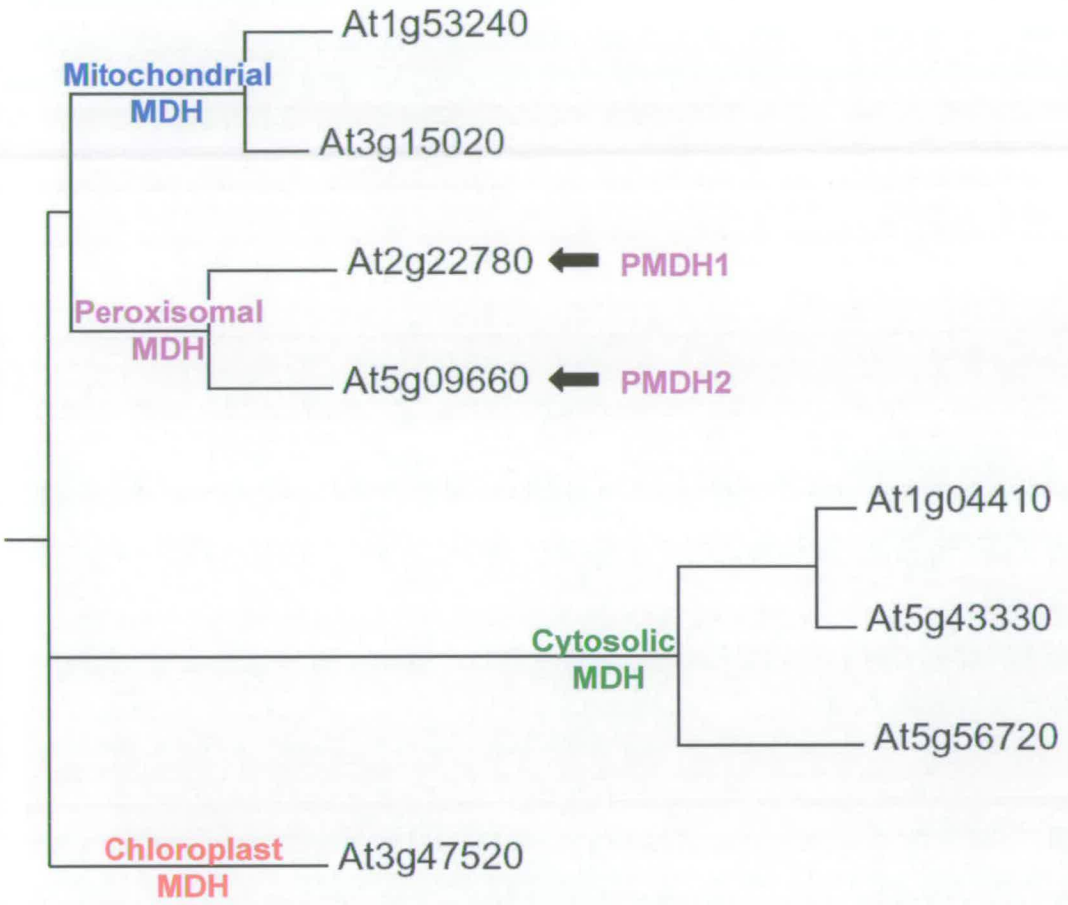

Figure 4.1 Phylogenetic tree of eight NAD^+-dependent MDH proteins from Arabidopsis. Sequences were aligned with ClustalX (Thompson et al., 1997) and the tree was constructed by Phylodendron (version 0.8d, by D.G. Gilbert, http://iubio.bio.indiana.edu/treeapp/).

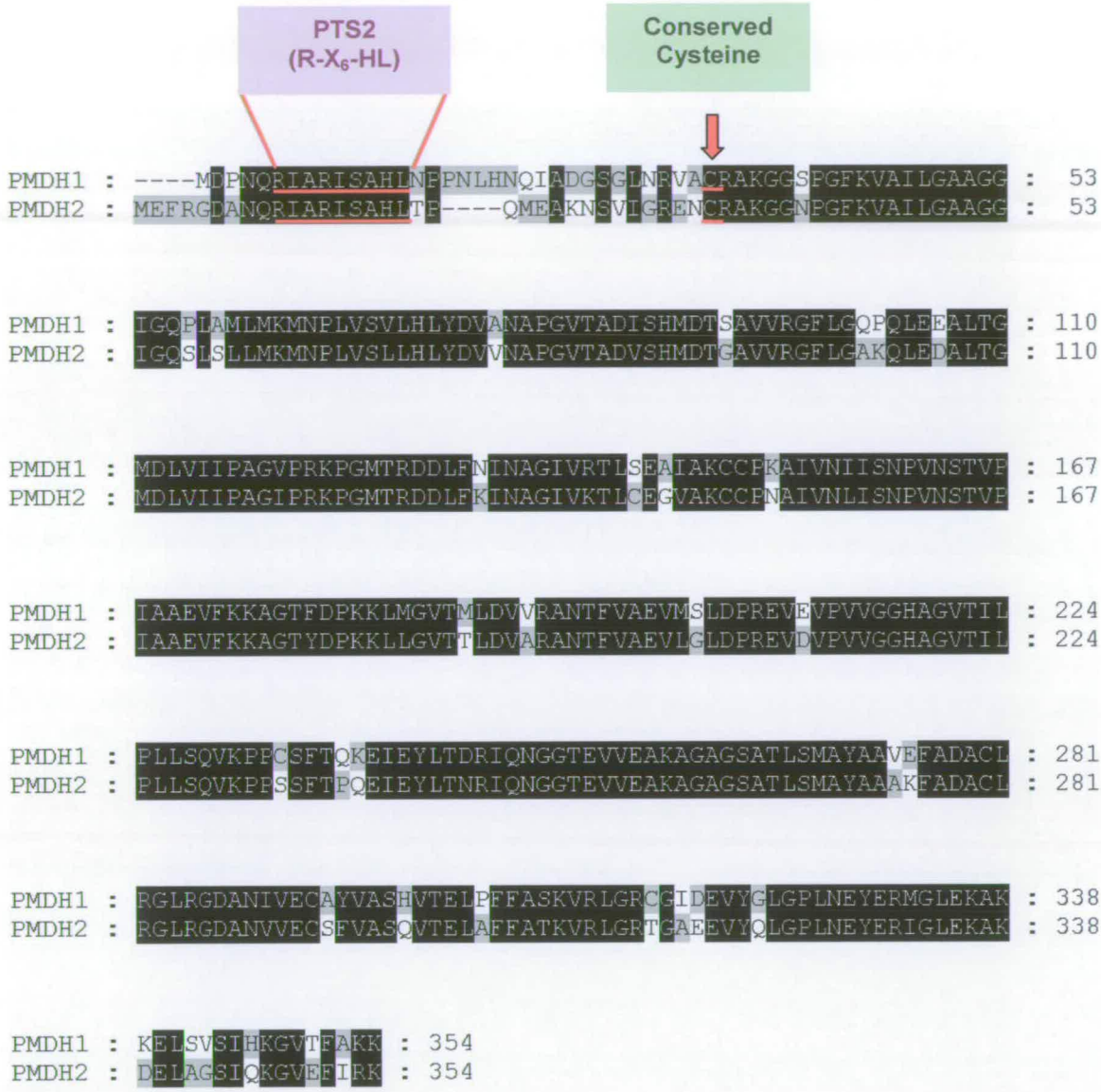

Figure 4.2 Multiple alignments of putative peroxisomal malate dehydrogenase proteins (PMDH) were carried out using ClustalX and GeneDoc programmes (Thompson et al., 1997; Nicholas et al., 1997). The peroxisomal targeting signal type 2 sequences (PTS2) and conserved cysteine residues are highlighted.

proteins following import into peroxisomes, at least in plants and mammals (Kato et al., 1998, Kato et al., 2000).

Table 4.1 Genes predicted to encode malate dehydrogenase in the Arabidopsis genome[a]

Gene	Number of exons	Prediction of subcellular localization	Encoded protein		Protein property		
			N-terminus (first 20 aa)	C-Terminus (last 3 aa)	PI	Length (aa)	MW (kDa)
At1g53240[b]	7	Mitochondria	MFRSMLVRSSASAKQAVIRR	ANQ	8.58	341	35.8
At3g15020[b]	7	Mitochondria	MFRSMIVRSASPVKQGLLRR	ANQ	8.44	341	35.9
At2g22780	**9**	**Peroxisome**	MDPNQRIARISAHLNPPNLH[c]	AKK	**8.06**	**354**	**37.4**
At5g09660	**8**	**Peroxisome**	MEFRGDANQRIARISAHLTP[c]	IRK	**8.11**	**354**	**37.4**
At1g04410	7	Cytosol	MAKEPVRVLVTGAAGQIGYA	CLS	6.51	332	35.6
At5g43330	7	Cytosol	MAKEPVRVLVTGAAGQIGYA	CLS	6.78	332	35.7
At5g56720	2	Cytosol	MCNLLNIEKDPIRVLITGAA	LNV	5.98	339	36.9
At3g47520[d]	2	Chloroplast	MATATSASLFSTVSSSYSKA	AAN	8.81	403	42.4

[a]Information for gene/protein annotations was obtained from The Arabidopsis Information Resource (Huala et al., 2001; www.arabidopsis.org)

[b]Mitochondrial malate dehydrogenase (Millar et al., 2002; Hazelwood et al., 2004)

[c]Highlighted are peroxisome targeting sequence type 2 (PTS2) : R-X_6-HL

[d]Chloroplast malate dehydrogenase (Berkemeyer et al., 1998)

In addition to the PTS2 sequence found in PMDH1 and PMDH2 leader sequences, both share similar characteristics in terms of sequence identity, gene structure and protein properties (Figure 4.2, Table 4.1). There are 9 exons in *PMDH1* and 8 exons in *PMDH2*. Each exon in PMDH1 appears to be similar to individual exons in PMDH2, apart from the fifth and the sixth exons in *PMDH1* which are combined into one exon (fifth exon) in *PMDH2*. In contrast there are 7 and 2 exons in other *MDH* genes, in which exon structure and arrangement are completely different from *PMDH* genes. Furthermore, the protein properties in PMDHs are found to be unique from other MDHs. Both PMDH1 and PMDH2 polypeptides are 354 amino acids in length; have isoelectric points of about 8.1 and the calculated molecular weight of 37.4 kDa. Therefore PMDH1 and PMDH2 are proposed to be peroxisomal and chosen for this study of peroxisomal malate dehydrogenase.

4.2 Analysis of PMDH genes expression

To determine the expression of *PMDH1* and *PMDH2*, gene-specific oligonucleotide primers were designed so that transcripts of each gene could be detected by RT-PCR. Due to the nucleotide coding sequence of *PMDH1* showing strong similarity to *PMDH2* (77% identity), the specificity of particular primer pairs to such desired template to be amplified was monitored. To test the RT-PCR products obtained with each primer combination, they were digested with restriction endonucleases *Acc*I which could distinguish *PMDH1* and *PMDH2* gene products (Figure 4.3A). The *Acc*I sites were located at the position 849 on *PMDH1* cDNA and on position 357 on *PMDH2* cDNA (where A of start codon = 1). The results showed that RT-PCR

Figure 4.3 Characterisation of two Arabidopsis PMDH cDNAs. **(A)**, Schematics of the primer locations (red arrows) and unique *Acc*I restriction endonuclease sites (pink arrows) in the *PMDH1* and *PMDH2* cDNAs. **(B)**, RT-PCR products from each *PMDH* cDNA using primers illustrated, without (-) and with (+) subsequent digestion with *Acc*I restriction endonuclease.

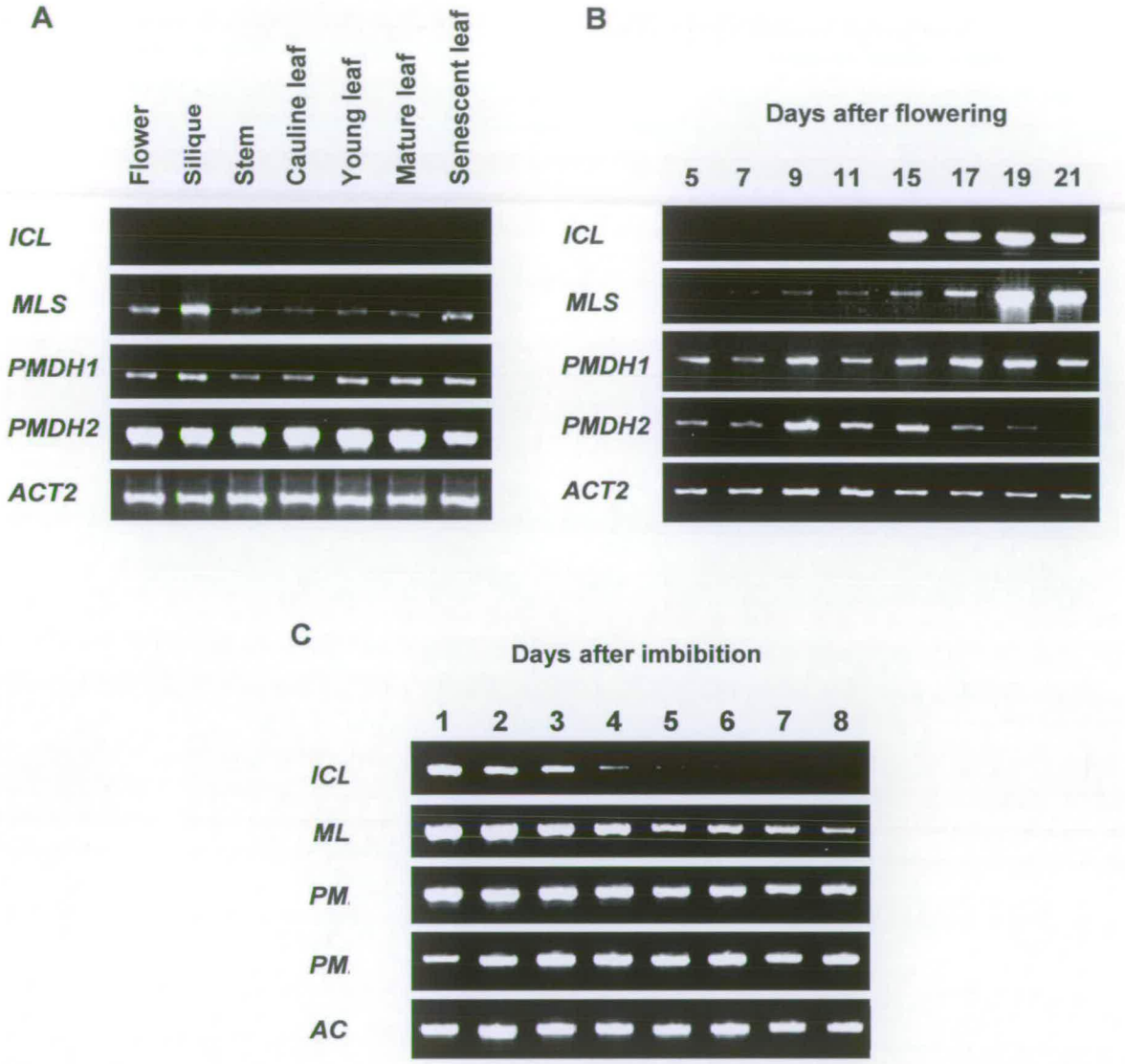

Figure 4.4 Expression pattern of peroxisomal *PMDH* genes detected by RT-PCR; **(A),** in different organs of 5 week old Arabidopsis plants; **(B)**, in maturing Arabidopsis seeds; **(C)**, in developing seedlings.

products obtained with each primer pair were of the predicted sizes and were digested with *Acc*I to products of the expected sizes (Figure 4.3B). The RT-PCR products were subsequently identified by nucleotide sequencing to confirm that RT-PCR products corresponded to the predicted gene in each case (results not shown).

The expression profiles of the predicted peroxisomal *PMDH* genes were then examined. RT-PCR analysis using RNA template isolated from various tissues of mature Arabidopsis showed that *PMDH1* and *PMDH2* genes are expressed throughout the shoot (Figure 4.4A). Even though RT-PCR is a semi-quantitative technique to detect gene expression, the result showed that *PMDH2* is expressed more highly than *PMDH1* in every organ of 5 week old mature plants (Figure 4.4A). *PMDH1* and *PMDH2* expression are also found in developing seeds (Figure 4.4B). To examine expression of *PMDH* genes in seedlings, RNA was isolated at daily intervals from day 1 to day 8. RT-PCR analysis showed that *PMDH1* and *PMDH2* are both expressed strongly during the germination and seedling development stages (Figure 4.4C). Expression of both genes could also be detected in imbibed seeds (day 0) but the RNA template from such seeds was less reliable for RT-PCR (results not shown).

4.3 Analysis of peroxisomal malate dehydrogenase subcellular localisation

The peroxisomal targeting signal type 2 (PTS2), nonapeptide motif R-$(X)_6$-HL, at the N-termini is believed to compartmentalise peroxisomal proteins into the peroxisomes (Kato et al., 1995; Johnson and Olsen, 2003; Fulda et al., 2002; Hyashi et al., 2002; Mano et al., 2002). To confirm that Arabidopsis PMDH1 and PMDH2 are localised in the peroxisome and are targeted by the PTS2 located in their leader sequences, constructs were generated encoding the putative PTS2 sequences of PMDH1 and PMDH2 fused to green fluorescent protein (GFP). The binary vectors were constructed by PCR using Pfu polymerase. The strategies of plasmid construction were carried out as same as that mentioned previously in section 3.3.1 (using primers 780_HindIII_For, 780_GFP_For, 780_GFP_Rev and GFP_EcoRI_Rev for PMDH1 construct , and primers 660_HindIII_For, 660_GFP_For, 660_GFP_Rev and GFP_EcoRI_Rev for PMDH2 construct). These binary vector constructs were named 'p35S::PMDH1-GFP' and 'p35S::PMDH2-GFP' (Figure 4.5A and 4.5B).

Arabidopsis plants were subjected to Agrobacterium floral dipping transformation using the p35S::PMDH1-GFP and p35S::PMDH2-GFP binary vectors. The T_0 transgenic plants, PMDH1-GFP and PMDH2-GFP, were obtained through hygromycin selection and subsequently the presence of the transgenes was determined by PCR analysis. The GFP expression in leaves was then confirmed under fluorescence microscopy (results not shown). In order to confirm that the GFP expression is in peroxisomes, the transgenic plants, PMDH1-GFP and PMDH2-GFP,

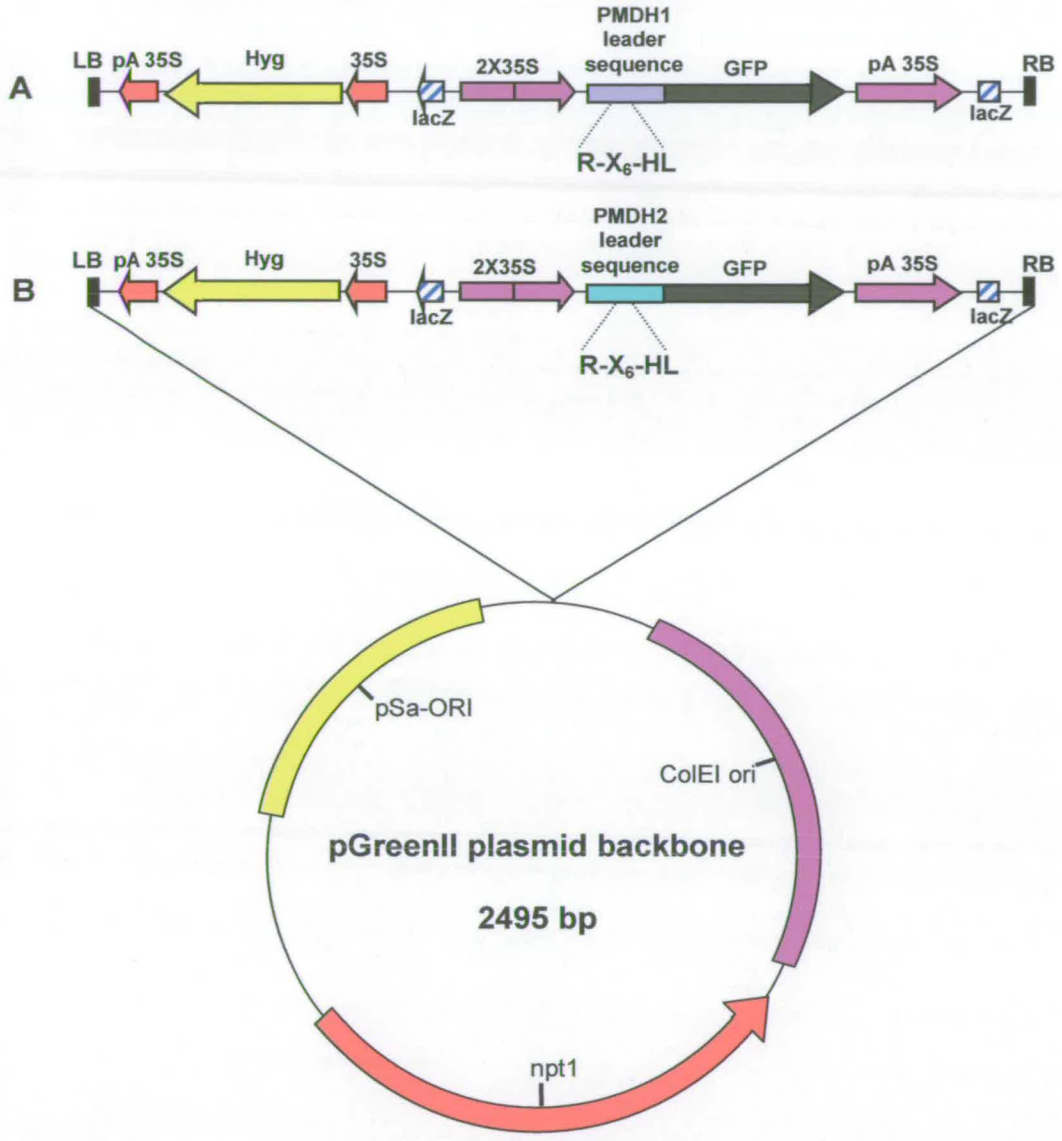

Figure 4.5 Schematic diagram of binary vector p35S::PMDH1-GFP **(A)** and p35S::PMDH2-GFP **(B)**

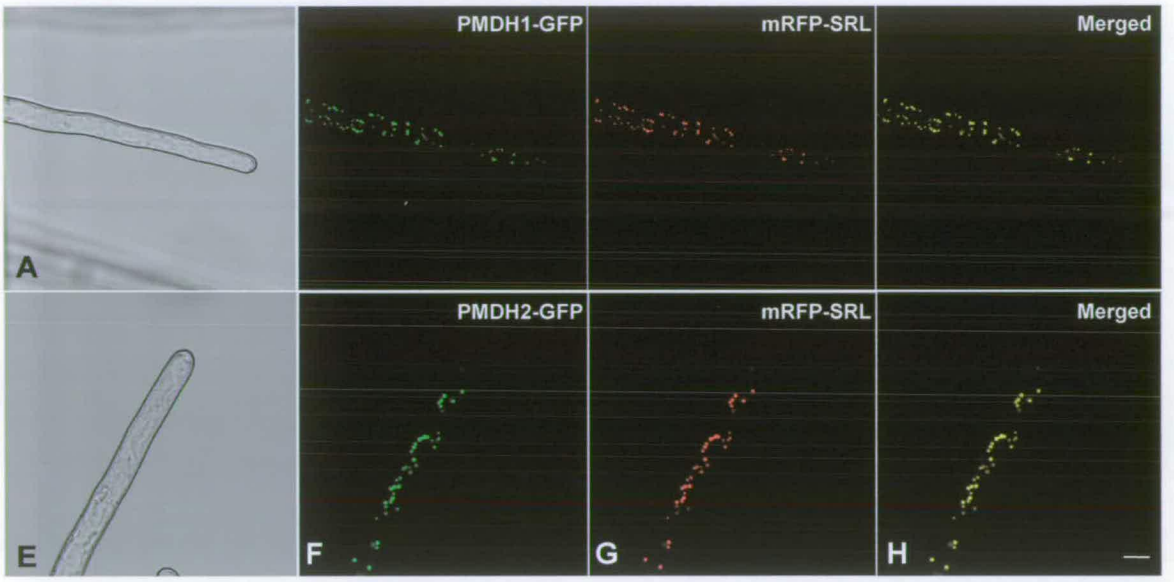

Figure 4.6 Confocal images of root hair cells of transgenic Arabidopsis plants expressing PMDH1-GFP/PMDH2-GFP and mRFP-SRL. Images are bright-field **(A and E)**, GFP signal **(B and F)**, mRFP signal **(C and G)** and merged GFP and mRFP **(D and H)** images. Scale bar = 10 μm.

were crossed with transgenic plants mRFP-SRL (confering kanamycin resistant). This mRFP-SRL line was generated from the peroxisomal marker construct p35S::mRFP-SRL (section 3.3.2), encoding monomeric red fluorescent protein (mRFP) (Campbell et al., 2002) fused to the C-terminal 10 amino acids of pumpkin (Cucurbita cv Kurokawa Amakuri) malate synthase which contain the PTS1 signal sequence Ser-Arg-Leu (SRL) (Hayashi et al., 1996). The seeds derived from crossing were grown on media containing both hygromycin (for GFP screening) and kanamycin (for mRFP screening). The transgenic plants with GFP and mRFP co-expression (PMDH1-GFP/PMDH2-GFP and mRFP-SRL) were obtained through the selection.

To demonstrate co-localisation of GFP and mRFP, confocal microscopic observation of root hair cells from 7 day old seedlings co-expressing PMDH1-GFP or PMDH2-GFP with mRFP-SRL was performed (Figure 4.6A and 4.6E). The images revealed that the distribution of PMDH1-GFP and PMDH2-GFP is located in punctate spherical structures similar in size to plant peroxisomes (0.5-1.5 μm) (Figure 4.6B and 4.6F) and resemble the distribution of the peroxisomal marker mRFP-SRL (Figure 4.6C and 4.6G). The merged images of GFP and mRFP confirmed that PMDH1-GFP and PMDH2-GFP co-localised with mRFP-SRL (Figure 4.6D and 4.6H). No evidence was found for targeting of GFP or mRFP to organelles other than peroxisomes. Thus, PMDH1 and PMDH2 are concluded to be peroxisomal proteins which are targeted by PTS2 signals.

4.4 Isolation of *pmdh1* and *pmdh2* knockout mutants

Arabidopsis knockout mutants with T-DNA insertions in the structural genes for *PMDH1* and *PMDH2* have been searched throughout the Arabidopsis mutant databases. Both *pmdh1* and *pmdh2* mutants were available from GABI-Kat knockout centre (Rosso et al., 2003; Strizhov et al., 2003; Li et al., 2003). The mutants were obtained and PCR-based screening carried out (section 3.4, Figure 3.10). The primers used for screening procedure are designed to the 5' end [primer 780_For (*PMDH1*) and 660_For (*PMDH2*)] and 3' end [primer 780_Rev (*PMDH1*) and 660_Rev (*PMDH2*)] portions of the target genes and used in combination with GABI-Kat LB primer.

In the *pmdh1* mutant, the PCR junction fragment was obtained using GABI-Kat LB and 780_For primers. The nucleotide sequencing using GABI-Kat LB primer revealed that the T-DNA is inserted in exon 3 at position 645 (where A of start codon = 1). The left border is toward the 5' end of *PMDH1* structural gene (Figure 4.7A). Seeds from a plant that is heterozygous for the T-DNA insertion in *PMDH1* were used for segregation analysis for resistance to sulfadiazine. The result show that 69.1% of those seeds were resistant to sulfadiazine, indicating a good fit to the 3:1 hypothesis for a single gene insertion ($\chi^2 = 1.86$, $P > 0.1$).

In the *pmdh2* mutant, the PCR junction fragment was obtained using GABI-Kat LB and 660_For primers. The nucleotide sequencing using GABI-Kat LB primer revealed that the T-DNA is inserted in intron 6 at position 1,641 (where A of start

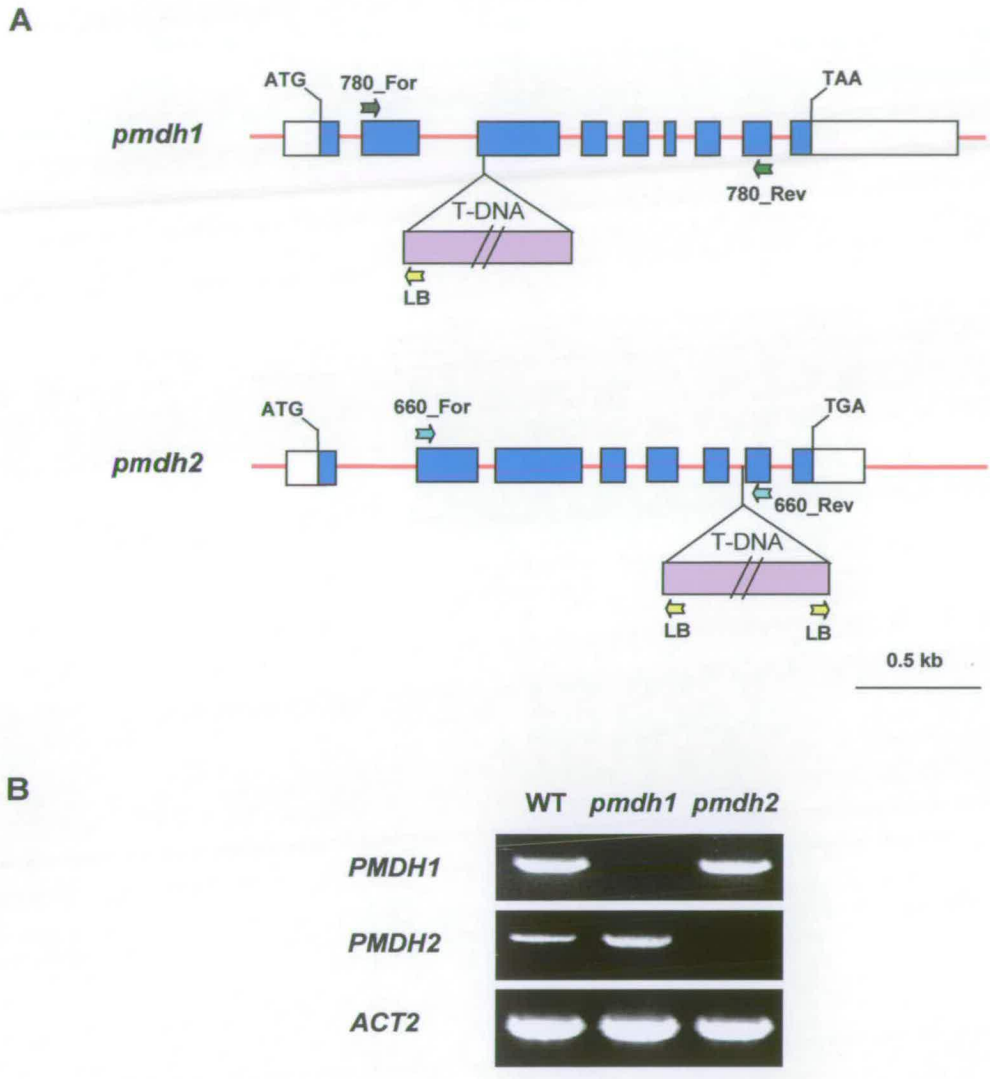

Figure 4.7 (A), Diagram showing gene structure of *PMDH1* and *PMDH2* with positions of the T-DNAs in each mutant. Exons are blue boxes, introns red lines and untranslated regions white boxes. **(B),** RT-PCR with RNA isolated from 2-day old seedlings.

codon = 1). The Left border is toward the 5' end of the *PMDH2* structural gene (Figure 4.7A). However there is another LB toward the 3' end, as this LB allowed a PCR product to be amplified using GABI-Kat LB primer and 660_Rev primer. Seeds from a plant that is heterozygous for the T-DNA insertion in *PMDH2* were used and segregation analysis for resistance to sulfadiazine carried out. The result showed that 70.4 % of those seeds were resistant to sulfadiazine, consistent with the agreement of the 3:1 hypothesis for a single gene insertion ($\chi^2 = 1.13$, $P > 0.1$).

Both homozygous *pmdh1* and *pmdh2* were isolated and the absence of transcript confirmed using RT-PCR analysis (Figure 4.7B). PMDH is believed to be involved in lipid mobilisation which is required for germination and seedling growth. Knocking out *PMDH* genes might reveal phenotypes similar to either those of glyoxylate cycle mutants or β-oxidation mutants. The germination and seedling growth in *pmdh1* and *pmdh2* was tested on media with various conditions, with or without sucrose, in the light or dark, but there was no appreciable phenotype when compared to wild type. This might be due to the redundancy of *PMDH* genes, so that knocking out just one *PMDH* does not do enough to reveal obvious phenotypes.

4.5 Analysis of the double mutant

Mutants of *pmdh1* and *pmdh2* were crossed to make the double mutant. The F_1 heterozygotes were allowed to self fertilise to generate F_2 seeds. The F_2 seeds were plated on media containing 1% (w/v) sucrose as shown to be sufficient for seedling establishment in several β-oxidation mutants (Hayashi et al., 1998; Richmond and Bleecker, 1999; Germain et al., 2001; Zolman et al., 2001; Fulda et al., 2004). All F_2 seeds appeared to germinate normally on the media in the presence of 1% (w/v) sucrose. The seedlings were then transferred into soil and the *pmdh1:pmdh2* double mutants were isolated through PCR-based genotype screening. The F_3 homozygous double mutant (*pmdh1:pmdh2*) seeds were harvested and used for further phenotypic analysis.

4.5.1 The absence of PMDH in the double mutant

Seedlings of wild type, and *pmdh1:pmdh2* were imbibed and grown on media containing 1% (w/v) sucrose for two days and subjected to RT-PCR analysis and total MDH activity assay. RT-PCR analysis revealed that there is an absence of transcripts for PMDH1 and PMDH2 in *pmdh1:pmdh2* (Figure 4.8A). In addition the total MDH activity demonstrated that there is a reduction of MDH activity in *pmdh1*, *pmdh2* and *pmdh1:pmdh2* day 2 seedlings when compared to wild type (Figure 4.8B). The most reduction was found in *pmdh1:pmdh2*. On the other hand the activity of total MDH observed in *pmdh1* is slightly less than in *pmdh2*, indicating that PMDH1 might be responsible for the major PMDH activity, compared to PMDH2.

PMDH is believed to be involved in lipid metabolism occurring in germinated seeds and seedling, and photorespiration occurring in mature plants. The observation of PMDH in cucumber demonstrated that *PMDH* is highly expressed during germination and early seedling growth but thereafter decreased, but then expression markedly increased again beyond the seedling stage together with hydroxy pyruvate reductase (HPR) expression, the unique enzyme for photorespiration (Kim and Smith, 1994). In Arabidopsis, the total MDH activity assayed using samples from seedlings day 0 to day 7 showed that there is an impaired total MDH activity through germination and seedling growth in *pmdh1:pmdh2* when compared to wild type. The missing MDH activity in *pmdh1:pmdh2* double mutant is believed to be the peroxisomal isoforms, so it can be used indirectly to represent PMDH activity. This showed that the PMDH activity increased rapidly following imbibition and was highest on days 2 and 3 (Figure 4.8C). After that the PMDH activity decreased during days 3 to 6. The PMDH activity is presumably increased again as it is required for photorespiration beyond the seedling stage. The high PMDH activity observed during day 2-3 is consistent with the role of PMDH in germination and consistent with PMDH observation in cucumber.

RT-PCR is successful to demonstrate the absence of PMDH1 and PMDH2 at the transcriptional level. On the other hand, as a result of redundancy of MDH, a reduction of MDH activity in *pmdh1:pmdh2* double mutant can not directly demonstrate the absence of PMDH1 and PMDH2 proteins. Western blot analysis using PMDH antibody was subsequently undertaken to examine the absence of PMDH in *pmdh1:pmdh2* double mutant. Results follow in section 4.6.

A

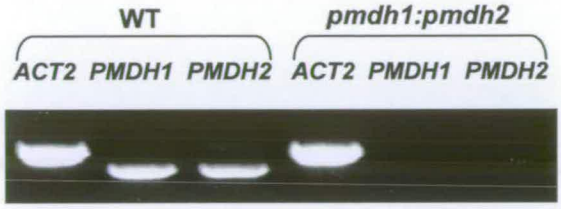
WT
pmdh1:pmdh2
ACT2 PMDH1 PMDH2
ACT2 PMDH1 PMDH2

B

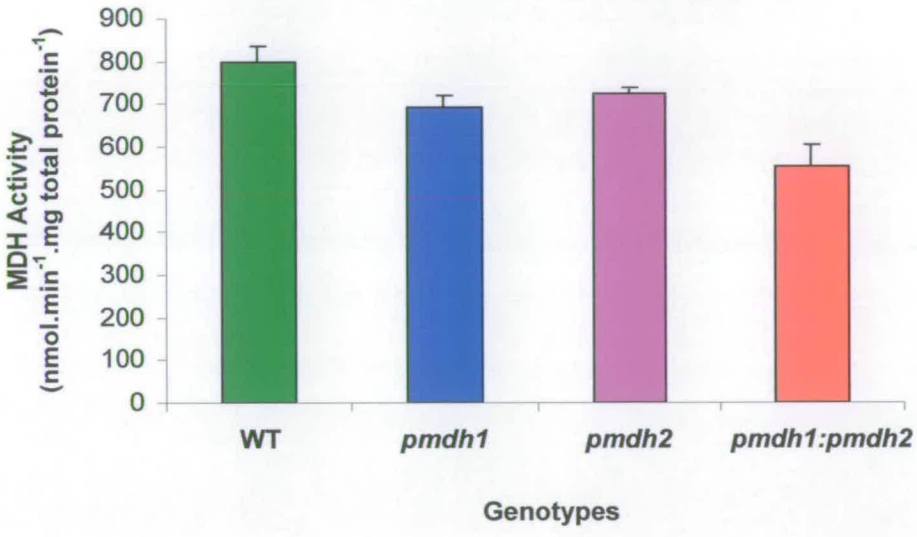
MDH Activity
(nmol.min-1.mg total protein-1)
900
800
700
600
500
400
300
200
100
0
WT
pmdh1
pmdh2
pmdh1:pmdh2
Genotypes

C

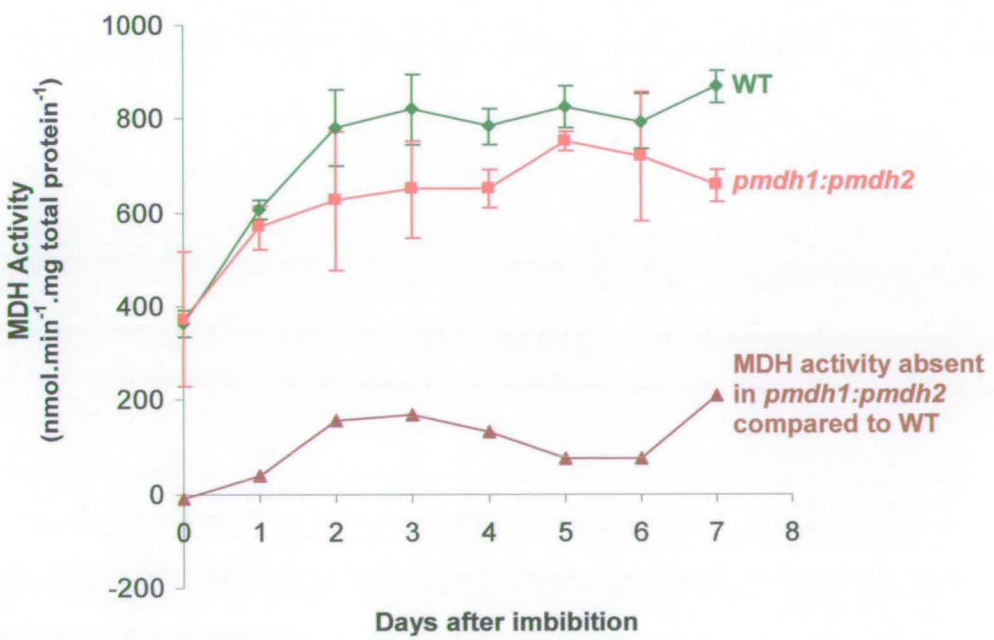
MDH Activity
(nmol.min-1.mg total protein-1)
1000
800
600
400
200
0
-200
0 1 2 3 4 5 6 7 8
Days after imbibition
WT
pmdh1:pmdh2
MDH activity absent
in pmdh1:pmdh2
compared to WT

Figure 4.8 (Previous Page) (A), RT-PCR of *ACT2* (actin), *PMDH1* and *PMDH2* RNAs from 2-day old wild type and *pmdh1:pmdh2* seedlings. **(B)**, Total MDH enzyme activity in 2-day old seedlings grown in continuous light on media containing 1% (w/v) sucrose. Data are the mean ± SD where green box is wild type, blue box is *pmdh1,* pink box is *pmdh2* and red is *pmdh1:pmdh2.* Three experiments each with three replicates were performed. **(C),** MDH activity in total cell extracts of wild type and *pmdh1:pmdh2* mutant seedlings from day 0 to day 7 following imbibition. Data plotted are the mean ± SD, where green symbols are wild type and red symbols are *pmdh1:pmdh2*. The missing MDH activity in *pmdh1:pmdh2* when compared to wild type is shown as brown symbols. Three experiments each with three replicates were performed.

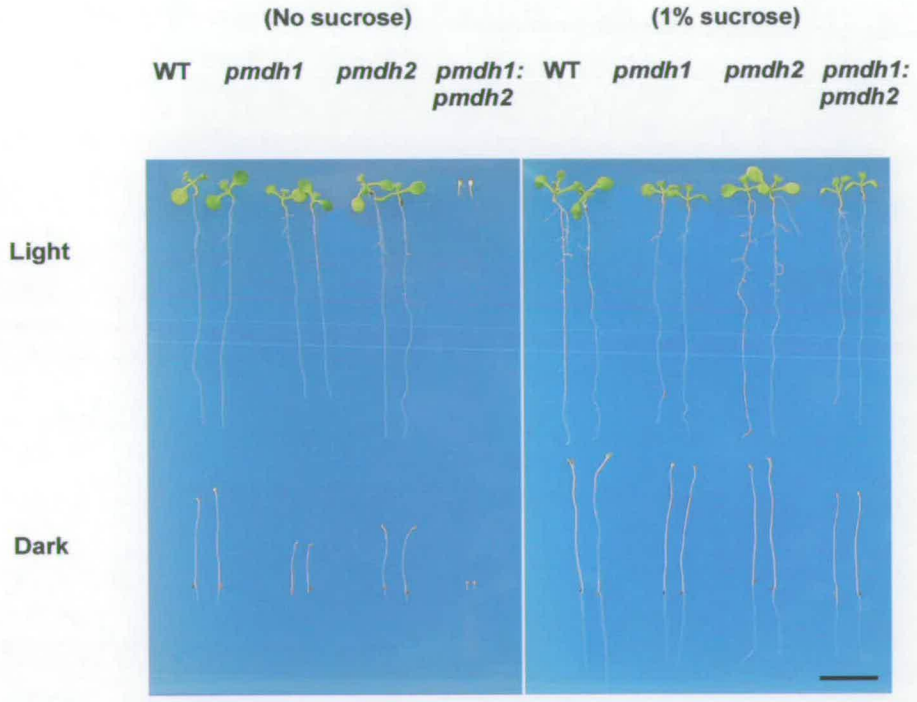

Figure 4.9 Phenotypes of *pmdh1, pmdh2* and *pmdh1:pmdh2* mutants. Seedlings were grown vertically on plates in continuous light or dark in the presence or absence of 1% (w/v) sucrose for 7 days. Scale bar = 1 cm.

4.5.2 Germination and seedling growth phenotypes

Previous observations on *icl* and *mls* mutants defective in the glyoxylate cycle, showed that seeds are able to germinate and establish as seedlings normally even without exogenous sucrose (Eastmond et al., 2000, Cornah and Smith, 2002). On the other hand, mutants defective in β-oxidation, such as *lacs6:lacs7* and *kat2*, are able to germinate but unable to establish as seedlings, unless exogenous sucrose is supplied (Germain et al., 2001; Fulda et al., 2004). To test whether *pmdh1:pmdh2* has a similar arrested seedling phenotype as those mutants defective in β-oxidation, double mutant seeds as well as single mutants *pmdh1* and *pmdh2* and wild type, were imbibed for 2 days and plated on media for 7 days with or without sucrose, in light or dark conditions. Then seedling growth phenotypes were subsequently observed. The result showed that wild type, *pmdh1* and *pmdh2* seedlings are indistinguishable in the presence of sucrose in both light and dark conditions (Figure 4.9). The *pmdh1:pmdh2* is able to establish such seedlings, but the seedlings are slightly smaller when compared to wild type. By contrast, in the absence of sucrose, *pmdh1:pmdh2* germinates but stall in their post germinative growth (Figure 4.9 and 4.10A). The cotyledons remained unexpanded and there was no true leaf. The cotyledon and hypocotyl showed a slightly green colour at day 5 (Figure 4.10A). The *pmdh1:pmdh1* seedlings that were grown on media without sucrose for 4 weeks still remained as arrested phenotype (Figure 4.10B). The cotyledon slightly expanded and sometimes true leaves emerged, but those leaves are very tiny and showed sign of chlorosis. This result demonstrated that *pmdh1:pmdh2* has a more severe phenotype in seedlings when compared to glyoxylate cycle mutants (*mls* and *icl*), but has a

similar phenotype when compared to β-oxidation mutant seedlings, *kat2* and *lacs6:lacs7* (Germain et al., 2001; Fulda et al., 2004).

Lipid mobilization is known to be essential for seed germination. For instance, disruption of Comatose leads to the seed dormancy phenotype (Footitt et al., 2002), and dormancy is also revealed when two peroxisomal citrate synthase genes are mutated (section 3.5). To test whether *pmdh1:pmdh2* has a defect in seed germination, seeds which were imbibed for two days were grown on the media supplemented with or without 1% (w/v) sucrose and the percent germination was scored as judged by the emergence of radicle from the seed coat during the period of the following seven days. The results showed that wild type and *pmdh2* seeds germinate rapidly, although it appeared to be slightly quicker in the absence of sucrose (Figure 4.11A and 4.11B). Nearly all of the wild type and *pmdh2* seeds germinate by day 2. In contrast *pmdh1:pmdh2* showed an impaired germination phenotype, and stop at about 80% germination rate (both with and without sucrose) at day 3 (Figure 4.11A and 4.11B). In addition, *pmdh1* revealed an intermediate effect when compared to *pmdh1:pmdh2* and wild type. The more impaired phenotype observed in *pmdh1* when compared to *pmdh2* agrees with the greater loss of PMDH activity observed in 2-day old *pmdh1* seedlings compared to *pmdh2* seedlings. The results in *pmdh1:pmdh2* is consistent with the delay in emergence of the radical as observed in the *lacs6:lacs7* mutant defective in β-oxidation (Fulda et al., 2004). This indicates that germination is defective in the absence of PMDH which is similar to the phenotype of β-oxidation mutants.

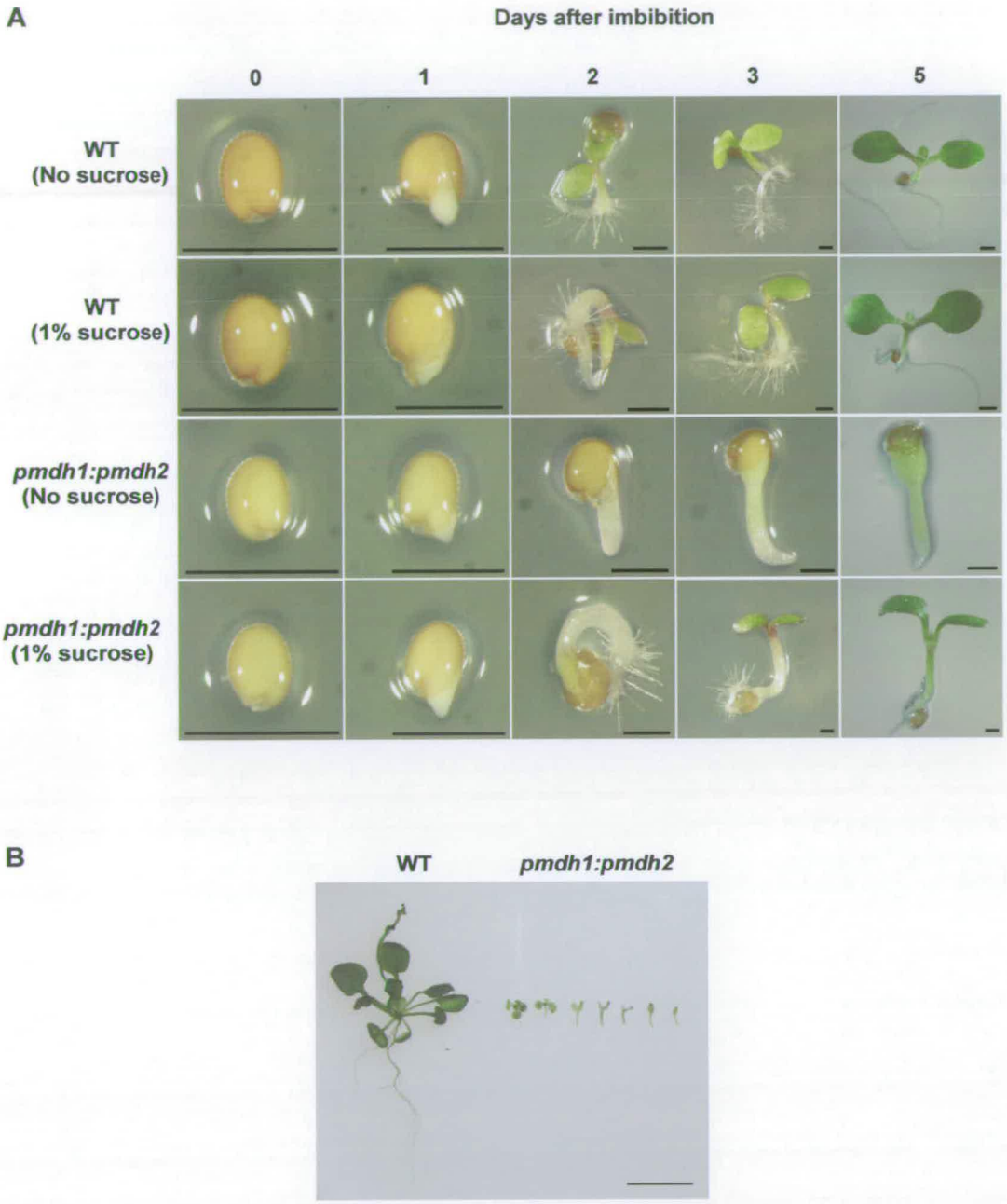

Figure 4.10 (A), Phenotype of *pmdh1:pmdh2* mutant compared to wild type. Seedlings were grown vertically on plates under continuous light in the presence or absence of 1% (w/v) sucrose. Scale bar = 1 mm. **(B)**, Phenotype of *pmdh1:pmdh2* mutant grown under continuous light in the absence of sucrose for 4 weeks, compared to wild type. Scale bar = 1 cm.

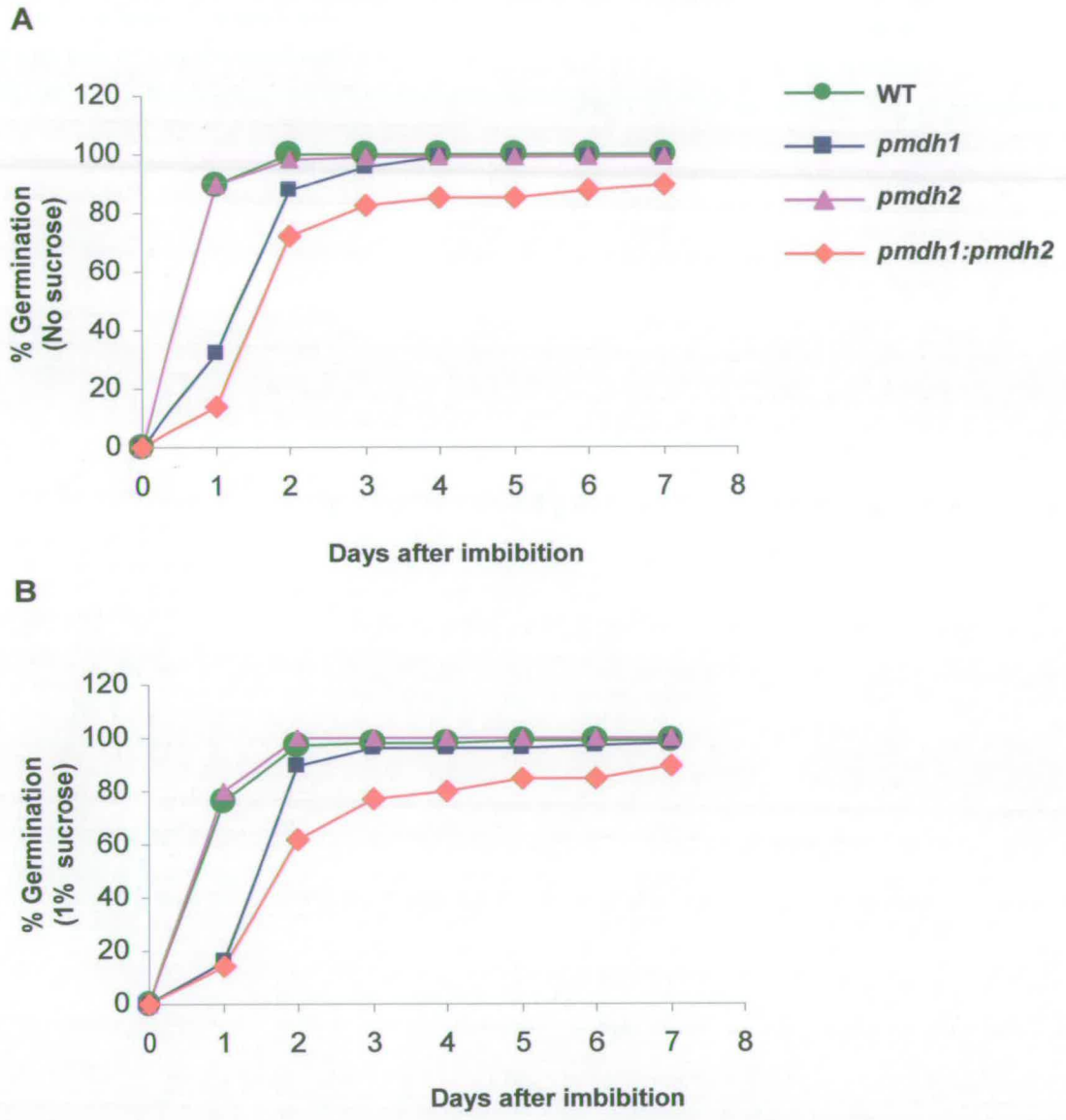

Figure 4.11 Germination rate of *pmdh1*, *pmdh2* and *pmdh1:pmdh2* mutants following imbibition. Seeds were grown under continuous light in the presence **(A)** or absence of 1% (w/v) sucrose **(B)**. Two batches of 100 seeds were scored as judged by the emergence of radicle.

In summary the *pmdh1:pmdh2* double mutant exhibits a slightly impaired seed germination phenotype shown by a delay in emergence of radicle and impaired seedling growth phenotype such that they are unable to establish in the absence of sucrose. These results are consistent with the phenotype observed in other β-oxidation mutants, suggesting that PMDH is involved in β-oxidation rather than the glyoxylate cycle.

4.5.3 Defect in fatty acid β-oxidation

To examine lipid reserve mobilisation in the *pmdh1:pmdh2* double mutant, transmission electron microscopic examination of cotyledons was carried out. The sections were prepared from seedlings grown on media with 1% (w/v) sucrose for 5 days. The results showed an impaired ability to break down lipid bodies in the *pmdh1:pmdh2* double mutant (Figure 4.12A and 4.12B). In comparison lipid bodies are not present in wild type seedlings at day 5 (Figure 4.12C and 4.12D). These results are consistent with those observed with mutant seedlings defective in β-oxidation (Hayashi et al., 1998; Germain et al., 2001; Footitt et al., 2002; Fulda et al., 2004). However, the lipid bodies present in *pmdh1:pmdh2* double mutant are less than those observed in *cts*, *kat2* and *csy2:csy3* (Germain et al., 2001; Footitt et al., 2002; Chapter 3). This indicates that disruption of PMDH results in a less severe effect when compared to those mutants.

To provide further information on the reduction of lipid mobilisation in *pmdh1:pmdh2*, triacylglycerol (TAG) content was measured in *pmdh1:pmdh2* double mutants compared to wild type. TAG was determined by the quantitation of

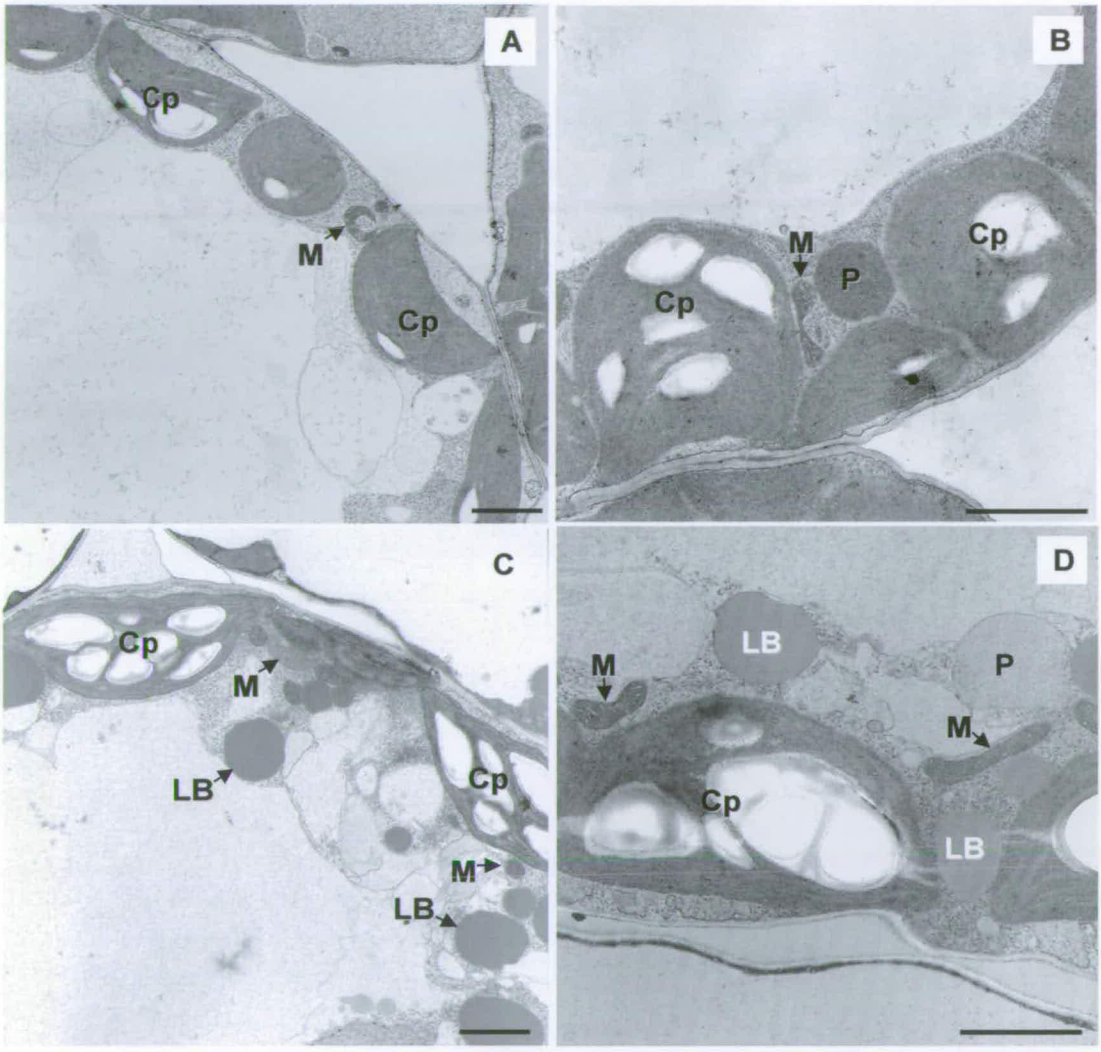

Figure 4.12 Transmission electron micrograph from cotyledon of 5-day old wild type **(A and B)** and *pmdh1:pmdh2* **(C and D)**. Seedlings were grown under continuous light in the presence of 1% (w/v) sucrose. Scale bars are 1 μm. P, peroxisomes; M, mitochondria; Cp, chloroplasts; LB, lipid bodies.

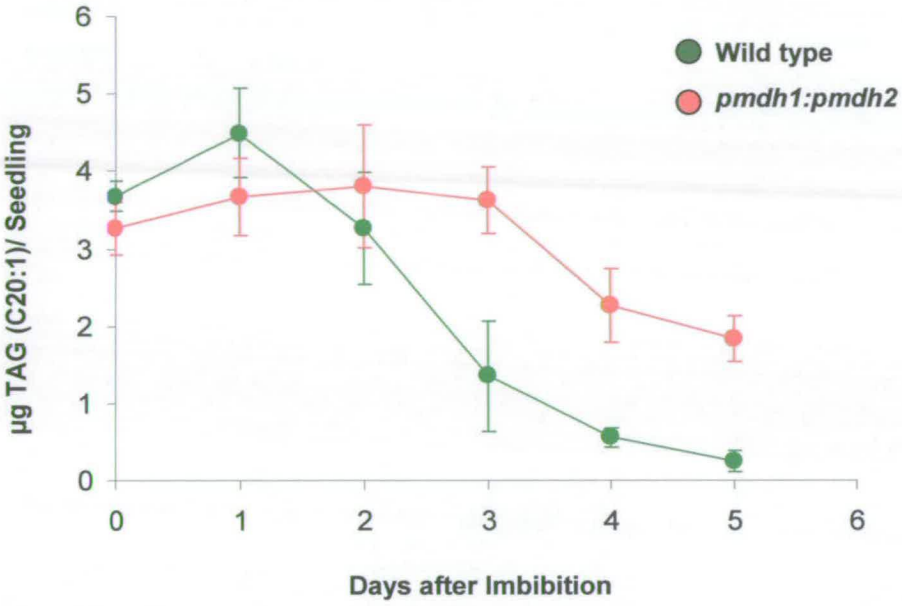

Figure 4.13 TAG content of wild type (green symbols) and *pmdh1:pmdh2* (red symbols) seedlings. C20:1, used as a marker for TAG, was detected by GC-MS in triplicate batches of 20 seedlings grown in continuous light on medium plus 1% (w/v) sucrose. Data are the mean ± SD.

eicosenoic acid (20:1) using gas chromatography and mass spectrometry (Browse et al., 1986). Samples were prepared from seedlings which were imbibed for 2 days and grown on media with 1% (w/v) sucrose, at daily intervals from day 0 to day 5 and TAG quantification was carried out. The results shows that the TAG content in wild type decreases rapidly and is almost absent at day 5 (Figure 4.13). In contrast the TAG content in *pmdh1:pmdh2* double mutants does not change during the first three days, but gradually decreases thereafter and, at day 5, TAG content remains about 50% when compared to the original amount at day 0 (Figure 4.13). The TAG content observed at day 5 is similar to that observed in *lacs6:lacs7*, which showed that about 40% of TAG remained at day 5. This was explained by the redundancy of *LACS* genes, so that β-oxidation is not completely blocked in *lacs6:lacs7*, and ability to break down TAG is only partially impaired. On the other hand, KAT2 and Comatose are predominantly responsible for β-oxidation, so that TAG is not broken down at all in *kat2* and *cts*. Hence, in *pmdh1:pmdh2*, there might be some other way to complement the disruption of PMDH since the deficiency in lipid breakdown is only partial.

To establish that the block of TAG mobilisation in *pmdh1:pmdh2* double mutants is due to a defect in β-oxidation, the resistance to the pro-herbicide 2,4-dichlorophenoxybutyric acid (2,4-DB) was tested. This compound can be converted by peroxisomal β-oxidation to the herbicide 2,4-dichlorophenoxyacetic acid (2,4-D) resulting in an inhibition of root growth (Wain and Wightman, 1954). Previous experiments showed that mutants defective in β-oxidation are unable to metabolise 2,4-DB and seedlings were then found to be resistant to 2,4-DB (Hayashi et al.,

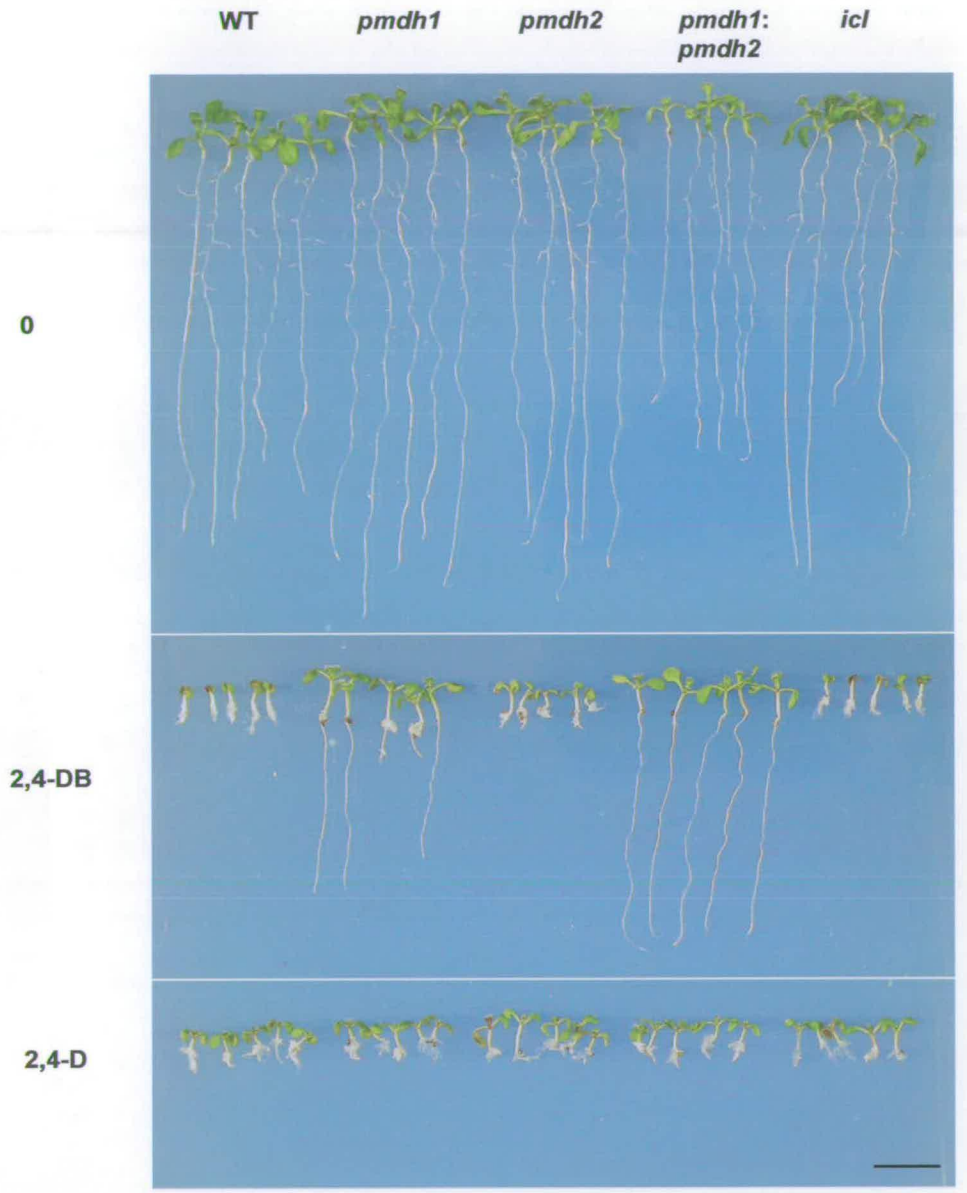

Figure 4.14 Response of *pmdh1, pmdh2, pmdh1:pmdh2* and *icl* mutants to 2,4-DB. Seedlings on media plus 1% (w/v) sucrose (control) and plus 200 ng/ml 2,4-DB or 50 ng/ml 2,4-D. Scale bar = 1 cm.

1998; Richmond and Bleecker, 1999; Zolman et al., 2001; Footitt et al., 2002). The *pmdh1:pmdh2* together with *pmdh1*, *pmdh2*, wild type and *icl* seeds were grown on medium containing 2,4-DB and 1% (w/v) sucrose. The results showed that the *pmdh1:pmdh2* double mutant seedlings are resistant to 2,4-DB but wild type and *pmdh2* are sensitive while *pmdh1* showed a partial effect when compared to *pmdh1:pmdh2* (Figure 4.14). In addition, the *icl* mutant in which the glyoxylate cycle is disrupted showed 2,4-DB sensitivity as β-oxidation is still functional in the absence of the glyoxylate cycle. The 2,4-DB insensitivity observed in *pmdh1*, but not *pmdh2*, indicates that PMDH1 is responsible for a major role during germination and seedling growth, when compared to PMDH2. This agrees with the more severe germination phenotype observed in *pmdh1* when compared to *pmdh2*. These results demonstrated that peroxisomal β-oxidation deficiency is detectable in the *pmdh1* and even more in *pmdh1:pmdh2* double mutant. Therefore PMDH appears to be required for peroxisomal β-oxidation.

4.5.4 Expression of genes involved in lipid mobilisation

It is expected that blocking PMDH leads to an imbalance in the NADH/NAD^+ ratio in the peroxisome. During germination this ratio is presumably high as a lot of NADH is produced from β-oxidation. The high NADH/NAD^+ ratio might result in pleiotropic effects that could influence lipid mobilization indirectly such as through an effect on gene expression. To determine whether disruption of PMDH affects the expression of other genes, RT-PCR analysis was carried out to detect the expression of a number of genes which are involved in β-oxidation and glyoxylate cycle, as well as genes encoding other MDH isoforms. The samples were prepared from seedlings

which were imbibed and grown on media containing 1% (w/v) sucrose for two days. The results revealed that expression of those genes in *pmdh1* and *pmdh2* are normal when compared to wild type. By contrast, the expression of *LACS7, ACX2, MFP2* and *MLS* genes in *pmdh1:pmdh2* is shown to be suppressed when compared to wild type (Figure 4.15A). Other genes such as *KAT2, ICL* and *PEPCK2* are still expressed normally. In *pmdh1*, *pmdh2* and *pmdh1:pmdh2*, other MDH genes encoding mitochondrial and cytosolic isoforms are expressed normally, suggesting that the phenotype observed in these mutants is not due to disruption of MDH other than the peroxisomal isoforms. Although expression of some genes associated with β-oxidation is apparently reduced in *pmdh1:pmdh2* seedlings, it is not known if this is sufficient to explain the defect in β-oxidation and TAG catabolism.

It is known that NADH can be consumed in the photorespiration reaction by hydroxypyruvate reductase. Therefore, in green leaves (beyond the seedling stage), the expected high NADH/NAD^+ ratio in *pmdh1:pmdh2* peroxisomes might be recovered as flux through β-oxidation activity reduces and photorespiration is markedly increased. To detect whether there is any gene suppression in *pmdh1:pmdh2* green leaves, RT-PCR analysis was performed using samples prepared from mature green leaves from 5 week old plants. Results showed that, in contrast to gene expression in seedlings, genes encoding *LACS7, ACX2* and *MFP2* in *pmdh1:pmdh2* are expressed normally when compared to wild type (Figure 4.15B). This could be interpreted to indicate that a high NADH/NAD^+ ratio in seedlings results in suppression of expression of some β-oxidation genes. In order to obtain a more complete analysis of changes in gene expression that may result from a

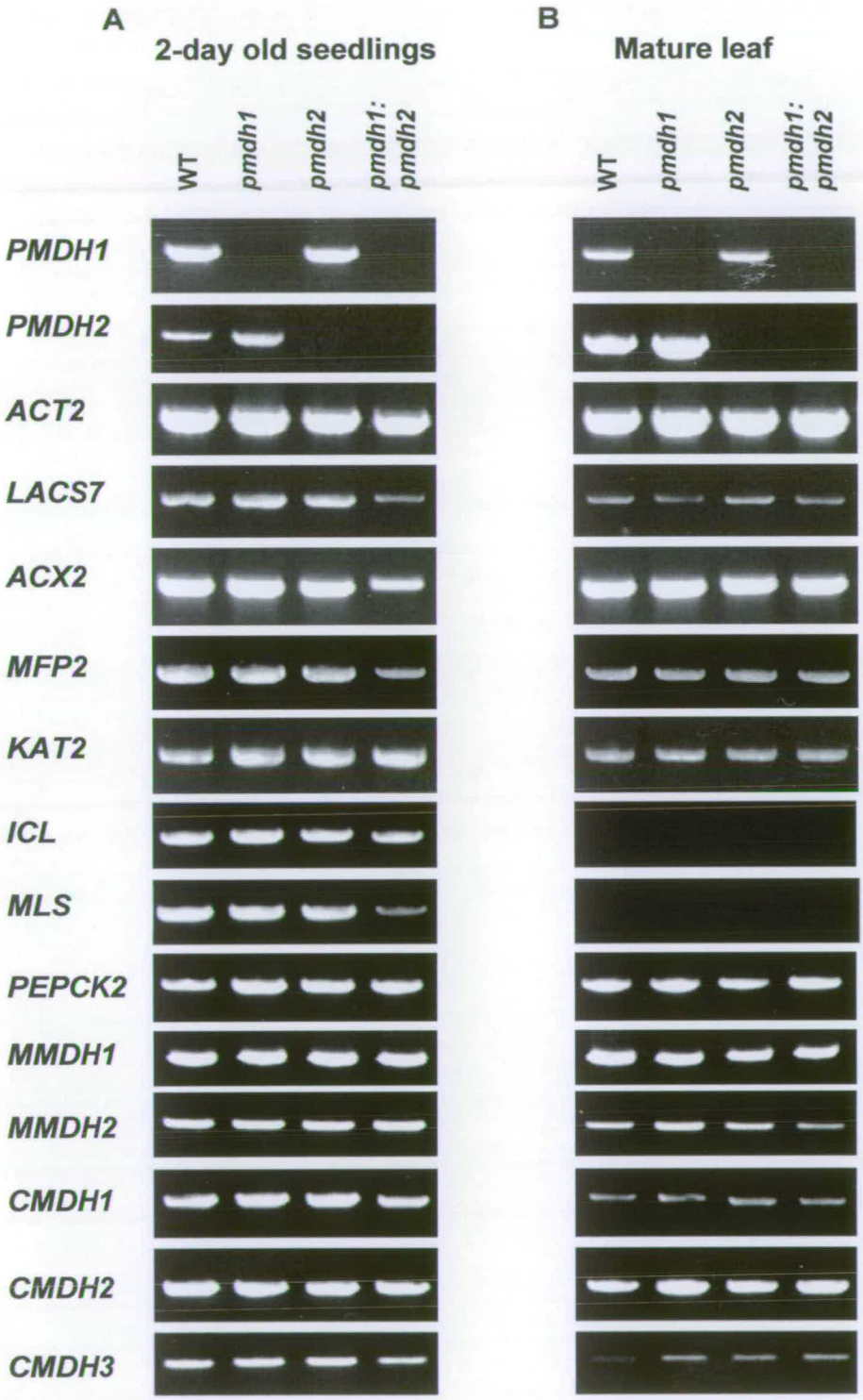
A
2-day old seedlings
B
Mature leaf
WT
pmdh1
pmdh2
pmdh1: pmdh2
PMDH1
PMDH2
ACT2
LACS7
ACX2
MFP2
KAT2
ICL
MLS
PEPCK2
MMDH1
MMDH2
CMDH1
CMDH2
CMDH3

Figure 4.15 (Previous Page) Expression of malate dehydrogenase (MDH), β-oxidation and glyoxylate cycle genes detected by RT-PCR using RNA isolated from 2-day old light-grown seedlings **(A)** and green leaves from 5-week old mature plants **(B)**. The amount of cDNA template in each RT-PCR reaction was normalised to the signal from the *ACT2* (Actin) gene. *PMDH*, peroxisomal malate dehydrogenase; *MMDH*, mitochondrial malate dehydrogenase; *CMDH*, cytosolic malate dehydrogenase; *LACS7*, peroxisomal long chain acyl CoA synthetase; *ACX2*, acyl CoA oxidase 2; *MFP2*, multifunctional protein 2; *KAT2*, 3-ketoacyl CoA thiolase; *MLS*, malate synthase; *ICL*, isocitrate lyase; *PEPCK2*, phosphoenolpyruvate carboxykinase.

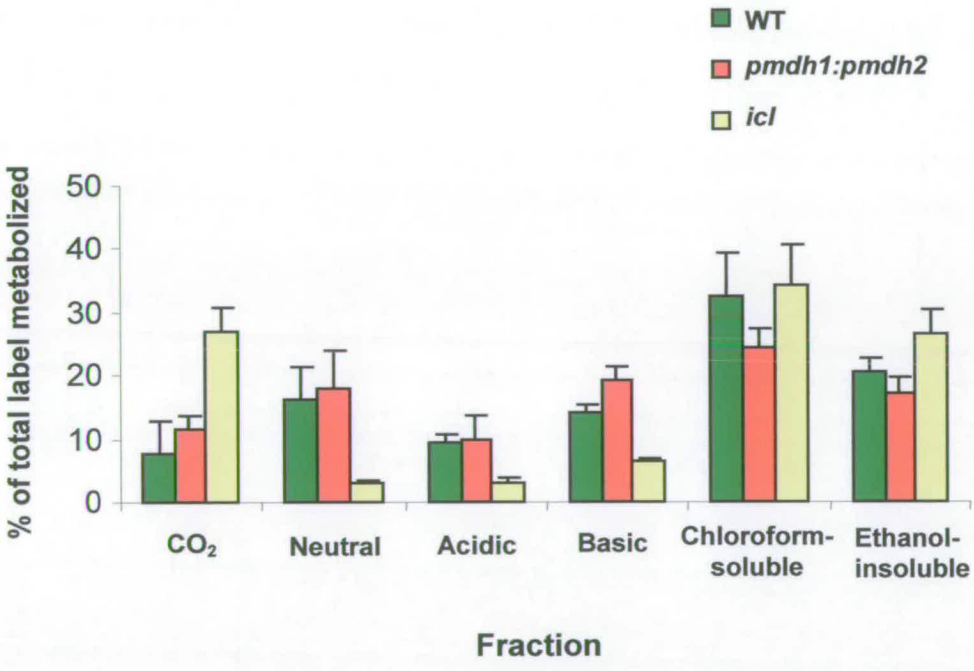

Figure 4.16 Metabolism of [2-^{14}C]-acetate in wild type, *pmdh1:pmdh2 and icl* mutant seedlings. Incorporation of ^{14}C into sugars, organic acids and amino acids is represented as neutral, acidic and basic fraction respectively.

disruption in PMDH gene expression in seedlings, Affymetrix microarray analysis was undertaken. The RNA samples were prepared from wild type and *pmdh1:pmdh2* seeds that were imbibed for 2 day and grown on media containing 1% sucrose for 2 day under continuous light. Results (obtained by the Nottingham Arabidopsis Stock Centre) showed that there was no significant change in the expression of β-oxidation and glyoxylate cycle genes (result not shown). It is concluded that the RT-PCR analysis that indicated a reduction in expression of some genes in the *pmdh1:pmdh2* mutant, is probably inaccurate for technical reasons. Alternatively, the repression of these genes is not reproducible.

4.5.5 Metabolism of [2-^{14}C] acetate

To test the requirement for PMDH in glyoxylate cycle activity, 2-day old seedlings were fed with [2-^{14}C]-acetate and then the incorporation of ^{14}C into sugars, organic acids and amino acids was analysed (Cornah et al., 2004). This experiment was carried out by Dr Johanna Cornah. The neutral, acidic and basic fractions represent sugars, organic acids and amino acids respectively. The results showed that a significant proportion of ^{14}C is incorporated into sugars in both wild type and *pmdh1:pmdh2* double mutant seedlings, indicating that the glyoxylate cycle is functioning normally and so enables acetate to be converted into sugars. In contrast ^{14}C labeling of sugars in the glyoxylate cycle mutant *icl* is at a background level (Figure 4.16). In the *icl* mutant, most of [2-^{14}C]-acetate is respired as revealed by $^{14}CO_2$ release, but in the *pmdh1:pmdh2* double mutant, seedlings respired equivalent amounts of acetate when compared to wild type. This experiment indicates that the glyoxylate cycle functions normally in the absence of PMDH.

4.6 In vitro expression of PMDH proteins and western blot analysis

In order to obtain antibodies to detect PMDH1 and PMDH2 proteins, first *in vitro* expression of PMDH1 and PMDH2 recombinant proteins was undertaken in *E. coli* so that these recombinant proteins can be used to raise rabbit antibodies. Two constructs were made to encode PMDH1 and PMDH2 fused to six histidine residues at the carboxyl terminus. To construct these genes, primers were designed to amplify the coding sequence from *PMDH1* and *PMDH2* cDNA using Pfu polymerase and to allow the cloning in the expression vector pET20a(+) (Novagen, Nottingham, UK) at *Nhe*I and *Xho*I sites. These expression vectors are called 'pET-PMDH1 and pET-PMDH2'. The vectors were then transformed into *E. coli* strain BL21 (DE3) which was used as a host for expression of the recombinant His-tagged protein. Following an induction with IPTG (final concentration 1 mM), the recombinant proteins were expressed rapidly as detected on SDS-PAGE even just 10 minutes after an induction (Figure 4.17A). After 3 hours expression, both PMDH1 and PMDH2 recombinant his-tagged proteins showed strong bands on the SDS-gel and exhibited molecular weights of about 37 kDa, which is similar to the molecular weight calculated from the coding sequences on the constructs. Then *E. coli* cells were broken and recombinant his-tagged proteins PMDH1 and PMDH2 were purified by column chromatography (Figure 4.17B and 4.17C). Subsequently, antibodies were raised commercially in rabbits against the PMDH1 and PMDH2 polypeptides.

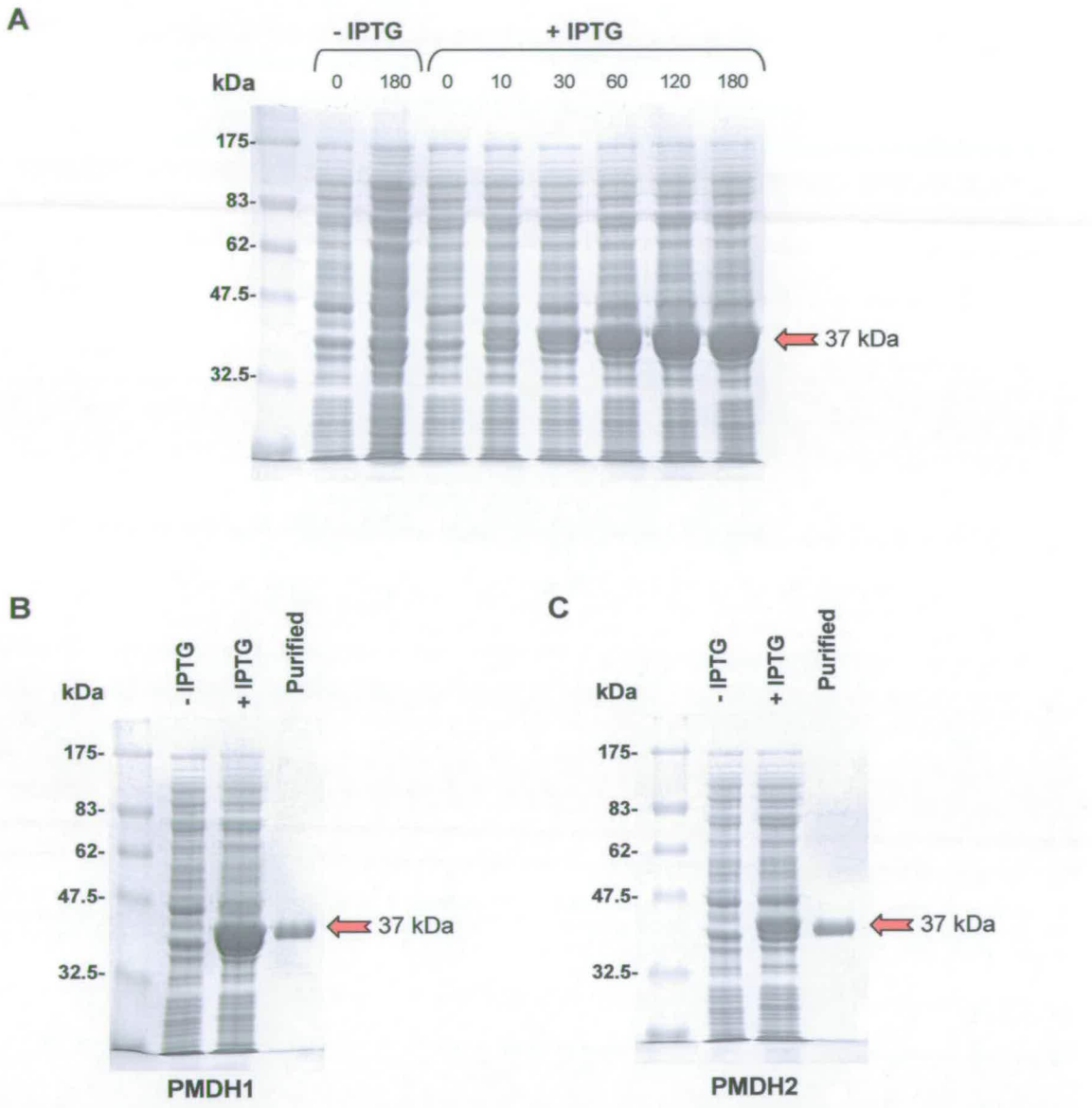

Figure 4.17 (A), SDS-PAGE of total protein from *E. coli* harbouring plasmid encoding PMDH1. The expression was induced by 1 mM IPTG. Following 3 hours of induction, the PMDH1 **(B)** and PMDH2 **(C)** proteins were purified by column chromatography and 2 µg of protein analysed.

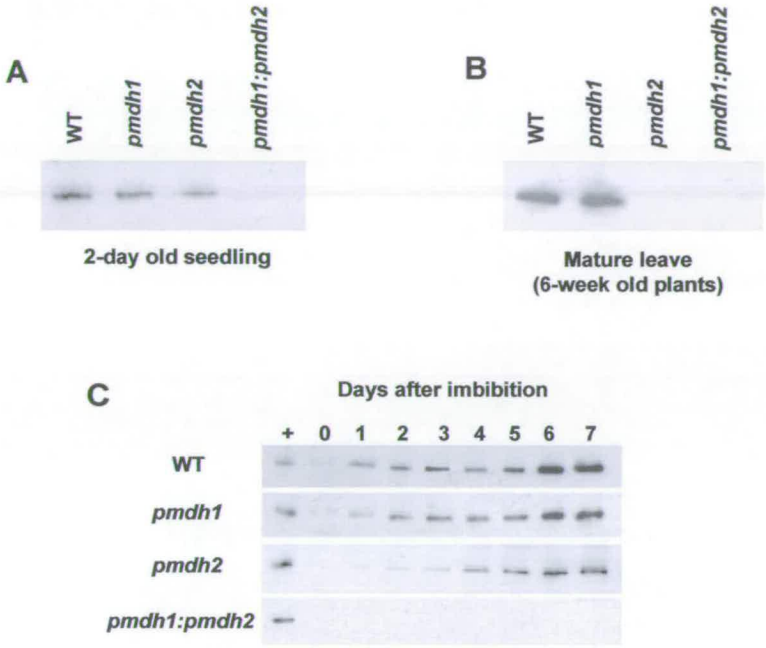

Figure 4.18 Western blot of PMDH proteins in wild type, *pmdh1*, *pmdh2*, *pmdh1:pmdh2* using 10 µg of total protein prepared from 2-day old seedlings **(A)**, green leaves from 5-week old mature plants **(B)** and seedlings day 0-7 following imbibition **(C)**.

The rabbit antibodies raised against PMDH1 and PMDH2 were obtained and subsequently tested for their ability to recognise PMDH1 and PMDH2 recombinant proteins, and PMDH1 and PMDH2 from Arabidopsis. To test them, western blotting was carried out using protein samples from PMDH1 and PMDH2 recombinant his-tagged proteins as well as total proteins from Arabidopsis. Results showed that both PMDH1 and PMDH2 antibodies are able to detect either PMDH1 or PMDH2 recombinant proteins (result not shown). By contrast, only the antibody for PMDH2 was able to detect Arabidopsis PMDH in crude extracts. Western blotting results using Arabidopsis total protein from *pmdh1*, *pmdh2* and *pmdh1:pmdh2* revealed that the PMDH2 antibody was capable of detecting both PMDH1 and PMDH2 proteins, in agreement with the high sequence identity of these two polypeptides. However, when using PMDH2 antibody to detect PMDH1 protein (which exists in wild type and the *pmdh2* mutant) the signal may not be representative of the amount of PMDH1 protein. The western blot signal showed that the molecular weight of PMDH1 and PMDH2 are about 34 kDa, consistent with the calculated molecular weight of mature proteins after the predicted transit peptides are cleaved.

To demonstrate the absence of PMDH in mutants, western blot analysis using 2-day old seedlings from wild type, *pmdh1*, *pmdh2* and *pmdh1:pmdh2* was employed. Seeds were imbibed for two days and plated on media containing 1% (w/v) sucrose for 2 days. The results showed the presence of PMDH in wild type, *pmdh1*and *pmdh2*, and revealed signals at 34 kDa, while there was no PMDH in *pmdh1:pmdh2* double mutant (Figure 4.18A). The western blot using protein samples prepared from mature leaves from 5 week old plants again revealed that there was no signal for

PMDH in the *pmdh1:pmdh2* double mutant (Figure 4.18B). Furthermore PMDH1 protein is low to undetectable as shown by the missing signal in *pmdh2*. This is in agreement with the low level of *PMDH1* transcript detected by RT-PCR in mature leaf when compared to *PMDH2*.

To determine the pattern of change in PMDH during germination and seedling growth, samples were prepared from seedlings of wild type, *pmdh1*, *pmdh2* and *pmdh1:pmdh2* that were imbibed for two days and then grown on media containing 1% sucrose. Samples were collected at daily intervals from day 0 to day 7 and then western blot analysis was carried out. Results reveal that in wild type the PMDH level increased following imbibition and led to a high level at day 2-3 (Figure 4.18C). Thereafter the PMDH signal slightly decreased but then the signal was markedly increased again from day 5. This result is consistent with the pattern of the amount of missing PMDH activity observed in the *pmdh1:pmdh2* double mutant when compared to wild type. The pattern of PMDH2 in *pmdh1* showed a similar, but weaker signal when compared to wild type. In addition, the PMDH1 in *pmdh2* increased gradually but strong signal showed from day 4 (This result might not be directly representative as the antibody was raised from PMDH2). There was no signal in *pmdh1:pmdh2* indicating that there is an absence of PMDH in the *pmdh1:pmdh2* double mutant.

4.7 Complementation of the double mutant with *PMDH* genes

To confirm that the phenotype observed in *pmdh1:pmdh2* is due to the lack of a functional *PMDH* gene and not due to inherent disruption of expression of other specific genes caused as a consequence of T-DNA insertion in a *PMDH* gene, transgenic complementation was undertaken. The constructs for complementation were generated from full-length *PMDH1* and *PMDH2* cDNAs. These contain the native PTS2 targeting sequence at the N-terminus. The strategies for binary vector construction are the same as that mentioned in section 3.6 (using primers 780_HindIII_For and 780_XbaI Rev for PMDH1 construct and primers 660_HindIII_For and 660_XbaI Rev for PMDH2 construct). These constructs are called p35S::PMDH1 and p35S::PMDH2 (Figure 4.19A and 4.19B).

A previous study showed that a PTS2 sequence can be responsible for dual targeting of citrate synthase to both peroxisome and mitochondria in yeast (Lee et al., 2000). To demonstrate that the homozygous *pmdh1:pmdh2* mutant phenotype is due to the disruption of PMDH in the peroxisome but not mitochondria, another construct was made. The construct with a modified *PMDH1* cDNA was generated in which the first 60 bases, corresponding to the PTS2 signal sequence were deleted. The cDNA was then provided with a PTS1 sequence, corresponding to last 10 amino acids of the pumpkin *MLS* gene (as in section 3.3.2). This PTS1 sequence has been confirmed to be a peroxisomal targeting sequence (Hayashi et al., 1996). The construct was made using the same strategies as in section 3.6 (using primers 780_HindIII_62,

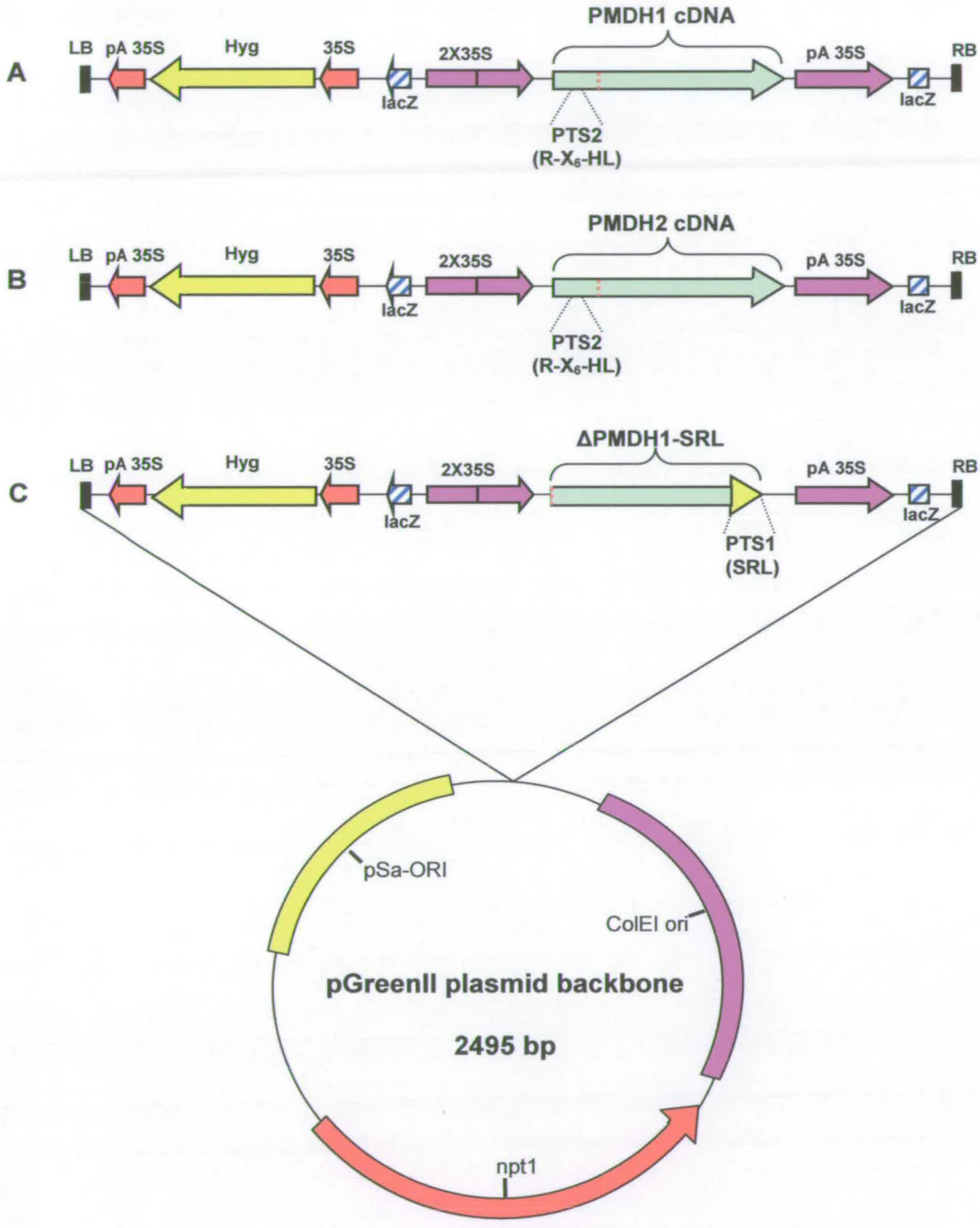

Figure 4.19 Schematic diagram of binary vector p35S::PMDH1 **(A)**, p35S::PMDH2 **(B)**, and p35S::ΔPMDH1-SRL **(C)**.

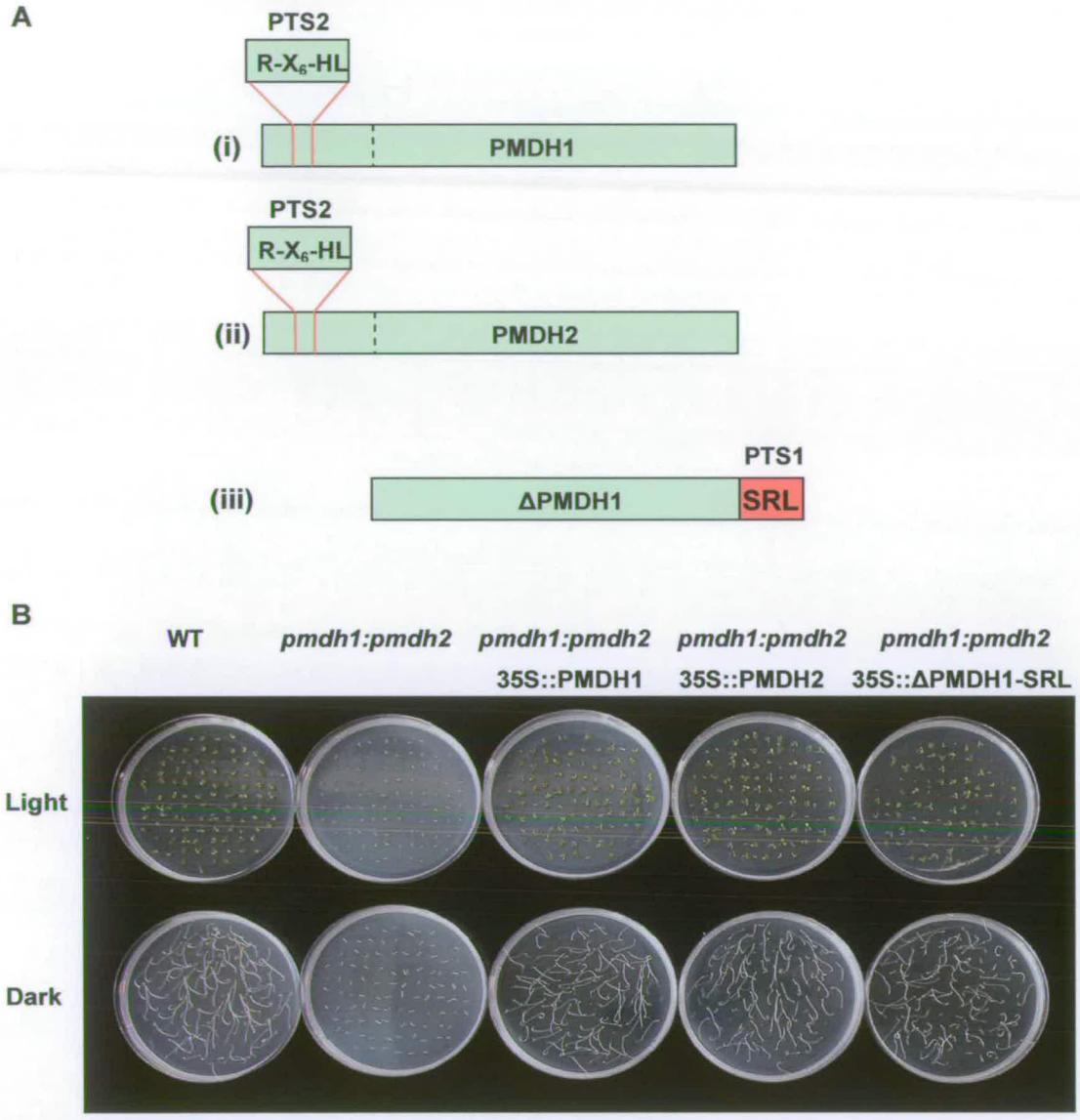

Figure 4.20 (A), Diagram showing PMDH1 and PMDH2 containing the native PTS2 (R-X_6-HL) at the N-terminus (i, ii) and ΔPMDH1-SRL which is truncated PMDH1 in which PTS2 is replaced with PTS1 (SRL) (iii). **(B)**, 5-day old seedlings of T_1 complemented lines grown on media in the absence of sucrose in the light or dark.

780_SRL_Rev and EcoRI_SRL_Rev for PMDH1 construct). This construct was named p35S::ΔPMDH1-SRL (Figure 4.19C).

Flowering *pmdh1:pmdh2* plants were subjected to *Agrobacterium* floral dipping transformation with binary vectors p35S::PMDH1, p35S::PMDH2 and p35S::ΔPMDH1-SRL. In all cases, the T_0 transformants were obtained through hygromycin selection and PCR was subsequently used to verify the presence of the transgene in those T_0 plants. The T_0 plants were grown and allowed to produce T_1 seeds, then the restoration of seedling phenotype in T_1 was tested. As observed by the ability of seedlings to establish in the absence of sucrose in both light and dark conditions, the restored seedling phenotype obtained from transgenic complementation experiments occured at the expect frequency (Figure 4.20, Table 4.2, Table 4.3). These results correlate with inheritance of the hygromycin resistance gene used as plant selectable marker, in agreement with a 3:1 hypothesis for a single gene insertion (Table 4.4). This result indicates that the phenotype in *pmdh1:pmdh2* seedlings is due to the absence of PMDH which is compartmentalised in peroxisomes.

Table 4.2 Light grown seedling phenotypes from the complementation of *pmdh1:pmdh2* with PMDH genes

Genetic Background	Transgene Construct	Light grown phenotype[a] (%)			
		Not germinatated	*pmdh* phenotype[b]	WT phenotype[c]	Intermediate phenotype
Wild type	-	0.33 ± 0.58	0	99.67 ± 0.58	0
pmdh1:pmdh2	-	7.33 ± 1.15	91.33 ± 2.31	0	1.67 ± 0.58
pmdh1:pmdh2	35S::PMDH1	2.67 ± 2.00	21.33 ± 1.53	71.33 ± 1.00	4.67 ± 2.08
pmdh1:pmdh2	35S::PMDH2	3.33 ± 1.53	20.67 ± 7.51	71.67 ± 6.66	4.33 ± 0.58
pmdh1:pmdh2	35S::ΔPMDH1-SRL	8.67 ± 6.35	17.67 ± 5.77	67.00 ± 2.65	6.67 ± 2.52

[a]Seeds germinated and grown without sucrose for 5 days

[b]Growth arrested, no expanded cotyledons

[c]Seedlings fully established with expanded green cotyledons

Table 4.3 Dark grown seedling phenotypes from the complementation of *pmdh1:pmdh2* with PMDH genes

Genetic Background	Transgene Construct	Dark grown phenotype[a] (%)			
		Not germinatated	*pmdh* phenotype[b]	WT phenotype[c]	Intermediate phenotype
Wild type	-	1.33±0.58	0	98.33±0.58	0
pmdh1:pmdh2	-	9.33±1.15	90.67 ± 1.15	0	0
pmdh1:pmdh2	35S::PMDH1	3.33 ± 2.08	18.00 ± 3.61	78.67± 5.69	0
pmdh1:pmdh2	35S::PMDH2	5.33 ± 4.16	15.67 ± 9.87	79.33 ± 6.66	0
pmdh1:pmdh2	35S::ΔPMDH1-SRL	13.33 ± 10.07	13.67 ± 2.52	73.00 ± 11.53	0

[a]Seeds germinated and grown without sucrose for 5 days in the dark

[b]Growth arrested, hypocotyls are not elongated

[c]Seedlings fully established with elongated hypocotyls

Table 4.4 Hygromycin resistance phenotype from the complementation of *pmdh1:pmdh2* with PMDH genes

Genetic Background	Construct	Hygromycin Resistance (%)	χ^2 Value (*P*)
Wild type	-	0	-
pmdh1:pmdh2	-	0	-
pmdh1:pmdh2	35S::PMDH1	72.33 ± 0.47	0.38 (> 0.5)
pmdh1:pmdh2	35S::PMDH2	75.67 ± 7.04	0.02 (> 0.5)
pmdh1:pmdh2	35S::ΔPMDH1-SRL	71.33 ± 3.09	0.72 (> 0.1)

Chapter 5

Discussion

5.1 Requirement for peroxisomal CSY in germination and post-germinative growth

5.2 Fate of carbon skeletons derived from β-oxidation

5.3 Role of PMDH in seedling establishment

5.4 Redundancy in the pathway for NADH re-oxidation

5.5 Proposed pathway for lipid catabolism during germination and seedling growth

5.6 Prospective research and biotechnological applications of lipid catabolism

Chapter 5

Discussion

5.1 Requirement for peroxisomal CSY in germination and post-germinative growth

Based on the phenotypes observed in *csy2:csy3* double mutants, it is deduced that peroxisomal CSY is required for lipid mobilisation in germinating Arabidopsis. Arabidopsis *icl* or *mls* mutants in which key enzymes in the glyoxylate cycle are disrupted revealed milder phenotypes when compared to *csy2:csy3* (Eastmond et al., 2000b; Cornah and Smith, 2002; Cornah et al., 2004). Germination and seedling growth are achievable in *icl* and *mls* mutant seedlings, even though the seedlings showed slightly impaired growth phenotypes in the absence of sucrose. The mutant seedlings are still able to utilise TAGs and are sensitive to 2,4-DB, indicating that β-oxidation is functional and there is an alternative means to metabolise carbon skeletons derived from β-oxidation besides the glyoxylate cycle. In contrast, *csy2:csy3* double mutants reveal a severe phenotype by which germination cannot be achieved even if exogenous sucrose is supplied, showing that disruption of peroxisomal CSY is more than a simple block in the glyoxylate cycle. The *csy2:csy3* seeds require the special treatments of removing seed coats and providing sucrose, and even then the seedlings are unable to break down TAGs. The seedlings are

resistant to 2,4-DB, indicating that β-oxidation is blocked. These results indicate that peroxisomal CSY plays a key role in β-oxidation and fatty acid respiration. It has not been possible to directly demonstrate a block in β-oxidation using biochemical approaches such as ^{14}C feeding, because it is not possible to obtain enough homozygous *csy2:csy3* seed.

The *csy2:csy3* phenotype is similar to that observed in the *cts* mutant in which an ABC transporter is disrupted (Footitt et al., 2002). Seeds exhibit dormancy and require special treatments to drive germination. The seed coat is known to be a physiological barrier, which exerts its restrictive action by impermeability to water and oxygen or by its mechanical resistance to radicle protrusion (Debeaujon et al., 2000). Like *cts,* the *csy2:csy3* mutant can be forced to germinate by removing the seed coat and supplying sucrose. This treatment allows the embryo to be exposed to oxygen and sucrose in the media. In addition, *cts* can also germinate in the presence of short chain fatty acids such as propionic acid or butyric acid, as these are believed not to require the ABC transporter for their import (Footitt et al., 2002). However these short-chain fatty acids have no effect to *csy2:csy3* seeds (results not shown). The seed dormancy phenotype observed in *csy2:csy3* double mutants may result from the energy being inadequate to initiate the germination process. In fact, seeds contain extant carbohydrate and protein reserves, but just these may not be sufficient to commence germination. However, sucrose in *cts* seeds is not metabolised in imbibed seeds, suggesting that there is some block in its utilisation (Footitt et al., 2002). The catabolism of sugar and protein reserves in *csy2:csy3* seeds has not been studied due to the difficulty in obtaining enough seed. Products derived from lipid

breakdown may be responsible for a vital energy source or signal. However, without removing the seed coat, exogenous sucrose cannot trigger germination to begin. This indicates that β-oxidation plays a role beyond carbon and energy provision. Possibly there is a mechanism of lipid signalling to control germination and metabolism. The mechanism is not yet known but β-oxidation may remove or create particular signalling molecules.

So far no β-oxidation mutants reveal severe phenotypes to such an extent as *csy2:csy3*. However, all cases can be explained by the redundancy of gene families, by which the remaining isoforms are sufficient to compensate. For example in *lacs6:lacs7*, *acx3:acx4*, *aim1* and *kat2* mutants, wild type genes encoding different isoforms are present (Fulda et al., 2004; Rylott et al., 2003b; Richmond and Bleecker, 1999; Hayashi et al., 1998; Germain et al., 2001). As shown previously, there are three peroxisomal CSY isoforms in Arabidopsis. During germination and seedling growth, only CSY2 and CSY3 are active. Mutation in only CSY2 or CSY3 results in a mild seedling phenotype in the absence of sucrose, indicating that there is a functional overlap between CSY2 and CSY3. Knocking out one *CSY* gene, another one can compensate and is sufficient for germination and post-germinative growth. In contrast, the seed phenotypes observed in *csy2:csy3* cannot be compensated by CSY1, as it is expressed only in developing seed during TAG accumulation. β-oxidation has been observed in developing seed and has been shown to be required for seed development. The *acx3:acx4* mutant revealed an embryo lethal phenotype (Rylott et al., 2003b). However, *csy2:csy3* seed is able to develop seed as normal;

this can be explained by CSY1 being able to compensate for CSY2 and CSY3 during seed development.

In Arabidopsis, beyond the seedling stage, mutants lacking the glyoxylate cycle are indistinguishable from wild type as the glyoxylate cycle has no apparent role apart from germination and seedling growth. On the other hand, β-oxidation is active in all stages of plant development. Expression of peroxisomal CSY genes is consistent with a role associated with β-oxidation as it is found in all developmental stages and is highly induced during senescence. Beyond the seedling stage β-oxidation is essential, even if the activity is at a low basal level (Graham and Eastmond, 2002). In other β-oxidation mutants that have been characterised, they may be compensated or attenuated by other isoforms in the gene family. Therefore, in most cases, no obvious phenotype shows after the seedling stage. The exceptions are the altered inflorescence meristem in *aim1* (Richmond and Bleecker, 1999) and embryo abortion in *acx3:acx4* (Rylott et al, 2003b). In contrast, *csy2:csy3* mutants showed an arrested phenotype and crucially are unable to flower and produce seeds, indicating that CSY is also required in post-germinative growth.

5.2 Fate of carbon derived from β-oxidation

In the *icl* mutant, fatty acids are still broken down and respired; in contrast, these processes cannot be carried out in *csy2:csy3* mutants. This suggests that peroxisomal CSY is required for respiration of TAGs by forming citrate from acetyl-CoA and oxaloacetate. Citrate is then transported out of the peroxisomes into the cytosol. Due

to the localisation of aconitase in both cytosol (Courtois-Verniquet and Douce, 1993; De Bellis et al., 1994; Hayashi et al., 1995) and mitochondria, either citrate or isocitrate can possibly enter mitochondria via a tricarboxylic acid transporter located on the mitochondrial membrane (Picault et al., 2002). Acetyl-CoA itself or other forms of metabolites cannot be transported from peroxisomes as indicated by the complete block in TAG mobilisation in the absence of CSY.

In yeast, as acetyl units can be transported for respiration in mitochondria via an acetyl-carnitine shuttle (van Roermund et al., 1995; 1999), knocking out peroxisomal CSY has no effect. However, acetyl units produced from β-oxidation can potentially be transported to mitochondria in the form of citrate as found in Arabidopsis. Citrate is normally exported into the cytosol in both yeast and plants as part of the glyoxylate cycle since aconitase is cytosolic (van Roermund et al., 2003). Therefore, in yeast, either citrate or isocitrate could be imported to mitochondria rather than being metabolised via the glyoxylate cycle.

The function of BOU, the acylcarnitine carrier-like protein on the mitochondrial membrane, still needs to be elucidated (Lawand et al., 2002). However its function is not consistent with a role in TAG breakdown as it is required only in the light. The glyoxylate cycle is functional in both light and dark conditions (Eastmond et al., 2000b; Cornah and Smith, 2002), and this can metabolise acetyl-CoA produced from β-oxidation. Moreover there is no gene candidate in Arabidopsis that shows similarity to the carnitine acetyl-CoA transferase (CAT) gene found in yeast. As previously mentioned the phenotypes observed in *csy2:csy3* suggested that besides

citrate, acetyl-CoA itself or other forms of metabolite cannot be transported as indicated by the complete block of β-oxidation in the absence of peroxisomal CSY. Therefore Arabidopsis is unable to use an alternative pathway such as the acetyl-carnitine shuttle discovered in yeast, but uses the citrate export pathway to transport carbon out of peroxisomes. Hence in Arabidopsis and potentially other plants, peroxisomal CSY is critical.

5.3 Role of PMDH in seedling establishment

Results obtained from phenotypic characterisation of *pmdh1:pmdh2* are consistent with the hypothesis that PMDH serves to oxidise NADH produced by β-oxidation, and does not oxidise malate to provide oxaloacetate for the glyoxylate cycle. Without the glyoxylate cycle, *icl* seedlings are unable to perform the metabolism of acetate into sucrose (Eastmond et al., 2000b; Cornah et al., 2004). This is because the glyoxylate cycle plays a key role to condense two acetyl-CoA molecules into succinate. Succinate is then converted into sucrose via gluconeogenesis. However, mutants in which PMDH is disrupted are still able to metabolise acetate into sucrose at a level similar to wild type. This indicates that PMDH is not required for the glyoxylate cycle.

Seedlings of *pmdh1:pmdh2* mutants reveal a defect in β-oxidation rather than a defect in the glyoxylate cycle. Germination and seedling growth can be achieved normally in *icl* and *mls* mutant seedlings, even if the seedlings show slightly impaired growth phenotypes when without sucrose (Eastmond et al., 2000b; Cornah

and Smith, 2002; Cornah et al., 2004). In contrast, *pmdh1:pmdh2* seeds germinate but are unable to establish as seedlings unless exogenous sucrose is supplied. In this respect, the *pmdh1:pmdh2* phenotype is similar to a range of β-oxidation mutants. The *pmdh1:pmdh2* mutant seedling are also insensitive to 2,4-DB, indicating that β-oxidation is deficient, while *icl* and *mls* are sensitive. These observations suggest that PMDH is involved in β-oxidation rather than the glyoxylate cycle.

Because β-oxidation produces NADH at the β-hydroxyacyl-CoA dehydrogenase step (catalysed by the MFP), NAD^+-malate dehydrogenase activity of PMDH is likely to be involved at this point. This will enable NADH to be reoxidised to NAD^+ which can be reused to allow the pathway to flow. A previous study in yeast has demonstrated that PMDH is required for re-oxidation of NADH produced from β-oxidation, into NAD^+ (van Roermund et al., 1999). Upon disruption of PMDH, β-hydroxyacyl-CoA, the substrate for the β-hydroxyacyl-CoA dehydrogenase step, is accumulated. As NAD^+ is not regenerated, this step cannot be carried out. The function of PMDH in Arabidopsis is potentially the same as that found in yeast. The direction of the reaction catalysed by PMDH depends on the balance of the reactants under physiological conditions. Thus the reduction of oxaloacetate toward malate by PMDH using NADH as a co-factor is apparently a favourable reaction since a high ratio of $NADH/NAD^+$ is generated during β-oxidation (Esher and Widmer, 1997).

5.4 Redundancy in the pathway for NADH re-oxidation

As mentioned previously, *cts* or *csy2:csy3* exhibit dormancy. This may result from the complete block in β-oxidation. Unlike these mutants, *pmdh1:pmdh2* seeds are not dormant, they only fail to establish as seedling in the absence of sucrose. This phenotype is similar to that observed in range of β-oxidation mutants (Fulda et al., 2004; Rylott et al., 2003b; Richmond and Bleecker, 1999; Hayashi et al., 1998; Germain et al., 2001). In all cases, β-oxidation may not be completely blocked because of the redundancy in gene families. For example, as observed in the *lacs6:lacs7* mutant in which two isoforms of long-chain acyl-CoA synthethase are disrupted, TAG content can be reduced to a 40% at day 5 (Fulda et al., 2004). The missing TAG content is presumably catabolised by other LACS isoforms within the LACS family. There are two isoforms of PMDH in Arabidopsis. Knocking out only one of the two isoforms does not reveal an obvious phenotype, indicating that one isoform can compensate for the other. When both PMDH isoforms are knocked out, a phenotype is revealed as the failure to establish as seedlings. This indicates a defect in β-oxidation in *pmdh1:pmdh2,* although it seems not to be a complete block in β-oxidation since the phenotype is not as severe as observed in *cts* or *csy2:csy3,* and about half of the total lipid content disappears by day 5. This suggests that there is an alternative means to reoxidise NADH instead of PMDH.

Presumably, there might be other isoforms of NAD^+-dependent malate dehydrogenase that could be targeted into peroxisomes or other NADH/NAD^+-oxidoreductase proteins may exist. The NADH-dehydrogenase protein (At4g21490)

containing a PTS1 signal could be a good candidate as significant expression was found in seedlings (Kamada et al., 2003).

The hypothesis that a NADH-driven electron transport chain is located on the peroxisomal remains to be established. A reductase protein, probably a flavoprotein, may exist and enable NADH to be reoxidised to NAD^+ (Hicks and Donaldson, 1982; Donaldson and Fang, 1987; Luster and Donaldson, 1987). In addition, although the evidence in yeast demonstrated that the peroxisomal membrane is likely to be impermeable to NADH, export of NADH out of the peroxisome may occur at a low level or might even take place in Arabidopsis *pmdh1:pmdh2* mutants due to a high NADH accumulation inside peroxisomes.

Based on the data obtained, the TAG profile in *pmdh1:pmdh2* seedlings begins to decrease after day 3, whereas in wild type TAG can be utilised from day 1. It is likely that some mechanism may be able to compensate for absence of PMDH function in the peroxisome at the later stage of seedling growth. Photorespiration is known to require NADH as a co-factor in the reaction of hydroxypyruvate reductase (HPR) to convert hydroxypyruvate into glycerate (Figure 5.1). During plant development the cotyledon is transformed from an oil-rich storage organ to photosynthetic tissue. Previous work showed that in Arabidopsis seedlings, HPR activity increases two fold from day 2 to day 5 (Cornah et al., 2004). Thus, at the later stage of seedling growth (in this case after day 3), NADH produced from β-oxidation might be consumed by HPR. Therefore β-oxidation in *pmdh1:pmdh2*

seedlings might be possible when photorespiratory activity, and HPR activity in particular, is present at an adequate level.

Beyond the seedling stage, *pmdh1:pmdh2* mature plants do not reveal any apparent defect in growth. This may be due to the reasons previously described. Specifically, HPR can play a major role as this enzyme requires NADH as a co-factor and appreciable activity is found in mature leaves.

During photorespiration, reducing equivalent produced from the chloroplasts and mitochondria as malate, is transported for re-oxidation by PMDH inside the peroxisomes. PMDH is known to catalyse malate oxidation into oxaloacetate, giving NADH for the HPR reaction in peroxisomes (Figure 5.1). As the *pmdh1:pmdh2* mature plant is indistinguishable from wild type, it indicates that a defect in photorespiration is not apparent under the growth conditions used. It might be that malate could be oxidised into oxaloacetate in the cytosol by cytosolic MDH or in mitochondria by mitochondrial MDH. Also in mitochondria the electrons from NADH could be directly transfered to the electron transport chain rather than generating malate. On the other hand, in *pmdh1:pmdh2*, there is no PMDH to provide NADH into HPR reaction; however, NADH produced from β-oxidation, if it is enough, could complement the absence of PMDH (Figure 5.2). Moreover, it is proposed that there might be a cytosolic isoform of HPR which prefers NADPH over NADH as a co-factor (Kleczkowski and Randall, 1988; Kleczkowski et al., 1988), so in this case hydroxypyruvate might be exported out of the peroxisome and reduced by cytosolic HPR (Figure 5.2).

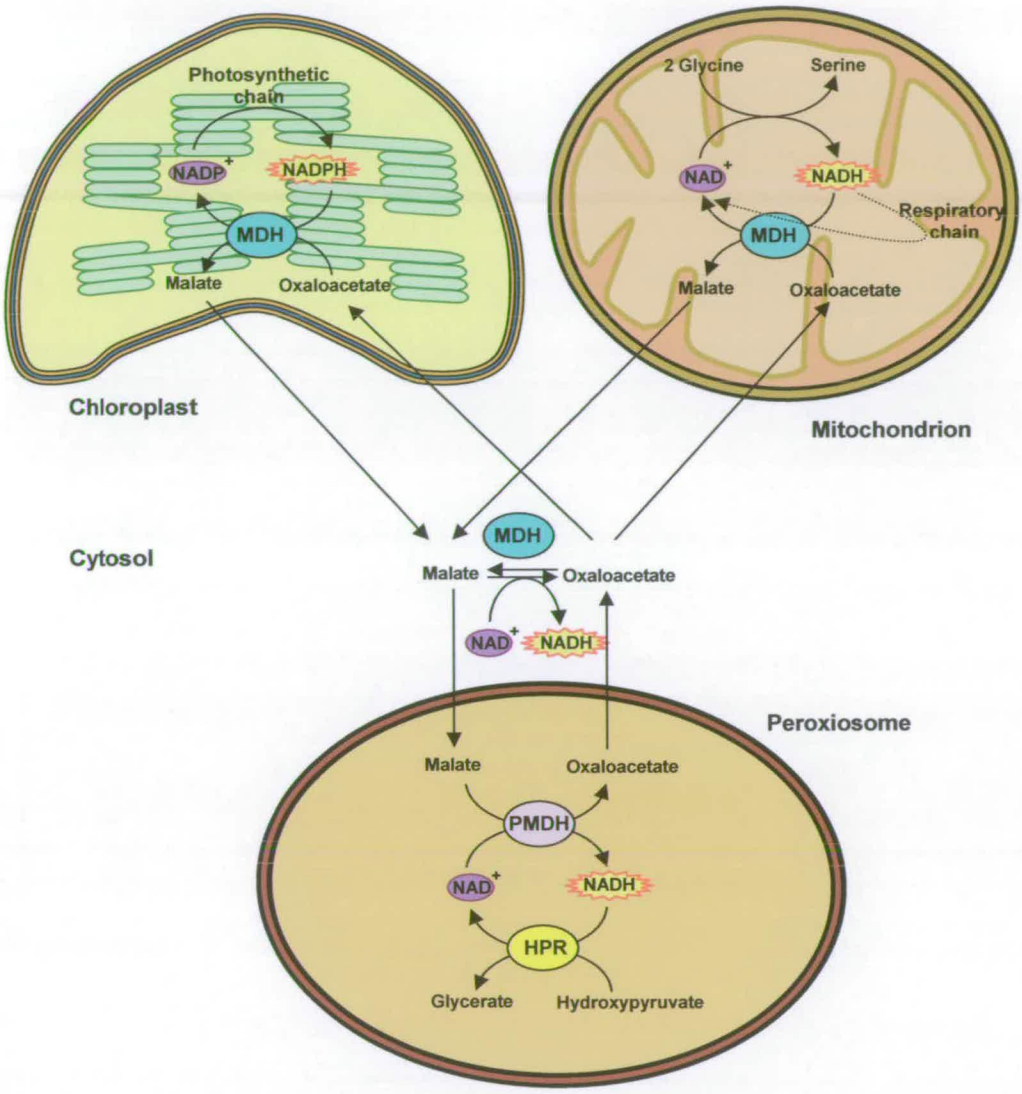

Figure 5.1 Role of PMDH in Photorespiration

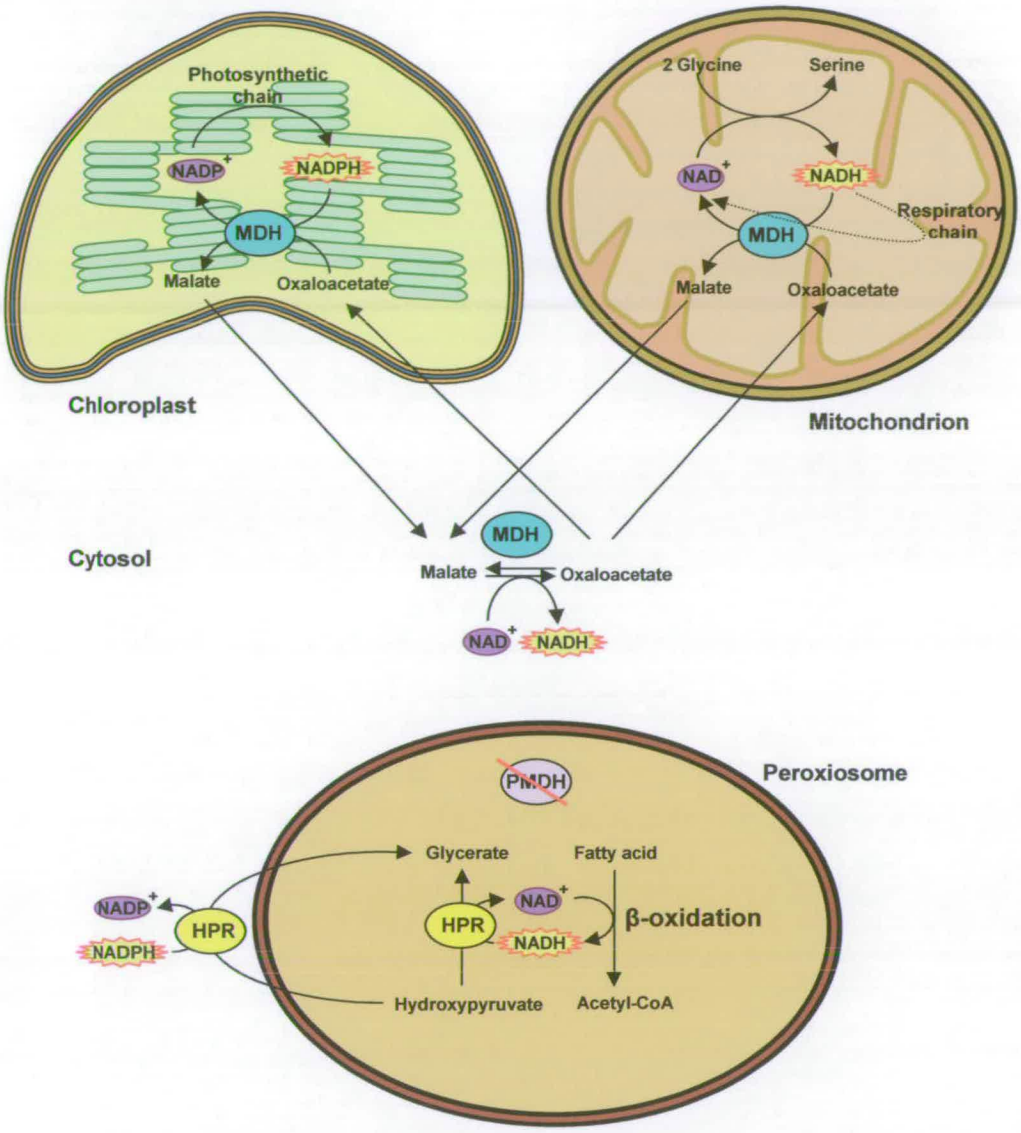

Figure 5.2 Proposed photorespiratory pathway in mutants lacking PMDH.

5.5 Proposed pathway for lipid catabolism during germination and seedling growth

Based on the results obtained so far, the pathways for lipid catabolism and gluconeogenesis can be revised and proposed as in figure 5.3. In this model, the metabolism of acetyl-CoA can be achieved by using two routes. Firstly acetyl-CoA is metabolised through the glyoxylate pathway (glyoxylate cycle) to form succinate and malate. This process requires CSY, ACO, ICL and MLS. Both succinate and malate can subsequently be converted into sucrose via gluconeogenesis. Secondly, using CSY, acetyl-CoA can be formed into citrate. Citrate and/or its derivative, isocitrate, are then respired in mitochondria. In Arabidopsis *icl* and *mls* mutants in which the glyoxylate cycle is disrupted, the seedlings are still able to use the latter route. In contrast, in mutants without CSY, both routes are interrupted.

Based on data from Arabidopsis with the disruption of PEPCK1, the gluconeogenesis seems to be very important (Rylott et al., 2003a). Mutant seedlings cannot be established in the absence of sucrose. This phenotype is more severe than that of mutants lacking the glyoxylate cycle. Hence, sucrose synthesis from lipid or other carbon sources is still absolutely required for other growing tissues such as the root which is different to fat-rich cotyledons or hypocotyls that are able to utilise and respire lipid stored within the tissue itself.

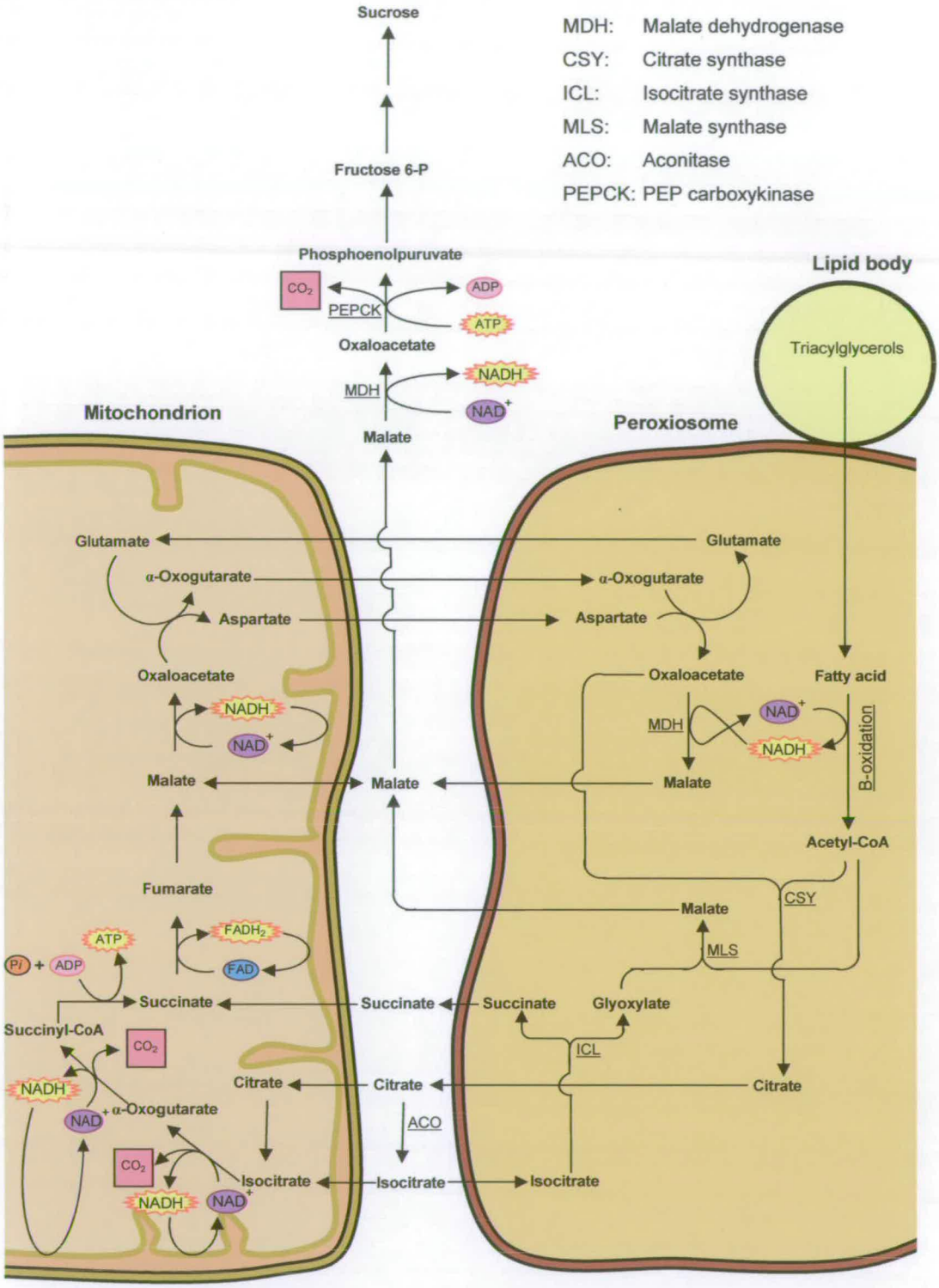

Figure 5.3 Proposed pathways for lipid catabolism during germination and seedling growth. Note that this figure does not intend to show the stoichiometry of the reactants.

Mutants lacking the glyoxylate pathway are able to germinate and establish as seedlings relatively normally because the CSY respiration route can compensate for the glyoxylate pathway and provide a means to respire lipid. The small amounts of stored sucrose in Arabidopsis seeds can be used for export to root meristems, and stored protein can be hydrolysed to amino acids which can provide three- and four-carbon skeletons for gluconeogenesis (Thomas and ap Rees, 1972).

The proposal that PMDH is involved in β-oxidation at the β-hydroxy-CoA dehydrogenase step remains to establish by using further biochemical analysis. However, based on the evidence from yeast and the phenotypes observe in *pmdh1:pmdh2*, PMDH appears to be required for β-oxidation. The direction of catalysis of PMDH is likely to depend on the physiological conditions inside peroxisomes. The carbon skeletons that influx into peroxisomes and the NADH/NAD^+ ratio are likely to be the key factors to determine the direction of the PMDH reaction. During germination large amounts of fatty acids import into the peroxisome and a significant amount of NADH is generated from β-oxidation. Thus reduction of oxaloacetate toward malate by PMDH using NADH as a co-factor is probably favoured. By contrast, beyond the seedling stage, photorespiration is probably predominant and surpasses flux through fatty acid β-oxidation. The photorespiration intermediates such as malate and hydroxypyruvate are abundant. This determines the function of PMDH to oxidise malate into oxaloacetate, generating a high concentration of NADH, which drives the HPR reaction. Therefore, PMDH serves to oxidise NADH produced by β-oxidation into NAD^+ during

germination and seedling growth (Figure 5.4A), but reduce NAD^+ into NADH to drive photorespiration beyond the seedling stage (Figure 5.4B).

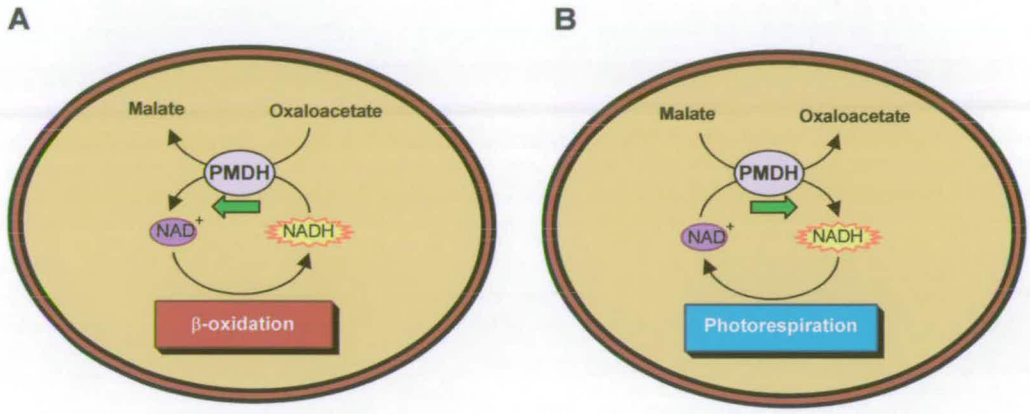

Figure 5.4 Role of PMDH in β-oxidation during germination and seedling growth **(A)** and in photorespiration beyond the seedling stage **(B)**.

5.6 Prospective research and biotechnological applications of lipid catabolism

Despite the results that have been obtained from Arabidopsis mutants with disruptions of CSY and PMDH, an overwhelming amount of work involved in this field of research still remains. Firstly, to test if the BOU pathway (Lawand et al., 2002) exists and is required for fatty acid breakdown to transport acetyl-CoA from the peroxisomes to mitochondria, the double mutant *icl:bou* is required to test this theory. This will result in a complete block of lipid mobilisation, if BOU is responsible for the acetyl-carnitine shuttle pathway. Based on a previous study in yeast (van Roermund et al., 1995), CAT and CAC in Arabidopsis are also needed to

establish this metabolic route. To test whether BOU is functional as the carnitine-acetylcarnitine carrier proteins (CACs), complementation of yeast *cac* mutant (van Roermund et al., 1995) with *BOU* might support this hypothesis. However, based on results from *icl* and *csy2:csy3* mutants, it is likely that the BOU pathway is not responsible for transferring carbon skeletons produced from TAG degradation during germination; however BOU function might be involved in mitochondrial fatty acid metabolism or polar lipid synthesis in the light. The CSY respiratory route is more likely, nevertheless the question is raised how peroxisome and mitochondria maintain the charge balance, as in this route tricarboxylate is exported and returned as dicarboxylate. The influx/efflux of these organic acids through tricarboxylate transporter/dicarboxylate transporter remains to be established (Picault et al., 2002). There might be some metabolites or ions taking part in maintaining the charge balance in each compartment.

Recently the mitochondrial succinate/fumarate transporter has been discovered and its role seems potentially linked to the glyoxylate cycle, TCA cycle and gluconeogenesis (Catoni et al., 2003). In yeast, it is proposed that succinate (from the cytosol or peroxisome) is potentially transported into mitochondria via this transporter (van Roermund et al., 2003). The fumarate is then exported into the cytosol and converted by cytosolic fumarase to malate which can then be converted to oxaloacetate and to sugar by gluconeogenesis enzymes. The function of the succinate/fumarate transporter in plants is still unknown. The role of the succinate/fumarate transporter and cytosolic fumarase might be another key point in

the pathway of lipid catabolism in plants. All in all, the knockout mutants with the disruption of these genes will be invaluable.

In the yeast mutant lacking acetyl-carnitine transferase, during fatty acid respiration, the acetyl-CoA unit cannot be transported to be respired in the mitochondria (van Roermund et al., 1995). However this is not necessary in yeast as the peroxisomal CSY can compensate, by providing citrate instead of mitochondrial CSY. It is possible that mitochondrial CSY is not absolutely required in plants, because citrate could be formed in the peroxisomes prior to import to mitochondria. Also some organic acids could be imported into the mitochondria via appropriate mitochondrial transporters. Therefore it would be worth knocking out mitochondrial CSY genes in plants, and the phenotype will reveal whether peroxisomal isoforms could compensate in these circumstances. Evidence from antisense experiments in potato suggests that this is not possible in ovary tissue, but might be in other tissues (Landschutze et al., 1995).

The role of PMDH in lipid catabolism has been tested and is consistent with the malate-aspartate shuttle proposed by Mettler and Beevers (1980). In this scheme, there are some other facts that still remain to be established. Firstly, further biochemical analysis is required to establish that PMDH is part of β-oxidation at the β-hydroxyl-CoA dehydrogenase step. β-hydroxyl-CoA potentially accumulates in *pmdh1:pmdh2* Arabidopsis, based on evidence from yeast (van Roermund et al., 1999). Secondly, whether the transfer of 2-oxoglutarate and aspartate are required to maintain the carbon and nitrogen balance during exchange of reducing equivalents,

needs to be established. To test this, a knockout mutant lacking 2-oxoglutarate-aspartate aminotransferases may reveal a defect in lipid mobilisation. Additionally, as the PMDH is involved in β-oxidation, the cytosolic MDH is implicated as responsible for part of the glyoxylate pathway. The cytosolic MDH knock out mutants may reveal a phenotype similar to those glyoxylate cycle mutants.

Understanding the mechanism of seed germination will lead to commercial applications in agriculture and brewing industries in the future. There are problems related to seed germination. For example pre-harvest seeds are unable to germinate; some seeds are dormant until the right conditions are encountered; conversely in some crops, seeds germinate too quickly, even still inside the fruit. In oilseeds including Arabidopsis, a lipid signalling molecule is believed to exist (Graham and Eastmond, 2002). This is a big challenge for researchers in this field to discover because this knowledge will be vital for application in other commercial crops. The recent availability of transcriptome and metabolome profiles has facilitated the determination of increases or decreases of particular transcripts or metabolites in the mutants. Through this analysis, mutants with defects in germination and lipid metabolism can be used to find evidence of a lipid signal mechanism. Furthermore, in the future, forward genetics might be adopted and applied with reverse genetic approaches. For example, mutant seeds such as *cts* (Footitt et al., 2002) can be subjected to mutagenesis, then seeds lacking the *cts* phenotype can be isolated and used to isolate genes potentially involved in the lipid signalling mechanism.

It is unknown whether lipid metabolism can control germination in cereals. Despite the fact that cereal seeds contain large amounts of carbohydrate source stored in the endosperm, evidence suggests that β-oxidation and glyoxylate cycle are active in cereal embryo and aleurone, to metabolise store lipid (Cornah and Smith, 2002). These mechanisms might be required to trigger germination rather than simply to provide energy. Therefore, besides Arabidopsis, the characterisation of cereal mutants with disruption of genes (such as by RNA interference) involved in this pathway will be important in the future.

Many challenges have been addressed in biotechnology research. Introducing novel genes into plants for the synthesis of valuable lipids has been carried out. Because lipid breakdown occurs constitutively, over expressing a gene does not necessarily result in accumulation of the required fatty acid. Another approach is to overcome breakdown by trying to minimise lipid degradation by suppressing β-oxidation activity (Rylott and Larson, 2002). It is also possible that fatty-rich nuts could be engineered to contain low lipid content by overexpressing genes to increase β-oxidation activity in their developing seeds. In particular, knowledge gained in this field of research is important for applications in the future. The more knowledge we have about the lipid metabolic pathways of both breakdown and synthesis, the better our understanding about how to manipulate it. From Arabidopsis, we can develop schemes to guide applications to commercial crop species.

References

Alonso, J.M., Stepanova, A.N., Leisse, T.J., Kim, C.J., Chen, H., Shinn, P., Stevenson, D.K., Zimmerman, J., Barajas, P., Cheuk, R., Gadrinab, C., Heller, C., Jeske, A., Koesema, E., Meyers, C.C., Parker, H., Prednis, L., Ansari, Y., Choy, N., Deen, H., Geralt, M., Hazari, N., Hom, E., Karnes, M., Mulholland, C., Ndubaku, R., Schmidt, I., Guzman, P., Aguilar-Henonin, L., Schmid, M., Weigel, D., Carter, D.E., Marchand, T., Risseeuw, E., Brogden, D., Zeko, A., Crosby, W.L., Berry, C.C. and Ecker, J.R. (2003) Genome-wide insertional mutagenesis of *Arabidopsis thaliana*. *Science*, **301**, 653-657.

Altschul, S.F., Gish, W., Miller, W., Myers, E.W. and Lipman, D.J. (1990) Basic local alignment search tool. *J. Mol. Biol.*, **215**, 403-410.

Bechtold, N., Ellis, J. and Pelletier, G. (1993) *In planta Agrobacterium* mediated gene transfer by infiltration of adult *Arabidopsis thaliana* plants. *C. R. Acad. Sci. Paris, Life Sci.*, **316**, 1194-1199.

Beeching, J.R. and Northcote, D.H. (1987) Nucleic acid (cDNA) and amino acid sequences of isocitrate lyase from castor bean. *Plant Mol. Biol.*, **8**, 471-475.

Beevers, H. (1979) Microbodies in higer plants. *Annu. Rev. Plant Physiol.*, **30**, 159-193.

Berkemeyer, M., Scheibe, R. and Ocheretina, O. (1998) A novel, non-redox-regulated NAD-dependent malate dehydrogenase from chloroplasts of *Arabidopsis thaliana* L. *J. Biol. Chem.*, **273**, 27927 –27933.

Bevan, M., Mayer, K., White, O., Eisen, J.A., Preuss, D., Bureau, T., Salzberg, S.L. and Mewes, H. (2001) Sequence and analysis of the Arabidopsis genome. *Curr. Opinion Plant Bio.*, **4**, 105-110.

Bewley, D.J., Hempel, F.D., McCormick, S. and Zambryski, P. (2000) Reproductive development. In Buchanan, B.B., Gruissen, W., and Jones, R.L. (eds), *Biochemistry & Molecular Biology of Plants*. American Society of Plant Physiologist, Maryland, pp. 988-1043.

Bewley, J. D. (1997): Seed germination and dormancy. *Plant Cell*, **9**, 1055-1066.

Bewley, J. D. and Black, M. (1982) *Physiology and biochemistry of seeds.* Vol 2. Viability, dormancy and environmental control. Springer-Verlag, Berlin.

Bowditch, M.I. and Donaldson, R.P. (1990) Ascorbate free-radical reduction by glyoxysomal membranes. *Plant Physiol.*, **94**, 531-537.

Boyes, D.C., Zayed, A.M., Ascenzi, R., McCaskill, A.J., Hoffman, N.E., Davis, K.R. and Gorlach, J. (2001) Growth stage-based phenotypic analysis of Arabidopsis: a model for high throughput functional genomics in plants. *Plant Cell,* **13,** 1499-1510.

Bradford, M.M. (1976) A rapid and sensitive method for quantitation of microgram quantities of protein utilizing the principle of protein-dye-binding. *Anal. Biochem.,* **72**, 248-254.

Breidenbach, R.W., and Beevers, H., (1967). Association of the glyoxylate cycle enzymes in a novel subcellular particle from castor bean endosperm. *Biochem. Biophys. Res. Commun.*, **27**, 462-469.

Brickner, D.G., Brickner, J.H. and Olsen, J.J. (1998) Sequence analysis of a cDNA encoding Pex5p, a peroxisomal targeting signal type 1 receptor from *Arabidopsis*. (Accession No. AF07843). *Plant Physiol.*, **118**, 330.

Brown, L.-A. and Baker, A. (2003) Peroxisome biogenesis and the role of protein import. *J. Cell. Mol. Med.*, **7**, 388-400.

Browse, J., McCourt, P.J. and Somerville, C.R. (1986) Fatty-acid composition of leaf lipids determined after combined digestion and fatty-acid methyl-ester formation from fresh tissue. *Anal. Biochem.*, **152**, 141-145.

Campbell, R.E., Tour, O., Palmer, A.E., Steinbach, P.A., Baird, G.S., Zacharias, D.A. and Tsien, R.Y. (2002) A monomeric red fluorescent protein. *Proc. Natl. Acad. Sci. U S A.*, **99**, 7877-7882.

Carde, J.P. (1987) Electron Microscopy of Plant Cell Membranes. *Methods Enzym.*, **148**, 599-622.

Catoni, E., Schwab, R., Hilpert, M., Desimone, M., Schwacke, R., Flugge, U.I., Schumacher, K. and Frommer, W.B. (2003) Identification of an Arabidopsis mitochondrial succinate-fumarate translocator. *FEBS Lett.*, **534**, 87-92.

Chory, J. (1993) Out of darkness: Mutants reveal pathways controlling light-regulated development in plants. *Trends Genet.*, **9**, 167-172.

Clough, S.J. and Bent, A.F. (1998) Floral dip: a simplified method for *Agrobacterium*-mediated transformation of Arabidopsis thaliana. *Plant J.*, **16**, 735-743.

Comai, L., Dietrich, R.A., Maslyar, D.J., Baden, C.S. and Harada, J.J. (1989) Coordinate expression of transcriptionally regulated isocitrate lyase and malate synthase genes in *Brassica napus* L. *Plant Cell*, **1**, 293-300.

Cooper, T.G. and Beevers, H. (1969a) Mitochondria and glyoxysomes from castor bean endosperm. Enzyme constituents and catalytic capacity. *J. Biol. Chem.*, **214**, 3507-3513.

Cooper, T.G. and Beevers, H. (1969b) β-oxidation in glyoxysomes from castor bean endosperm. *J. Biol. Chem.*, **244**, 3514-3520.

Cooper, T.G., (1971) Activation of fatty acids in castor bean endosperm. *J. Biol Chem.*, **246**, 3451-5.

Cornah, J.E. and Smith, S.M. (2002) Synthesis and function of glyoxylate cycle enzymes. In Baker,A. and Graham,I.A. (eds), *Plant Peroxisomes*. Kluwer Academic Publishers, London, pp. 57-101.

Cornah, J.E., Germain, V., Ward, J.L., Beale, M.H. and Smith, S.M. (2004) Lipid utilization, gluconeogenesis, and seedling growth in *Arabidopsis* mutants lacking the glyoxylate cycle enzyme malate synthase. *J. Biol. Chem.*, **279,** 42916-42923.

Corpas, F.J., Barroso, J.B. and del Rio, L.A. (2001) Peroxisomes as a source of reactive oxygen species and nitric oxide signal molecules in plant cells. *Trends Plant Sci.*, **6,** 145-150.

Cosgrove, D.J. (1997). Relaxation in a high-stress environment: The molecular bases of extensible cell walls and cell enlargement. *Plant Cell*, **9**, 1031-1041.

Courtois-Verniquet, F. and Douce, R. (1993) Lack of aconitase in glyoxysomes and peroxisomes. *Biochem. J.*, **294,** 103-107.

Crowe, J.H. and Crowe, L.M. (1992). Membrane integrity in anhydrobiotic organisms: Toward a mechanism for stabilizing dry seeds. In Somero, G.N., Osmond, C.B. and Bolis, C.L. (eds), *Water and Life*. Springer-Verlag, Berlin, pp. 87-103.

Daddow, L. Y. M. (1983) A double lead stain method for enhancing contrast of ultrathin sections in electron microscopy: a modified multiple staining technique. *J. Microscopy,* **129**, 147-153.

De Bellis, L., Hayashi, M., Biagi, P.P., Haranishimura, I., Alpi, A. and Nishimura, M. (1994) Immunological analysis of aconitase in pumpkin cotyledons - the absence of aconitase in glyoxysomes. *Physiol. Plant,* **90**, 757-762.

Debeaujon, I., Léon-Kloosterziel, K.M. and Koornneef, M. (2000) Influence of the testa on seed dormancy, germination and longevity in *Arabidopsis*. *Plant Physiol.*, **122**, 403–413.

Dieuaide, M, Brouquisse, R., Pradet, A. and Raymond, P. (1992) Increased fatty acid β-oxidation after glucose starvation in maize root tips. *Plant Physiol.*, **99**, 595-600.

Donaldson, R.P. (1982) Nicotinamide cofactors (NAD and NADP) in glyoxysomes, mitochondria and plastids isolated from castor bean endosperm. *Arch. Biochem. Biophys.*, **215**, 274-279.

Donaldson, R.P. and Fang, T.K. (1987) β-oxidation and glyoxylate cycle coupled to NADH: cytochrome c and ferricyanide reductases in glyoxysomes. *Plant Physiol.*, **85**, 792-795.

Eastmond, P. J., Hooks, M. and Graham, I. A. (2000a) The Arabidopsis acyl-CoA oxidase gene family. *Biochem. Soc. Trans.*, **28**, 755–757.

Eastmond, P.J. and Graham, I.A. (2000) The multifunctional protein AtMFP2 is co-ordinately expressed with other genes of fatty acid beta-oxidation during seed germination in Arabidopsis thaliana (L.) Heynh. *Biochem. Soc. Trans.*, **28**, 95-99.

Eastmond, P.J. and Graham, I.A. (2001) Re-examining the role of glyoxylate cycle in oilseeds. *Trends Plant Sci.*, **6**, 72-77.

Eastmond, P.J., Germain, V., Lange, P.R., Bryce, J.H., Smith, S.M. and Graham, I.A. (2000b) Postgerminative growth and lipid catabolism in oilseeds lacking the glyoxylate cycle. *Proc. Natl. Acad. Sci. USA*, **97**, 5669-5674.

Eccleston, V.S. and Ohlrogge, J.B. (1998) Expression of lauroyl-acyl carrier protein thioesterase in *Brassica napus* seeds induces pathways for both fatty acid oxidation and biosynthesis and implies a set point for triacylglycerol accumulation. *Plant Cell*, **10**, 613-622.

Edwards, K., Johnstone, C. and Thompson, C. (1991) A simple and rapid method for the preparation of plant genomic DNA for PCR analysis. *Nucleic. Acids Res.*, **19**, 1349.

Einwachter, H., Sowinski, S., Kunau, W.H. and Schliebs, W. (2001) Yarrowia lipolytica Pex20p, Saccharomyces cerevisiae Pex18p/Pex21p and mammalian Pex5pL fulfil a common function in the early steps of the peroxisomal PTS2 import pathway. *EMBO Rep.*, **2**, 1035-1039.

Elgersma, Y., Van Roermund, C.W.T., Wanders, R.J.A. and Tabak, H.F. (1995) Peroxisomal and mitochondrial carnitine acetyltransferases of *Saccharomyces cerevisiae* are encoded by a single gene. *EMBO J.*, **14**, 3472-3479.

Escher, C. L. and Widmer, F., 1997. Lipid mobilization and gluconeogenesis in plants: Do glyoxylate cycle enzyme activities constitute a real cycle? A hypothesis. *Biol. Chem.*, **378**, 803-813.

Footitt, S., Slocombe, S.P., Larner, V., Kurup, S., Wu, Y., Larson, T., Graham, I., Baker, A. and Holdsworth, M. (2002) Control of germination and lipid mobilization by *COMATOSE*, the *Arabidopsis* homologue of human ALDP. *EMBO J.*, **21**, 2912-2922.

Froman, B.E., Edwards, P.C., Bursch, A.G. and Dehesh, K. (2000) ACX3, a novel medium-chain acyl-coenzyme A oxidase from Arabidopsis. *Plant Physiol.*, **123**,733-42.

Fulda, M., Schnurr, J., Abbadi, A., Heinz, E. and Browse, J. (2004) Peroxisomal acyl-CoA synthetase activity is essential for seedling development in *Arabidopsis thaliana*. *Plant Cell,* **16,** 394-405.

Fulda, M., Shockey, J., Werber, M., Wolter, F.P. and Heinz, E. (2002) Two long-chain acyl-CoA synthetases from *Arabidopsis thaliana* involved in peroxisomal fatty acid beta-oxidation. *Plant J.*, **32**, 93-103.

Garciarrubio, A., Legaria, J.P. and Covarrubias, A.A. (1997) Abscisic acid inhibits germination of mature *Arabidopsis* seeds by limiting the availability of energy and nutrients. *Planta*, **203**, 182–187.

Gasteiger, E., Gattiker, A., Hoogland, C., Ivanyi, I., Appel, R.D. and Bairoch, A. (2003) ExPASy: the proteomics server for in-depth protein knowledge and analysis. *Nucleic Acids Res.*, **31**, 3784-3788.

Gerbling, H. and Gerhardt, B. (1987) Activation of fatty acids by non-glyoxysomal peroxisomes. *Planta,* **171,** 386-392.

Gerhardt, B. (1985) Substrate specificity of peroxisomal acyl-CoA oxidase. *Phytochemistry,* **24**, 351–352.

Germain, V., Rylott, E.L., Larson, T.R., Sherson, S.M., Bechtold, N., Carde, J.P., Bryce, J.H., Graham, I.A. and Smith, S.M. (2001) Requirement for 3-ketoacyl-CoA thiolase-2 in peroxisome development, fatty acid β-oxidation and breakdown of triacylglycerol in lipid bodies of *Arabidopsis* seedlings. *Plant J.,* **28,** 1-12.

Gietl, C. (1990) Glyoxysomal malate dehydrogenase from watermelon is synthesized with an amino-terminal transit peptide. *Proc. Natl. Acad. Sci. USA,* **87**, 5773-5777.

Gietl, C., Faber, K.N., van der Klei, I.J. and Veenhuis M. (1994) Mutational analysis of the N-terminal topogenic signal of watermelon glyoxysomal malate dehydrogenase using the heterologous host Hansenula polymorpha. *Proc. Natl. Acad. Sci. USA,* **91**, 3151-3155.

Gish, W. and States, D.J. (1993) Identification of protein coding regions by database similarity search. *Nature Genet.,* **3**, 266-272.

Graham, I.A. and Eastmond, P.J. (2002) Pathways of straight and branched chain fatty acid catabolism in higher plants. *Prog Lipid Res.,* **41**, 156-181.

Graham, I.A., Baker, C.J. and Leaver, C.J. (1994a) Analysis of the cucumber malate synthase gene promoter by transient expression and gel retardation assays. *Plant J.*, **6**; 893-902.

Graham, I.A., Denby, K.J. and Leaver, C.J. (1994b) Carbon catabolite repression regulates glyoxylate cycle gene expression in cucumber. *Plant Cell,* **6,** 761–772.

Graham, I.A., Leaver, C.J. and Smith, S.M. (1992) Induction of malate synthase gene expression in senescent and detached organs of cucumber. *Plant Cell,* **4,** 349-357.

Guhnemann-Schafer, K. and Kindl, H. (1995) Fatty acid beta-oxidation in glyoxysomes. Characterization of a new tetrafunctional protein (MFP III). *Biochim Biophys Acta.,* **1256,** 181-186.

Gut, H. and Matile, P. (1988) Apparent induction of key enzymes of the glyoxylic acid in senescent barley. *Planta*, **176,** 548-550.

Hayashi, M. and Nishimura, M. (2002) Genetic approaches to understand plant peroxisomes. In Baker, A. and Graham, I.A. (eds), *Plant Peroxisomes.* Kluwer Academic Publishers, London, pp. 279-303.

Hayashi, M. and Nishimura, M. (2003) Entering a new era of research on plant peroxisomes. *Curr. Opin. Plant Biol.,* **6,** 577-582.

Hayashi, M., Aoki, M., Kondo, M. and Nishimura, M. (1997) Changes in targeting efficiencies of proteins to plant microbodies caused by amino acid substitutions in the carboxy-terminal tripeptide. *Plant Cell Physiol.*, **38,** 759–768.

Hayashi, M., De Bellis, L., Alpi, A. and Nishimura, M. (1995) Cytosolic aconitase participates in the glyoxylate cycle in etiolated pumpkin cotyledons. *Plant Cell Physiol.,* **36,** 669-680.

Hayashi, M., Masahiro, A., Kato, A., Kondo, M. and Nishimura, M. (1996) Transport of chimeric proteins that contains a carboxy-terminal targeting signal into plant microbodies. *Plant J.,* **10,** 225-234.

Hayashi, M., Nito, K., Takei-Hoshi, R., Yagi, M., Kondo, M., Suenaga, A., Yamaya, T. and Nishimura, M. (2002) Ped3p is a peroxisomal ATP-binding cassette transporter that might supply substrates for fatty acid beta-oxidation. *Plant Cell Physiol.*, **43**, 1-11.

Hayashi, M., Nito, K., Toriyama-Kato, K., Kondo, M., Yamaya, T. and Nishimura, M. (2000a) AtPex14p maintains peroxisomal functions by determining protein targeting to three kinds of plant peroxisomes. *EMBO J.*, **19**, 5701-5710.

Hayashi, M., Toriyama, K., Kondo, M. and Nishimura, M. (1998) 2,4-dichlorophenoxybutyric acid-resistant mutants of *Arabidopsis* have defects in glyoxysomal fatty acid ß-oxidation. *Plant Cell,* **10,** 183-195.

Hayashi, M., Toriyama, K., Kondo, M., Kato, A., Mano, S., De Bellis, L., Hayashi-Ishimaru, Y., Yamaguchi, K., Hayashi, H. and Nishimura, M. (2000b) Functional transformation of plant peroxisomes. *Cell Biochem Biophys.*, **32**, 295-304.

Heazlewood, J.L., Tonti-Filippini, J.S., Gout, A.M., Day, D.A., Whelan, J. and Millar, A.H. (2004) Experimental analysis of the *Arabidopsis* mitochondrial proteome highlights signaling and regulatory components, provides assessment of targeting prediction programs, and indicates plant-specific mitochondrial proteins. *Plant Cell,* **16,** 241-256.

Hellens, R.P., Edwards, E.A., Leyland, N.R., Bean, S. and Mullineaux, P.M. (2000) pGreen: a versatile and flexible binary Ti vector for *Agrobacterium*-mediated plant transformation. *Plant Mol. Bio.,* **42,** 819-832.

Hettema, E.H., van Roermund, C.W., Distel, B., van den Berg, M., Vilela, C., Rodrigues-Pousada, C., Wanders, R.J. and Tabak, H.F. (1996) The ABC transporter proteins Pat1 and Pat2 are required for import of long-chain fatty acids into peroxisomes of Saccharomyces cerevisiae. *EMBO J.*, **15**, 3813-3822.

Hicks, D.B., and Donaldson, R.P. (1982) Electron transport in glyoxysomal membranes. *Arch. Biochem. Biophys.*, **215**, 280-288.

Holdsworth, M., Kurup, S. and McKibbin, R. (1999) Molecular and genetic mechanisms regulating the transition from embryo development to germination. *Trends in Plant Sci.*, **4**, 275-280.

Hong, Y., Wang, T.-W., Hudak, K. A., Schade, F., Froese, C. D., and Thompson, J. E. (2000) An ethylene-induced cDNA encoding a lipase expressed at the onset of senescence. *Proc. Natl. Acad. Sci. USA,* **97**, 8717–8722.

Hooks, M A (2002) Molecular biology, enzymology and physiology of β-oxidation. In Baker,A. and Graham,I.A. (eds), *Plant Peroxisomes*. Kluwer Academic Publishers, London, pp.19-55.

Hooks, M. A., Kellas, F. and Graham, I.A. (1999) Long-chain acyl-CoA oxidases of Arabidopsis. *Plant J.* **20**, 1-13.

Huala, E., Dickerman, A., Garcia-Hernandez, M., Weems, D., Reiser, L., LaFond, F., Hanley, D., Kiphart, D., Zhuang, J., Huang, W., Mueller, L., Bhattacharyya, D., Bhaya, D., Sobral, B., Beavis, B., Somerville, C. and Rhee, S.Y. (2001) The Arabidopsis Information Resource (TAIR): A comprehensive database and web-based information retrieval, analysis, and visualization system for a model plant. *Nucleic Acids Res.*, **29**, 102-105.

Huang, A.H. (1992) Oil bodies and oleosins in seeds. *Annu. Rev. Plant Physiol.*, **43**, 177-200.

Ismail, I., De Bellis, L., Alpi, A. and Smith, S. M. 1997 Expression of glyoxylate cycle genes in cucumber roots responds to sugar supply and can be activated by shading or defoliation of the shoot. *Plant Mol Biol.*, **35**; 633-640.

Johnson, T.L. and Olsen, L.J. (2001) Building new models for peroxisome biogenesis. *Plant Physiol.*, **127**, 731-739.

Johnson, T.L. and Olsen, L.J. (2003) Import of the peroxisomal targeting signal type 2 protein 3-ketoacyl-coenzyme a thiolase into glyoxysomes. *Plant Physiol.*, **133**, 1991-1999.

Kagawa, T. and Beevers, H. (1975) The development of microbodies (glyoxysomes and leaf peroxisomes) in cotyledons of germinating seedling. *Plant physiol.*, **55**, 258-264.

Kamada, T., Nito, K., Hayashi, H., Mano, S., Hayashi, M. and Nishimura, M. (2003) Functional differentiation of peroxisomes revealed by expression profiles of peroxisomal genes in Arabidopsis thaliana. *Plant Cell Physiol.*, **44**, 1275-1289.

Karnovsky. M. J. (1965) A Formaldehyde Glutaraldehyde fixative of high osmolality for use in electron microscopy. *J. Cell Biol.*, **27**, 137A.

Kato, A., Hayashi, M. and Nishimura, M. (1999) Oligomeric proteins containing N-terminal targeting signals are imported into peroxisomes in transgenic Arabidopsis. *Plant Cell Physiol.*, **40**, 586-591.

Kato, A., Hayashi, M., Kondo, M. and Nishimura, M. (1996) Targeting and processing of a chimeric protein with the N-terminal presequence of the precursor to glyoxysomal citrate synthase. *Plant Cell*, **8**, 1601-1611.

Kato, A., Hayashi, M., Kondo, M. and Nishimura, M. (2000) Transport of peroxisomal proteins that are synthesized as large precursors in plants. *Cell Biochem. Biophys.*, **32**, 269-275.

Kato, A., Hayashi, M., Mori, H. and Nishimura, M. (1995) Molecular characterization of a glyoxysomal citrate synthase that is synthesized as a precursor of higher molecular mass in pumpkin. *Plant Mol Biol.*, **27**, 377-390.

Kato, A., Takeda-Yoshikawa, Y., Hayashi, M., Kondo, M., Hara-Nishimura, I. and Nishimura, M. (1998) Glyoxysomal malate dehydrogenase in pumpkin:

cloning of a cDNA and functional analysis of its presence. *Plant Cell Physiol.*, **39**, 186-195.

Kersey, P. J., Duarte, J., Williams, A., Karavidopoulou, Y., Birney, E. and Apweiler, R. (2004) The International Protein Index: An integrated database for proteomics experiments. *Proteomics,* **4**, 1985-1988.

Kim, D.-J. and Smith, S.M. (1994) Expression of a single gene encoding microbody NAD-malate dehydrogenase during glyoxysome and peroxisome development in cucumber. *Plant. Mol. Biol.,* **26,** 1833-1841.

Kleczkowski, L.A. and Randall, D.D. (1988) Purification and characterization of a novel NADPH (NADH)-dependent hydroxypyruvate reductase from spinach leaves. Comparison of immunological properties of leaf hydroxypyruvate reductases. *Biochem J.,* **250**, 145-152.

Kleczkowski, L.A., Givan, C.V., Hodgson, J.M. and Randall, D.D. (1988) Subcellular localisation of NADPH-dependent hydroxyl pyruvate reductase of leaf protoplasts of *Pisum sativum* L. and its role in photorespiratory metabolism. *Plant physiol.*, **88**, 1182-1185.

Koncz, C. and Schell, J. (1986) The promoter of TL-DNA gene 5 controls the tissue-specific expression of chimaeric genes carried by a novel type of *Agrobacterium* binary vector. *Mol. Gen. Genet.*, **204**, 383-396.

Kozaki, A. and Takeba, G. (1996) Photorespiration protects C_3 plants from photooxidation. *Nature,* **384**, 557-560.

Krysan, P.J., Young, J.C., and Sussman, M.R. (1999) T-DNA as an insertional mutagen in *Arabidopsis*. *Plant Cell,* **11**, 2283-2290.

Krysan, P.J., Young, J.C., Tax, F. and Sussman, M.R. (1996) Identification of transferred DNA insertions within *Arabidopsis* genes involved in signal transduction and ion transport. *Proc. Natl. Acad. Sci. USA,* **93**, 8145-8150.

Kunau, W.H., Dommes, V. and Schulz, H. (1995) β-oxidation of fatty acids in mitochondria, peroxisomes and bacteria: a century of continued progress. *Prog. Lipid Res.*, **34**, 267-342.

Laibach, F. (1943) *Arabidopsis thaliana* (L.) Heynh. als Objekt für genetische und entwicklungsphysiologische Untersuchungen. *Bot. Archiv.*, **44**, 439–455.

Landschutze, V., Willmitzer, L., and Muller-Rober, B. (1995) Inhibition of flower formation by antisense repression of mitochondrial citrate synthase in transgenic potato plants leads to a specific disintegration of the ovary tissues of flowers. *EMBO J.*, **14**, 660-666.

Lawand, S., Dorne, A.J., Long, D., Coupland, G., Mache, R. and Carol, P. (2002) Arabidopsis *A BOUT DE SOUFFLE*, which is homologous with mammalian carnitine acyl carrier, is required for postembryonic growth in the light. *Plant Cell,* **14,** 2161-2173.

Lazarow, P.B. (2003) Peroxisome biogenesis: advances and conundrums. *Curr. Opin. Cell Biol.*, **15**, 489-497.

Lee, J.G., Cho, S.P., Lee, H.S., Lee, C.H., Bae, K.S. and Maeng, P.J. (2000) Identification of a cryptic N-terminal signal in *Saccharomyces cerevisiae* peroxisomal citrate synthase that functions in both peroxisomal and mitochondrial targeting. *J. Biochem.*, **128,** 1059-1072.

Li, Y., Rosso, M.G., Strizhov, N., Viehoever, P. and Weisshaar, B. (2003) GABI-Kat Simple Search: a flanking sequence tag (FST) database for the identification of T-DNA insertion mutants in Arabidopsis thaliana. *Bioinformatics.*, **19**, 1441-1442.

Liepman, A.H. and Olsen, L.J. (2001) Peroxisomal alanine:glyoxylate aminotransferase (AGT1) is a photorespiratory enzyme with multiple substrates in *Arabidopsis thaliana. Plant J.*, **25**, 487-498.

Lin, Y., Cluette-Brown, J.E. and Goodman, H.M. (2004) The peroxisome deficient *Arabidopsis* mutant *sse1* exhibits impaired fatty acid synthesis. *Plant Physiol.*, **135**, 814-827.

López-Huertas, E., Corpas, F.J., Sandalio, L.M. and del Río, L.A. (1999) Characterization of membrane polypeptides from pea leaf peroxisomes involved in superoxide radical generation. *Biochem J.*, **337**, 531-536.

López-Huertas, E., Sandalio, L.M., Gomez, M. and del Río, L.A. (1997) Superoxide radical generation in peroxisomal membranes: evidence for the participation of the 18-kD integral membrane polypeptide. *Free Radical Res.*, **26**, 497-506.

Lovegrove, A. and Hooley, R. (2000) Gibberellin and abscisic acid signalling in aleurone. *Trends Plant Sci.*, **5**, 102-110.

Luster, D.G. and Donaldson, R.P. (1987) Glyoxysomal membrane electron transport proteins. In: Fahimi, D.D. and Sies, H. (editors), *Peroxisomes in biology and medicine*, Spinger-Verlag, Heidenberg, pp. 189-193.

Madden, T.L., Tatusov, R.L. and Zhang, J. (1996) Applications of network BLAST server. *Meth. Enzymol.*, **266**, 131-141.

Mano, S., Nakamori, C., Hayashi, M., Kato, A., Kondo, M. and Nishimura, M. (2002) Distribution and characterization of peroxisomes in Arabidopsis by visualization with GFP: dynamic morphology and actin-dependent movement. *Plant Cell Physiol.*, **43**, 331-341.

Martin, T., Oswald, O. and Graham, I.A. (2002) Arabidopsis seedling growth, storage lipid mobilization, and photosynthetic gene expression are regulated by carbon:nitrogen availability. *Plant Physiol.*, **128**, 472-481.

Matsumura, T., Otera, H. and Fujiki, Y. (2000) Disruption of the interaction of the longer isoform of Pex5p, Pex5pL, with Pex7p abolishes peroxisome targeting signal type 2 protein import in mammals. Study with a novel Pex5-impaired Chinese hamster ovary cell mutant. *J. Biol. Chem.*, **275**, 21715-21721.

McLaughlin, J.C. and Smith, S.M. (1994) Metabolic regulation of glyoxylate-cycle enzyme synthesis in detached cucumber cotyledons and protoplasts. *Planta*, **195**, 22-28.

McQueen-Mason, S. and Cosgrove, D.J. (1995). Expansin mode of action on cell walls. Analysis of wall hydrolysis, stress relaxation, and binding. *Plant Physiol.*, **107**, 87-100.

Mettler, I.J. and Beevers, H. (1980) Oxidation of NADH in glyoxysomes by a malate-aspartate shuttle. *Plant Physiol.*, **66**, 555-560.

Millar, A.H., Sweetlove, L.J., Giege, P. and Leaver, C.J. (2001) Analysis of the Arabidopsis Mitochondrial Proteome. *Plant Physiol.*, **127**, 1711-1727.

Mosser, J., Douar, A.M., Sarde, C.O., Kioschis, P., Feil, R., Moser, H., Poustka, A.M., Mandel, J.L. and Aubourg, P. (1993) Putative X-linked adrenoleukodystrophy gene shares unexpected homology with ABC transporters. *Nature*, **361**, 726-730.

Mullen, R.T. (2002) Targeting and import of matrix proteins into peroxisomes. In Baker,A. and Graham,I.A. (eds), *Plant Peroxisomes*. Kluwer Academic Publishers, London, pp. 339-383.

Mullen, R.T., Flynn, C.R. and Trelease, R.N. (2001) How are peroxisomes formed? The role of the endoplasmic reticulum and peroxins. *Trends Plant Sci.*, **6**, 273-278.

Mullen, R.T., Lee, M.S. and Trelease, R.N. (1997) Identification of the peroxisomal targeting signal for cotton seed catalase. *Plant J.*, **12**, 313-322.

Murashige, T. and Skoog, F. (1962) A revised medium for rapid growth and bioassays with tobacco tissue cultures. *Physiol. Plant.*, **15**, 473-497.

Nicholas, K.B., Nicholas Jr., H.B. and Deerfield II, D.W.. (1997). GeneDoc: Analysis and Visualization of Genetic Variation. *EMBNET.NEWS*, **4**, 1-4.

Nishimura, M., and Beevers, H. (1979) Subcellular distribution of gluconeogenetic enzymes in germinating castor bean endosperm. *Plant Physiol.*, **64**, 31-37.

Nishimura, M., Yamaguchi, J., Mori, H., Akazawa, T. and Yokota, S. (1986) Immunocytochemical analysis shows that glyoxysomes are directly transformed to leaf peroxisomes during greening of pumpkin cotyledon. *Plant Physiol.*, **81**, 313-316.

Nito, K., Hayashi, M. and Nishimura, M. (2002). Direct interaction and determination of binding domains among peroxisomal import factors in *Arabidopsis thaliana*. *Plant Cell Physiol.*, **43**, 355-366.

Old, R. W. and Primrose, S. B. (1994) *Principles of Gene Manipulation, (5th ed).* Blackwell Science, Oxford.

Olsen, L. J. (1998) The surprising complexity of peroxisome biogenesis. *Plant Mol. Biol.*, **38**, 163-189.

Penfield, S., Rylott, E.L., Gilday, A.D., Graham, S., Larson, T.R. and Graham, I.A. (2004) Reserve mobilization in the Arabidopsis endosperm fuels hypocotyl elongation in the dark, is independent of abscisic acid, and requires *PHOSPHOENOLPYRUVATE CARBOXYKINASE1*. *Plant Cell.* **16**, 2705-2718.

Picault, N., Palmieri, L., Pisano, I., Hodges, M. and Palmieri, F. (2002) Identification of a novel transporter for dicarboxylates and tricarboxylates in plant mitochondria. Bacterial expression, reconstitution, functional characterization, and tissue distribution. *J. Biol. Chem.*, **277**, 24204-24211.

Pires, J.R., Hong, X., Brockmann, C., Volkmer-Engert, R., Schneider-Mergener, J., Oschkinat, H. and Erdmann, R. (2003) The ScPex13p SH3 domain exposes two distinct binding sites for Pex5p and Pex14p. *J. Mol. Biol.*, **326**, 1427-1435.

Purdue, P. E. and Lazarow, P.B. (2001) Peroxisome biogenesis. *Annu. Rev. Cell Dev. Biol.*, **17**, 701-752.

Raymond, P., Spiteri, A., Dieuaide, M., Gerhardt, B. and Pradet, A. (1992) Peroxisomal β-oxidation of fatty acids and citrate formation by a particulate fraction from early germinating sunflower seeds. *Plant Physiol. Biochem.*, **30**, 153-161.

Reumann, S. (2000) The structural properties of plant peroxisomes and their metabolic significance. *Biol. Chem.*, **381**, 639-648.

Reumann, S. (2002) The photorespiratory pathway of leaf peroxisomes. In Baker, A. and Graham, I.A. (eds), *Plant Peroxisomes*. Kluwer Academic Publishers, London, pp. 141-190.

Richmond, T. and Bleecker, A.B. (1999). A defect in β-oxidation causes abnormal inflorescence development in *Arabidopsis*. *Plant Cell,* **11**, 1911-1924.

Ritchie, S. and Gilroy, S. (1998) Gibberellins: regulation genes and germination. *New Phytol.*, **140**, 363-383.

Rosso, M.G., Li, Y., Strizhov, N., Reiss, B., Dekker, K. and Weisshaar, B. (2003) An Arabidopsis thaliana T-DNA mutagenized population (GABI-Kat) for flanking sequence tag-based reverse genetics. *Plant Mol Biol.*, **53**, 247-259.

Russell, L., Larner, V., Kurup, S., Bougourd, S. and Holdsworth, M.J. (2000) The *Arabidopsis COMATOSE* locus regulates germination potential. *Development*, **127**, 3759–3767.

Rylott, E. and Larson, T. (2002) Futile cycling through β-oxidation as a barrier to increased yields of novel oils. In Baker, A. and Graham, I.A. (eds), *Plant Peroxisomes*. Kluwer Academic Publishers, London, pp. 445-464.

Rylott, E.L., Gilday, A.D., and Graham, I.A. (2003a) The gluconeogenic enzyme Phosphoenolpyrubate carboxykinase in Arabidopsis is essential for seedling establishment. *Plant Physiol.*, **131**, 1834-1842.

Rylott, E.L., Hooks, M.A., and Graham, I.A. (2001) Co-ordinate regulation of genes involved in storage lipid mobilization in *Arabidopsis thaliana. Biochem. Soc. Trans.*, **29**, 283-287.

Rylott, E.L., Rogers, C.A., Gilday, A.D., Edgell, T., Larson, T.R. and Graham, I.A. (2003b) *Arabidopsis* mutants in short- and medium-chain acyl-CoA oxidase activities accumulate acyl-CoAs and reveal that fatty acid β-oxidation is essential for embryo development. *J. Biol. Chem.*, **278**, 21370-21377.

Sacksteder, K.A. and Gould, S.J. The genetics of peroxisome biogenesis. *Annu. Rev. Genet.*, **34**, 623-652.

Salon, C., Raymond, P. and Pradet, A. (1988) Quantification of carbon fluxes through the tricarboxylic acid cycle in early germinating lettuce embryos. *J. Biol. Chem.*, **263**, 12278-12287.

Sambrook, J., Fritsch, E.F. and Maniatis, T. (1989) *Molecular Cloning: A Laboratory Manual, Vol. 1, 2, 3. (2nd ed).* Cold Spring Harbor Laboratory Press, NY, USA.

Schnarrenberger, C., Fitting, K.H., Tetour, M. and Zehler, H. (1980) Inactivation of the glyoxysomal citrate synthase from caster bean endosperm by 5,5'-dithio-bis(2-nitrobenzoic acid) (DTNB). *Protoplasm*, **103**, 299-307.

Schumann, U., Gietl, C. and Schmid, M. (1999) Sequence analysis of a cDNA encoding Pex7p, a peroxisomal targeting signal 2 receptor from *Arabidopsis thaliana* (accession no. AF130973). (PGR99-060). *Plant Physiol.*, **120,** 339.

Seki, M., Narusaka, M., Kamiya, A., Ishida, J., Satou, M., Sakurai, T., Nakajima, M., Enju, A., Akiyama, K., Oono, Y., Muramatsu, M., Hayashizaki, Y., Kawai, J., Carninci, P., Itoh, M., Ishii, Y., Arakawa, T., Shibata, K., Shinagawa, A.

and Shinozaki, K. (2002) Functional annotation of a full-length *Arabidopsis* cDNA collection. *Science,* **296**, 141-145.

Sessions, A., Burke, E., Presting, G., Aux, G., McElver, J., Patton, D., Dietrich, B., Ho, P., Bacwaden, J., Ko, C., Clarke, J.D., Cotton, D., Bullis, D., Snell, J., Miguel, T., Hutchison, D., Kimmerly, B., Mitzel, T., Katagiri, F., Glazebrook, J., Law, M. and Goff, S.A. (2002) A high-throughput Arabidopsis reverse genetics system. *Plant Cell.*, **14**, 2985-2994.

Sherson, S.M., Hemmann, G., Wallace, G., Forbes, S., Germain, V., Stadler, R., Bechtold, N., Sauer, N. and Smith, S.M. (2000) Monosaccharide/proton symporter AtSTP1 plays a major role in uptake and response of Arabidopsis seeds and seedlings to sugars. *Plant J.*, **24**, 849-857.

Shockey, J., Schnurr, J. and Browse, J. (2000) Characterization of the AMP-binding protein gene family in Arabidopsis thaliana: will the real acyl-CoA synthetases please stand up? *Biochem. Soc. Trans.*, **28**, 955–957.

Shockey, J.M., Fulda, M.S. and Browse, J.A. (2002) Arabidopsis contains nine long chain acyl-Coenzyme A synthetase genes that participate in fatty acid and glycerolipid metabolism. *Plant Physiol.*, **129**, 1710-1722.

Somerville, C., Browse, J., Jaworski, J.G., and Ohlrogge, J.B., 2000. Lipids. In Buchanan, B.B., Gruissen, W., and Jones, R.L. (eds), *Biochemistry & Molecular Biology of Plants*. American Society of Plant Physiologist, Maryland, pp. 456-527.

Sommerville, C. and Koornneef, M. (2002) A fortunate choice: the history of Arabidopsis as a model plant. *Nature Rev. Genet.*, **3**, 883-889.

Sparkes, I.A., Brandizzi, F., Slocombe, S.P., El-Shami, M., Hawes, C. and Baker A. (2003) An Arabidopsis pex10 null mutant is embryo lethal, implicating peroxisomes in an essential role during plant embryogenesis. *Plant Physiol.*, **133**, 1809-1819.

Srere, P.A. (1969) Citrate synthase. *Methods Enzym.*, **13**, 3-11.

Stintzi, A. and Browse, J. (2000) The *Arabidopsis* male-sterile mutant, *opr3*, lacks the 12-oxophytodienoic acid reductase required for jasmonate synthesis. *Proc. Natl. Acad. Sci. USA,* **97,** 10625-10630.

Strizhov, N., Li, Y., Rosso, M.G., Viehoever, P., Dekker, K.A. and Weisshaar, B. (2003) High-throughput generation of sequence indexes from T-DNA mutagenized Arabidopsis thaliana lines. *BioTechniques.,* **35,** 1164-1168.

Struglics, A., Fredlund, K.M., Rasmusson, A.G. and Møller, I.M. (1993) The presence of a short redox chain in the membranes of intact potato tuber peroxisomes and the association of malate dehydrogenase with the peroxisome membrane. *Physiol. Plant,* **88,** 19-28.

Suzuki, H. and Verma, D. (1991) Soybean nodule-specific uricase (nodulin-35) is expressed and assembled into a functional tetrameric holoenzyme in *Escherichia coli. Plant Physiol.*, **95**, 384-389.

Taiz, L. and E. Zeiger. (1998) *Plant Physiology, (2nd ed).* Sinauer Associates, Sunderland, MA, USA.

The Arabidopsis Genome Initiative (2000) Analysis of the genome sequence of the flowering plant *Arabidopsis thaliana. Nature*, **408**, 796–815.

Theodoulou, F.L. (2000). Plant ABC transporters. *Biochim. Biophys. Acta.,* **1465,** 79–103.

Thomas, S.M. and ap Rees, T. (1972) Glycolysis during gluconeogenesis in cotyledons of *Cucurbita pepo. Phytochemistry.*, **11**, 2187–2194.

Thompson, J.D., Gibson, T.J., Plewniak, F., Jeanmougin, F. and Higgins, D.G. (1997) The CLUSTAL_X windows interface: Flexible strategies for multiple sequence alignment aided by quality analysis tools. *Nucleic Acids Res.,* **25l,** 4876-4882.

Thorneycroft, D., Sherson, S. M. and Smith, S. M. (2001). Using gene knockouts to investigate plant metabolism. *J. Exp. Bot.*, **52**, 1593-1601.

Tissier, A.F, Marillonnet, S., Klimyuk, V., Patel, K., Torres, M.A., Murphy, G. and Jones, J.D. (1999) Multiple independent defective suppressor-mutator transposon insertions in Arabidopsis: a tool for functional genomics. *Plant Cell*, **11**, 1841-52.

Trelease, R N. (1984) Biogenesis of glyoxysomes. *Ann. Rev. Plant Physiol.*, **35**, 321-347.

Trelease, R.N., Becker, W.M., Grubber, P.J. and Newcomb, E.H. (1971) Microbodies (glyoxysomes and peroxisomes) in cucumber cotyledons. *Plant Physiol.*, **48**, 461–475.

Van Larabeke, N., Engler, G., Holsters, M., Elcacker, S.V.D., Zaenen, I., Schilperoort, R.A. and Schell, J. (1974). Large plasmid in *Agrobacterium tumefaciens* essential for crown gall-inducing ability. *Nature,* **252**, 169.

van Roermund, C.W., Waterham, H.R., Ijlst, L. and Wanders, R.J. (2003) Fatty acid metabolism in *Saccharomyces cerevisiae. Cell Mol Life Sci.*, **60**, 1838-1851.

van Roermund, C.W.T., Elgersma, Y., Singh, N., Wanders, R.J.A. and Tabak, H.F. (1995) The membrane of peroxisomes in *Saccharomyces cerevisiae* is impermeable to NAD(H) and acetyl-CoA under in vivo conditions. *EMBO J.*, **14**, 3480-3486.

van Roermund, C.W.T., Hettema, E.H., van den Berg, M., Tabak, H.F. and Wanders, R.J.A. (1999) Molecular characterisation of carnitine-dependent transport of acetyl-CoA from peroxisomes to mitochondria in *Saccharomyces cerevisiae* and identification of a plasma membrane carnitine transporter, Agp2p. *EMBO J.*, **18**, 5843-5852.

Verleur, N., Hettema, E.H., van Roermund, C.W.T., Tabak, H.F. and Wanders, R.J.A. (1997) Transport of activated fatty acids by the peroxisomal ATP-

binding-cassette transporter Pxa2 in a semi-intact yeast cell system. *Eur. J. Biochem.*, **249**, 657-661.

Volokita, M. and Somerville, C.R. (1987) The primary structure of spinach glycolate oxidase deduced from the DNA sequence of a cDNA clone. *J. Biol. Chem.*, **262**, 15825-15828.

Wain, R.L. and Wightman, F. (1954) The growth-regulating activity of certain α-substituted alkyl carboxylic acids in relation to their β-oxidation within the plant. *Proc. R. Soc. Lond. Biol. Sci.*, **142**:525-536.

Webb, M.A. and Newcomb, E.H. (1987) Cellular compartmentation of ureide biogenesis in root nodules of cowpea (*Vigna unguiculata* (l.) Walp.). *Planta*, **172**, 162-175.

Wheeler, D.L., Chappey, C., Lash, A.E., Leipe, D.D., Madden, T.L., Schuler, G.D., Tatusova, T.A. and Rapp, B.A. (2000) Database resources of the National Center for Biotechnology Information. *Nucleic Acids Res.*, **28**, 10-14.

Wu, Y., Spollen, W.G., Sharp, R.E., Hetherington, P.R. and Fry, S.C. (1994). Root growth maintenance at low water potentials. Increased activity of xyloglucan endotransglycosylase and its possible regulation by abscisic acid. *Plant Physiol.*, **106**, 607-615.

Yamada, K., Lim, J., Dale, J., Chen, H., Shinn, P., Palm, C.J., Wu, H.C., Pham, P., Liu, S.X., Sakano, H., Yu, G., Quach, H.L., Akiyama, K., Arakawa, T., Carninci, P., Seki, M., Davis, R.W., Theologis, A. and Ecker, J.R. (2003) Empirical Analysis of Transcriptional Activity in the Arabidopsis Genome. *Science,* **302,** 842-846.

Zhang, J. and Madden, T.L. (1997) PowerBLAST: A new network BLAST application for interactive or automated sequence analysis and annotation. *Genome Res.*, **7**, 649-656.

Zhang, Z., Schwartz, S., Wagner, L. and Miller, W. (2000) A greedy algorithm for aligning DNA sequences. *J. Comput. Biol.*, **7**, 203-214.

Zolman, B.K., Silva, I.D. and Bartel, B. (2001) The *Arabidopsis pxa1* mutant is defective in an ATP-binding cassette transporter-like protein required for peroxisomal fatty acid β-oxidation. *Plant Physiol.*, **127,** 1266-1278.

Zolman, B.K., Yoder, A. and Bartel, B. (2000) Genetic analysis of indole-3-butyric acid responses in *Arabidopsis thaliana* reveals four mutant classes. *Genetics,* **156,** 1323-1337.